UNIVERSIDAD DE BURGOS

DEPARTMENT OF BIOTECHNOLOGY AND FOOD SCIENCE

Valorization of industrial solid residue from macroalgae by emerging technologies

PhD Thesis

Ester Trigueros Andrés

Burgos, 2021

Valorization of industrial solid residue from macroalgae by emerging technologies

Memoria que para optar al grado de Doctor por la Universidad de Burgos en el programa de Avances en Ciencia y Biotecnología Alimentarias presenta:

ESTER TRIGUEROS ANDRÉS

Burgos, 2021

UNIVERSIDAD DE BURGOS

Departamento de Biotecnología y Ciencia de los Alimentos

Dña. MARÍA TERESA SANZ DÍEZ y Dña. SAGRARIO BELTRÁN CALVO, Profesoras del Departamento de Biotecnología y Ciencia de los Alimentos de la Universidad de Burgos,

CERTIFICAN:

Que la Graduada en Nutrición Humana y Dietética y Máster en Seguridad y Biotecnología Alimentarias **Dña. Ester Trigueros Andrés** ha realizado bajo su dirección el trabajo titulado "**Valorization of industrial solid residue from macroalgae by emerging technologies**", cuyo título en castellano es: "Valorización del residuo sólido industrial de macroalgas mediante tecnologías emergentes".

Considerando que dicho trabajo reúne los requisitos exigidos para ser presentado como Tesis Doctoral, expresan su conformidad con dicha presentación.

Para que conste, firman el presente certificado.

En Burgos, a 24 de Marzo de 2021

Fdo. María Teresa Sanz Díez

Fdo. Sagrario Beltrán Calvo

UNIVERSIDAD DE BURGOS

Departamento de Biotecnología y Ciencia de los Alimentos

D. JOSÉ MANUEL BENITO MORENO, coordinador del programa de doctorado "Avances en Ciencia y Biotecnología Alimentarias" de la Universidad de Burgos,

CERTIFICA:

Que la memoria titulada "**Valorization of industrial solid residue from macroalgae by emerging technologies**" presentada por Dña. Ester Trigueros Andrés, Graduada en Nutrición Humana y Dietética y Máster en Seguridad y Biotecnología Alimentarias, ha sido realizada en el Departamento de Biotecnología y Ciencia de los Alimentos bajo la dirección de las Dras. María Teresa Sanz Díez y Sagrario Beltrán Calvo, y en representación de la Comisión Académica del Programa de Doctorado, autoriza su presentación para ser defendida como Tesis Doctoral.

Para que conste, y surta los efectos oportunos, firmo el presente certificado.

En Burgos, a 24 de Marzo de 2021

BENITO MORENO JOSE MANUEL - 10868960B

Firmado digitalmente por BENITO MORENO JOSE MANUEL - 10868960B
Fecha: 2021.03.24 10:26:17 +01'00'

Fdo. José Manuel Benito Moreno

Coordinador del Programa de Doctorado

El trabajo presentado ha sido desarrollado en el seno del Grupo de Investigación Biotecnología Industrial y Medioambiental, reconocido por la UBU (GIR-UBU BIOIND) y por la Junta de Castilla y León como Unidad de Investigación Consolidada UIC-128, en el marco de los siguientes proyectos de investigación:

- VALORIZACIÓN DE LA FRACCIÓN PROTEICA DE SUBPRODUCTOS DE LA INDUSTRIA AGROALIMENTARIA DE CASTILLA Y LEÓN MEDIANTE TECNOLOGÍAS DE FLUIDOS PRESURIZADOS (PROVALOR), financiado por la Junta de Castilla y León y el Fondo Europeo de Desarrollo Regional (BU050P20).

- VALORIZACIÓN DE SUBPRODUCTOS MARINOS MEDIANTE TECNOLOGÍAS DE FLUIDOS SUB- Y SUPERCRÍTICOS PARA LA OBTENCIÓN DE BIOCOMPUESTOS VALIOSOS, financiado por la Agencia Estatal de Investigación (10.13039/501100011033).

- VALORIZACIÓN INTEGRAL DE SUBPRODUCTOS DE LA INDUSTRIA AGROALIMENTARIA MEDIANTE TECNOLOGÍAS EMERGENTES (ALVALOR), financiado por la Junta de Castilla y León y el Fondo Europeo de Desarrollo Regional (BU301P18).

Agradecimientos

A la Junta de Castilla y León y al Fondo Social Europeo por financiar mi contrato predoctoral y a la JCyL, la AEI y los Fondos FEDER por financiar los proyectos 10.13039/501100011033, BU050P20 y BU301P18 en los que he trabajado.

A mis directoras de Tesis. A Tere, por todo lo que me ha enseñado, por su gran dedicación y el enorme apoyo que me ha ofrecido todo este tiempo. A Sagrario, por haber depositado en mí su confianza para comenzar este proyecto y por toda la ayuda que me ha ofrecido durante estos años.

A todos los compañeros del Área de Ingeniería Química que han colaborado en esta Tesis. En especial, agradecer a Beti su total disposición, su ayuda, y por contribuir a mi formación. A Olga, por todo lo que me ha enseñado y por su infinita ayuda en esta última etapa. A Patricia, por su apoyo y compañía durante todos estos años. A Cipri, por estar siempre dispuesto a encontrar una solución a los problemas. A toda la gente con la que he trabajado durante estos años y que también han colaborado de una forma u otra en esta Tesis. A Mansoore, Óscar y Rodrigo.

A la Dra. Maria Manuel Gil, del Instituto Politécnico de Leiria, por ofrecerme la posibilidad de colaborar con su grupo para realizar mi estancia de investigación predoctoral. A Sónia Duarte por su recibimiento y su disposición a contribuir a mi formación investigadora.

A mi familia y amigos, por sus consejos, su apoyo y su confianza y por ser partícipes de esta etapa.

A Nacho, por su infinito apoyo, por acompañarme en esta aventura desde el primer día y por transmitirme ánimos siempre, a pesar de la distancia.

GENERAL INDEX

GENERAL INDEX

SUMMARY OF THE THESIS.....3

INTRODUCTION.....7

OBJECTIVES.....45

RESULTS.....49

Recovery of the protein fraction with high antioxidant activity from red seaweed industrial solid residue after agar extraction by subcritical water treatment.....53

Effect of heating rate and residence time on subcritical water macroalgae residue hydrolysis.....93

Subcritical water extraction scale-up from laboratory to pilot system for red algae residue after agar extraction valorization.....129

Enzymatic hydrolysis of the industrial solid residue of red seaweed after agar extraction: Extracts characterization and modelling.....163

Fractionation of bioactive compounds from a red alga subcritical water extract by ultrafiltration.....201

CONCLUSIONS.....237

h

SUMMARY / RESUMEN

SUMMARY OF THE THESIS

Nowadays, increasing wastes generation, as consequence of the growing population and higher quality of life, is one of the biggest problems that society faces with. The concept of biorefinery, in which residues are treated as new raw materials to be reincorporated into industrial processes, emerges as a solution. In this work, a complete valorization of the red alga *Gelidium sesquipedale* solid by-product generated after industrial agar extraction has been proposed. Despite being usually discarded, it still contains high content of interesting bioactive compounds such as carbohydrates, proteins or amino acids with high antioxidant activity that can be recovered.

Traditional extraction methods have several drawbacks. They are usually time-consuming and have low selectivity and extraction yields. In addition, large volumes of organic solvents, which are dangerous, too expensive and can be harmful for environment and human health, are used.

As an alternative, subcritical water extraction has been proposed as a novel technology within the green chemistry concept. Under subcritical conditions, water properties such as density, dielectric constant or ionic product can be modified by temperature modulation, which gives water the ability to selectively extract different target compounds from the selected raw material.

In addition, aimed to compare subcritical water extraction with other technologies, different hydrolytic enzymes have been also evaluated on bioactive compounds recovery from the marine alga residue through enzymatic assisted extraction technology.

Finally, after testing the effectiveness of subcritical water extraction on the marine alga by-product valorization, pressure-driven membrane technology has been evaluated for fractionation and concentration of subcritical water extracts, with the purpose of obtaining isolated and high-purity concentrates of the extracted bioactive compounds.

RESUMEN DE LA TESIS

Uno de los principales problemas que afronta la sociedad actual es la acumulación de residuos, consecuencia de una creciente población y una mayor calidad de vida. Sin embargo, el concepto de biorrefinería, donde los residuos son tratados como nuevas materias primas que puedan ser reincorporadas al proceso industrial, surge como posible solución a este problema. En este sentido, se ha propuesto la valorización integral del subproducto del alga roja *Gelidium sesquipedale* tras la extracción industrial del agar, ya que, a pesar de ser un residuo, aún contiene importantes cantidades de compuestos bioactivos de interés como carbohidratos, proteínas o aminoácidos con alta actividad antioxidante que pueden proporcionarle un valor añadido.

Las técnicas de extracción convencionales presentan numerosas desventajas, entre las que destacan: tiempos de tratamiento prolongados, baja selectividad y rendimientos de extracción y uso de grandes volúmenes de disolventes orgánicos, que no sólo son peligrosos, sino que además encarecen el proceso de extracción y dañan el medio ambiente. Como alternativa, se ha propuesto el estudio de una tecnología novedosa integrada en el concepto de la química verde, como es la extracción con agua subcrítica. En condiciones subcríticas, propiedades como la densidad, la constante dieléctrica o el producto iónico del agua pueden variar a través de la modulación de la temperatura, lo que otorga al agua la capacidad de extraer selectivamente diferentes compuestos de interés.

Además, con el objetivo de comparar los resultados obtenidos mediante la extracción con agua subcrítica con otras tecnologías, se ha evaluado la actuación de distintas enzimas hidrolíticas sobre la recuperación de compuestos bioactivos en el residuo algal a través de la extracción enzimática asistida.

Por último, tras demostrar la efectividad del agua en condiciones subcríticas en la valorización del subproducto algal con altos rendimientos de extracción, se ha estudiado la tecnología de separación con membranas para el fraccionamiento y concentración de los extractos utilizando presión como fuerza impulsora, con el objetivo de obtener concentrados de compuestos bioactivos aislados y de elevada pureza.

INTRODUCTION

1. Macroalgae: *Gelidium sesquipedale*

Algae are photosynthetic organisms capable of fixing carbon dioxide from the atmosphere by using solar energy. These organisms can survive in hard conditions, although composition is very sensitive to parameters like pH, temperature, light or carbon dioxide concentration (Bitog et al., 2011).

Algae are divided in two main groups: microalgae and macroalgae. Microalgae are cellular microorganisms that can be found in unicellular form or simple colony structures (Mata et al., 2010), whereas macroalgae, also known as seaweeds, are plants that are classified in three general types based on their pigments: red (*Rodophyta*), brown (*Phaeophyta*) and green (*Chlorophyta*) (Jung et al., 2013).

The chemical composition of macroalgae significantly varies depending on the type, the species and the cultivation conditions (Hong et al., 2014). Carbohydrate fraction in seaweeds is constituted of complex polysaccharides which, according to their biological function, can be storage or structural polysaccharides. Red macroalgae are classified based on the presence of major structural carbohydrates, agar and carrageenans, into agarophytes and carrageenophytes, respectively (Ju et al., 2016).

Agar is a hydrocolloid which forms a thermoreversible gel when it is dissolved in hot water and then cooled (Guerrero et al., 2014). Solubilization takes places in hot water (85 to 100 °C) while it solidifies from 30 to 40 °C. Structural reorganization of the conformation is made during this process to obtain a rigid and ordered structure of co-axial double helix (Delattre et al., 2011).

Agar structure is composed by two polysaccharides: agarose and agaropectin. Agarose, the main constituent of agar, is a neutral linear heteropolysaccharide of alternatively repeated residues of D-galactopyranose and 3,6-anhydro-L-galactopyranose, linked through α-1,3-glycosidic linkages. The resulting heterodimers of α-neoagarobiose are linked to each other by β-1,4-glycosidic bonds to form the polysaccharide agarose (**Figure I.1**) (Araki, 1956). Agaropectin is a more complex and charged heteropolysaccharide characterized by the

same backbone as agarose with many acid groups such as sulphate, pyruvate but also glycuronate and methylated residues (Duckworth & Yaphe, 1971; Knutsen, 1994).

The ratio of agarose and agaropectin varies depending on the agarophyte genus, the origin and the harvesting season. Moreover, the amount of agarose determines the quality of agar, as well as the gel strength and gelling temperature (Ju et al., 2016).

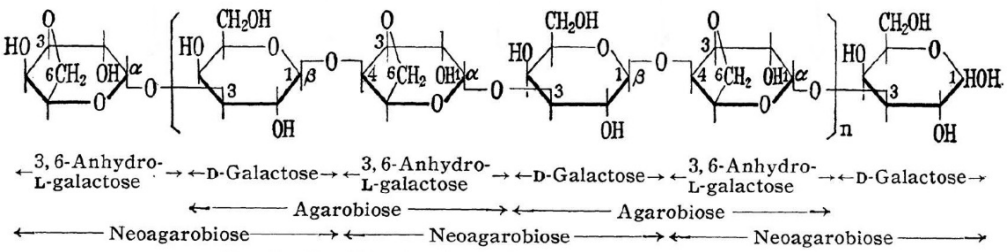

Figure I.1. Chemical structure of agarose as constituent of agar. Adapted from Araki. (Araki, 1956).

Besides the agar, cellulose, a polysaccharide consisting of a linear chain of β-1,4 D-glucose units, is also presented in red macroalgae but in lower amount (Park et al., 2012).

Agar is mostly extracted from the macroalgal genera *Gelidium*, *Gracilaria* and *Euchema* (Park et al., 2011) and it is a very appreciated component for food and cosmetic industries where it is used as a gelling, thickening and stabilizing agent in food formulations and microbiological media (Murano, 1995).

Gelidium sesquipedale (*Rhodophyta, Gelidiaceae*) is a red alga that is able to live three or four years. It grows between 9 and 10 centimetres per year to a total size of 30 centimetres and it can be found in the Atlantic coasts of France, Spain, Portugal and Morocco (Borja, 1987). This alga is the major seaweed resource in the Spanish agar industry since it is the most abundant specie of *Gelidium* in Spain and it provides the best raw material to obtain the highest quality agar (Carmona et al., 1998; Fernández, 1991; Mouradi-givernaud et al., 1999; Maria Torres et al., 1991).

The industrial process generally used to produce agar from *G. sesquipedale* macroalga consists of a first alkaline treatment with NaOH in order to eliminate components such as colorants and salts, followed by a washing step with cold water. Then, the agar-agar extraction takes place through a boiling water bath, an intermediate filtration stage and a final second extraction. A diagram of the process is represented in **Figure I.2**.

As a result of the industrial process, a solid residue is generated, being mainly destined to fodder and fertilizer, although most of it is disposed of (Ferrera-Lorenzo et al., 2014). However, despite being a residue, this solid still contains high-value bioactive compounds such as carbohydrates, proteins or amino acids with high antioxidant activity (Ennouali et al., 2006) that makes it a very valuable and functional product rather than just a waste.

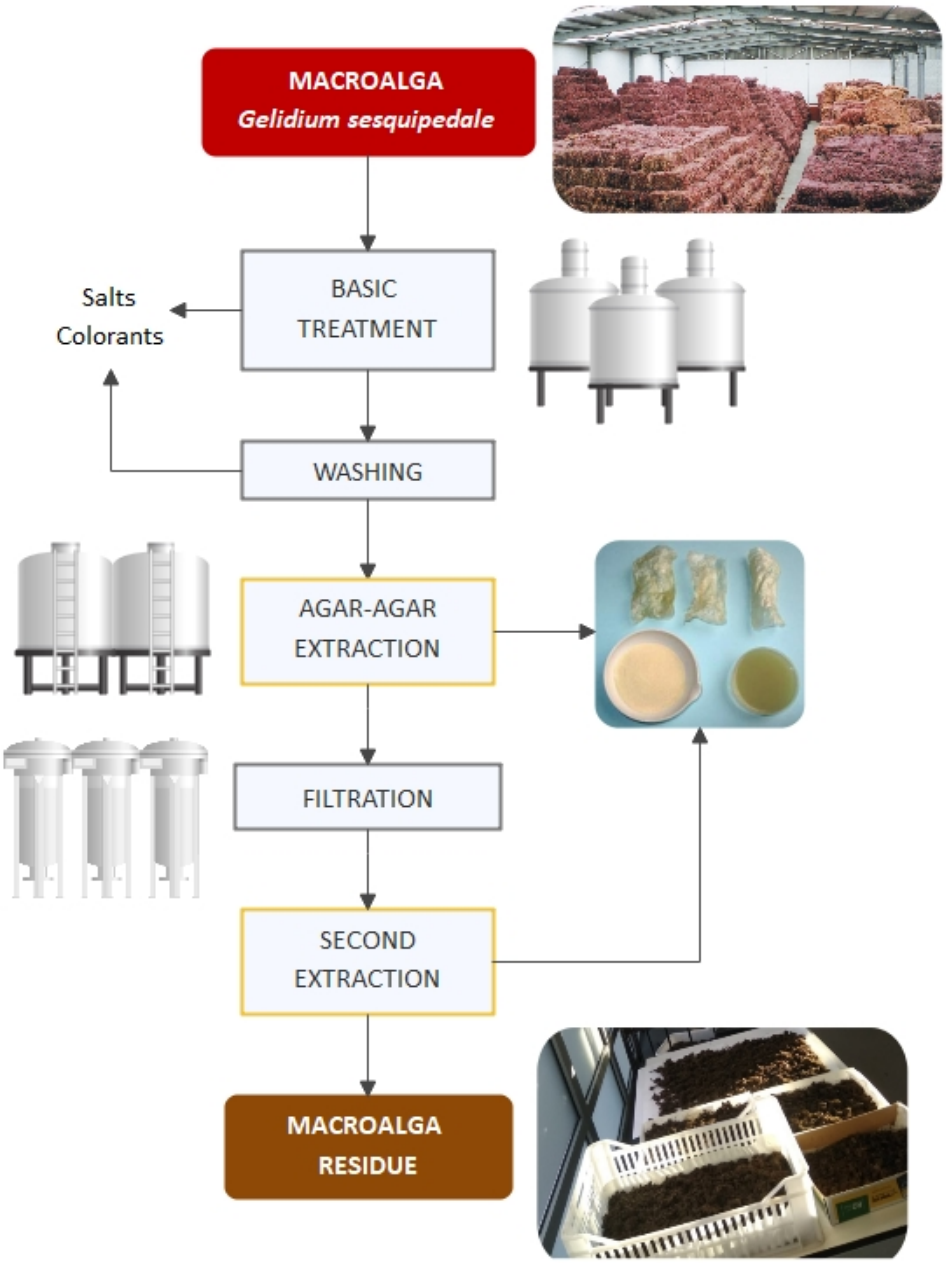

Figure I.2. Industrial agar extraction process from *Gelidium sesquipedale* red macroalga.

2. Sustainable valorization of macroalga by-product within an integrated biorefinery concept

Nowadays, the increasing generation of solid wastes is one of the biggest problems that society faces with, consequence of the growing population and the increase in quality of life (Blikra et al., 2018). Organic solid wastes are one of the largest groups of wastes produced worldwide and the rate at which they are being generated is constantly increasing (Méndez et al., 2019).

Biorefinery concept refers to the transformation of a raw material – biomass – into energy and several products, such as chemicals and biomaterials, by fractionation or conversion processes (Cabeza et al., 2016). To this purpose, identifying sources of valuable compounds, taking into account both environmental and economic aspects, is needed (Jung et al., 2013).

Biorefineries are classified according to feedstock nature in first, second and third generation biorefineries, depending on the utilization of classical agricultural biomass, lignocellulosic biomass or high-yield feedstocks of algae, respectively (Elmekawy et al., 2013).

Algal biorefineries are based on the sequential fractionation of the biomass and subsequent transformation into the target final products (Torres et al., 2019). Seaweeds, as a third-generation biomass, are characterized with no or low lignin content, therefore, unlike other biomasses with higher amount of lignin, macroalgae overcome the drawbacks of second-generation biomasses, such as agricultural and forest residues, owing to the fact that a pre-treatment step to lignin degradation or removal is not needed (Anto et al., 2020; Rajak et al., 2020; Tuma et al., 2020). This is a great advantage over terrestrial biomass in which lignin obstructs the enzymatic hydrolysis and further conversion of bioactive compounds (Fasahati et al., 2015; Jung et al., 2013).

In this work, the by-product from *Gelidium sesquipedale* after industrial agar extraction was studied as an interesting source of valuable compounds. Worldwide, agar production exceeds 14,500 t annually with a sale value of 246 million US$ (Porse & Rudolph, 2017) and,

consequently, large amounts of waste are generated. Utilization of this seaweed by-product by using a biorefinery model through the complete valorization besides phycocolloids extraction, reduces the accumulation of solid waste, as well as the associated economic expenses, in addition to a more efficient use of resources. For that reason, a circular economy system, where wastes are treated as raw materials which can be reincorporated into industrial processes, is desired.

Within a biorefinery concept, different technologies are used to transform biomass into biofuels and high value-added products that will be reincorporated into different production processes in the industry (**Figure I.3**). These technologies are classified into physical, thermal, chemical and biochemical processes (González-Delgado & Kafarov, 2011).

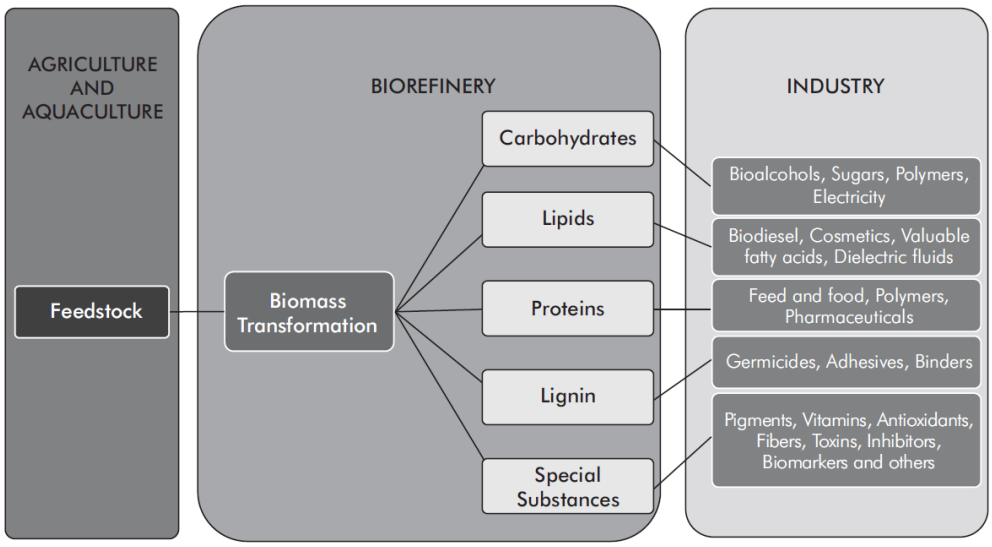

Figure I.3. Systematic process in biorefinery concept (González-Delgado & Kafarov, 2011).

Physical processes involve homogenization, destruction, separation or particle size decrease through mechanical procedures. Thermal processes are based on the thermal decomposition of organic components and include direct combustion, thermal liquefaction, gasification or pyrolysis. Chemical processes refer to hydrolysis by acid, basic or enzymatic reagents, esterification and transesterification, whereas biochemical processes are

anaerobic digestion for biogas production and fermentation, in which fermentable substrates are transformed into organic acids and alcohols by the action of enzymes or microorganisms (Elmekawy et al., 2013; González-Delgado & Kafarov, 2011; Suganya et al., 2016).

Nevertheless, some of these methods have several drawbacks: not only are time-consuming and have low selectivity and extraction yields, but also use large volumes of organic solvents that are dangerous (Gbashi et al., 2016; Herrero et al., 2006), too expensive and can corrode the equipment (Greiserman et al., 2019).

Nowadays, not only efficiency of the extraction techniques is sought, but the development of environmental and friendly extraction processes is desired instead of conventional extraction methods. This fact is related to the Green Chemistry concept, that, according to its definition, "*is based on the discovery and design of extraction processes, which will reduce energy consumption, allows use of alternative solvents and renewable natural products, and ensures a safe and high-quality extract/product*" (Chemat et al., 2012). In this sense, as a part of a biorefinery approach, suitable, efficient, fast, cheap and green extraction techniques are needed (Herrero et al., 2006).

3. Subcritical water extraction/hydrolysis

In relation to a sustainable approach in which new environment respectful technologies are sought, water seems to play a key role. This fact is due to the non-toxic, non-flammable, inexpensive, safe and environmental benign character of water, that makes it an excellent solvent for obtaining valuable compounds from biomass or turn it on fuels and chemicals (Liang & Fan, 2013; Knez et al., 2015).

3.1. Principle of Subcritical water extraction/hydrolysis

Subcritical water extraction (SWE), also known as superheated water extraction or pressurized hot-water extraction, consists of using hot pressurized water as solvent, at temperatures above its boiling point (100 °C) and below its critical point (374 °C) and pressure enough to keep it at its liquid state (**Figure I.4**) (Herrero et al., 2006; Zakaria & Mustapa Kamal, 2016).

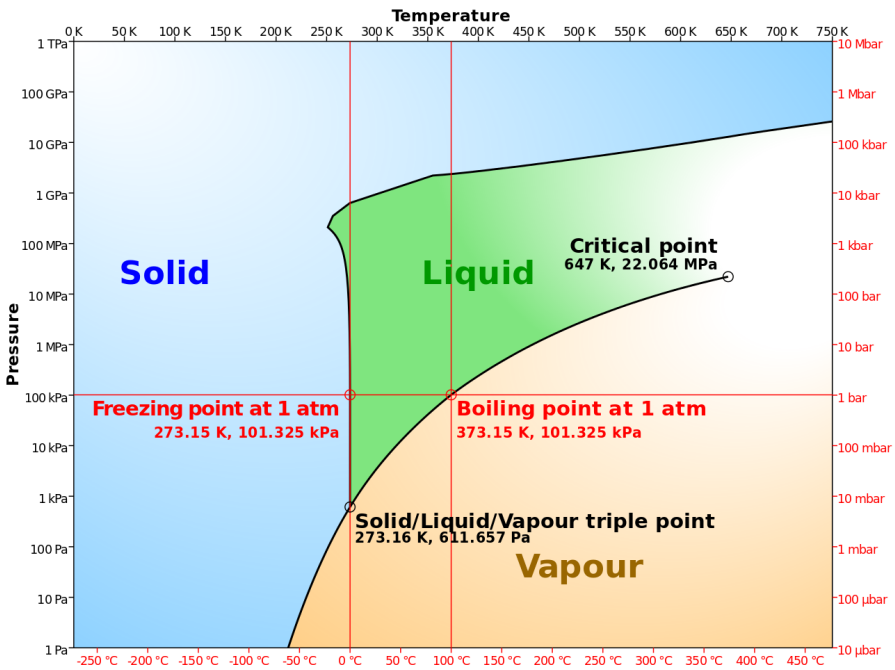

Figure I.4. Water phase diagram. Adapted from Plaza & Turner. (Plaza & Turner, 2015).

The breaking of hydrogen-bonds with temperature promotes low viscosity and high diffusivity that facilitate water to diffuse into the matrix. Furthermore, concentrations of H^+ and OH^- ions are higher than in ambient liquid state, thus, it provides an effective medium for acid- and base-catalyzed reactions (Akiya & Savage, 2002).

Under subcritical conditions, density, surface tension, polarity, viscosity and diffusion of water change and provide water unique properties as solvent (Martínez-abad et al., 2018). **Figure I.5** shows how density, ionic product (pKw) and dielectric constant (ε) vary as a function of temperature. When temperature of pressurized water increases, parameters such as density, dielectric constant and ionic product of water change. Below its critical point (374 °C), both density, ε and pKw decrease with increasing temperature.

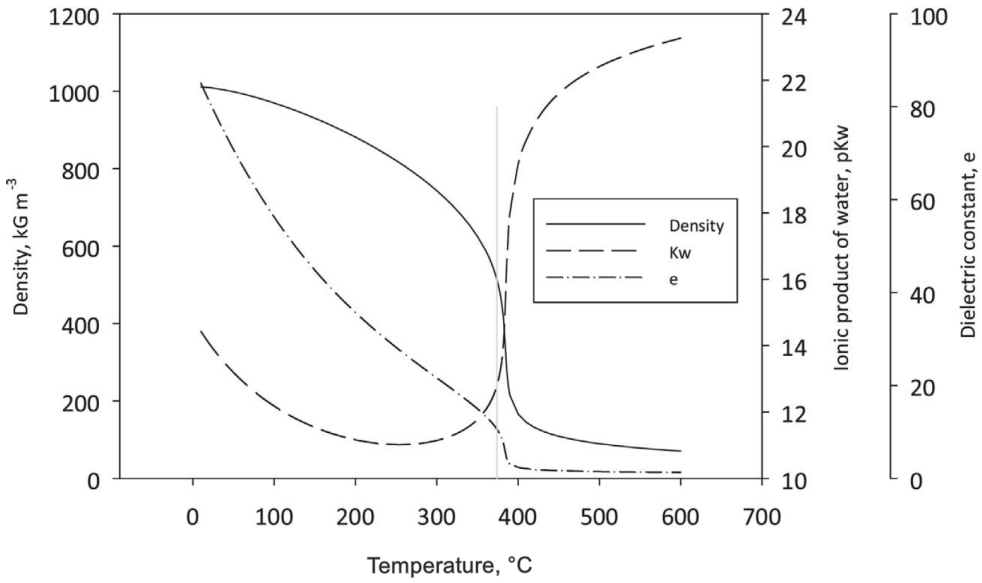

Figure I.5. Water properties around the critical point depending on the temperature (Cocero et al., 2018).

Dielectric constant is related to polarity of water. Water presents a dielectric constant nearly 80 at room temperature; however, this value can decrease below 40 when temperature is above 200 °C and pressure enough to keep it in liquid state, and it will be close to 27 when pressurized water is heated up to 250 °C (Plaza et al., 2010).

Consequently, through the dielectric constant modulation with temperature, water can acquire similar values to organic solvents such as methanol (ε = 32.6), ethanol (ε = 24.3) and acetone (ε = 20.7), which give water both polar and non-polar properties (Park et al., 2019). Owing to the ability of water to imitate the solvent capacity of organic solvents, subcritical water extraction can be suggested as a green and useful alternative technology to organic solvents for selectively extract hydrophobic organic compounds from different sources (Carr et al., 2011; Herrero et al., 2015).

3.2. Industrial applications

Subcritical water treatment has been used in literature to extract contaminants such as sulfonates (Priego-López & Castro, 2004), dioxins (Hashimoto, 2004), pesticides (Richter & Sepulveda, 2003; Rodil & Popp, 2006) or herbicides (Chienthavorn et al., 2007; Tajuddin & Smith, 2005) mainly from soil matrixes.

Subcritical water has also been reported as a good solvent for bioactive compounds recovery from different plants and foods as rice bran (Wataniyakul et al., 2012) or mango leaves (Fernández-Ponce et al., 2012) and from vegetal wastes such as onion skin (Benito-Román et al., 2020) and brewer's spent grain (Alonso-Riaño et al., 2021).

Algae have been also treated by subcritical water for bio-oil production (Alba et al., 2012; Gai et al., 2015; Jin et al., 2013) and protein, amino acids and sugars extraction, with a maximum recovery yield of 20.2, 6.3 and 36.7 %, respectively (Park et al., 2019). However, the use of subcritical water has not been reported for treating algae residues.

In comparison to other conventional techniques and treatments, Gámiz-Gracia & Castro (Gámiz-Gracia & Castro, 2000) found subcritical water faster for essential oils extraction with higher purity and productivity than hydro-distillation and dichloromethane extraction. Along the same lines, Budrat & Shotipruk (Budrat & Shotipruk, 2009) obtained subcritical water extracts from bitter melon with three times antioxidant capacity than by using methanol or ultrasonic extraction.

3.3. Parameters affecting extraction with subcritical water

3.3.1. Effect of operational mode

In subcritical water treatment, three operational modes are possible: static or discontinuous, dynamic or continuous and static-dynamic or semicontinuous mode.

In static or discontinuous mode, a certain amount of biomass is charged in the reactor with a fixed volume of water, while in dynamic or continuous mode both water and sample flow continually through the reactor. Static-dynamic or semicontinuous mode is a combination of the other two modes: biomass remains in the reactor during the extraction process while there is a continuous supply of fresh water to the reactor (Morales-Muñoz et al., 2002).

In discontinuous mode, as there is not fresh water running through the sample, the reaction inside the reactor will change according to the equilibrium constant at each point of the extraction process. Dilution of the final extracts will not be a problem, however, degradation reactions resulting from long exposure times of the sample to water at high temperatures will probably take place (Carr et al., 2011). Nevertheless, in a hybrid-semicontinuous mode, the equilibrium is completely displaced because fresh water is continuously pumped through the sample (Morales-Muñoz et al., 2002).

Continuous mode is generally faster than discontinuous one because of the constant renewal of water solvent, which stimulates the mass transfer from biomass to the aqueous medium. However, since greater volume of water is used in dynamic mode, a more diluted product will be collected (Carr et al., 2011).

A diagram of the different operational modes in SWE is shown in **Figure I.6.**

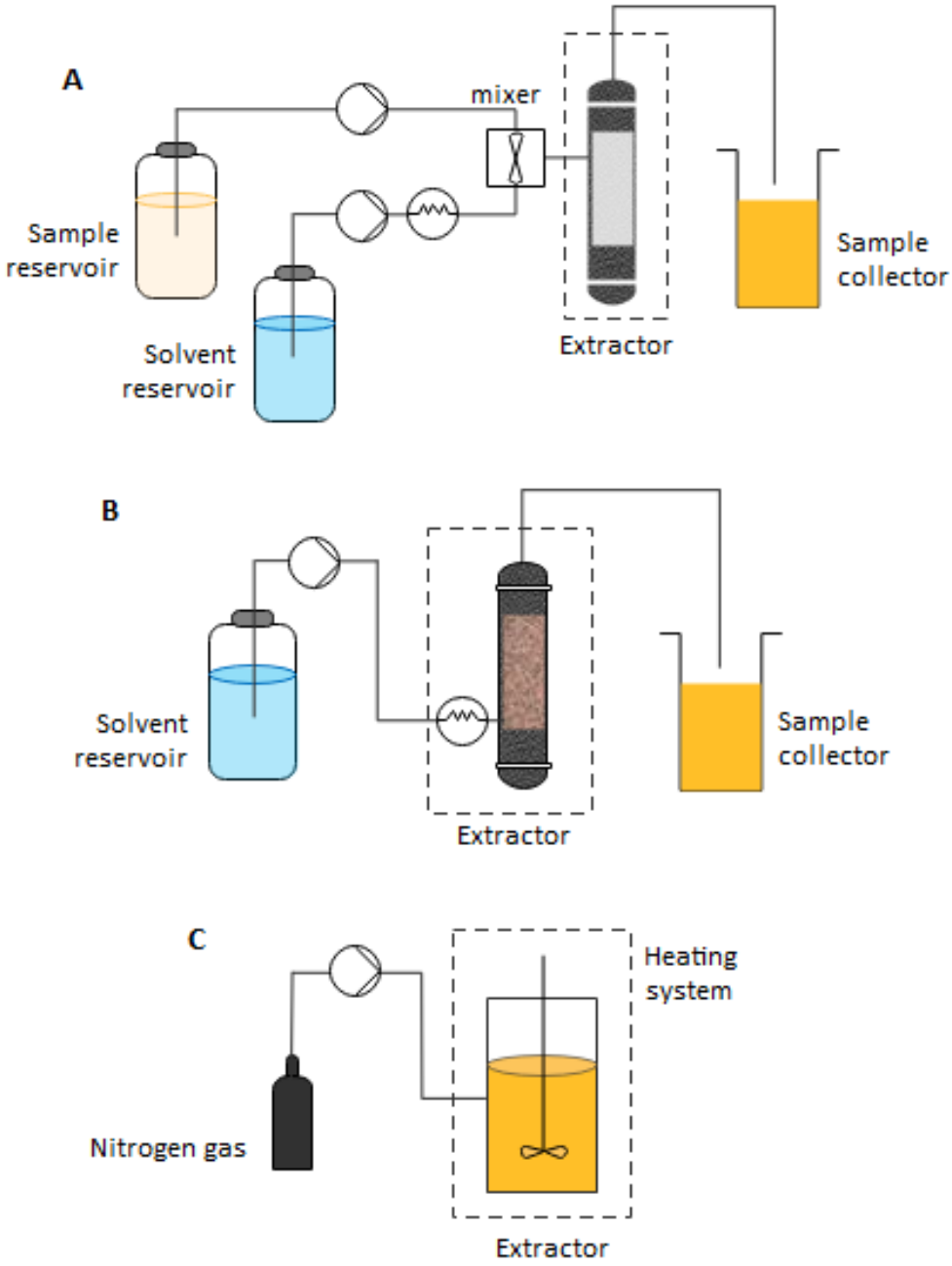

Figure I.6. Different operational modes in subcritical water extraction system. **A** continuous (dynamic), **B** semicontinuous (static-dynamic), **C** discontinuous mode (static).

3.3.2. Effect of temperature

Temperature is one of the most important operational parameters in subcritical water extraction (Peterson et al., 2008; Thiruvenkadam et al., 2015). As shown before, temperature affects directly the polarity of water, defining the type of compound that will be extracted. Thus, it is possible to vary temperature of subcritical water selectively according to the desired compound to be extracted.

Higher temperatures of subcritical water usually lead to higher extraction yields, but it is necessary to take into account that some compounds start degradation and decomposition reactions when temperature is too high (Chen et al., 2014). Consequently, the effect of temperature in subcritical water extraction must be studied for target components (Carr et al., 2011). The selected working temperature should be the optimal temperature at which maximum yield for components is reached and no degradation reactions take place.

For instance, Plaza et al. (Plaza et al., 2012) found the highest yield and maximum antioxidant activity from green microalga *Chlorella vulgaris* subcritical water extraction at 200 °C, the maximum temperature studied. Similar results from the same raw material were found for the protein fraction recovery with a maximum at 200 °C and lower protein content at higher temperatures due to further degradation (Phusunti et al., 2017). For brown and red algae, 175 °C was the optimal temperature found for total polyphenol extraction and antioxidant activity in discontinuous subcritical water extraction (Plaza et al., 2010).

3.3.3. Effect of pressure

Pressure has a negligible effect on the extraction yield by using subcritical water. Varying the working pressure, little or non-effect on the extraction efficiency has been discovered during subcritical water extraction (Carr et al., 2011; Zakaria & Mustapa Kamal, 2016).

3.3.4. Effect of extraction time

Extraction time is also an important parameter to control in subcritical water extraction. Degradation and hydrolysis products may appear as a result of the sample exposure to high temperatures for long reaction times. In consequence, understanding the combined effect of temperature and reaction time during hydrothermal processes is needed to improve the process selectivity (Cocero et al., 2018). For this purpose, severity factor is a commonly used variable for temperature and treatment time combination:

$$logR_o = log\left(t \cdot exp^{((T-T_{ref})/14.75)}\right) \quad \textbf{[I.1]}$$

where t is the treatment time (min), T is the operating temperature (°C) and T_{ref} is equal to 100 °C.

For example, Valdez et al. (Valdez et al., 2012) found that extraction of water-soluble compounds from microalgae with subcritical water at 300 °C and 350 °C resulted in a yield decrease with increasing process time due to the formation of volatile compounds such as H_2, CO, CO_2, CH_2 and C_2H_6. This fact evidenced the decomposition of extracted liquid compounds to volatile component because of high temperatures and long processes.

3.3.5. Effect of the flow rate and residence time

In continuous subcritical water processes, the solvent flow rate can affect the velocity at which the compounds are extracted (Carr et al., 2011). The flow solvent rate and the reactor volume determine the residence time of water in the reactor:

$$\tau = \frac{V}{F_v} = \frac{V}{F_{v,o}}\frac{\rho_r}{\rho_o} \quad \textbf{[I.2]}$$

where τ is the residence time, V is the reactor volume (m^3), $F_{v,o}$ the water flow rate at ambient conditions (m^3/s), ρ_o is the water density at ambient conditions (kg/m^3) and ρ_r the water density at the reaction conditions (kg/m^3).

Lower residence times, as a result of greater flow solvent rate, have been reported in literature to be more efficient in subcritical water treatment by obtaining faster (Anekpankul et al., 2007; Haghighi & Khajenoori, 2013; Ozel et al., 2003) and higher extraction yields (Thiruvenkadam et al., 2015). Increasing flow rate enhances superficial velocity that results in a mass transfer improvement (Jansen et al., 2002).

Longer residence times have been reported in the literature to let degradation of solubilized compounds take place, in comparison with shorter residence times at the same temperature, where the degradation compounds found at higher residence times were not detected (Karagoz et al., 2004; Zhong & Wei, 2004).

In continuous mode, water and biomass residence time depend on flow rate, while in a semicontinuous process, the residence time of biomass refers only to process time. Moreover, to determine the severity factor in dynamic modes, the treatment time is replaced by the residence time.

During subcritical water extraction, degradation reactions may take place. These reactions transform extracted compounds into different degradation products (Peterson et al., 2008). Consequently, composition and concentration of liquid extracts collected during subcritical water treatment can be modified as a result of flow rate and residence time modulation and it will determine directly the final composition (Akhtar et al., 2011).

In spite of the improvement in the extraction yield with subcritical water at high flow rates because of lower residence times, obtaining final extracts with more dilute components could be a problem owing to large volumes of water used (Carr et al., 2011). Therefore, the optimal flow rate should be selected taking into account both extraction time and final extracts concentration in order to get more concentrated extracts in shorter treatment times (Haghighi & Khajenoori, 2013).

3.3.6. Effect of heating rate

The heating rate has been also identified as an important parameter in subcritical water technology which, along with the other influencing parameters, determines the hydrolysis degree of biomass (Brand et al., 2014).

High heating rates stimulate fragmentation and biomass hydrolysis, accompanied by the cell disruption and the limitation of unwanted reactions (Thiruvenkadam et al., 2015). On the opposite, slow heating rates generally lead to secondary reactions with char formation (Akhtar et al., 2011). Therefore, finding the appropriate heating rate of the subcritical water reactor is essential to solve heat transfer limitations and achieve high yields. However, the great impact of heating rate on subcritical water extraction/hydrolysis makes it very difficult to compare results between different heating operational systems found in bibliography.

3.3.7. Effect of biomass loading

Water is a green solvent that participates as a catalyst, hydrogen donor and hydrolyzing solvent of the high molecular weight compounds from the raw material. For this reason, biomass:water ratio in the reactor is another important parameter that influences the extraction of target components by using subcritical water (Anastasakis & Ross, 2011; Brand et al., 2014).

Anastakasis & Ross (Anastasakis & Ross, 2011) found an optimum loading rate of 1:10 (biomass:water) for brown alga *L. saccharina* in discontinuous mode subcritical water extraction and water volume increasing did not produce any change in extraction yield. However, the interactions between components of biomass and water may be blocked as a consequence of the increase in solid biomass concentration, avoiding these components from being released into the aqueous medium (Akhtar et al., 2011).

4. Enzyme assisted extraction

In this work, subcritical water extraction/hydrolysis results have been compared with other biomass treatments. For this purpose, enzyme assisted extraction (EAE) has emerged as a potential alternative to conventional extraction methods because of being an efficient, benign, sustainable and eco-friendly technology (Nadar et al., 2018).

The main advantage of EAE compared to conventional methods is a great specifity for the substrate (Gligor et al., 2019). It is an environmentally friendly technology owing to the general use of water instead of organic solvents and it uses low temperature preventing for heat degradation reactions (Panja, 2017).

EAE consists of using hydrolytic enzymes as a catalyst to disrupt the cell walls from raw materials in order to easily release intracellular compounds to the reactive medium (Boulila et al., 2015; Puri et al., 2012). The mechanism to break the cell wall by using hydrolytic enzymes starts with a complex formed between the active site of the enzyme and the cell wall of the substrate. This interaction causes the change of the enzyme shape with the consequent greater enzyme-substrate interaction. Finally, the breakage of cell wall bonds due to hydrolytic reactions causes the release of intracellular and wall-linked components to the extraction medium (**Figure I.7**) (Sheldon & Pelt, 2013; Sowbhagya et al., 2010).

Enzymes are able to carry out hydrolysis reactions specifically and selectively under mild conditions at controlled temperature, which is very useful for thermosensitive compounds extraction with retention of their biological activity (Puri et al., 2012).

EAE has been reported in the literature as a successfully way to recover sugars, proteins and polyphenols with high antioxidant activity from different seaweeds (Habeebullah et al., 2020; Hardouin et al., 2014; Wijesinghe & Jeon, 2012).

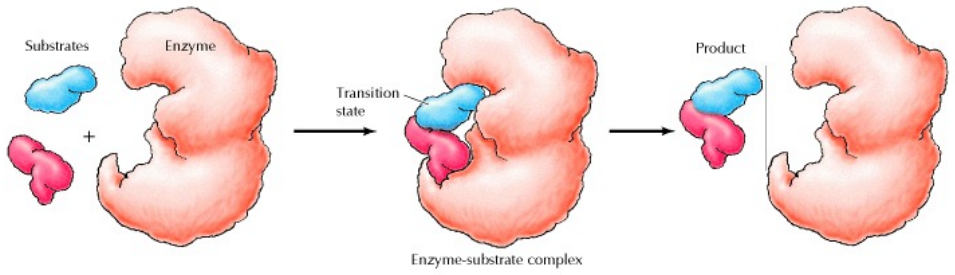

Figure I.7. Enzymatic catalysis of two substrates reaction (Cooper, 2000)

There are several parameters that directly influence the enzymatic activity and, hence, the release of the bioactive compounds from the raw material:

4.1. Effect of enzyme type

Selection of the hydrolytic enzyme or enzymes mixture is essential to reach high extraction yields.

The type of enzyme selected will depend on the nature of the raw material (Puri et al., 2012). Marine algae cell wall is constituted of a complex mixture of heteromolecules that could be broken down by using carbohydrases and proteases (Grosso et al., 2015). Common enzymes used for breaking the cell wall from algae are xylanase, arabinose, cellulase, amylase, protease and glucanase (Kadam & Tiwari, 2013). For instance, cellulases hydrolyse cellulose to cellobiose and glucose when the hydrolysis is completed, while proteases hydrolyse proteins into varied-sized peptides and free amino acids (Muniglia et al., 2014).

4.2. Effect of extraction temperature

Generally, increasing temperature results in higher enzymatic activity because it leads to a viscosity medium decrease and easier compounds solubilization (Gligor et al., 2019). The optimum temperature is known as the temperature at which the highest enzymatic activity is reached. However, due to the protein enzymes nature, high temperatures promote

enzymatic configuration alteration with a reduction in enzyme activity (Peterson et al., 2007; Wijesinghe & Jeon, 2012) and extracted bioactive compounds degradation (Muniglia et al., 2014).

4.3. Effect of extraction time and enzyme concentration

Longer treatment times are related to more expensive processes and lower quality extracts. Solubilized compounds during enzymatic hydrolysis can be transformed into degradation products due to long exposure times at elevated temperatures (Muniglia et al., 2014; Nadar et al., 2018). Extraction time is related to the concentration of enzyme, as the former can be reduced up to half the initial value if the latter is increased twice. Same results are obtained by reversing the values (Gligor et al., 2019).

4.4. Effect of extraction pH

pH also influences the rate of enzymatic reaction. pH value at which enzyme shows its highest activity is known as the optimum pH (Wijesinghe & Jeon, 2012). In general, acid media are desired to achieve good enzymatic activity as a consequence of hydrogen bonds destabilization with greater cellular wall plasticity. This modifies protein configuration and binding capacity of substrates to the active centre (Gligor et al., 2019; Muniglia et al., 2014).

5. Purification and separation process

In this PhD Thesis, fractionation and concentration steps after subcritical water extraction has been proposed by using membrane technology. As a result of the extraction methods described above, aqueous mixtures of different valuable compounds such as carbohydrates, polyphenols, proteins and free amino acids are obtained. These compounds are highly valued in food, cosmetic and pharmaceutical industries, however, they are found in heterogenous and diluted aqueous solutions. Hence, developing a purification and concentration process is desired in order to obtain isolated and concentrated valuable compounds from an economic and health point of view.

5.1. Membranes for separation processes

Membrane separation technology has been proven to be an environmentally friendly and cost-effective alternative for the separation and fractionation of valuable compounds from by-products of food industry (Saidi et al., 2014; Yu et al., 2016).

In pressure-driven membrane processes, the membranes act like a selective barrier capable of separating different components from a fluid based mainly on its size. In **Figure I.8** different pressure-driven membranes processes covering a wide range of particle sizes are shown. The main and more common pressurized membrane processes, microfiltration (MF), ultrafiltration (UF), nanofiltration (NF) and reverse osmosis (RO), are differenced by the application of hydraulic pressure, but the main responsible for controlling what compounds are filtered is the nature of the membrane. By RO, all components are retained except for the solvent, while UF and MF retain macromolecules or particles larger than 10-200 Å and 0.1-5 µm, respectively. Hence, UF and MF are considered to be useful methods for purifying, concentrating and fractionating macromolecules immersed in heterogenous solutions (Cheryan, 1998).

The main advantages of pressure-driven membrane technology in comparison with conventional dewatering processes are: low energy consumption, high selectivity, free of organic solvents and moderate conditions of pressure and temperature. The last-

mentioned benefit is very important when thermolabile components separation or concentration is sought because no heat degradation of target compounds takes place (Cissé et al., 2011). In fact, membrane processes can operate at ambient temperatures, therefore, thermal and oxidative degradation reactions common in evaporation traditional methods are avoided (Cheryan, 1998).

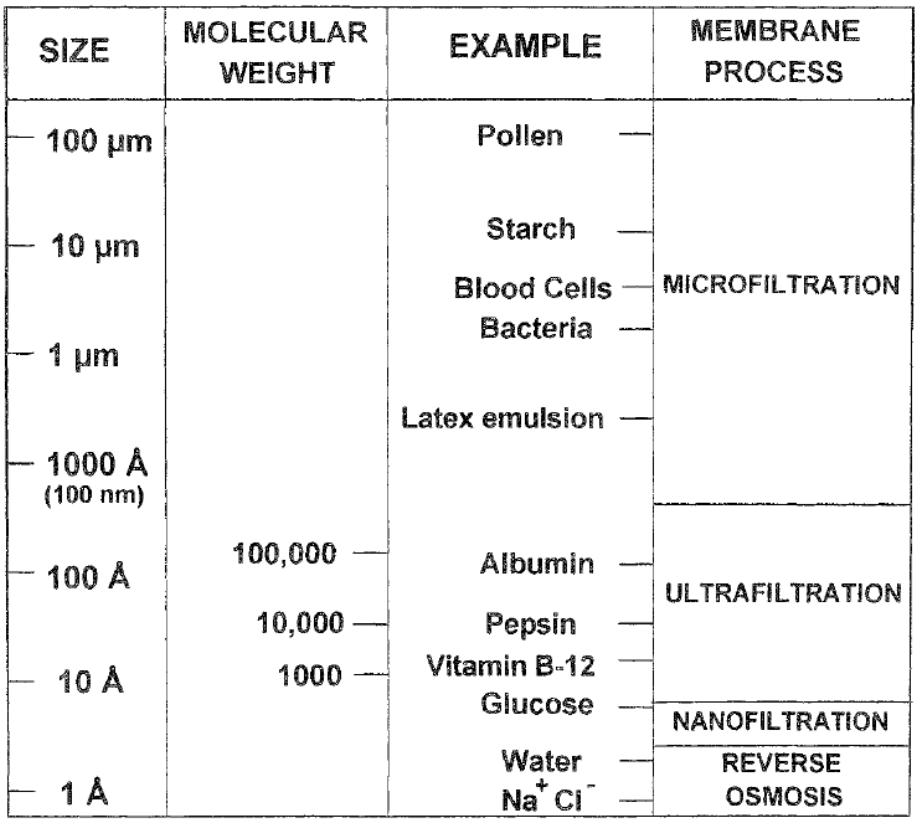

Figure I.8. Compounds separation according to its size by using different pressure-driven membrane processes (Cheryan, 1998).

One of the most important advantages of pressure-driven membrane processes compared to traditional processes is the non-appearance of change in solvent state during concentration process. Among traditional dewatering processes, evaporation and freeze concentration for liquid product are based on water phase change from liquid to vapor and solid state, respectively, consequently resulting in high energy consumption.

5.2. Principle of membrane separation technology

Pressure-driven membrane separation technology consists of pumping the desired feed solution over the selected membrane under low pressure. During MF and UF processes, the pressure gradient of the membrane forces the lower-size components from the feed solution through the pores of the membrane, while the higher-size components are retained. The fraction capable of crossing the pore of the membrane constitutes the "permeate", while the fraction not crossing the membrane is the "retentate" or "concentrate" fraction (Cheryan, 1998).

In pressure-driven membrane processes there are two different ways to operate: "dead-end" or perpendicular mode and "cross-flow" or tangential mode (**Figure I.9**). In "dead-end" mode, total volume of feed is pumped perpendicularly through the membrane and only the fraction passing through the pore of the membrane is collected at the end of the filtration process and called as permeate fraction. Therefore, insoluble and larger components will accumulate on the membrane, forming a bio-gel layer (Ambrosi et al., 2014). On the other hand, in tangential or "cross-flow" mode, feed is tangentially pumped over the surface of the membrane and there is one stream getting into and two streams leaving the module, the retentate and the permeate fraction (Cheryan, 1998). Therefore, solids remain in suspension in the recirculating feed stream resulting in less gel layer formation and less resistance on the membrane with higher permeate flux (Ambrosi et al., 2014).

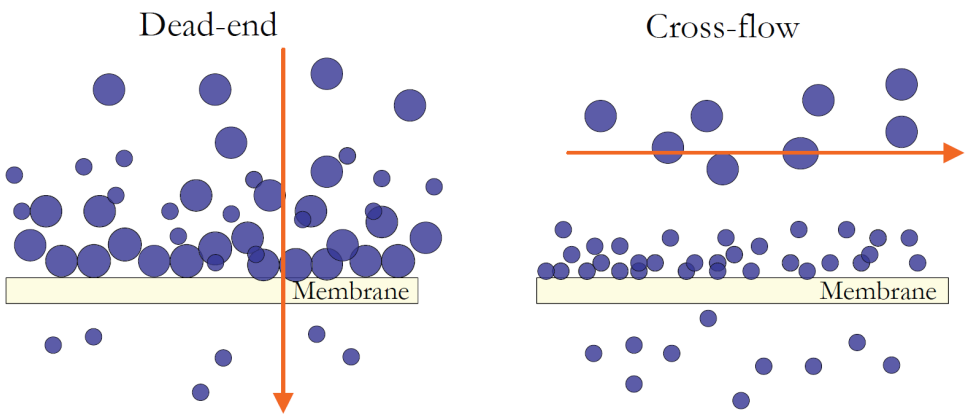

Figure I.9. Typical operational modes in ultrafiltration membrane processes (Ruiz-García et al., 2017).

5.3. Important operation parameters in ultrafiltration processes

Among the different parameters affecting the separation membrane process, the following stand out:

5.3.1. Transmembrane pressure (TMP)

TMP is the major driven-force for the pressure-driven filtration processes, defined as the difference between the pressure at the feed inlet and the pressure at the outlet of the permeate (Kresnowati et al., 2017). The higher TMP, the higher permeate flux (Audinos & Branger, 1992), although greater fouling rate is also found because of layer gel formation at high pressures (Cheryan, 1998).

5.3.2. Feed flow rate

As mentioned above, tangential or cross-flow mode is more suitable than perpendicular feed supply due to its lower fouling tendency. Moreover, in cross-flow mode, by increasing feed flow rate, greater and improved molecules circulation is reached because of higher tangential velocity, resulting in a decrease in the thickness of the gel layer (Takaç et al., 2000).

5.3.3. Feed compounds concentration

More concentrated feed stream results in lower permeate flux because of greater membrane fouling (Audinos & Branger, 1992). Increasing feed concentration results in continuous reduction in permeate flux owing to concentration polarization phenomenon (Takaç et al., 2000).

5.3.4. Membrane pore size

As mentioned in previous sections, selectivity of pressure-driven membrane separation is determined by its pore size. Because of that, it is common to find the membranes classified according to its pore size, although for UF membranes is more common to talk about "molecular weight cut-off" (MWCO) (Cheryan, 1998).

The greater the membrane pore size, the lower the retention rate owing to a greater number of components permeating through the membrane (**Figure I.10**) (Timmer et al., 1998).

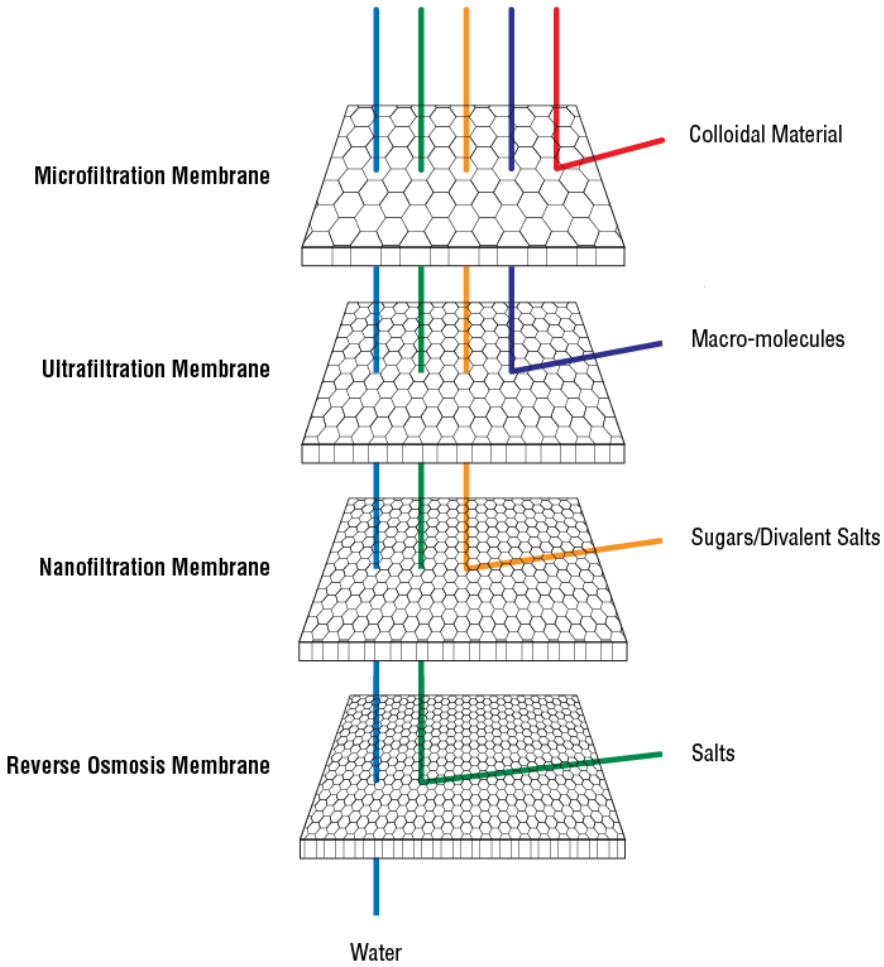

Figure I.10. Separation of different compounds by pressure-driven membrane processes. Retrieved from (https://membranespecialists.com/)

5.3.5. Membrane material

Membranes can be made of polymers such as cellulose, polyamide, nylon, polypropylene, polycarbonate and so on, or use inorganic materials for its manufacture. In the last case, membranes are called as “ceramic” or “mineral” membranes, and they can be flat or tubular as a single channel or multichannel (**Figure I.11**). Since ceramic membranes are made of inorganic materials, they are very versatile and have numerous advantages over polymeric membranes such as wide temperature and pH limits or extended operating lifetimes. Moreover, they are inert to chemicals and solvents (Cheryan, 1998).

Figure I.11. Different examples of tubular mono- and multichannel ceramic membranes. Obtained from (https://ceramics.org/)

References

Akhtar, J., Aishah, N., & Amin, S. (2011). A review on process conditions for optimum bio-oil yield in hydrothermal liquefaction of biomass. *Renewable and Sustainable Energy Reviews*, *15*, 1615–1624.

Akiya, N., & Savage, P. E. (2002). Roles of water for chemical reactions in high-temperature water. *Chemical Reviews*, *102*(8), 2725–2750.

Alba, L. G., Torri, C., Samorì, C., Spek, J. Van Der, Fabbri, D., Kersten, S. R. A., & Brilman, D. W. F. W. (2012). Hydrothermal Treatment (HTT) of Microalgae: Evaluation of the Process as Conversion Method in an Algae Biorefinery Concept. *Energy & Fuels*, *26*, 642–657.

Alonso-Riaño, P., Sanz, M. T., Benito-Román, O., Beltrán, S., & Trigueros, E. (2021). Subcritical water as hydrolytic medium to recover and fractionate the protein fraction and phenolic compounds from craft brewer's spent grain. *Food Chemistry*, *351*, 129264.

Ambrosi, A., Sérgio, N., Cardozo, M., & Tessaro, I. C. (2014). Membrane Separation Processes for the Beer Industry: A Review and State of Membrane Separation Processes for the Beer Industry: a Review and State of the Art. *Bioprocess Technology*, *7*, 921–936.

Anastasakis, K., & Ross, A. B. (2011). Hydrothermal liquefaction of the brown macro-alga *Laminaria Saccharina*: Effect of reaction conditions on product distribution and composition. *Bioresource Technology*, *102*, 4876–4883.

Anekpankul, T., Goto, M., & Sasaki, M. (2007). Extraction of anti-cancer damnacanthal from roots of Morinda citrifolia by subcritical water. *Separation and Purification Technology*, *55*, 343–349.

Anto, S., Sankha, S., Muthappa, R., Mathimani, T., Deviram, G., Kumar, S. S., Nath, T., & Pugazhendhi, A. (2020). Algae as green energy reserve: Technological outlook on biofuel production. *Chemosphere*, *242*.

Araki. (1956). Structure of the Agarose Constituent of Agar-agar. *Bulletin of the Chemical Society of Japan*, *29*(4), 543.

Audinos, R., & Branger, J. L. (1992). Ultrafiltration concentration of enzyme hydrolysates. *Journal of Membrane Science*, *68*, 195–204.

Benito-Román, O., Blanco, B., Sanz, M., & Beltran, S. (2020). Subcritical Water Extraction of Phenolic Compounds from Onion Skin Wastes (*Allium cepa cv. Horcal*): Effect of Temperature and Solvent Properties. *Antioxidants*, *9*.

Bitog, J. P., Lee, I., Lee, C., Kim, K., Hwang, H., Hong, S., Seo, I., Kwon, K., & Mostafa, E. (2011). Application of computational fluid dynamics for modelling and designing photobioreactors for microalgae production: A review. *Computers and Electronics in Agriculture*, *76*, 131–147.

Blikra, E., Romeo, D., & Thomsen, M. (2018). Biowaste valorisation in a future circular bioeconomy. *Procedia CIRP Engineering (LCE) Conference 2018*, *69*, 591–596.

Borja, A. (1987). *El alga "Gelidium" en la costa guipuzcoana*. Servicio de Gestión oceanográfica Gobierno Vasco.

Boulila, A., Hassen, I., Haouari, L., Mejri, F., Amor, I.B., Casabianca, H., & Hosni, K. (2015). Enzyme-assisted extraction of bioactive compounds from bay leaves (*Laurus nobilis L*). *Industrial Crops and Products*, *74*, 485–493.

Brand, S., Hardi, F., Kim, J., & Jin, D. (2014). Effect of heating rate on biomass liquefaction: Differences between subcritical water and supercritical ethanol. *Energy*, *68*, 420–427.

Budrat, P., & Shotipruk, A. (2009). Enhanced recovery of phenolic compounds from bitter melon (*Momordica charantia*) by subcritical water extraction. *Separation and Purification Technology*, *66*, 125–129.

Cabeza, A., Piqueras, C. M., Sobrón, F., & García-serna, J. (2016). Modeling of biomass fractionation in a lab-scale biorefinery: Solubilization of hemicellulose and cellulose from holm oak wood using subcritical water. *Bioresource Technology*, *200*, 90–102.

Carmona, R., Vergara, J. J., Lahaye, M., & Niell, F. X. (1998). Light quality affects morphology and polysaccharide yield and composition of Gelidium sesquipedale (Rhodophyceae). *Journal of Applied Phycology*, *10*, 323–331.

Carr, A. G., Mammucari, R., & Foster, N. R. (2011). A review of subcritical water as a solvent and its utilisation for the processing of hydrophobic organic compounds. *Chemical Engineering Journal*, *172*(1), 1–17.

Chandra, R., Jacob, S., & Soo, B. (2020). A holistic zero waste biorefinery approach for macroalgal biomass utilization: A review. *Science of the Total Environment*, *716*, 137067.

Chemat, F., Vian, M. A., & Cravotto, G. (2012). Green Extraction of Natural Products: Concept and Principles. *International Journal of Molecular Sciences*, *13*, 8615–8627.

Chen, W., Zhang, Y., Zhang, J., Yu, G., Schideman, L. C., Zhang, P., & Minarick, M. (2014). Hydrothermal liquefaction of mixed-culture algal biomass from wastewater treatment system into bio-crude oil. *Bioresource Technology*, *152*, 130–139.

Cheryan, M. (1998). *Ultrafiltration and microfiltration handbook* (B. Raton (Ed.); Second). Technomic Pub.

Chienthavorn, O., Pengpumkiat, S., Noomhorm, A., & Smith, R. M. (2007). Superheated water extraction and phase transfer methylation of phenoxy acid herbicides from solid matrices. *Journal of Chemical Technology and Biotechnology*, *1152*, 268–273.

Cissé, M., Vaillant, F., Bouquet, S., Pallet, D., Lutin, F., Reynes, M., & Dornier, M. (2011). Athermal concentration by osmotic evaporation of roselle extract, apple and grape juices and impact on quality. *Innovative Food Science and Emerging Technologies*, *12*, 352–360.

Cocero, M. J., Cabeza, Á., Abad, N., Adamovic, T., Vaquerizo, L., Martínez, C. M., & Pazo-cepeda, M. V. (2018). Understanding biomass fractionation in subcritical & supercritical water. *The Journal of Supercritical Fluids*, *133*, 550–565.

Cooper, G.M. (2000) The Cell: A Molecular Approach. 2nd Edition, Sunderland (MA): Sinauer Associates, The Development and Causes of Cancer.

Delattre, C., Fenoradosoa, T. A., & Michaud, P. (2011). Galactans: An Overview of their Most Important Sourcing and Applications as Natural Polysaccharides. *Brazilian Archives of Biology and Technology*, *54*(6), 1075–1092.

Duckworth, M., & Yaphe, W. (1971). The structure of agar. *Carbohydrate Research*, *16*, 189–197.

Elmekawy, A., Diels, L., Wever, H. De, & Pant, D. (2013). Valorization of Cereal Based Biorefinery Byproducts: Reality and Expectations. *Environmental Science & Technology*, *47*, 9014–9027.

Ennouali, M., Ouhssine, M., Ouhssine, K., & Elyachioui, M. (2006). Biotransformation of algal waste by biological fermentation. *African Journal of Biotechnology*, 5(13), 1233–1237.

Fasahati, P., Woo, H. C., & Liu, J. J. (2015). Industrial-scale bioethanol production from brown algae: Effects of pretreatment processes on plant economics. *Applied Energy*, *139*, 175–187.

Fernández, C. (1991). Biological and economic importance of the genus Gelidium in Spain. *Informes Técnicos de Scientia Marina*, *163*, 1–20.

Fernández-ponce, M. T., Casas, L., Mantell, C., Rodríguez, M., Martínez, E., & Ossa, D. (2012). Extraction of antioxidant compounds from different varieties of Mangifera indica leaves using green technologies. *The Journal of Supercritical Fluids*, *72*, 168–175.

Ferrera-Lorenzo, N., Fuente, E., Bermúdez, J. M., & Ruiz, B. (2014). Conventional and microwave pyrolysis of a macroalgae waste from the Agar – Agar industry. Prospects for bio-fuel production. *Bioresource Technology*, *151*, 199–206.

Gai, C., Li, Y., Peng, N., Fan, A., & Liu, Z. (2015). Co-liquefaction of microalgae and lignocellulosic biomass in subcritical water. *Bioresource Technology*, *185*, 240–245.

Gámiz-Gracia, L., & Castro, M. D. L. De. (2000). Continuous subcritical water extraction of medicinal plant essential oil: comparison with conventional techniques. *Talanta*, *51*, 1179–1185.

Gbashi, S., Njobeh, P., Steenkamp, P., Tutu, H., & Madala, N. (2016). The effect of temperature and methanol – water mixture on pressurized hot water extraction (PHWE) of anti-HIV analogoues from Bidens pilosa. *Chemistry Central Journal*, 1–12.

Gligor, O., Mocan, A., Moldovan, C., Locatelli, M., Crișan, G., & Ferreira, I. C. F. R. (2019). Enzyme-assisted extractions of polyphenols – A comprehensive review. *Trends in Food Science & Technology*, *88*, 302–315.

González-Delgado, A., & Kafarov, V. (2011). BIOREFINERY: ISSUES. *Journal Ciencia, Tecnología y Futuro*, 4, 5–22.

Greiserman, S., Epstein, M., Chemodanov, A., Steinbruch, E., Prabhu, M., Guttman, L., Jinjikhashvily, G., Shamis, O., Gozin, M., Kribus, A., & Golberg, A. (2019). Co-production of Monosaccharides and Hydrochar from Green Macroalgae *Ulva* (Chlorophyta) sp. with Subcritical Hydrolysis and Carbonization. *BioEnergy Research*, *12*, 1090–1103.

Grosso, C., Ferreres, F., National, S., & Andrade, P. (2015). Alternative and Efficient Extraction Methods for Marine-Derived Compounds. *Marine Drugs*, *13*, 3182–3230.

Guerrero, P., Etxabide, A., Leceta, I., Peñalba, M., & de la Caba, K. (2014). Extraction of agar from Gelidium sesquipedale (Rodhopyta) and surface characterization of agar based films. *Carbohydrate Polymers*, 99, 491–498.

Habeebullah, S. F. K., Alagarsamy, S., Sattari, Z., & Al-haddad, S. (2020). Enzyme-assisted extraction of bioactive compounds from brown seaweeds and characterization. *Journal of Applied Phycology*, *32*, 615–629.

Haghighi, A., & Khajenoori, M. (2013). Subcritical Water Extraction. In Mass Transfer - Advances in Sustainable Energy and Environment Oriented Numerical Modeling (pp. 460–487).

Hardouin, K., Burlot, A. S., Umami, A., Tanniou, A., Stiger-Pouvreau, V., Widowati, I., Bedoux, G., & Bourgougnon, N. (2014). Biochemical and antiviral activities of enzymatic hydrolysates from different invasive French seaweeds. *Journal of Applied Phycology*, *26*, 1029–1042.

Hashimoto, S. (2004). Remediation of soil contaminated with dioxins by subcritical water extraction. *Chemosphere*, *54*, 89–96.

Herrero, M., Cifuentes, A., & Iban, E. (2006). Sub- and supercritical fluid extraction of functional ingredients from different natural sources: Plants, food-by-products, algae and microalgae A review. *Food Chemistry*, *98*, 136–148.

Herrero, M., Sánchez-Camargo, A. P., Cifuentes, A., & Ibáñez, E. (2015). Plants, seaweeds, microalgae and food by-products as natural sources of functional ingredients obtained using pressurized liquid extraction and supercritical fluid extraction. *Trends in Analytical Chemistry*, *71*, 26–38.

Hong, I. K., Jeon, H., & Lee, S. B. (2014). Comparison of red, brown and green seaweeds on enzymatic saccharification process. *Journal of Industrial and Engineering Chemistry*, *20*(5), 2687–2691.

Jansen, B., Kubatova, A., & Hawthorne, S. B. (2002). Thermodynamic and kinetic models for the extraction of essential oil from savory and polycyclic aromatic hydrocarbons from soil with hot (subcritical) water and supercritical CO2. *Journal of Chemical Technology and Biotechnology*, *975*, 175–188.

Jin, B., Duan, P., Xu, Y., Wang, F., & Fan, Y. (2013). Co-liquefaction of micro- and macroalgae in subcritical water. *Bioresource Technology*, *149*, 103–110.

Ju, E., Taek, H., Mun, K., Yu, S., Kim, S., Choi, I., & Heon, K. (2016). Pretreatment and saccharification of red macroalgae to produce fermentable sugars. *Bioresource Technology*, *199*, 311–318.

Jung, K. A., Lim, S., Kim, Y., & Moon, J. (2013). Potentials of macroalgae as feedstocks for biorefinery. *Bioresource Technology*, *135*, 182–190.

Kadam, S. U., & Tiwari, B. K. (2013). Application of Novel Extraction Technologies for Bioactives from Marine Algae. *Journal of Agricultural and Food Chemistry*, *61*, 4667–4675.

Karagoz, S., Bhaskar, T., Muto, A., Sakata, Y., & A, U. (2004). Low-Temperature Hydrothermal Treatment of Biomass: Effect of Reaction Parameters on Products and Boiling. Energy & Fuels, 18, 234–241.

Knez, Z., Markocic, E., Knez-Hrncic, M., Ravber, M., Skerget, M. (2015). High pressure water reforming of biomass for energy and chemicals: A short review. *The Journal of Supercritical Fluids*, *96*, 46–52.

Knutsen, S. H. (1994). A Modified System of Nomenclature for Red Algal Galactans. *Botanica Marina*, 37, 163–169.

Kresnowati, M. T. A. P., Desiriani, R., & Wenten, I. G. (2017). AIP Conference Proceedings. *Ultrafiltration of Hemicellulose Hydrolysate Fermentation Broth*, *1818*, *020024*.

Liang, X., & Fan, Q. (2013). Application of Sub-Critical Water Extraction in Pharmaceutical Industry. *Journal of Materials Science and Chemical Engineering*, *2013*, 1–6.

Martínez-abad, A., Giummarella, N., Vilaplana, F., & Lawoko, M. (2018). Differences in extractability under subcritical water reveal interconnected hemicellulose and lignin recalcitrance in birch hardwoods. *Green Chemistry*, *20*, 2534–2546.

Mata, T. M., Martins, A., & Caetano, N. S. (2010). Microalgae for biodiesel production and other applications: A review. *Renewable and Sustainable Energy Reviews*, 14, 217–232.

Méndez, A., Gascó, G., Ruiz, B., & Fuente, E. (2019). Hydrochars from industrial macroalgae "*Gelidium Sesquipedale*" biomass wastes. *Bioresource Technology*, *275*, 386–393.

Morales-Muñoz, S., Luque-García, J.L., & Luque de Castro, M.D. (2002). Pressurized Hot Water Extraction with On-Line Fluorescence Monitoring: a Comparison of the Static, Dynamic, and Static - Dynamic Modes for the Removal of Polycyclic Aromatic Hydrocarbons from Environmental Solid Samples. *Analytical Chemistry*, 74, 4213–4219.

Mouradi-givernaud, A., Hassani, L. A., Givernaud, T., & Lemoine, Y. (1999). Biology and agar composition of Gelidium sesquipedale harvested along the Atlantic coast of Morocco. *Hydrobiologia*, *398/399*, 391–392.

Muniglia, L., Claisse, N., Baudelet, P.-H., & Ricochon, G. (2014). Enzymatic Aqueous Extraction (EAE). In Alternative solvents for natural products extraction (pp. 167–204).

Murano, E. (1995). Chemical structure and quality of agars from *Gracilaria*. *Journal of Applied Phycology*, *7*, 245–254.

Nadar, S. S., Rao, P., & Rathod, V. K. (2018). Enzyme assisted extraction of biomolecules as an approach to novel extraction technology: A review. *Food Research International*, *108*, 309–330.

Ozel, M. Z., Gogus, F., & Lewis, A. C. (2003). Subcritical water extraction of essential oils from Thymbra spicata. *Food Chemistry*, *82*, 381–386.

Panja, P. (2017). Green extraction methods of food polyphenols from vegetable materials. *Food Science*, *17*, 173–182.

Park, J., Hong, J., Chul, H., Geun, S., Kim, S., Yoon, J., & Jin, Y. (2012). Use of *Gelidium amansii* as a promising resource for bioethanol: A practical approach for continuous dilute-acid hydrolysis and fermentation. *Bioresource Technology*, *108*, 83–88.

Park, J., Yoon, J., Park, H., Jin, Y., Jung, D., & Kim, S. (2011). Feasibility of biohydrogen production from Gelidium amansii. *International Journal of Hydrogen Energy*, *36*, 13997–14003.

Park, J., Jeong, Y., & Chun, B. (2019). Physiological activities and bioactive compound from laver (*Pyropia yezoensis*) hydrolysates by using subcritical water hydrolysis. *The Journal of Supercritical Fluids*, *148*, 130–136.

Peterson, A. A., Vogel, F., Lachance, R. P., Fröling, M., Antal, M. J., & Tester, J. W. (2008). Thermochemical biofuel production in hydrothermal media: A review of sub- and supercritical water technologies. *Energy & Environmental Science*, 32–65.

Peterson, M. E., Daniel, R. M., Danson, M. J., & Eisenthal, R. (2007). The dependence of enzyme activity on temperature: determination and validation of parameters. *Biochemical Journal*, *402*, 331–337.

Phusunti, N., Phetwarotai, W., & Tirapanampai, C. (2017). Subcritical Water Hydrolysis of Microalgal Biomass for Protein and Pyrolytic Bio-oil Recovery. *BioEnergy Research*, *10*, 1005–1017.

Plaza, M., Amigo-benavent, M., María, D., Ibáñez, E., & Herrero, M. (2010). Neoformation of antioxidants in glycation model systems treated under subcritical water extraction conditions. *Food Research International*, *43*(4), 1123–1129.

Plaza, M., Santoyo, S., Jaime, L., Avalo, B., Cifuentes, A., Reglero, G., Reina, G. G., Javier, F., & Ibáñez, E. (2012). Comprehensive characterization of the functional activities of pressurized liquid and ultrasound-assisted extracts from Chlorella vulgaris. *LWT - Food Science and Technology*, *46*(1), 245–253.

Porse, H., & Rudolph, B. (2017). The seaweed hydrocolloid industry: 2016 updates, requirements, and outlook. *Journal of Applied Phycology*, *29*(5), 2187–2200.

Priego-López, E., & Castro, M. D. L. De. (2004). Superheated water extraction of linear alquilbenzene sulfonates from sediments with on-line preconcentration / derivatization / detection. *Analytica Chimica Acta*, *511*, 249–254.

Puri, M., Sharma, D., & Barrow, C. J. (2012). Enzyme-assisted extraction of bioactives from plants. *Trends in Biotechnology*, *30*, 37–44.

Richter, P., & Sepulveda, B. (2003). Screening and determination of pesticides in soil using continuous subcritical water extraction and gas chromatography – mass spectrometry. *Journal of Chromatography A*, *994*, 169–177.

Rodil, R., & Popp, P. (2006). Development of pressurized subcritical water extraction combined with stir bar sorptive extraction for the analysis of organochlorine pesticides and chlorobenzenes in soils. *Journal of Chromatography A*, *1124*, 82–90.

Ruiz-García, A., Melián-Martes, N., & Nuez, I. (2017). Short Review on Predicting Fouling in RO Desalination. *Membranes*, 1–17.

Saidi, S., Deratani, A., Belleville, M., & Ben, R. (2014). Production and fractionation of tuna by-product protein hydrolysate by ultrafiltration and nanofiltration: Impact on interesting peptides fractions and nutritional properties. *Food Research International*, *65*, 453–461.

Sheldon, R. A., & Pelt, S. van. (2013). Enzyme immobilisation in biocatalysis: why, what and how. *Chemical Society Reviews*, 42, 6223–6235.

Sowbhagya, H. B., Srinivas, P., & Krishnamurthy, N. (2010). Effect of enzymes on extraction of volatiles from celery seeds. *Food Chemistry*, *120*, 230–234.

Suganya, T., Varman, M., Masjuki, H. H., & Renganathan, S. (2016). Macroalgae and microalgae as a potential source for commercial applications along with biofuels production: A biorefinery approach. *Renewable and Sustainable Energy Reviews*, *55*, 909–941.

Tajuddin, R., & Smith, R. M. (2005). On-line coupled extraction and separation using superheated water for the analysis of triazine herbicides in spiked compost samples. *Journal of Chromatography A*, *1084*, 194–200.

Takaç, S., Elmas, S., Çalik, P., Özdamar, T H. (2000). Separation of the protease enzymes of Bacillus licheniformis from the fermentation medium by crossflow ultrafiltration. *Journal of Chemical Technology and Biotechnology*, *75*, 491–499.

Thiruvenkadam, S., Izhar, S., Yoshida, H., Danquah, M. K., & Harun, R. (2015). Process application of Subcritical Water Extraction (SWE) for algal bio-products and biofuels production. *Applied Energy*, *154*, 815–828.

Timmer, J.M.K., Speelmans, M.P.J., van der Horst, H.C. (1998). Separation of amino acids by nanofiltration and ultrafiltration membranes. *Separation and Purification Technology*, *14*, 133–144.

Torres, M., Niell, F. X., & Algarra, P. (1991). Photosynthesis of Gelidium sesquipedale: effects of temperature and light on pigment concentration, C/N ratio and cell-wall polysaccharides. *International Workshop on Gelidium*, *221*(1), 77–82.

Torres, M., Flórez-Fernández, N., & Domínguez, H. (2019). Integral Utilization of Red Seaweed for Bioactive Production. *Marine Drugs*, 17, 314.

Tuma, S., Izaguirre, J. K., Bondar, M., Marques, M. M., Fernandes, P., Fonseca, M. M. R., & Cesário, M. T. (2020). Upgrading end-of-line residues of the red seaweed Gelidium sesquipedale to polyhydroxyalkanoates using Halomonas boliviensis. *Biotechnology Reports*, *27*(27).

Valdez, P. J., Nelson, M. C., Wang, H. Y., Lin, X. N., & Savage, P. E. (2012). Hydrothermal liquefaction of *Nannochloropsis sp*.: Systematic study of process variables and analysis of the product fractions. *Biomass and Bioenergy*, *46*, 317–331.

Wataniyakul, P., Pavasant, P., Goto, M., & Shotipruk, A. (2012). Microwave pretreatment of defatted rice bran for enhanced recovery of total phenolic compounds extracted by subcritical water. *Bioresource Technology*, *124*, 18–22.

Wijesinghe, W. A. J. P., & Jeon, Y. J. (2012). Enzyme-assistant extraction (EAE) of bioactive components: A useful approach for recovery of industrially important metabolites from seaweeds: A review. *Fitoterapia*, *83*, 6–12.

Yu, X., Bogaert, L., Hu, R., Bals, O., Grimi, N., & Vorobiev, E. (2016). A combined coagulation – ultrafiltration method for enhanced separation of proteins and polyphenols. *Separation Science and Technology*, *51:6*, 1030–1041.

Zakaria, S. M., & Mustapa Kamal, S. M. (2016). Subcritical Water Extraction of Bioactive Compounds from Plants and Algae: Applications in Pharmaceutical and Food Ingredients. *Food Engineering Reviews*, 23–34.

Zhong, C., & Wei, X. (2004). A comparative experimental study on the liquefaction of wood. *Energy*, *29*, 1731–1741.

OBJECTIVES

OBJECTIVES

The main objective of this PhD Thesis is to study the complete valorization of alga by-product after industrial agar extraction through a biorefinery concept by using subcritical water extraction/hydrolysis as a green technology.

Along the different chapters, several parameters during subcritical water extraction/hydrolysis are studied in order to determine the optimal process conditions for bioactive compounds recovery, as well as other technologies for comparison.

Firstly, subcritical water technology was studied from alga solid residue after agar extraction. Chapters 1-3 evaluate its effect on bioactive compounds extraction/hydrolysis by studying different process parameters and operational modes:

Chapter 1: "*Recovery of the protein fraction with high antioxidant activity from red seaweed industrial solid residue after agar extraction by subcritical water treatment*": The effect of subcritical water technology on bioactive compounds recovery from alga by-product was evaluated. Moreover, the study of different SWE parameters was carried out in a semicontinuous mode.

Chapter 2: "*Effect of heating rate and residence time on subcritical water macroalgae residue hydrolysis*": The effect of heating mode, reactor size and residence time during SWE was studied on the hydrolysis and degradation rate of the components from the alga solid residue.

Chapter 3: "*Subcritical water extraction scale-up from laboratory to pilot system for red alga residue after agar extraction valorization*": The feasibility of industrial-scale subcritical water system through scaling-up from laboratory to pilot system was studied in discontinuous mode.

Secondly, enzyme assisted extraction technology from alga solid residue was evaluated for comparison with subcritical water treatment.

Chapter 4: "*Enzymatic hydrolysis of the industrial solid residue of red seaweed after agar extraction: Extracts characterization and modelling*": To compare SWE with other technologies, enzymatic assisted extraction from alga residue after agar extraction was carried out. Different operational parameters were evaluated to determine optimal conditions. Finally, kinetic parameters were evaluated and modelling of the extraction curves was carried out.

Finally, membrane technology was proposed for bioactive compounds fractionation and concentration of subcritical water extracts.

Chapter 5: "*Fractionation of bioactive compounds from a red alga subcritical water extract by ultrafiltration*": The viability of membrane technology for bioactive compounds fractionation from subcritical water extracts was evaluated. Different operational parameters were studied for filtration process optimization and used for carbohydrates and proteins fractionation.

RESULTS

RESULTS

The more outstanding results of this PhD Thesis are presented as different chapters which correspond to the scientific publications detailed below. A brief summary in Spanish language of each publication is included at the beginning of each chapter.

Chapter 1: Recovery of the protein fraction with high antioxidant activity from red seaweed industrial solid residue after agar extraction by subcritical water treatment.

Chapter 2: Effect of heating rate and residence time on subcritical water macroalgae residue hydrolysis.

Chapter 3: Subcritical water extraction scale-up from laboratory to pilot system for red alga residue after agar extraction valorization.

Chapter 4: Enzymatic hydrolysis of the industrial solid residue of red seaweed after agar extraction: Extracts characterization and modelling.

Chapter 5: Fractionation of bioactive compounds from a red alga subcritical water extract by ultrafiltration.

CHAPTER 1

Recovery of the protein fraction with high antioxidant activity from red seaweed industrial solid residue after agar extraction by subcritical water treatment

Based on the article:

Trigueros E., Sanz M.T., Alonso-Riaño P., Beltrán S., Ramos C., Melgosa R. (2021). "Recovery of the protein fraction with high antioxidant activity from red seaweed industrial solid residue after agar extraction by subcritical water treatment". *Journal of Applied Phycology*

DOI: https://doi.org/10.1007/s10811-020-02349-0

Capítulo 1

Recuperación de la fracción proteica con alta actividad antioxidante a partir del residuo industrial del alga roja tras la extracción del agar mediante tratamiento con agua subcrítica

Resumen

En este trabajo se ha estudiado la valorización del residuo sólido industrial generado tras la extracción del agar de *Gelidium sesquipedale* mediante el uso de agua subcrítica en un reactor semicontinuo de lecho fijo. Primero, se realizó una caracterización completa del subproducto, determinando hasta 21% (p/p) de contenido de proteína (con un factor de nitrógeno de 4.9) con alto contenido de aminoácidos esenciales, 37% (p/p) de carbohidratos y alta cantidad de cenizas, 22% (p/p). Se estudió el efecto de la temperatura, en el rango de 129 a 200°C, y velocidad de flujo, en el rango de 2 a 6 mL/min, sobre la extracción/hidrólisis de la fracción de proteína y carbono. A caudal constante de 2 mL/min se alcanzó un máximo en la extracción de proteínas a 185°C. Temperaturas más altas condujeron a la degradación de las proteínas o a sus productos de hidrólisis. La liberación de aminoácidos libres siguió la misma tendencia. Los aminoácidos más termosensibles, determinados por cromatografía de gases (EZ: faast Phenomenex), fueron la serina y los ácidos aspártico y glutámico. Como consecuencia, la selectividad hacia los aminoácidos no polares aumentó al trabajar con factores de severidad altos. Se estableció una correlación de Pearson entre la capacidad antioxidante de los extractos recolectados con los compuestos bioactivos determinados (compuestos polifenólicos totales –TPC-, péptidos y aminoácidos libres), siendo más fuerte para TPC. El contenido de cenizas en el residuo sólido después del tratamiento aumentó constantemente con la temperatura debido a su no solubilización, siendo posible su aplicación en agricultura como fertilizante.

Palabras clave: extracción con agua subcrítica, biorrefinería, residuo macroalga, proteína, aminoácidos, actividad antioxidante.

Abstract

In this work, valorization of the underexploited industrial solid residue generated after agar extraction from *Gelidium sesquipedale* was studied by using subcritical water in a semicontinuous fix-bed reactor. First, a complete characterization of this by-product was carried out, determining up to 21 % (w/w) of protein content (for a nitrogen factor of 4.9) with high content of essential amino acids, 37 % (w/w) of carbohydrate fraction and high amount of ash, 22 % (w/w). The effect of temperature, in the range from 129 to 200 °C, and flow rate, in the range from 2 to 6 mL/min, on protein and carbon fraction extraction/hydrolysis was studied. At constant flow rate of 2 mL/min a maximum in the protein extraction was achieved at 185 °C. Higher temperatures led to degradation of protein or its hydrolysis products. Free amino acids release followed the same trend as the protein fraction. The most temperature sensitive amino acids, as determined by gas chromatography (EZ:faast *Phenomenex*), were serine and aspartic and glutamic acids. As a consequence, the selectivity towards non-polar amino acids increased by working at high severity factors. A Pearson correlation between antioxidant capacity of the collected extracts with the bioactive compounds determined in the extracts (total polyphenolic compounds –TPC-, peptides and free amino acids) was established, being stronger for TPC. The ash content in the solid residue after treatment steadily increased with temperature due to non-solubilization being possible its application in agriculture as fertilizers.

Keywords: subcritical water extraction, biorefinery, macroalgae residue, protein, amino acids, antioxidant activity.

1. Introduction

The industrial importance of phycocolloids from marine macroalgae is well known for food and cosmetic industries. Agar is a hydrocolloid that is dissolved in hot water and forms gels when it is cooled. Worldwide, agar production exceeds 14,500 t annually with a sale value of 246 million US$ (Porse & Rudolph, 2017). *Gelidium* (Rhodophyta Gelidiaceae) is a red alga mainly found in the Atlantic coasts of France, Spain, Portugal and Morocco and it is the major seaweed resource in the Spanish agar industry, providing a high quality agar.

The industrial process to produce agar generates a solid residue that is used for fodder and fertilizer although most of it is disposed of (Ferrera-Lorenzo et al., 2014a). However, this by-product still contains valuable compounds that can be recovered reducing the environmental impact by incorporating this by-product within a circular economy concept.

In the literature some studies can be found for macroalgae biomass valorisation (Bordoloi & Goosen, 2020; Gereniu et al., 2017; Meillisa et al., 2013; Pangestuti et al., 2019). However, only a few deal with macroalgal by-products valorization (Rajak et al., 2020). Regarding valorization of the solid waste generated in the industrial production of agar, previous studies have already been published by the Instituto Nacional del Carbon (CSIC) analysing the potential energetic uses of the product generated from the pyrolysis of this residual marine biomass and the potential as precursor of activated carbon (Ferrera-Lorenzo et al., 2014a,b).

In this work, a different approach has been considered to valorize this solid waste biomass, based on the use of subcritical water (subW) to hydrolyze and fractionate the different biomass compounds, mainly the protein fraction. subW treatment is a green technology that uses water as solvent at temperatures above its boiling point, 100 °C, and below its critical point, 374 °C, and pressure high enough to keep water at its liquid state. Water has unique properties with temperature. An increase in temperature leads to a decrease in the dielectric constant, increasing solubility of organic compounds in water. Due to the breaking of hydrogen-bonds with temperature, at these conditions, water presents low viscosity and high diffusivity that facilitate water to diffuse into the matrix. Furthermore, concentrations

of H^+ and OH^- ions are higher than in its ambient liquid state. Thus, it provides an effective medium for acid- and base-catalyzed reactions (Akiya & Savage, 2002).

Biomass can be hydrolyzed and fractionated into high value components such as amino acids, proteins, polysaccharides and other bioactive compounds. In this regard, it has been reported that among the three types of macroalgae, the red algae have the highest protein content containing, in general, all essential amino acids (Postma et al., 2018). The main goal of this work is to explore the subW treatment of *Gelidium sesquipedale* solid residue after agar extraction to valorize mainly its protein fraction and further obtain different bioproducts based on marine proteins, such as small bioactive peptides and free amino acids from the breakdown of the peptide bonds that could have potential applications in the field of the biotechnology, food and pharma industries. In this work, the effect of temperature and water flow rate in a semicontinuous fix-bed reactor on extraction and hydrolysis kinetics of proteins and free amino acids, as well as on the total organic fraction was determined. Furthermore, the antioxidant capacity and total polyphenol compounds released in the extracts were determined, as well as the composition of the solid residue after subW treatment that could be considered for further use.

2. Materials and methods

2.1. Raw material

The raw material used in this work has been kindly provided by Hispanagar (Burgos, Castilla y León, Spain, https://www.hispanagar.com/es). It consisted of the solid residue from *Gelidium sesquipedale* after agar extraction. This raw material was oven dried at 45 °C until constant weight to retard microbial growth, preserve the desirable quality and reduce storage volume. This final solid residue was called macroalgae residue (MR). The final moisture content of the MR was determined gravimetrically by weighing it before and after drying in an oven at 105 °C until constant weight, 5.0 ± 2.4 %. Sample moisture was used to express results per gram of dried MR (DMR).

2.2. Subcritical water equipment

subW treatment was carried in a laboratory scale semicontinuous apparatus (see **Figure 1.1**) equipped with a fixed-bed reactor (20.6 cm length and 2.8 cm internal diameter). Degassed distilled water at room temperature was pumped into the reactor through a HPLC pump (Gilson 305, head SC-10, 10 mL/min maximum flow) and was heated to the desired working temperature by circulating it through a heat exchanger (60 cm of 1/8" AISI 316 piping) placed inside an oven (Selecta T 204A) together with the fixed bed reactor where around 7 g of MR were placed. Two metallic filters were placed at the top and the bottom of the reactor to avoid loss of solid particles and clogging of the system. A back pressure regulator (Autoclave Engineers SWB2200) allowed pressure control. In this study, a constant pressure of 50 bar was fixed to keep water in its liquid state.

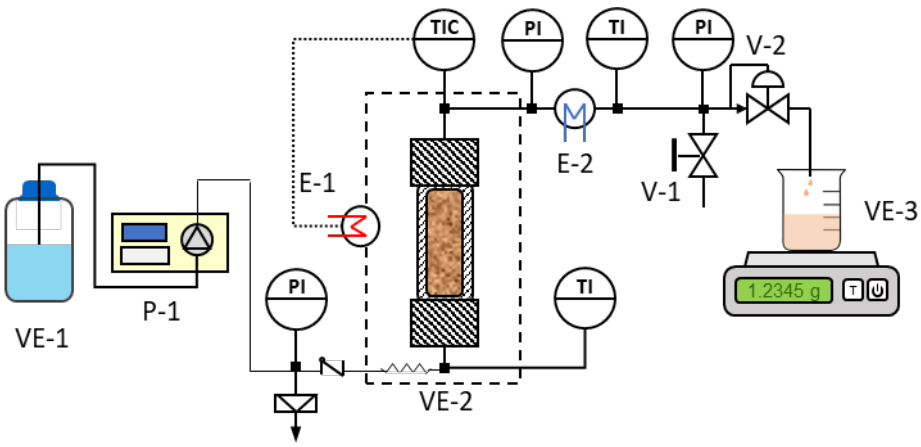

Figure 1.1. Diagram of the laboratory-scale pressurized water equipment. VE-1: solvent reservoir; P-1: Gilson 305 HPLC pump; VE-2: extractor; VE-3: collector; V-1: vent valve; (V-2) back-pressure valve.

subW treatment was carried out at different temperatures (T = 129, 142, 155, 171, 185 and 200 °C) and flow rates (F = 2 and 6 mL/min) for a total treatment time of 240 min. Before starting the extraction at the selected extraction temperature, the reactor was loaded with distilled water at room temperature. Temperature and pressure were steadily increased to the selected working conditions during a static holding time of 30 min, selected to improve

the DMR swelling and accessibility to water. Then the pump was turned on at the selected feed water flow selecting time 0 as the time at which liquid extract was obtained at the outlet pipe. Different liquid fractions were collected with time and stored at -18 °C until analysis.

The temperature profile from this zero time is presented in **Figure 1.2a**. In the experiments performed at low temperature, from 129 °C to 171 °C, it can be observed that 30 min of static holding time was enough to reach the working temperature; however, at the highest temperatures essayed in this work (185 and 200 °C), 30-40 min were still needed to reach the selected temperature. The temperature profile along heating is usually not reported in literature. For instance, Hata et al. (Hata et al., 2008) reported that 5 - 10 min were needed for a small vessel (9 mL) placed in an oven heating system, while it took 25 - 40 min for a 117 mL reactor when using a mantle heater to reach 260 -270 °C. The heating rate and time needed to reach the working temperature must be reported to compare the subW results. A Crison GLP 22 pH-meter was used to measure the pH of the subW extracts at the outlet vessel (**Figure 1.2b**).

2.3. Analysis

2.3.1. Biomass characterization

The chemical characterization of MR was performed according to the NREL protocols (https://www.nrel.gov/bioenergy/biomass-compositional-analysis.html). MR free of extractives was subjected to two acid hydrolysis steps. Carbohydrates were quantified by high-performance liquid chromatography (HPLC) with a Biorad Aminex-HPX-87 H column, a variable wavelength detector (VWD) and refractive index detector (RID) using a mobile phase constituted by 0.005 M sulphuric acid. Presence of galactose was confirmed by Megazyme L-Arabinose/D-Galactose assay kit. Total lipids were determined according to the Bligh and Dyer method (Bligh and Dyer 1959). Ash content was determined by placing the sample in a muffle furnace at 575 ± 25 °C for 24 ± 6 h until constant weight.

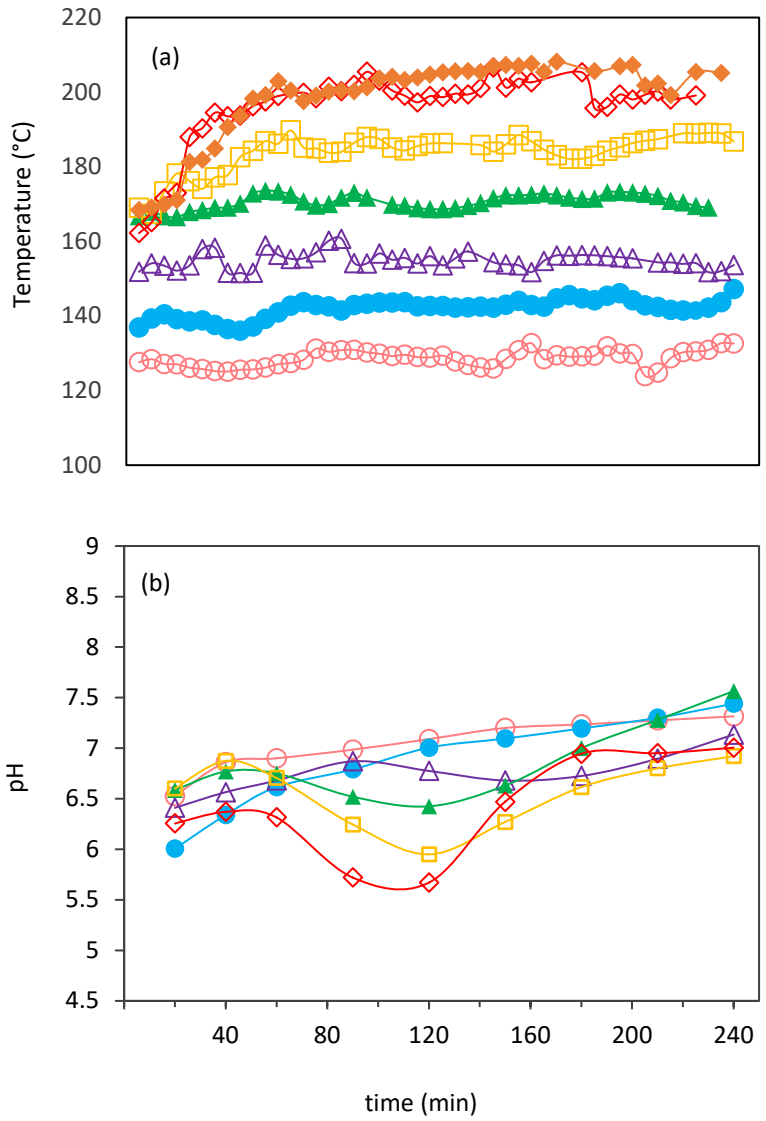

Figure 1.2 (a) Extraction temperature profile. **(b)** pH of the liquid extracts at the outlet pipe along treatment time at different working conditions (F = 2 mL/min: ○ 129 °C, ● 142 °C, △ 155 °C, ▲ 171 °C, □ 185 °C, ◇ 200 °C; F = 6 mL/min ◆ 200 °C). Continuous lines are guide for the eye.

2.3.1.1. Elemental and inorganic composition.

Elemental composition (C, H, N, S) of the MR was determined by an organic elemental microanalyzer (Thermo Scientific Model Flash 2000). Oxygen content was determined by mass balance. Inorganic composition of the MR was performed by inductively coupled plasma mass spectrometry (ICP-MS-Agilent 7500cx). Samples were digested with a HNO_3 solution (2 wt %) by using a microwave system. The digested samples were cooled and diluted with deionized water. Concentrations of inorganic elements were determined using standard solutions prepared in the same acid matrix.

2.3.1.2. Amino acid profile.

Protein content in the MR was obtained by the total nitrogen content as measured by the elemental analysis by using the corresponding nitrogen factor (NF). The NF was determined according to the amino acid profile of the MR determined after acid hydrolysis with 6 N HCl: 0.1-1.0 g of dried MR was weighed and 1 mL of HCl 6N was added. The mixture was incubated for 24 hours at 110 °C. Afterwards, 1 mL of a 1 N HCl and ethanol solution (1:1 v:v) was added and then filtered. It must be highlighted that during acid hydrolysis, asparagine and glutamine are quantitatively converted to aspartic and glutamic acid, respectively. Most amino acids can be determined by acid hydrolysis; however, tryptophan, cystine and cysteine were lost by acid hydrolysis, and methionine could be partially destroyed by acid hydrolysis. To quantify these amino acids, basic hydrolysis was carried out by mixing 0.1 g of MR with 7 mL of 4.2 M NaOH. The mixture was incubated at 110 °C for 24 hours, cooled and neutralized with 6M HCl in order to get a pH between 1.5 and 5.5. After hydrolysis, the amino acid profile was determined by using the EZ:faast *Phenomenex* procedure, consisting of a solid phase extraction followed by derivatization and a final liquid/liquid extraction. The resulting samples were analyzed by gas chromatography (Hewlett-Packard, 6890 series) with an EZ:faast AAA LC integrated column and FID detector. Norleucine was used as internal standard.

2.3.2. Characterization of liquid and solid products from subcritical water treatment

2.3.2.1. Liquid extract.

Protein content in the extracts was estimated by two different methods. A colorimetric assay based in a reaction similar to the Lowry assay by using the DC kit (Bio Rad Laboratories) and bovine serum albumin as standard. Protein determination was also carried out by total nitrogen content by using a TOC/TN analyzer (Shimadzu TOC-V CSN analyzer) using KNO_3 as standard and the corresponding nitrogen to protein conversion factor (NF).

The hydrolysis degree (DH), the percentage of hydrolyzed peptide bonds, was evaluated by the ninhydrin reaction method. Most amino acids react with ninhydrin but also primary and secondary amines. The measurement was carried out according to ninhydrin Sigma Aldrich protocol. Two milliliters of sample were gently mixed with 1 mL of ninhydrin reagent solution and placed into a boiling water bath for 10 min. Samples were cooled and 5 mL of 95 % ethanol were added. Absorbance was measured at 570 nm. A calibration curve was obtained by following the same protocol but substituting the 2.0 mL of sample by 2 mL of different standards of leucine solution that was prepared daily (Friedman, 2004). The DH was obtained as (Adler-Nissen et al., 1983):

$$DH\ (\%) = (h/h_{tot}) \cdot 100 \qquad [\mathbf{1.1}]$$

where h is the number of equivalent peptide bonds hydrolyzed, expressed as m_{eq}/g protein and h_{tot} is the total amount of millimol of individual amino acids per gram in the unhydrolyzed protein that can be evaluated from the amino acid profile.

Free amino acids in the subW extracts were determined by the EZ:faast Phenomenex procedure as described in the previous section ("**Biomass characterization**").

Total organic carbon (TOC) of the liquid extracts was measured with a TOC/TN analyzer by subtracting the measured inorganic carbon (IC) from the measured total carbon (TC).

Total polyphenolic compounds (TPC) were determined according to Folin-Ciocalteu procedure (Singleton et al., 1999), using gallic acid (GA) as standard. Results were expressed as mg of gallic acid equivalent (GAE) per g_{DMR}.

The reducing capacity of subW extracts was determined by the ferric reducing ability of Plasma (FRAP) method according to Benzie and Strain (Benzie & Strain, 1996). Results were expressed as µmol of $FeSO_4$ per g_{DMR}.

Colour of the extracts. The L*, a* and b* values were obtained by a suitable program installed in a Beckman DU-650 spectrophotometer with diode-array of UV–vis (Beckman Instruments), representing brightness, red to green colour and yellow to blue colour, respectively (Illera et al. 2018). Other conditions are illuminant D65 (daylight source) and a 10° standard observer (perception of a human observer) following the CIE recommendations.

Residual agar from MR was also co-extracted and determined in the subW extract similarly to Meena et al. (Meena et al., 2008). Frozen samples were thawed and air-dried for 24 hours at ambient temperature for gel formation. The gelled material was then oven-dried at 50 °C until constant weight. Finally, agar content was determined by weighing the dry agar.

2.3.2.2. Solid residue after subcritical water treatment

The solid residue after subW treatment was dried and weighed and subjected to elemental composition analysis (Thermo Scientific Model Flash 2000). The high heating value (HHV) of the solid residue was evaluated by the following equation and compared to the one evaluated for the MR (Friedl et al., 2005):

$$HHV\ (kJ/kg) = 3.55C^2 - 232C - 2230H + 51.2C \cdot H + 131N + 20600 \qquad [\mathbf{1.2}]$$

2.3.3. Statistical analysis

All determinations were taken at least in duplicate and expressed as mean ± standard deviation. To confirm significant differences, the Fisher's least significant differences (LSD)

method at p value ≤ 0.05 was applied. Correlations between variables were determined by the Pearson correlation method. Analyses were carried out by the Centurion Statgraphics software.

3. Results

3.1. Macroalgae residue characterization

Chemical characterization of *G. sesquipedale* residue after agar extraction is presented in **Table 1.1** in a dry weight basis. Carbohydrates constituted the main class of chemical compounds, mainly glucans, 23.4 ± 0.9 %, and galactans, 10.9 ± 0.5 %, with small amounts of arabinans, 2.9 ± 0.2 %. Galactans determined by the enzymatic kit yielded a value of 9.5 ± 0.3 %, similar to the one obtained by HPLC determination. Extractives represented 11.5 % of MR composition, 22.6 % of the extractives were proteins, 6.8 % glucuronic acid and 2.4 % total polyphenols compounds (2.6, 0.78 and 0.28 %, respectively when referred to global macroalgae residue composition).

Lipid content was very low, less than 1 % as it was also determined for other macroalgae species. MR presented also low insoluble lignin content, 3 ± 1 %, as corresponds to third generation biomass. Ash content represented 22 ± 2 %. The mineral and inorganic elements of MR have been listed in **Table 1.2**. This table also includes the composition for fresh macroalgae for comparison with the industrial solid residue generated. Fresh *G. sesquipedale* has a content of inorganic components equal to 100 ± 6 g/kg of dry algae, while in the MR, this content was reduced down to 54 ± 4 g/kg dry MR, mainly due to lower levels of Na and K in the MR, less than 3 % of the levels presented in the fresh macroalgae.

The nitrogen factor was obtained according to the amino acid profile obtained for MR that has been listed in **Table 1.3**. The ammonia content from the degradation of some amino acids during acid hydrolysis was included in the calculation of protein nitrogen (Lourenço et al., 2002). According to the amino acid profile, a NF of 4.9 was determined that yielded a total protein content of 21 % (**Table 1.1**).

The total amount of amino acids, as determined by gas chromatography, was 172 ± 9 mg aa/g_{DMR}. The major amino acid in the MR was aspartic acid with 20.4 ± 0.8 mg/g_{DMR} (97 ± 4 mg/$g_{prot\text{-}MR}$). Glutamic and aspartic acids were found to be the main amino acids for many algae, including red algae with mean values of 123 and 142 for aspartic and glutamic acid, respectively (Lourenço et al., 2002). Total content of essential amino acids (EAA) in the MR was 76 ± 5 mg EAA/g_{DMR} (362 ± 5 mg EAA/$g_{prot\text{-}MR}$). Therefore, valorization of this by-product is of great interest due to the high protein and essential amino acids content, which gives it a great interest as dietary supplement for humans, among other uses.

Table 1.1. Chemical composition of macroalgae residue expressed as % ± standard deviation in a dry weight basis. (*n* = 2, number of independent samples and 3 technical replicates)

Compound	Composition, %
Extractives	**11.5 ± 0.9**
Polyphenols	0.28 ± 0.02
Proteins	2.6 ± 0.3
Glucuronic acid	0.78 ± 0.06
Carbohydrates	**37 ± 2**
Glucans	23.4 ± 0.9
Galactans	10.9 ± 0.5
Arabinans	2.9 ± 0.2
Lignin	**12 ± 1**
Soluble	8.7 ± 0.1
Insoluble	3 ± 1
Proteins*	**21 ± 1**
Lipids	**0.87 ± 0.09**
Ashes	**22 ± 2**

*Protein includes also the protein content in the extractive fraction

Table 1.2. Inorganic composition of fresh *G. sesquipedale*, macroalgae residue (MR) after agar extraction and solid residue after subW extraction (200 °C - 2 mL/min) in ppm ± standard deviation (*n* = 3 number of technical replicates)

Element	*G. sesquipedale*	MR	Residue-subW$^{200\,°C}$
Li	1.2 ± 0.2	13.4 ± 0.6	23.7 ± 0.4
B	260 ± 6	100 ± 7	62 ± 22
Na	34484 ± 317	875 ± 31	3573 ± 623
Mg	12764 ± 187	8918 ± 214	8359 ± 1976
Al	175 ± 59	8156 ± 217	17831 ± 2102
Si	190 ± 62	109 ± 27	132 ± 28
P	956 ± 87	5786 ± 677	7709 ± 1129
S	11711 ± 1014	4993 ± 357	1161 ± 57
K	29352 ±1082	863 ± 9	1624 ± 401
Ca	449 ± 93	6584 ± 221	12742 ± 3105
Ti	0.7 ± 0.2	7.32 ± 0.03	15 ± 2
V	2.1 ± 0.1	6.23 ± 0.07	11 ± 2
Cr	1.3 ± 0.4	14 ± 1	47 ± 14
Mn	149 ± 56	386 ± 115	626 ± 206
Fe	251 ± 83	6330 ± 346	12509 ± 404
Co	0.6 ± 0.2	2.4 ± 0.1	4.1 ± 0.9
Ni	5 ± 1	10 ± 1	25 ± 9
Cu	6 ± 1	8.8 ± 0.7	14 ± 6
Zn	246 ± 2	247 ± 26	377 ± 188
Ga	0.3 ± 0.1	10.50 ± 0.01	21 ± 1
As	5.7 ± 0.2	7.6 ± 0.1	6.8 ± 0.1
Br	3755 ± 826	4871 ± 363	334 ± 133
Rb	29.8 ± 0.4	10.2 ± 0.2	19 ± 1
Sr	35 ± 9	267 ± 110	587 ± 206
Zr	0.21 ± 0.05	2.08 ± 0.01	4 ± 1
Cd	0.53 ± 0.05	1.3 ± 0.2	2 ± 1
I	5793 ± 1926	5766 ± 1381	79 ± 39
Ba	1.1 ± 0.3	39.5 ± 0.4	81 ± 10
La	0.21 ± 0.06	5 ± 1	9.2 ± 0.3
Ce	0.3 ± 0.1	10 ± 3	18 ± 1
Nd	0.15 ± 0.05	4 ±1	7.9 ± 0.1
Pb	4 ± 2	10.9 ± 0.3	21 ± 8
Total	100629 ± 5815	54417 ± 4111	68035 ± 10677

Table 1.3. Amino acid profile of macroalgae residue, MR, and of the subW extracts, expressed as mg/$g_{protein\text{-}MR}$ ± standard deviation.

	MR	129 °C, 2 mL/min		142 °C, 2 mL/min		155 °C, 2 mL/min		171 °C, 2 mL/min		185 °C, 2 mL/min		200 °C, 2 mL/min		200 °C, 6 mL/min	
	mg/g_{DMR}	mg/g_{prot}	Yield, %	mg/g_{prot}	Yield, %	mg/g_{prot}	Yield, %	mg/g_{prot}	Yield, %	mg/g_{prot}	Yield, %	mg/g_{prot}	Yield, %	mg/g_{prot}	Yield, %
Ala	19.8 ± 0.7	0.81 ± 0.01	0.86 ± 0.08	0.95 ± 0.01	1.0 ± 0.1	2.36 ± 0.01	2.5 ± 0.2	4.19 ± 0.01	4.4 ± 0.4	6.9 ± 0.2	7.3 ± 0.8	6.22 ± 0.02	6.6 ± 0.1	6.94 ± 0.02	7.4 ± 0.6
Gly	8.6 ± 0.5	0.91 ± 0.01	2.2 ± 0.3	1.44 ± 0.02	3.5 ± 0.4	3.43 ± 0.01	8.4 ± 0.9	6.92 ± 0.01	17 ± 2	10.04 ± 0.04	25 ±3	7.38 ± 0.05	18 ± 2	8.37 ± 0.05	20 ± 2
Val	14.0 ± 0.9	0.90 ± 0.01	1.3 ± 0.2	0.52 ± 0.01	0.8 ± 0.1	1.04 ± 0.01	1.6 ± 0.2	3.07 ± 0.03	4.6 ± 0.6	6.85 ± 0.07	10 ± 1	6.74 ± 0.02	10 ± 1	6.20 ± 0.03	9 ± 1
Leu	16.3 ± 0.8	0.85 ± 0.01	1.1 ± 0.1	0.73 ± 0.01	0.9 ± 0.1	1.18 ± 0.01	1.5 ± 0.2	2.16 ± 0.01	2.8 ± 0.3	3.83 ± 0.01	4.9 ± 0.5	2.95 ± 0.01	3.8 ± 0.4	3.80 ± 0.02	4.9 ± 0.5
Ile	9.4 ± 0.7	0.57 ± 0.01	1.3 ± 0.2	0.34 ± 0.01	0.8 ± 0.1	0.60 ± 0.01	1.3 ± 0.2	125 ± 0.01	2.8 ± 0.4	2.97 ± 0.02	6.6 ± 0.9	2.50 ± 0.01	5.6 ± 0.7	2.35 ± 0.02	5.3 ± 0.7
Thr	7.5 ± 0.1	0.31 ± 0.02	0.9 ± 0.1	0.29 ± 0.02	0.8 ± 0.1	0.50 ± 0.02	1.4 ± 0.1	0.87 ± 0.05	2.4 ± 0.3	1.03 ± 0.09	2.9 ± 0.4	0.80 ± 0.05	2.2 ± 0.3	1.19 ± 0.03	3.3 ± 0.3
Ser	8.0 ± 0.9	0.74 ± 0.01	1.9 ± 0.3	0.97 ± 0.01	2.5 ± 0.4	1.78 ± 0.01	4.7 ± 0.8	2.47 ± 0.04	6.5 ± 0.9	3.55 ± 0.05	9 ± 2	1.80 ± 0.04	4.7 ± 0.9	2.21 ± 0.09	6 ± 1
Pro	15.4± 0.1	0.64 ± 0.01	0.88 ± 0.06	0.97 ± 0.01	1.3 ± 0.1	1.57 ± 0.01	2.1 ± 0.1	2.51 ± 0.01	3.4 ± 0.2	3.67 ± 0.02	5.0 ± 0.3	3.05 ± 0.01	4.2 ± 0.2	4.27 ± 0.02	5.8 ± 0.3
Asp	20.4 ± 0.8	0.40 ± 0.01	0.41 ± 0.05	0.93 ± 0.13	1.0 ± 0.2	5.37 ± 0.01	5.5 ± 0.5	10.19 ± 0.02	10.5 ± 0.9	10.3 ± 0.2	11 ± 1	4.5 ± 0.1	4.6 ± 0.5	18.3 ± 0.1	19 ± 2
Met	1.7 ± 0.2	0.12 ± 0.01	1.5 ± 0.04	0.15 ± 0.01	1.9 ± 0.4	0.52 ± 0.06	7 ± 2	0.84 ± 0.01	10 ± 2	1.30 ± 0.01	16 ± 3	0.97 ± 0.01	12 ± 2	1.9± 0.3	24 ± 7
Glu	16.6 ± 0.2	1.47 ± 0.02	1.9 ± 0.1	1.04 ± 0.06	1.3 ± 0.2	0.89 ± 0.04	1.1 ± 0.1	1.15 ± 0.04	1.5 ± 0.1	2.48 ± 0.02	3.1 ± 0.2	1.19 ± 0.04	1.5 ± 0.1	3.3 ± 0.5	4.2 ± 0.8
Phe	10.6 ± 0.8	0.51 ± 0.01	1.0 ± 0.1	0.45 ± 0.01	0.9 ± 0.1	0.79 ± 0.08	1.6 ± 0.3	1.67 ± 0.01	3.3 ± 0.4	2.99 ± 0.04	5.9 ± 0.8	2.34 ± 0.06	4.6 ± 0.7	2.88 ± 0.03	5.7 ± 0.8
Lys	12.0 ± 0.8	1.26 ± 0.08	2.2 ± 0.4	1.26 ± 0.02	2.2 ± 0.3	1.42 ± 0.09	2.5 ± 0.4	1.71 ± 0.02	3.0 ± 0.4	2.85 ± 0.04	5.0 ± 0.6	1.92 ± 0.08	3.4 ± 0.5	6.9 ± 0.5	12 ± 2
His	3.4 ± 0.2	0.26 ± 0.05	1.6 ± 0.5	0.44± 0.02	2.7 ± 0.4	0.80± 0.15	5 ± 1	1.37 ± 0.01	9 ± 1	2.29 ± 0.06	14 ± 2	1.9 ± 0.2	11 ± 2	5.4 ± 0.4	34 ± 6
Tyr	7.3 ± 0.9	1.33 ± 0.05	3.8 ± 0.8	1.9 ± 0.2	5 ± 1	2.33 ± 0.03	7 ± 1	2.46 ± 0.02	7 ± 1	3.32 ± 0.06	10 ± 2	2.93 ± 0.09	8 ± 1	5.47 ± 0.05	16 ± 3
Trp	0.60 ± 0.02	--	--	--	--	--	--	0.55 ± 0.01	20 ± 2	2.22 ± 0.09	78 ± 10	1.50 ± 0.01	53 ± 5	8.13 ± 0.01	> 100
EAA	76 ± 5	4.8 ± 0.2	1.3 ± 0.2	4.2 ± 0.1	1.2 ± 0.2	6.8 ± 0.4	1.9 ± 0.3	13.5 ± 0.1	3.8 ± 0.4	26.3 ± 0.4	7.3 ± 0.9	21.6 ± 0.5	6.0 ± 0.8	39 ± 1	11 ± 2
TAA	172 ± 9	11.1 ± 0.3	1.4 ± 0.2	12.4 ± 0.6	1.5 ± 0.2	24.5 ± 0.6	3.0 ± 0.4	43.4 ± 0.3	5.3 ± 0.6	67 ± 1	8.1 ± 0.9	48.7 ± 0.8	6.0 ± 0.7	88 ± 2	11 ± 1
NPS	0.6 ± 0.1	0.55 ± 0.02		0.53 ± 0.03		0.55 ± 0.01		0.60 ± 0.01		0.67 ± 0.02		0.75 ± 0.01		0.56 ± 0.02	

1.80 mg NH_3/g_{DMR} liberated during acid hydrolysis due to amino acid degradation

Extraction yield percentage (yield, % ± error associated to the ratio of two variables) of individual amino acid in the subW extracts. (*EAA* essential amino acids, *TAA* total amino acids, *NPS* non-polar selectivity, *NP/TAA* molar ratio of non-polar amino acids to total amino acids (*n* = 3 technical replicates, in case of raw material the number of independent samples were 2)

Table 1.4. Ash content, elemental analysis and estimated heating value (HHV) of original fresh macroalgae, macroalgae residue (MR) and the solid residue after subW treatment (F = 2 mL/min)

Sample	C (%, w/w)	H (%, w/w)	N (%, w/w)	S (%, w/w)	O (%, w/w)	Ashes (%, w/w)	H:C	O:C	HHV (kJ/kg)
G. sesquipedale	36.0 ± 0.3^{d}	5.4 ± 0.2^{e}	3.5 ± 0.3^{d}	0.26 ± 0.07^{b}	40 ± 1^{e}	14.9 ± 0.9^{a}	1.80 ± 0.08^{d}	0.83 ± 0.03^{f}	15219 ± 73^{b}
DMR	35.6 ± 1.2^{d}	5.9 ± 0.2^{f}	4.2 ± 0.4^{e}	0.21 ± 0.05^{b}	32.3 ± 0.3^{d}	21.8 ± 1.1^{b}	2.0 ± 0.1^{e}	0.68 ± 0.03^{e}	14987 ± 466^{a,b}
Residue-SW-129 °C	33.5 ± 0.9^{b,c}	5.2 ± 0.3^{e}	4.2 ± 0.3^{e}	0.20 ± 0.03^{b}	29 ± 3^{c}	29.5 ± 0.8^{c}	1.9 ± 0.2^{d,e}	0.61 ± 0.08^{d}	14685 ± 149^{a,b}
Residue-SW-142 °C	33.3 ± 0.6^{a,b,c}	4.5 ± 0.4^{c,d}	3.5 ± 0.5^{c,d}	0.04 ± 0.03^{a}	27 ± 2^{b,c}	31.9 ± 1.8^{c,d}	1.6 ± 0.2^{c}	0.61 ± 0.06^{c,d}	14907 ± 136^{a,b}
Residue-SW-155 °C	32.8 ± 1.6^{a,b}	4.7 ± 0.1^{d}	3.0 ± 0.2^{c}	n.d.	21 ± 4^{a,b}	33.4 ± 2.4^{d,e}	1.7 ± 0.1^{c,d}	0.54 ± 0.05^{b,c,d}	14615 ± 133^{a}
Residue-SW-171 °C	34.9 ± 1.1^{c,d}	4.0 ± 0.2^{b}	2.2 ± 0.1^{b}	n.d.	22 ± 2^{a,b}	36.2 ± 2.6^{e,f}	1.4 ± 0.1^{a,b}	0.51 ± 0.02^{a,b}	15343 ± 188^{b}
Residue-SW-185 °C	34.6 ± 0.9^{b,c,d}	4.0 ± 0.3^{b,c}	1.8 ± 0.1^{b}	n.d.	22 ± 2^{a,}	37.9 ± 1.9^{f}	1.4 ± 0.1^{b}	0.47 ± 0.04^{a}	15225 ± 336^{b}
Residue-SW-200 °C	31.4 ± 1.6^{a}	3.1 ± 0.3^{a}	1.0 ± 0.2^{a}	n.d.	22 ± 3^{a}	42.7 ± 2.1^{g}	1.2 ± 0.2^{a}	0.52 ± 0.06^{b,c}	15017 ± 387^{a,b}

n.d.: non detected. Values with different letters in each column are significantly different when applying the Fisher's least significant differences (LSD) method at *p*-value ≤ 0.05

Errors in the calculated variables have been estimated using the theory of error propagation

(*C* carbon; *H* Hydrogen; *N* Nitrogen; *S* Sulfur; *O* Oxygen) expressed as % (w/w) ± standard deviation (*n* = 3 technical replicates)

Elemental composition of MR can be found in **Table 1.4**. This table also lists the elemental composition of fresh *G. sesquipedale* for comparison with its industrial by-product. Fresh algae and its by-product presented similar content of carbon, but higher nitrogen and hydrogen content and lower oxygen content. Consequently, higher H:C molar ratio and lower O:C molar ratio were obtained in the MR compared to the fresh macroalgae. The ash content was much higher for the MR compared to the fresh raw material. Ferrera-Lorenzo et al. (Ferrera-Lorenzo et al., 2014b) reported elemental analysis composition of *G. sesquipedale* by-product. These authors obtained higher C (43.99 %), N (5.21 %) and S (1.02 %) content compared to our results. The most important difference lies in the ash content; these authors reported 7.7 %, while more than double ash content was obtained in this work. The difference in elemental composition in the *G. sesquipedale* residue can be attributed to the different source of the macroalgae, seasonality, as well as differences in the agar extraction process. With the data of the elemental composition, the HHV was evaluated according to **Equation 1.2**. Similar values were obtained for fresh *G. sesquipedale* and the MR, 15219 ± 73 and 14987 ± 466 kJ/kg values, respectively.

3.2. Extraction/hydrolysis of the protein fraction

The extraction/hydrolysis kinetics of the protein fraction by subW have been plotted in **Figure 1.3a**, as determined by TOC/TN analyzer by using the NF of 4.9. Total protein content has also been determined by a spectrophotometric method by using the DC kit. A linear correlation was stablished between both methods:

mg protein/g_{DMR} N-kit =1.139 mg protein/g_{DMR} TOC/TN, R2 = 0.9862

The slope of this linear correlation was higher than the unit, indicating that protein determination by spectrophotometric methods was overestimated. In this work, TOC/TN analyzer was considered to evaluate the protein fraction extraction since it is reliable and easy.

At a constant flow rate of 2 mL/min, accumulative protein content in the liquid extracts increased with temperature in the range from 129 to 185 °C. At 185 °C the protein yield accounted for nearly 70 % of the protein content in the MR. However, at the highest

temperature studied in this work, 200 °C, the accumulative protein fraction in the extracts was lower than at 185°C (see **Figure 1.3a**).

To assess the effect of the residence time, **Figure 1.3a** also shows the protein fraction hydrolysis at 200°C but at higher water flow rate, 6 mL/min. It can be clearly observed that faster extraction/hydrolysis kinetic was achieved by working at higher flow rate at the same operating temperature, 200 °C. By working with pressurized water, a common variable is the severity factor that combines temperature and the treatment time:

$$logR_o = log\left(t \cdot exp^{((T-T_{ref})/14.75)}\right) \quad [1.3]$$

where t is the treatment time (min), T is the operating temperature (°C) and T_{ref} is equal to 100 °C. To evaluate a similar parameter in a semicontinuous fixed bed reactor, the treatment time has been replaced by the residence time of the water in the reactor. The residence time for the water in the reactor was evaluated as:

$$\tau = \frac{V}{F_v} = \frac{V}{F_{v,o}}\frac{\rho_r}{\rho_o} \quad [1.4]$$

where V is the reactor volume in m^3 calculated with the dimensions of the reactor, $F_{v,o}$ the flow rate measured at ambient conditions, in m^3/s, ρ_o is the water density at ambient conditions and ρ_r the water density at the reaction conditions. According to **Figure 1.3a**, a maximum around values of severity factor of 4.22-4.25 that corresponds to the experiments performed at 185 °C and 2 mL/min and at 200 °C and 6 mL/min, respectively, was achieved for protein fraction release.

3.3. Free amino acids production

The accumulative content of the free amino acids, expressed as mg free aa/$g_{protein\text{-}MR}$ obtained in the subW extracts are plotted in **Figure 1.3b**. The total content of free amino acids has been calculated as the sum of the individual amino acids determined by gas chromatography. A similar trend as the total protein-fraction was observed. At a constant flow rate of 2 mL/min, a maximum at 185 °C for free amino acids was observed. At 200 °C (F = 2 mL/min) lower content of free amino acids was determined due to the degradation

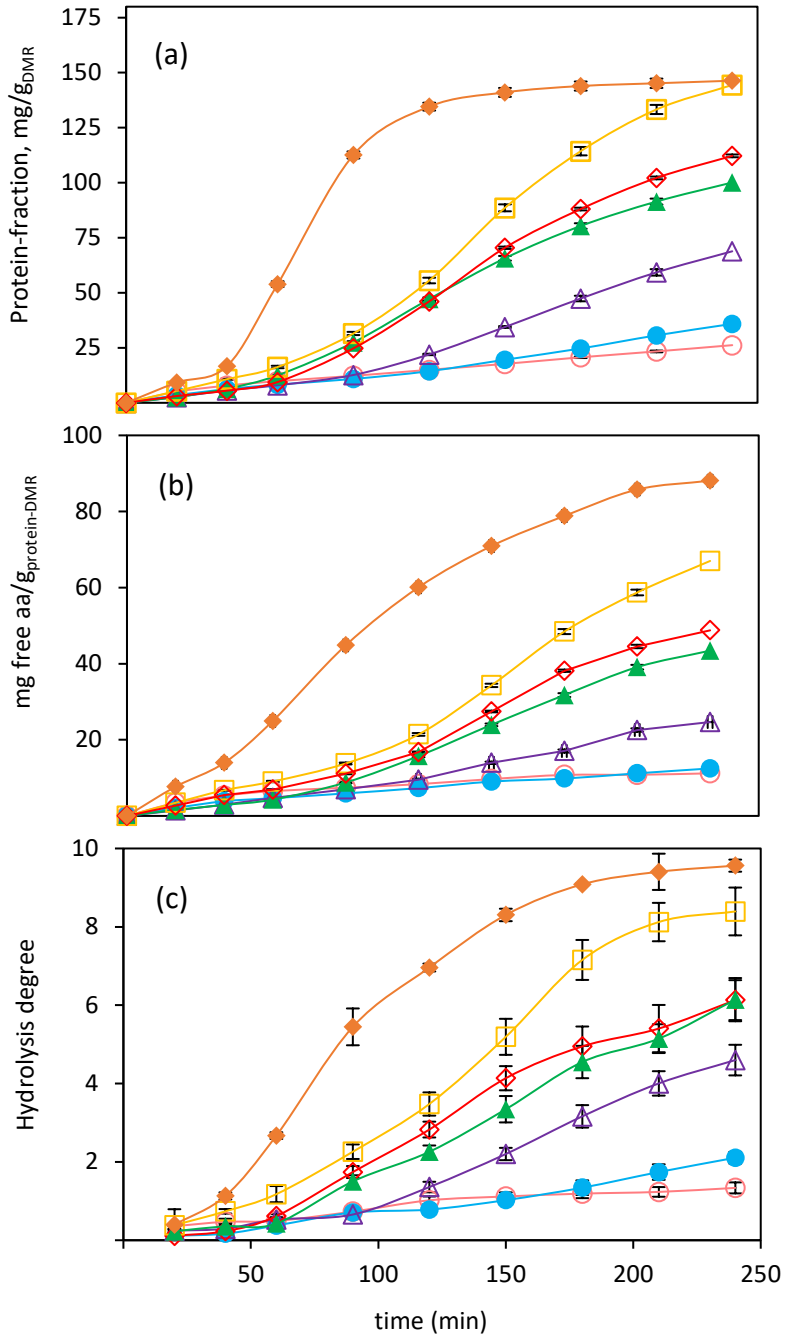

Figure. 1.3 (a) Accumulative protein (mg/g$_{DMR}$). **(b)** Accumulative free amino acid content (mg/g$_{protein-MR}$). **(c)** Hydrolysis degree in subW extracts from macroalgae solid residue. F = 2 mL/min (○ 129 °C, ● 142 °C, △ 155 °C, ▲ 171 °C, □ 185 °C, ◇ 200 °C), F = 6 mL/min and 200 °C (◆) (Experimental data include standard deviations, *n* = 3 technical replicates).

of amino acids at this temperature and such long residence time. Decreasing the residence time by working at higher flow rate, 6 mL/min, led to faster and higher amino acid yield.

As an example, **Figures 1.4a-1.4d** show the individual amino acid profile along extraction time for the experiments performed at 185 °C and 2 mL/min and at 200 °C and 6 mL/min, grouped into polar and non-polar amino acids. A slower release at 185 °C and 2 mL/min compared to the formation rate at 200 °C and 6 mL/min was also observed for individual free amino acids, obtaining the highest content for small amino acids, such as valine, alanine and glycine, as well as for aspartic acid (+ asparagine).

Table 1.3 lists the final free amino acid yield, evaluated as the ratio of the free amino acid content in the subW extracts to the initial amount of the amino acid in the MR. At a constant flow rate of 2 mL/min, for most of the amino acids, a maximum was observed at 185 °C. At this temperature, the total content of essential amino acids was 26.3 ± 0.4 mg of essential aa/$g_{protein}$. By increasing temperature up to 200 °C (F = 2 mL/min), the highest decrease in the accumulative amino acid fraction in the extracts was observed for polar amino acids such as serine and glutamic and aspartic acids.

Table 1.3 also lists the results for the production yield of the individual amino acids at 200 °C and 6 mL/min. By increasing flow rate, the water residence time in the reactor decreased, leading to lower severity factors than at 2 mL/min, and the formation yield for all the individual amino acids increased. This increase was especially noticeable for aspartic acid, methionine, lysine and histidine. Therefore, the selectivity towards non-polar amino acids decreased (see **Table 1.3**).

Figure 1.3c shows the hydrolysis degree for the different experiments carried out. According to the protein fraction release, the highest DH was obtained at 6 mL/min and 200 °C. The total content of free amino acids, expressed as mmol free amino acids/$g_{protein-MR}$, obtained as the sum of the individual amino acids as determined by gas chromatography, have been compared with the meq–NH_2/$g_{protein-MR}$ obtained by the ninhydrin assay. For that, a linear correlation between both values has been established and any statistically significant differences in the slopes from unity at the 90% or higher confidence level have been stablished (**Table 1.5**).

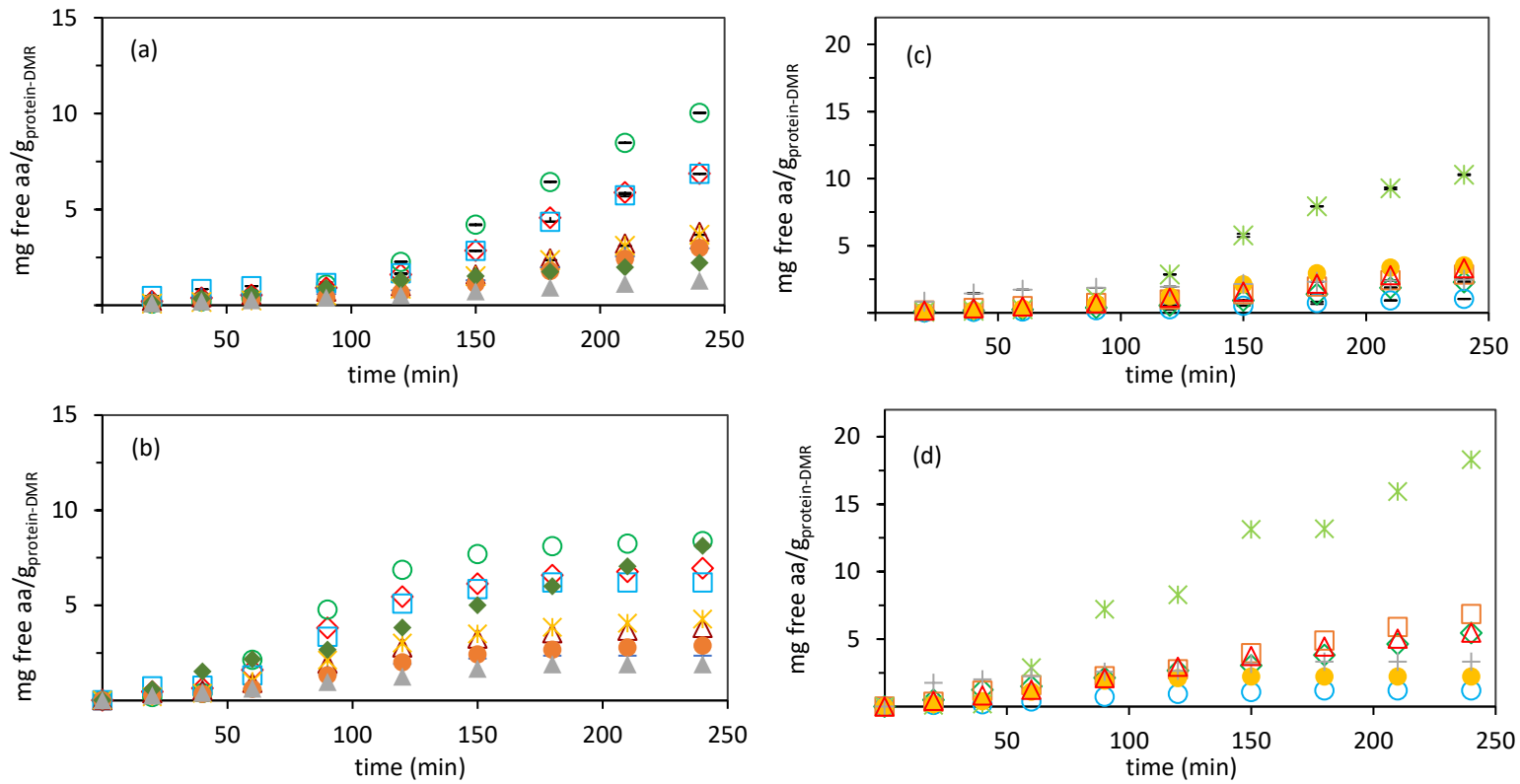

Figure 1.4 Accumulative formation of individual amino acids. Non-polar amino acids **(a)** at 185 °C and 2 mL/min **(b)** at 200 °C and 6 mL/min (◇ alanine, ○ glycine, □ valine, △ leucine, + isoleucine, ✳ proline, ● phenylalanine, ◆ tryptophan, ▲ methionine). Polar amino acids **(c)** at 185 °C and 2 mL/min **(d)** 200 °C and 6 mL/min (◇ histidine, ○ threonine, □ lysine, △ tyrosine, + glutamic acid, ✳ aspartic acid, ● serine). (experimental data include standard deviations, *n* = 3 technical replicates).

Although the ninhydrin assay determines all primary amines, be they amines, amino acids, peptides, proteins, and even ammonia (Friedman, 2004), no statistically significance difference between both analytical techniques was determined, except for 142 and 155 °C (see **Table 1.5**). From these data sets, it can be concluded that formation of small peptides could not be satisfactorily distinguished with the ninhydrin assay compared to the total amount of free amino acids detected by gas chromatography. According to Friedman (Friedman, 2004), the ninhydrin assay of amino groups in proteins was not as satisfactory as for amino acids since it does not always produce the theoretical yield.

Table 1.5. Linear relationship between meq–NH_2 determined by the ninhydrin assay and free amino acid, FAA, (mmol aa/$g_{protein\text{-}MR}$), determined by the sum of individual amino acids by gas chromatography: meq-NH2 = (intercept ± standard error) + (slope ± standard error) × FAA_{GC}

Experiment	slope	intercept	R^2
129 °C, 2 mL/min	1.08 ± 0.10	-0.006 ± 0.007	0.940
142 °C, 2 mL/min	1.49 ± 0.06*	-0.023 ± 0.004*	0.987
155 °C, 2 mL/min	1.53 ± 0.05*	-0.009 ± 0.006*	0.992
171 °C, 2 mL/min	1.15 ± 0.07	0.022 ± 0.015*	0.974
185 °C, 2 mL/min	1.09 ± 0.07	0.023 ± 0.021	0.975
200 °C, 2 mL/min	0.96 ± 0.05	0.006 ± 0.011	0.984
200 °C, 6 mL/min	0.94 ± 0.04	0.015 ± 0.020	0.988

*Significant difference from slope unity or 0 intercept. (*p* value ≥0.1)

3.4. Total phenolic content and antioxidant activity of subW extracts.

Figure 1.5a shows the accumulative curve of the total polyphenolic compounds (TPC), as determined by the Folin Ciocalteu assay. At 2 mL/min, TPC release increased by increasing temperature. Higher flow rate, 6 mL/min, led to faster release of TPC, at the same operating temperature of 200 °C, but similar TPC was obtained after 240 min, 25.9-26.5 mg GAE/g_{DMR}.

The antioxidant capacity of the extracts collected at the different time intervals was determined by the FRAP assay and results are presented in **Figure 1.5b**. Antioxidant capacity

increased with temperature and flow rate. The maximum antioxidant capacity in the collected extracts when working at 6 mL/min was obtained at 40-60 min, while at 2 mL/min, the maximum was reached later at 60-90 min.

These results agree with others obtained for different fresh red algae in literature that determined a greater antioxidant activity as temperature increased with a maximum at 210 °C (Park et al., 2019). In that study, the TPC obtained after subW treatment varied in the range from 4.70 ± 0.08 (at 120 °C) to 14.29± 0.33 (210 °C) mg GAE/$g_{dry\ algae}$ (Park et al., 2019).

Correlation coefficients between the antioxidant capacity and the components determined in the extracts (TPC, protein fraction and free amino acids) have been determined according to the Pearson product moment correlation. Analysis indicated a statistically significant non-zero correlations at the 95.0 % confidence level and positive correlation coefficients between antioxidant capacity and the TPC, solubilized protein and free amino acids in the extracts with values of the correlation coefficients of 0.882, 0.771 and 0.381, respectively (n = 63, the number of pairs of data values used to compute each coefficient).

Browning process along extraction could be clearly observed at first sight. To quantify the colour of the extract, the evolution of the colour of the collected extracts at the different time intervals, when working at 6 mL/min and 200 °C, was evaluated and colour parameters were compiled in **Table 1.6**. It can be observed that the lowest values of the luminosity and yellowness correspond to the highest value of the antioxidant capacity and the TPC of the extracts (60-90 min, see **Figure 1.5b**). Pearson correlation coefficients between these two variables and the colour parameters showed significant non-zero correlations at the 95.0 % confidence level. Negative correlations for L* and b* and positive correlation for a* were obtained and stronger correlations were determined for the antioxidant capacity than for TPC (see **Table 1.6**).

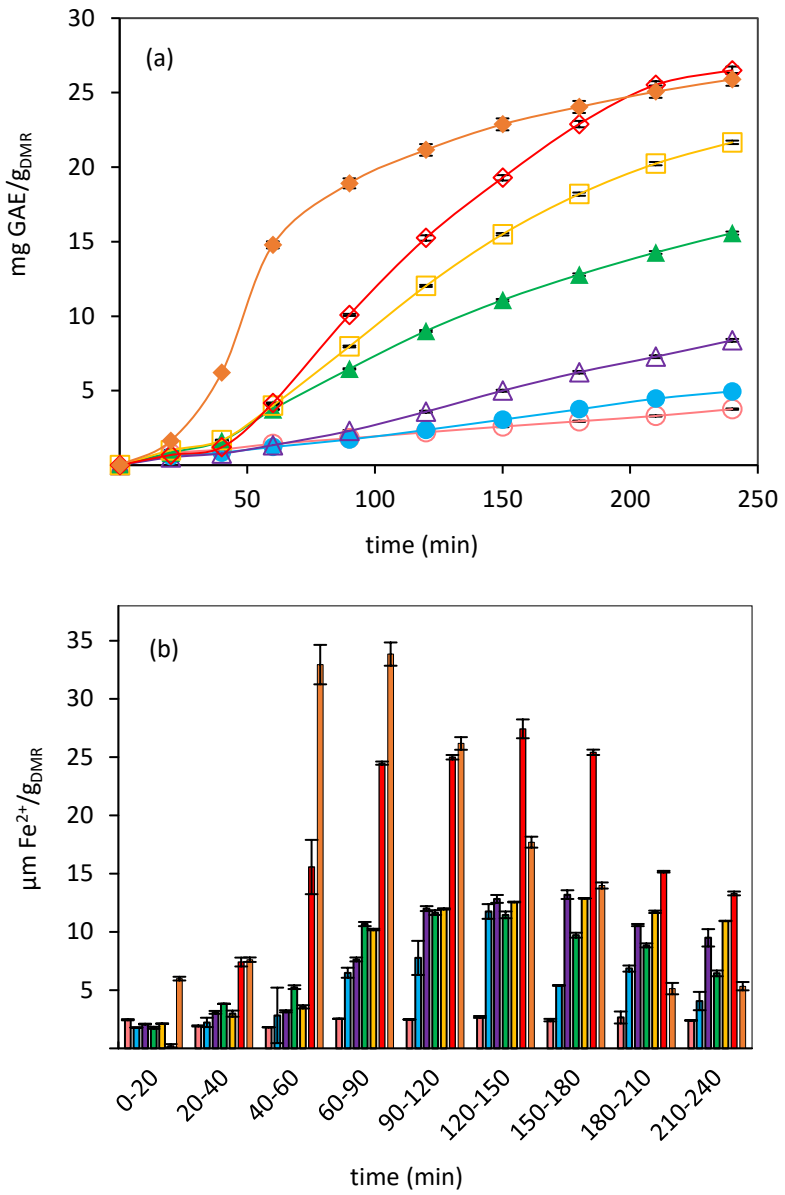

Figure 1.5 (a) Accumulative total phenolic compounds, as determined by Folin-Ciocalteu, (mg GAE/g_{DMR}). **(b)** Total antioxidant activity (µm $FeSO_4$/g_{DMR}) collected at the different time intervals in subW extracts from macroalgae residue: F = 2 mL/min (○, ■ 129 °C; ●, ■ 142 °C; △, ■ 155 °C; ▲, ■ 171 °C; □, ■ 185 °C; ◇, ■ 200 °C). F = 6 mL/min and 200 °C. (◆, ■). (Experimental data include standard deviations, *n* = 3 technical replicates).

Table 1.6. Colour parameters of the extracts collected at 200 °C (F = 6 mL/min) at different time intervals. CIElab parameters ± standard deviation (*n* = 3 technical replicates) Pearson correlation parameters for colour parameters and TPC and antioxidant capacity

Time interval	L*	a*	b*
0 - 20 min	31.6 ± 0.3^{h}	5.2 ± 0.7^{a}	32.9 ± 0.4^{f}
20 – 40 min	24.8 ± 0.5^{f}	9.4 ± 0.2^{d}	32.5 ± 0.5^{f}
40 – 60 min	3.0 ± 0.1^{a}	12.1 ± 0.3^{e}	5.1 ± 0.2^{a}
60 – 90 min	4.8 ± 0.2^{b}	16.9 ± 0.6^{h}	8.1 ± 0.3^{b}
90 – 120 min	8.1 ± 2.0^{c}	17.2 ± 0.9^{h}	13.7 ± 1.7^{c}
120 – 150 min	12.0 ± 0.1^{d}	15.3 ± 0.3^{g}	20.3 ± 0.1^{d}
150 – 180 min	17.8 ± 0.6^{e}	13.03 ± 0.08^{f}	29.1± 0.8^{e}
180 – 210 min	28.8 ± 1.3^{g}	6.2 ± 0.5^{b}	28.8 ± 3.1^{e}
210 – 240 min	25.3 ± 1.3^{f}	7.1 ± 0.3^{c}	30.0 ± 1.2^{e}
Correlation coefficients (*n* = 9)	TPC - L* = -0.8327 Fe^{2+} - L* = -0.9671	TPC - a* = 0.7392 Fe^{2+} - a* = 0.8108	TPC - b* = -0.8770 Fe^{2+} - b* = -0.9701

Values with different letters in each column are significantly different when applying the Fisher's least significant differences (LSD) method at *p* value ≤ 0.05
*$p < 0.05$ for all pair of variables

Table 1.7. Hydrolysis yield for the experiments carried out at F = 2 mL/min. Mass balances (MB) for C, N and ash

T, °C	Yield (%)	C_{inlet} (g)	C_{outlet} (g)	MB, C (%)	N_{inlet} (g)	N_{outlet} (g)	MB, N (%)	ash_{inlet}	ash_{outlet}	MB, ash (%)
129	21.2	3.359	3.021	89.9	0.396	0.363	91.7	2.057	2.194	106.7
142	26.2	2.352	2.118	90.1	0.278	0.223	80.2	1.441	1.557	108.1
155	31.5	2.353	2.220	94.3	0.278	0.229	82.4	1.441	1.512	104.9
171	40.7	2.349	2.220	94.5	0.277	0.221	79.8	1.438	1.415	98.4
185	44.3	2.371	2.313	97.6	0.280	0.261	93.2	1.452	1.406	96.8
200	50.7	2.356	2.066	88.0	0.277	0.197	71.1	1.437	1.388	96.3

7 g of DMR were charged into the reactor except for run at 129 °C that 10 g were charged
Mass or % (w/w) ± standard deviation (*n* = 3 technical replicates)

3.5. Total organic carbon in the subcritical water extracts

Accumulative total organic carbon (TOC) of the different extracts collected has been plotted in **Figure 1.6.** At 2 mL/min, TOC in the extracts increased with temperature, although no differences were observed between 185 °C and 200 °C.

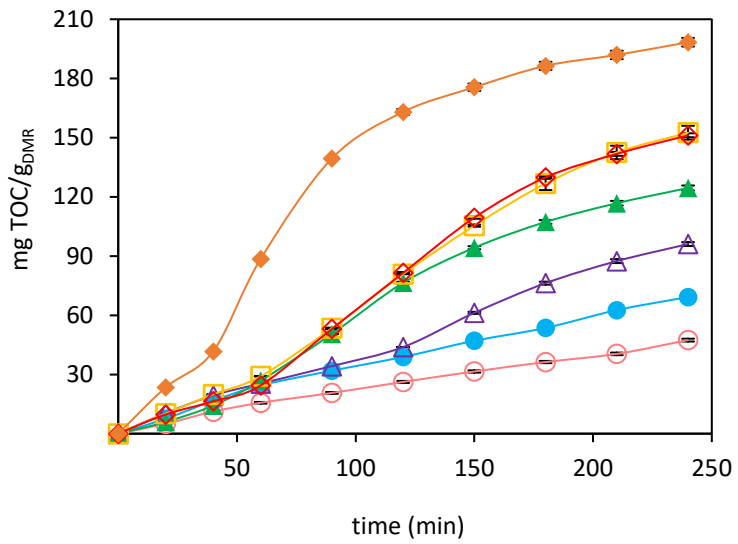

Figure 1.6. Accumulative total organic carbon (mg TOC/g_{DMR} obtained by subW treatment from macroalgae residue at F = 2 mL/min (○ 129 °C, ● 142 °C, △ 155 °C, ▲ 171 °C, □ 185 °C, ◇ 200 °C). F = 6 mL/min and 200 °C (◆). (Experimental data include standard deviations, *n* = 3 technical replicates).

Regarding the effect of flow rate, faster and higher release of TOC was observed by working at high flow rate. High flow rate led to lower residence time and higher yields of TOC, similar to proteins and amino acids.

3.6. Waste solid analysis

The solid residue was weighed after each extraction and the hydrolysis yield was estimated according to the equation:

$$Hydrolysis\ yield\ (\%) = \frac{W - W_1}{W} \cdot 100 \qquad [\mathbf{1.5}]$$

where w is the weight of the dry sample introduced in the reactor and w_1 is the weight of the dried residue after subW treatment. The values of the hydrolysis yield (%) are listed in **Table 1.7** where it can be observed that the hydrolysis yield increased by increasing the working temperature. For instance, at a flow rate of 2 mL/min, the hydrolysis yield increased from 21 to 51 % when varying temperature from 129 to 200 °C due to a greater solubilization of the extracted compounds at high temperatures.

Elemental composition of the residue collected in the different experiments carried out at F = 2 mL/min has been listed in **Table 1.4**. A significant decrease in C, H and especially in N was observed by increasing operating temperature, due to a higher organic and protein fraction solubilization. S content also decreased probably due to the extraction of the residual agar in the by-product. Ash content steadily increased with temperature, proving that ashes are not solubilized at the experimental conditions of this work.

Elemental composition of the MR before and after subW treatment and the accumulative content of C and N in the collected extracts help to perform the carbon and nitrogen balance:

$$C\ (or\ N)\ balance = \frac{C\ (or\ N)_{outlet}}{C(or\ N)_{inlet}} \cdot 100 \qquad [\mathbf{1.6}]$$

Deviations for C and N mass balances are collected in **Table 1.7**. Deviations ranged from 4 to 12 % for C and from 6.8 to 28.9 % for N. The greatest deviations for the mass balance were observed at the highest temperature studied. Some of the solid may also be converted to volatile compounds (Yoshida & Tavakoli, 2004) that were not measured in this work. Mass balance for the ashes was also performed, considering that the ashes were only present in the solid reside after subW treatment. For ashes, mass balance deviations ranged from 3.7 to 8.1 %. The inorganic content of the solid residue obtained at 2 mL/min and 200 °C was listed in **Table 1.2**. Compared to the macroalgae industrial residue, the concentration of most of the metals increased after subW treatment. For instance, Na concentration increased by a factor of 4, Cr by a factor of 3, while the concentration of K, Al, Ca, Fe, Ti, and Ni was doubled. From **Table 1.2** can be also observed the reduction in S content after subW

treatment as determined in **Table 1.4** by ICP-MS. HHV for the residues after subW treatment was also evaluated (see **Table 1.4**), but not a trend in these values was observed in the solid residue after subW treatment.

4. Discussion

The benefits of different components of marine algae have been well documented and described in literature. However, algae by-products generated during industrial activity have been hardly discussed. Macroalgae industry generates a large amount of by-products that still contain different valuable compounds being worthy their valorization. The solid residue generated from red algae after agar extraction still contains important amounts of carbohydrates (37 %, w/w) and proteins, 21 % (w/w). The NF determined for MR was 4.9, lower than the value of 6.25 commonly used (Park et al., 2019). However, for different types of macroalgae, lower values for NF have also been reported in literature. Lourenco et al. (Lourenço et al., 2002) determined an average value of 4.6 ± 0.5 for nine red algae species, with an overall average NF factor of 4.9 ± 0.6 for different macroalgae species including red, brown and green. The lower values of the NF for seaweeds are due to the presence of non-protein nitrogen compounds such as pigments and inorganic nitrogen (nitrite, nitrate and ammonia) that led to lower NF for algae species (Lourenço et al., 2004).

The low lipid content agreed with the range reported in the literature, between 0.3 and 3.6 g/100 g dry seaweed for different red, brown and green algae (Rodrigues et al., 2015). The elemental composition of the MR led to a HHV of 14987 ± 466 kJ/kg. The HHV for MR was slightly lower than the values reported for other types of biomass. Friedl et al (Friedl et al., 2005) reported HHV in the range from 15974 to 20321 kJ/kg for various types of wastes (including compost, waste from sugar, oil, and brewering industries, poultry litter and sewage sludge).

4.1. Extraction/hydrolysis of the protein fraction

Protein fraction in the extracts has been evaluated by the TOC/TN analyzer. In algae, spectrophotometric methods such as Lowry et al. (Lowry et al., 1951) and Bradford (Bradford, 1976), can be subjected to some interferences, such as degradation products of proteins, saccharides, amino acids and phenolic compounds (Hata et al., 2008), but also amino acid composition affects the results obtained by these two methods. According to literature (Lourenço et al., 2004), the Cu^{2+} ion present in the reagent is overly sensitive to some amino acids such as tryptophan and tyrosine. These could be the reasons that justify the difference in the protein fraction content obtained by the spectrophotometric method and the TOC analyzer determined in this work. The effect of subW treatment on hydrolysis and extraction of the protein fraction of the MR has been described. Both, temperature and solvent flow rate, have been determined as key parameters when dealing with protein hydrolysis. At constant flow rate of 2 mL/min, a maximum at 185 °C in the protein fraction hydrolysis was obtained. At subW conditions, the ionic product of water, K_w, increases with temperature that induced lower pH values in the medium due to the high levels of hydronium (H_3O^+) and hydroxide (OH^-) ions derived from autoionization of water that favours biomass hydrolysis (see **Figure 1.2b**) (Toor et al., 2011). At these conditions, the protein fraction would be probably hydrolyzed into valuable peptides and free amino acids (Marcet et al., 2016). Furthermore, an increase in temperature could cause the algae cell wall to swell and rupture enhancing diffusion of intracellular components and water interaction (Zainan et al., 2020). Additionally, insoluble proteins have a high surface hydrophobicity that can become hydrated when the dielectric constant of water decreases with temperature (Lamp et al., 2020). By increasing temperature up to 200 °C, the residence time of water with the soluble products in the fixed bed reactor was long enough to cause protein or its hydrolysis products to degrade.

An increase in flow rate, at 200 °C, led to better results in terms of extraction/hydrolysis rate and yield. To explain these results, a similar mechanism as the one proposed by Liu and Wyman (Liu & Wyman, 2003) for hemicellulose dissolution from corn stover, can be proposed. That is, water will hydrolyze long-chain peptides slower than short-chain peptides and therefore long-chain peptides could be accumulated on the solid surface; an

increase in the flow rate would reduce the thickness of the stagnant fluid layer surrounding the solid, facilitating water penetration into the solids and therefore hydrolyze and remove the protein fraction. The mass transfer limitation on protein extraction can be observed in the shape of the extraction accumulative curves, since protein release was quite slow at 2 mL/min but was much faster at 6 mL/min.

4.2. Free amino acids production

High severity factors (high temperature and high residence time) led to lower free amino acids due to amino acids decomposition. Toor et al. (Toor et al., 2011) reported that primary mechanisms of degradation of the amino acids were decarboxylation and deamination with loss of NH_3. Rogalinski et al. (Rogalinski et al., 2005) studied the production and decomposition of amino acids from bovine serum albumin (BSA) by continuous subW. These authors determined the main degradation products of BSA carboxylic acids such as acetic acid, propionic acid, n-butyric acid, isobutyric acid and isovaleric acid with only two nitrogen containing compounds, ethanolamine and the non-proteinogenic amino acid ornithine. Unfortunately, no results on NH_3 release were presented.

The results obtained in this work agree with literature that also reported serine and aspartic and glutamic acids as one of the most temperature-sensitive amino acids that decomposed faster than lower molecular weight amino acids such as glycine and alanine (Ahmed & Chun, 2018). A high yield loss by increasing temperature form 185 °C to 200 °C was also observed for lysine. Lysine and (other) polar amino acid side groups have a high tendency to undergo Maillard reactions with carbonyl groups or reducing carbohydrates (Lamp et al., 2020) generated during subW treatment. On the contrary, simple amino acids such as alanine and glycine presented higher stability under subW conditions, as it has also been reported by Rogalinski et al. (Rogalinski et al., 2005) in the study of amino acid production from bovine serum albumin by continuous subW. High stability was also observed by valine, but possible transformation of lysine to valine has also been reported (Zainan et al., 2020). As a consequence, the selectivity towards non-polar amino acids defined as the amount of free non-polar amino acids released in the subW extracts relative to total amount of free amino

acids on molar base increased by working on more severe conditions (higher severity factor) since polar amino acids seems to be more sensitive under subW conditions (see **Table 1.3**).

In general, amino acids with high molecular weight are more susceptible to degradation not only to ammonia, organic acids and amines but also to other amino acids with lower molecular weight that could compensate the degradation of these amino acids (Esteban et al., 2010). In the present study glycine, the smallest amino acid presented the highest formation yield. The high values of tryptophan yields are probably due to the error associated during its determination by basic hydrolysis. In any case, as reported by Esteban et al. (Esteban et al., 2010), it is difficult to stablish any relation between the type of side chain of the amino acid and the hydrolysis yield since for a specific type chain, not all amino acids are obtained in proportional amounts.

4.3. Total phenolic content and antioxidant

TPC release and antioxidant capacity increased by increasing flow rate and temperature. According to these results, it could be concluded that the temperature needed for phenolic compounds degradation present in the macroalgae residue was not yet reached. However, as reported in literature, Maillard reactions could take place between sugars and amino acids and new compounds can be obtained that contribute to the antioxidant capacity of the collected extracts (Plaza & Turner, 2017). Marcet et al. (Marcet et al., 2016) reported that antioxidant capacity increased when small peptides are obtained. However, the strength of the correlation between antioxidant capacity and TPC was the highest, concluding that TPC contributed in a larger extent to the determined antioxidant capacity than protein fraction or free amino acids.

4.4. Total organic carbon and waste solid

The effect of temperature and flow rate on TOC in subcritical water extracts was similar to the protein fraction. TOC would include hydrolysis products of carbohydrates such as oligomers, monomers and their degradation products, but also protein degradation products such as different organic acids (Kang et al., 2001). For instance, residual agar was

analyzed in the extracts obtained at 200 °C and 6 mL/min and accounted for 5.0 % ± 1.4 probably due to a non-complete industrial extraction. Degradation of carbohydrates and proteins can release NH_3 and CO_2 or other gas products that would have led to similar TOC yield at 200 °C and 185°C, due to a higher degradation degree of the macroalgae residue components. Although gas product formation has not been studied in this work, it has been reported previously (Kang & Chun, 2004a; Sereewatthanawut et al., 2008).

The greater solubilization of the carbon and nitrogen fraction of the MR with temperature led to an increase of the hydrolysis yield and lower N and C content of the solid residue after subW treatment. Ash content increased in the solid residue as temperature increased due to non-solubilization. Toor et al (Toor et al., 2011) reported that the decrease of the dielectric constant of water with temperature led to an increase of the solubility of non-polar organic compounds, but the solubility of salts significantly decreased. Thiruvenkadam et al. (Thiruvenkadam et al., 2015), in their review concluded that the solid residue after subW treatment had a high concentration of ash and low concentrations of hydrogen, nitrogen and sulphur. This can be also appreciated in **Table 1.4** where the experiment carried out at 200 °C and 2 mL/min presented the lowest H and N content and the highest ash content.

Conclusions

SubW treatment led to an efficient extraction/hydrolysis of the protein fraction of the macroalgae industrial solid residue after agar extraction. The best experimental conditions in the semicontinuous fix-bed reactor used in this work were 200 °C and 6 mL/min with nearly 70 % of the solubilized protein content. The highest content of individual amino acids was obtained for small amino acids such as valine, alanine and glycine as well as aspartic acid. Therefore, an increase in the non-polar selectivity was observed by working at high severity factors. Positive and strong correlation was obtained for TPC and the reducing capacity of the subW extracts. The solid residue after subW treatment presented lower H, N and O content, but higher ash content due to non-solubilization of this fraction, being possible its application in agriculture as fertilizers.

References

Adler-Nissen J, Eriksen S, Olsen HS (1983) Improvement of the functionality of vegetable proteins by controlled enzymatic hydrolysis. *Qual Plant Plant Foods Hum Nutr* 32:411–423.

Ahmed R, Chun BS (2018) Subcritical water hydrolysis for the production of bioactive peptides from tuna skin collagen. *J Supercrit Fluids* 141:88–96.

Akiya N, Savage PE (2002) Roles of water for chemical reactions in high-temperature water. *Chem Rev* 102:2725–2750.

Benzie IFF, Strain JJ (1996) The Ferric Reducing Ability of Plasma (FRAP) as a Measure of "Antioxidant Power": The FRAP Assay. *Anal Biochem* 239:70–76.

Bligh EG, Dyer WJ (1959) A rapid method of total lipid extraction and purification. Canadian Journal of Biochemistry and Physiology. *Can J Biochem Physiol* 37:911–917

Bordoloi A, Goosen NJ (2020) A greener alternative using subcritical water extraction to valorize the brown macroalgae Ecklonia maxima for bioactive compounds. *J Appl Phycol*. 32: 2307-2319

Bradford MM (1976) A Rapid and Sensitive Method for the Quantitation of Microgram Quantities of Protein Utilizing the principle of protein-dry bingin. *Anal Biochem* 72:248–254.

Esteban MB, García AJ, Ramos P, Márquez MC (2010) Sub-critical water hydrolysis of hog hair for amino acid production. *Bioresour Technol* 101:2472–2476.

Ferrera-Lorenzo N, Fuente E, Suárez-Ruiz I, Gil RR, Ruiz B (2014a) Pyrolysis characteristics of a macroalgae solid waste generated by the industrial production of Agar-Agar. *J Anal Appl Pyrolysis* 105:209–216.

Ferrera-Lorenzo N, Fuente E, Suárez-Ruiz I, Ruiz B (2014b) KOH activated carbon from conventional and microwave heating system of a macroalgae waste from the Agar-Agar industry. *Fuel Process Technol* 121:25–31.

Friedl A, Padouvas E, Rotter H, Varmuza K (2005) Prediction of heating values of biomass fuel from elemental composition. *Anal Chim Acta* 544:191–198.

Friedman M (2004) Applications of the Ninhydrin Reaction for Analysis of Amino Acids, Peptides, and Proteins to Agricultural and Biomedical Sciences. *J Agric Food Chem 52:385–406.*

Gereniu CRN, Saravana PS, Getachew AT, Chun BS (2017) Characteristics of functional materials recovered from Solomon Islands red seaweed (Kappaphycus alvarezii) using pressurized hot water extraction. *J Appl Phycol* 29:1609–1621.

Hata S, Wiboonsirikul J, Maeda A, Kimura Y, Adachi S (2008) Extraction of defatted rice bran by subcritical water treatment. *Biochem Eng J* 40:44–53.

Illera AE, Sanz MT, Beltrán S, Melgosa R, Solaesa AG, Ruiz MO (2018) Evaluation of HPCD batch treatments on enzyme inactivation kinetics and selected quality characteristics of cloudy apple juice from Golden delicious apples. *J. Food Eng.* 221:141-150.

Kang KY, Chun BS (2004) Behavior of amino acid production from hydrothermal treatment of fish-derived wastes. *Korean J Chem Eng* 21:1147–1152.

Kang K, Quitain AT, Daimon H, Noda R, Goto N, Hu H-Y, Fujie K (2001) Optimization of amino acids production from waste fish entrails by hydrolysis in sub- and supercritical water. *Can J Chem Eng* 79:65–70.

Lamp A, Kaltschmitt M, Lüdtke O (2020) Protein recovery from bioethanol stillage by liquid hot water treatment. *J Supercrit Fluids* 155:104624.

Liu C, Wyman CE (2003) The effect of flow rate of compressed hot water on xylan, lignin, and total mass removal from corn stover. *Ind Eng Chem Res* 42:5409–5416.

Lourenço SO, Barbarino E, De-Paula JC, da S. Pereira LO, Lanfer Marzques UM (2002) Amino acid composition, protein content and calculation of nitrogen-to-protein conversion factors for 19 tropical seaweeds. *Phycol Res* 50:233–241.

Lourenço SO, Barbarino E, Lavín PL, Lanfer Marquez UM, Aidar E. (2004) Distribution of intracellular nitrogen in marine microalgae: Calculation of new nitrogen-to-protein conversion factors. *Eur J Phycol* 39:17–32.

Lowry OH, Rosebrough NJ, Farr AL, Randall RJ (1951) Protein measurement with the folin reagent. *J Biol Chem* 193:265–275

Marcet I, Álvarez C, Paredes B, Díaz M (2016) The use of sub-critical water hydrolysis for the recovery of peptides and free amino acids from food processing wastes. Review of sources and main parameters. *Waste Manag* 49:364–371.

Meena R, Prasad K, Ganesan M, Siddhanta AK (2008) Superior quality agar from Gracilaria species (Gracilariales, Rhodophyta) collected from the Gulf of Mannar, *India. J Appl Phycol* 20:397–402.

Meillisa A, Siahaan EA, Park JN, Woo HCh, Chun BS (2013) Effect of subcritical water hydrolysate in the brown seaweed Saccharina japonica as a potential antibacterial agent on food-borne pathogens*. J Appl Phycol* 25:763–769.

Pangestuti R, Getachew AT, Siahaan EA, Chun BS (2019) Characterization of functional materials derived from tropical red seaweed Hypnea musciformis produced by subcritical water extraction systems. *J Appl Phycol* 31:2517–2528.

Park JS, Jeong YR, Chun BS (2019) Physiological activities and bioactive compound from laver (Pyropia yezoensis) hydrolysates by using subcritical water hydrolysis. *J Supercrit Fluids* 148:130–136.

Plaza M, Turner C (2017) Pressurized Hot Water Extraction of Bioactives. *Compr Anal Chem* 76:53–82.

Porse H, Rudolph B (2017) The seaweed hydrocolloid industry: 2016 updates, requirements, and outlook*. J Appl Phycol* 29:2187–2200.

Postma PR, Cerezo-Chinarro O, Akkerman RJ, et al (2018) Biorefinery of the macroalgae Ulva lactuca: extraction of proteins and carbohydrates by mild disintegration. *J Appl Phycol* 30:1281–1293.

Rajak RC, Jacob S, Kim BS (2020) A holistic zero waste biorefinery approach for macroalgal biomass utilization: A review. *Sci Total Environ* 716:137067.

Rodrigues D, Freitas AC, Pereira L, Rocha-Santos TAP, Vasconcelos MW, Roriz M., Rodríguez-Alcalá LM, Gomes AMP, Duarte AC (2015) Chemical composition of red, brown and green macroalgae from Buarcos bay in Central West Coast of Portugal. *Food Chem* 183:197–207.

Rogalinski T, Herrmann S, Brunner G (2005) Production of amino acids from bovine serum albumin by continuous sub-critical water hydrolysis. *J Supercrit Fluids* 36:49–58.

Sereewatthanawut I, Prapintip S, Watchiraruji K, Goto M, Sasaki M, Shotipruk A (2008) Extraction of protein and amino acids from deoiled rice bran by subcritical water hydrolysis. *Bioresour Technol* 99:555–561.

Singleton VL, Orthofer R, Lamuela-Raventós RM (1999) Analysis of Total Phenols and Other Oxidation Substrates and Antioxidants by Means of Folin-Ciocalteu Reagent. *Methods Enzymol* 299:152–178.

Thiruvenkadam S, Izhar S, Yoshida H, Danquah MK, Harun R (2015) Process application of Subcritical Water Extraction (SWE) for algal bio-products and biofuels production. *Appl Energy* 154:815–828.

Toor SS, Rosendahl L, Rudolf A (2011) Hydrothermal liquefaction of biomass: A review of subcritical water technologies. *Energy* 36:2328–2342.

Yoshida H, Tavakoli O (2004) Sub-critical water hydrolysis treatment for waste squid entrails and production of amino acids, organic acids, and fatty acids. *J Chem Eng Japan* 37:253–260.

Zainan NH, Thiruvenkadam S, Danquah MK, Harun R (2020) Biochemical analysis and potential applications of aqueous and solid products generated from subcritical water extraction of microalgae Chlorella pyrenoidosa biomass. *J Appl Phycol* 32:111–126.

CHAPTER 2

Effect of heating rate and residence time on subcritical water macroalgae residue hydrolysis

Based on the article:

Trigueros E., Sanz M.T., Beltrán S., Alonso-Riaño P., Ramos C.

"Effect of heating rate and residence time on subcritical water macroalgae residue hydrolysis".

(Submitted to Journal of Cleaner Production)

Capítulo 2

Efecto de la velocidad de calentamiento y el tiempo de residencia en la hidrólisis de residuos de macroalga con agua subcrítica

Resumen

Se ha estudiado la valorización del residuo sólido procedente del alga roja tras la extracción del agar mediante el empleo de agua subcrítica. Los experimentos se llevaron a cabo en un reactor de lecho fijo semicontinuo a 185 °C empleando como sistema de calentamiento una camisa calefactora. El uso de una sección de by-pass para calentar el agua antes de entrar en contacto con la muestra, evitó la exposición de la biomasa a altas temperaturas durante el período de calentamiento, reduciendo así la formación de productos de degradación. Se determinaron las distintas curvas de hidrólisis para la fracción de polisacáridos (glucosa, galactosa, arabinosa, ácidos urónicos y productos de degradación) y la fracción proteica a distintos tiempos de residencia. Disminuyendo el tiempo de residencia, se obtuvieron tasas de hidrólisis mayores debido a la mejora en la difusividad de los productos de hidrólisis hacia la disolución. Se estableció una relación de tipo Arrhenius entre la tasa inicial de hidrólisis y el tiempo de residencia. Se determinó una dependencia del tiempo de residencia similar para la fracción de carbohidratos y de proteínas, sin embargo, la liberación de aminoácidos libres mostró menor dependencia del tiempo de residencia, debido a mayores coeficientes de difusión para moléculas pequeñas.

Palabras clave: extracción con agua subcrítica (subW), calentamiento, tiempo de residencia, biorrefinería, residuos macroalga, biocompuestos.

Abstract

The valorization of the underexploited solid residue after agar extraction from red marine algae was studied by subcritical water treatment. Experiments were carried out in a semicontinuous fix-bed reactor configuration at 185 °C by heating the system by means of an oven or a heating jacket. The use of a by-pass section to heat the water previous contact to the sample, avoided the exposure of the biomass to high temperatures during the heating procedure, reducing the formation of degradation products. Hydrolysis curves were determined at different residence times for the polysaccharide fraction (glucose, galactose, arabinose, uronic acids and degradation products) and the protein fraction. By decreasing the residence time, higher initial hydrolysis rates were obtained due to enhancing diffusion of the hydrolysis products into the bulk solution. An Arrhenius type relationship was established between the initial hydrolysis rate and the residence time. It was determined a similar dependence of residence time for carbohydrates and the protein fraction but the release of free amino acids was less dependent of the residence time due to higher diffusion coefficients for small molecules.

Keywords: subcritical water extraction (subW), heating, residence time, biorefinery, macroalgae by-products, biocompounds.

1. Introduction

Subcritical water (subW) is pressurized water in its liquid state in the temperature range from 100 °C to 374 °C (T_c = 374 °C, p_c = 22 MPa). Under these conditions, water presents unique properties such as H-bonding weakening allowing dissociation of water into hydronium ions (H_3O^+) and basic hydroxide ions (OH^-), thus leading to higher ionization constant, K_w. Also, at these conditions, the dielectric constant of water drops from 80 to 20, which allows the solubilization of different organic compounds in subcritical water (Kumar et al., 2010). Due to its properties, subW is an attractive alternative solvent to be integrated in the valorization process of different sources of biomass for hydrolysing and dissolving its different components in order to obtain high added-value products with application in food, cosmetic and pharma industries. The use of subW meets the green chemistry and green chemical engineering concepts, avoiding the use of harsh reagents and minimizing the environmental impact (Pińkowska et al., 2019).

Among the different types of biomass, algae biomass presents several advantages as feedstock since algae productivity is higher than for terrestrial plants, they are lignin-free and not used as a food crop (Jang et al., 2012; Thiruvenkadam et al., 2015). The use of subW to valorize different marine algae in a biorefinery context has been recently reviewed (Ciko et al., 2018). Nevertheless, valorization of industrial by-products from marine algae has been hardly considered.

Phycocolloids are the main commercial seaweed extracts. However, during processing, only 15-30 % of the total dry mass of seaweed is used and important amounts of waste are generated (Álvarez-Viñas et al., 2019). *Gelidium* (Rhodophyta *Gelidiaceae*) is a red alga used as the major seaweed resource in the Spanish agar industry, providing a high quality agar. The industrial extraction process generates a solid residue that is usually disposed of, although it presents a valuable chemical composition since it still contains an important fraction of polysaccharides and a high protein content with all the essential amino acids (Trigueros et al., 2021).

Most of the works reported in the literature have been carried out in a static mode (Ciko et al., 2018). In this operation mode, a certain amount of the biomass is charged in a batch reactor and put in contact during a certain time with water in subcritical conditions. In a previous work on our group, subW treatment was carried out in a semi-continuous fixed bed reactor to hydrolyse and recover the protein fraction of the industrial solid by-product generated after agar extraction from the red algae *Gelidium sesquipedale* (Trigueros et al., 2021). In a semi-continuous reactor, there is a continuous supply of fresh water enhancing the mass transfer due to high concentration gradients at the solid-liquid interface (Gallina et al., 2018). In this configuration, more than the 70 % of the protein fraction was recovered. Experimental conditions such as temperature and flow rate determined the degree of hydrolysis, as well as the formation of degradation products from biomass. However, other important variables must be also considered, such as reactor size and geometry. The heating rate has been also identified as a key parameter in the subW treatment of the biomass and it also influences the degree of hydrolysis obtained (Brand et al., 2014). Furthermore, heating effects are also important in technical applications for the design of the heat exchanger (Sinağ et al., 2004). In literature, many of the subW heating set-ups consist of a preheating coil placed inside an oven together with the subW reactor. However, the heating of water can also be reached by using a heating jacket or belt (Zhang et al., 2020).

The aim of this work was to study the effect of the heating mode, reactor size and residence time on the hydrolysis and degradation rate of the components from the solid residue generated after agar extraction. A detailed characterization of biomass and its hydrolysis products, including carbohydrates, uronic acids and protein fraction was carried out to help to understand the effect of the above experimental conditions on the kinetics and yield of the process.

2. Materials and methods

2.1 Raw material

The raw material consisted of the industrial solid residue from *Gelidium sesquipedale* after agar extraction and it was kindly provided by Hispanagar (Burgos, Castilla y León, Spain, (https://www.hispanagar.com/es). It was oven dried at 45 °C and the final moisture content of the macroalgae residue (MR), 5.0 ± 2.4 %, was determined gravimetrically by weighing it before and after drying in an oven at 105 °C until constant weight. Sample moisture was used to express results per gram of dried MR (DMR).

A complete chemical characterization of the MR was performed according to the National Renewable Energy Laboratory (NREL) standard protocols to determine total extractives, structural carbohydrates, lignin, moisture, total solids, ash and protein (Sluiter et al., 2010). Uronic acids were determined according to the method of Filisetti-Cozzi (Filisetti-Cozzi & Carpita, 1991; Manns et al., 2013). A detailed description of the experimental procedures has been reported elsewhere (Trigueros et al., 2021). Chemical composition has been listed in **Table 2.S-1**.

2.2 Subcritical Water Equipment

Experiments were carried out in two different fixed-bed reactors of different size by using different heating modes. In the first configuration, a fixed-bed reactor (length 20.6 cm and internal diameter of 2.8 cm) was placed inside an oven (Selecta T 204A). A detailed description of this configuration can be found elsewhere (Trigueros et al., 2021). Briefly, 7 g of MR were placed inside the reactor and water was heated up to the desired working temperature by circulating it through a preheating coil (60 cm of 1/8" AISI 316 piping) placed also inside the oven. In this configuration, the sample is subjected to high temperature during the heating procedure. In the second configuration, a smaller reactor was used (length 20.3 cm and internal diameter of 1.3 cm) with 2.3 g of MR loaded into the reactor (**Figure 2.1**). In this case, water was heated up by circulating through the preheating coil

rolled up on the heating jacket. A second heating jacket covering the reactor allows to keep temperature during total treatment time. The reactor vessel loaded with the biomass was first flooded with a small amount of water and kept around 70 °C until water circulating through the preheating coil reached the selected temperature by-passing the reactor vessel. Then, the by-pass section was closed allowing the hot and pressurized water to circulate through the reactor at the working temperature. This way, the exposure of the biomass to heat during the heating procedure is avoided.

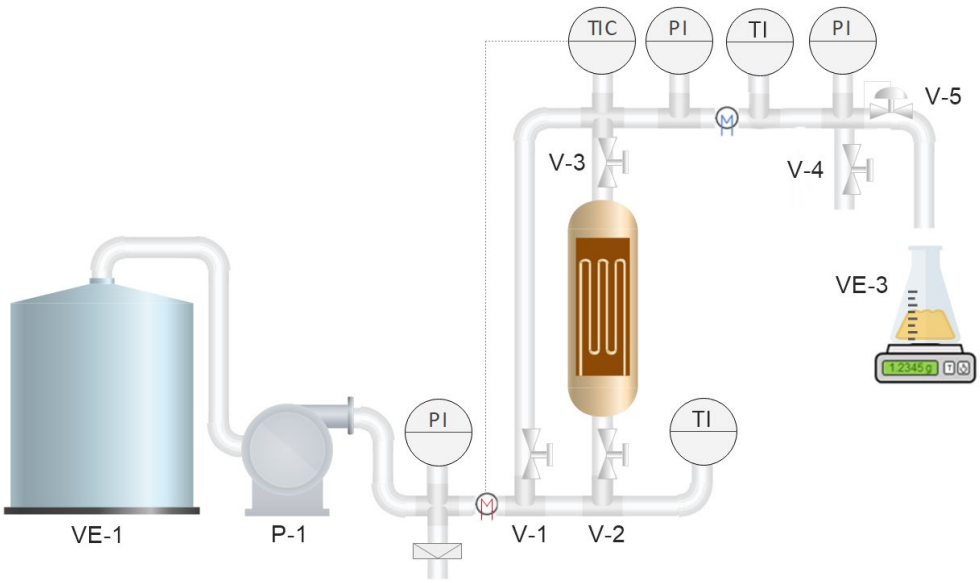

Figure 2.1. Subcritical water equipment provided by a by-pass system.

In both configurations, an HPLC pump (Gilson 305, SC-10 head with a maximum flow of 10 mL/min) was used for pressurization and water pumping at different flow rates. Two metallic filters were place at the top and the bottom of the reactors to avoid loss of solid particles and clogging of the system. Pressure was controlled by a pressure regulating valve (pressure Tech 6784 V962 max 414 bar). Temperature was continuously registered with Pt100 sensors at different points of the experimental set ups including the inlet and outlet of the reactor. Pt 100 sensors were connected to PID systems that controlled the temperature of the heating elements. Initial zero time was taken to be the time at which liquid extract was obtained at the outlet pipe. Effluents were cooled and periodically

collected for later characterization. Results were calculated as accumulative values along treatment time. The yields of the different biomass components were evaluated as the ratio of the mass of the component determined in the subW extracts and the total amount of such component in the raw material.

Four experiments were carried out: one experiment in the first configuration at 185 °C and a working flow rate of 2 mL/min and three experiments in the second configuration at 185 °C and different working flow rates in the range from 4 to 8 mL/min. Taking into account the reactor volume and working flow rate, the residence time for the water in the reactor, τ, was evaluated as:

$$\tau = \frac{V}{F_v} = \frac{V}{F_{v,o}} \frac{\rho_r}{\rho_o} \qquad [\mathbf{2.1}]$$

where V is the reactor volume in m^3 calculated with the dimensions of the reactor, $F_{v,o}$ the flow rate measured at ambient conditions in m^3/s, ρ_o is the water density at ambient conditions and ρ_r the water density at the reaction conditions. The calculated residence times were 56.2 min in the first configuration and 3, 4.2 and 6 min in the second configuration, decreasing by increasing flow rate.

The solid residue that remained in the reactor after subW treatment was washed, oven dried at 45 °C until constant weight, weighted and analyzed. The hydrolysis yield at the end of each experiment was evaluated as:

$$Hydrolysis\ yield\ (\%) = \frac{MR_{initial\ weight} - MR_{after\ subW\ weight}}{MR_{initial\ weight}} \cdot 100 \qquad [\mathbf{2.2}]$$

2.3 Analytical methods

2.3.1 Polysaccharide fraction

Identification and quantification of polysaccharides and their degradation products were performed by HPLC equipped with a Biorad Aminex-HPX-87 H column (300 × 7.8 mm, Bio-Rad) and its corresponding pre-column, with two detectors, a variable wavelength detector

(VWD) and a refractive index detector (RID) using 0.005 M sulfuric acid as mobile phase with a flow rate of 0.6 mL/min. The column and RID detector were maintained at 40 °C. Monosaccharides and degradation products were directly analyzed in the subW hydrolysates previously filtered through a 0.22 µm pore size syringe filter (Scharlab). Total sugars were determined after sample hydrolysis according to the Laboratory Analytical Procedure (Sluiter et al., 2010) to hydrolyze all the oligomers into monomeric sugars. Sugar yield was calculated as monomer yield and oligomer yield (Sánchez-Bastardo et al., 2017):

$$Monomer\ yield\ (\%) = \frac{Monomeric\ sugar\ in\ the\ hydrolysate}{Sugar\ in\ the\ raw\ material} \cdot 100 \qquad [\mathbf{2.3}]$$

$$Total\ yield\ (\%) = \frac{Monomeric\ and\ oligomeric\ sugar\ in\ the\ hydrolysate}{Sugar\ in\ the\ raw\ material} \cdot 100 \qquad [\mathbf{2.4}]$$

The standards employed for the HPLC analysis were cellobiose (99 %), glucose (99.5 %), xylose (99 %), rhamnose (99 %), galactose (99 %), arabinose (99 %), mannose (99 %), glyceraldehyde (98 %), glycoaldehyde (99 %), acrylic acid (99 %), pyruvaldehyde (40 %) and furfural (99 %) purchased from Sigma Aldrich (Spain); fructose (99 %), lactic acid (50 %) and formic acid (98 %) purchased from Fluka; 5-hydroxymethilfurfural (97 %) from Alfa Aesar; acetic acid (99.8 %) from VWR Chemicals and levulinic acid (98 %) from Merck.

2.3.2 Protein content and free amino acids

Protein content in raw material was estimated from the elemental nitrogen content present in the samples by using the corresponding N-factor of 4.9 as previously reported by Trigueros et al. (Trigueros et al., 2021). Nitrogen in the subW extracts was determined by using a Shimadzu TOC-V CSN analyzer using KNO_3 as standard.

The amino acid profile of the MR and the free amino acids in the subW extracts were analyzed by gas chromatography by using the EZ:faast kit (Phenomenex). It consists of a solid phase extraction followed by derivatization and a final liquid/liquid extraction. The derivatized amino acids were analyzed using a GC-FID instrument (Hewlett Packard; HP, 5890 Series II) equipped with an auto-sampler (Avondale, PA, USA). Details of the experimental procedure can be found elsewhere (Trigueros et al., 2021).

The hydrolysis degree (DH) in the subW extracts was evaluated by the ninhydrin reaction method according to the Sigma Aldrich protocol previously described in detail (Trigueros et al., 2021). A calibration curve was obtained by using a leucine solution that was prepared daily (Friedman, 2004). The DH was obtained as (Adler-Nissen et al., 1983):

$$DH = h/h_{tot} \cdot 100\ (\%) \quad [\mathbf{2.5}]$$

where *h* is the number of equivalent peptide bonds hydrolyzed expressed as $m_{eq}/g_{protein}$ and h_{tot} is the total amount of milimols of individual amino acids per gram in the unhydrolyzed protein that can be evaluated from the amino acid profile of the raw material. It must be highlighted that most amino acids react with ninhydrin but also primary and secondary amines.

2.3.3 Total organic carbon

A Total Organic Carbon (TOC) Analyzer Shimadzu (TOC-V CSN) was used to quantify the concentration of total carbon (TC) and inorganic carbon (IC). Potassium hydrogen phthalate and sodium hydrogen carbonate were used as standards. Then, TOC concentration was calculated by subtracting the IC concentration from the obtained TC concentration.

2.3.4 Total Polyphenols Content (TPC) and Antioxidant Activity

TPC was determined by using the Folin–Ciocalteu reagent following the method described by Singleton (Singleton et al., 1999). A calibration curve was prepared with standard solutions of gallic acid by following the same colorimetric method. Results were expressed as mg of gallic acid equivalent (GAE) per gram of DMR.

The FRAP method was used to determine the antioxidant activity. It was performed according to Benzie and Strain (Benzie & Strain, 1996). As standard, a solution of 0.1 M $FeSO_4 \cdot 7H_2O$ was used. Results were expressed in µmoles of Fe^{2+} per gram of DMR.

2.4. Statistical Analysis

All values were expressed as mean ± standard deviation of at least three replicates. To confirm significant differences, the Fisher's least significant differences (LSD) method at p-value ≤ 0.05 was applied. Correlations between variables were determined by the Pearson correlation method. Analysis were carried out by the Centurion Statgraphics software.

3. Results and discusión

3.1 Macroalgae residue characterization

Table 2.S-1 collects the chemical composition of the solid residue from the red macroalgae used in this work. The composition of fresh *Gelidium sesquipedale* before agar extraction was also presented for comparison. Extractives and galactans content decreased after agar extraction. This fact is consequence of agar extraction process, since agar is a mixture of two components: agarose, a linear polysaccharide made up of repeating sequences of (β-1→4) linked 3,6-anhydro-L-galactopyranose and (α-1→3) linked D-galactose, and agaropectin, a sulphated galactan with different percentages of ester sulfates, pyruvic acid and D-glucuronic acid (Araki, 1956). Furthermore, extractives were also reduced in the MR as a result of soluble compounds extraction together with agar (Duckworth & Yaphe, 1971). As a result, the percentage of other compounds, such as glucans, arabinans, proteins and ashes, is higher in the MR than in fresh algae. Uronic acids mass percent in the MR was 3.8 ± 0.1 % while only slightly higher mass percent was determined in fresh algae (4.3 ± 0.1 % (w/w)). Uronic acids are highly valuable chemicals used in the pharmaceutical, cosmetic and food industries due to its potential as platform chemicals (Pińkowska et al., 2019). The value of uronic acids determined in this work was lower than the value reported by Cui et al. (Cui et al., 2019) in a purified polysaccharide fraction from *Gelidium pacificum* and also lower than the value reported by Mohamad (Mohamad et al., 2017), who determined nearly 20 % of uronic acids in this polysaccharide fraction. For fresh *G. sesquipedale*, uronic acids accounted for 11.3 % of the total carbohydrates.

3.2 Heating rate

The temperature profile in both reactor configurations is presented in **Figure 2.2**. When the oven was used as the heating element, the biomass was exposed to high temperature during the time needed to reach the selected working temperature, approximately 60 min. However, in the second configuration, water entered the reactor when the working temperature was reached in the by-pass configuration (time zero). The by-pass system reduced the contact time of the biomass with water at high temperatures during the heating procedure and the heating jacket led to higher heating rates compared to the oven system due to the different heat exchange mechanism.

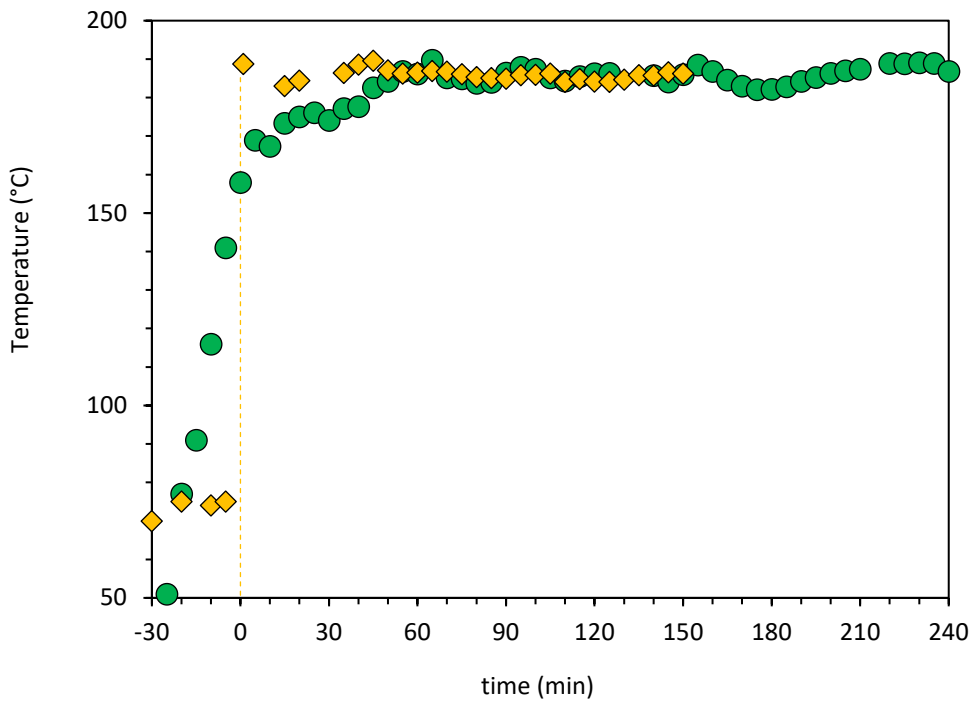

Figure 2.2. Temperature profile for the different reactor configurations to reach 185 °C (● first configuration: $V_{reactor}$ = 127 cm^3 and oven as heating element; ◆ second configuration: $V_{reactor}$ = 27 cm^3 and heating jacket as heating element with a by-pass configuration).

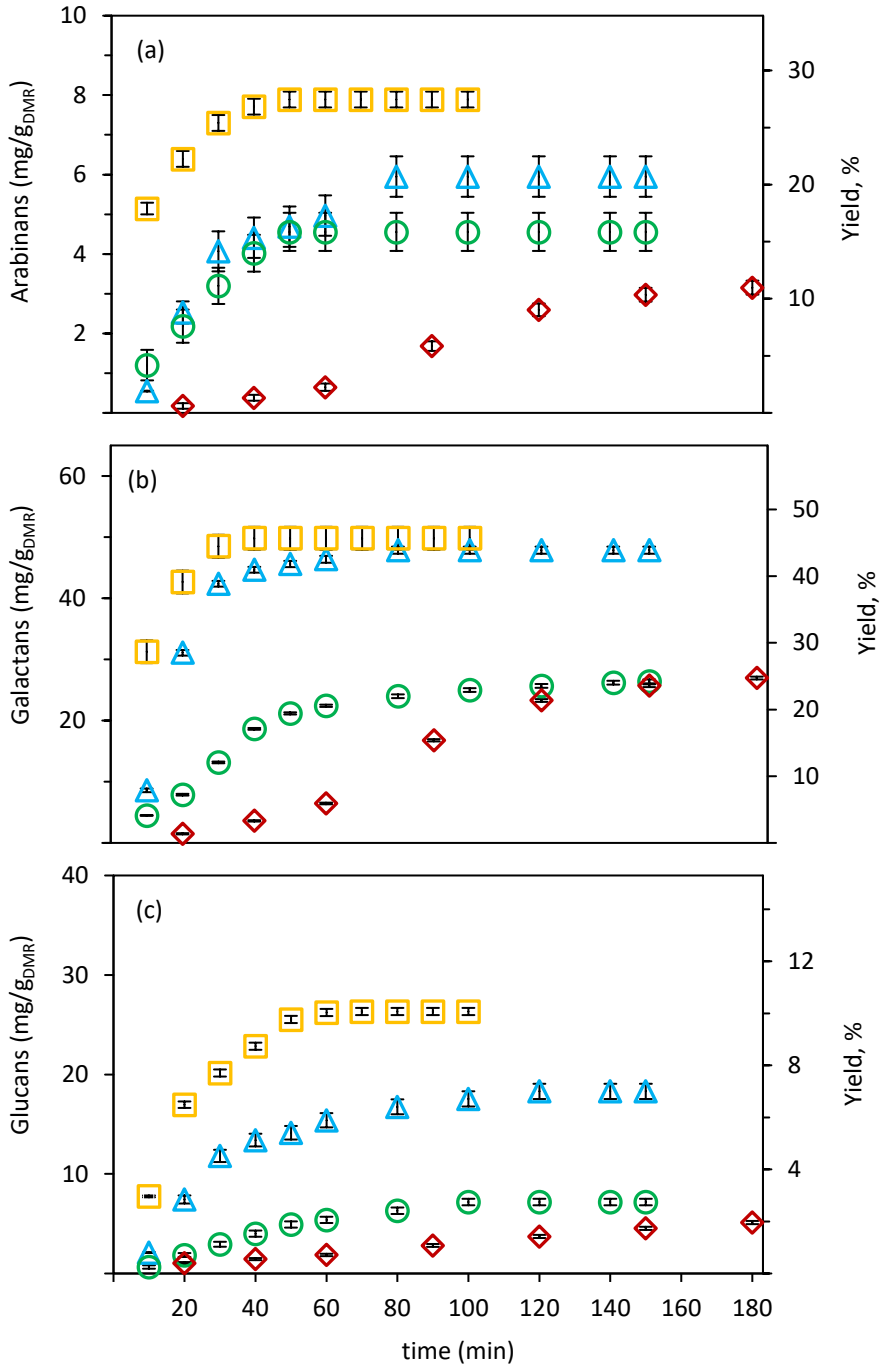

Figure 2.3. Extraction/hydrolysis yield by subW treatment for **(a)** arabinans **(b)** galactans and **(c)** glucans. ($V_{reactor}$ = 27 cm^3 and different residence time: 3 min (□), 4.2 min (△), 6 min (○); $V_{reactor}$ = 127 cm^3, 56.2 min of residence time (◇). T = 185 °C).

3.3 Polysaccharide fraction hydrolysis

Figure 2.3 shows the accumulated hydrolysis curves for arabinans, galactans and glucans expressed as mg/g_{DMR} and percentage yield. At the working conditions selected in this work, the carbohydrate fraction was recovered as sugar oligomers, since no monomers were observed in the subW extracts collected. For all the experiments carried out, preferential hydrolysis was observed for galactans followed by arabinans, with the lowest yield obtained for glucans.

The hydrolysis curves indicated that configuration 2, with the smallest reactor and a heating jacket as heating element, the maximum yield was reached at approximately 40-60 min of subW treatment. However, by using configuration 1, with the biggest reactor inside the oven, the maximum yield was not reached until 160-180 min. The difference in the extraction/hydrolysis rate determined in both configurations can be also observed in **Figure 2.S-1** that shows the elution profile in the concentration of the oligomers in the different subW extracts collected with time. The maximum oligomer concentration was reached earlier, at around 10-20 min, in the experiments performed in configuration 2, with the smallest reactor by using the heating jacket as the heating element. On the other hand, by using configuration 1, with the oven as the heating element and the biggest reactor, the maximum level of oligomer concentration in the extracts was reached much later, at around 90 min. It must be highlighted that the high concentration determined for glucans after 20 min of treatment by using the oven as heating element was probably due to the presence of soluble glucans in the extractives that would have been easily extracted during the heating period in the oven (see **Figure 2.2**) since, after this first point, glucans concentration in the extracts sharply decreased due to the lower extraction rate in the oven.

Figure 2.3 shows that the initial slopes of the solubilisation curves increase by decreasing residence time (increasing flow rate), indicating that external mass transfer limitations can play an important role in the transport of the soluble oligomer carbohydrates from the biomass surface to the bulk of the solvent. Liu & Wyman (Liu & Wyman, 2003) studied the effect of flow rate of subW on hemicellulose removal from corn stover concluding that water could hydrolyze long-chain oligomers more slowly than short chain oligomers. Therefore, long chain oligomers could build up on the biomass surface creating an “icelike”

layer, due to slower dissolution and diffusion than shorter oligomers that slows the access of water to carbohydrates. An increase in flow rate would decrease the thickness of this "icelike" layer enhancing diffusion of oligomers into the bulk solution. This effect led to an increase in carbohydrate solubilisation, as can be observed in **Figures 2.3** and **2.S-1**. The initial extraction rate of oligomers at the different flow rates (or residence time) essayed in this work were evaluated through the initial slope of the accumulated curves expressed as percentage yield, for a better comparison between the different carbohydrates. An Arrhenius type relationship was established between the initial rate and the residence time (evaluated from **Equation 2.1**):

$$r_o = k \cdot exp\left(\frac{E_{diff}}{\tau}\right) \qquad [\mathbf{2.6}]$$

where r_o is the initial extraction rate (min^{-1}), τ is the residence time (min) and k and E are parameters obtained by fitting experimental data. The linear regressions of **Equation 2.6** are shown in **Figure 2.4a**. **Table 2.1** shows the quality of the fitting together with statistical significance of the terms in the model to compare the different regression lines. There were not statistically significant differences among the slopes at the 90 % or higher confidence level while there were statistically significant differences among the intercepts at the 99 % confidence level. The higher the value of the intercept, the higher the extraction/hydrolysis rate for the oligomer, following the order galactans, arabinans and glucans. However, the similar values of the slopes of the linear regression showed that the effect of increasing flow rate (decreasing residence time) on oligomer hydrolysis/solubilisation was of the same order regardless the type of oligomer.

In subW treatment, it is usually defined (a) hydrolysis products as the combination of oligomers and monomers of polysaccharides, (b) degradation products such as organic acids, hydroxymethyl furfural (HMF) and furfural and retroaldol condensation products of C6 sugars such as glycoaldehyde or glyeraldehyde (Sasaki et al., 2000). **Figure 2.5** shows the final extraction/hydrolysis yield for oligomers as a function of the residence time, together with the total production of the degradation products identified in this work. According to **Figure 2.3**, oligomers yield decreased by increasing residence time (decreasing flow rate) because of higher degradation products concentration. Therefore, lower residence times

reduce the degradation reactions leading also to higher yields of carbohydrates. Sugar degradation products identified in the subW experiments carried out in the smallest reactor included mainly furfural, hydroxymethylfurfural (HMF) and acetic and formic acids. HMF is a typical product of glucose degradation in subW (Sinağ et al., 2004) while furfural is the major degradation product from pentoses. Due to the low amount of pentoses in the raw material, the amount of furfural detected in the subW extracts was much lower than the amount of HMF, being less than 15 % of the total amount of HMF.

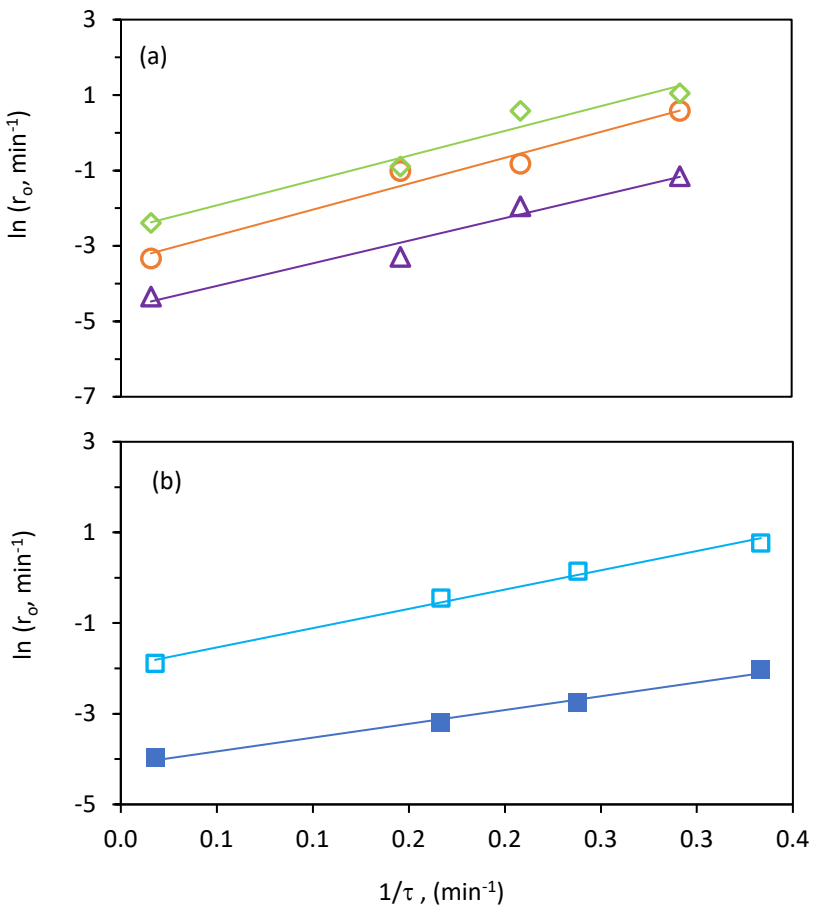

Figure 2.4. Arrhenius relationship of the different biocompounds: Initial extraction/hydrolysis rate as a function of the residence time in the reactor. **(a)** Glucans (△), arabinans (○), galactans (◇), **(b)** protein fraction (□), free amino acids (■). T = 185 °C.

Table 2.1. Linear regression parameters from Arrhenius type relationship of initial extraction rate and residence time, **Equation 2.6**, for different chemical compounds: $\ln r_o = \ln k + E_{diff}/\tau$

Compounds	Slope	Intercept	R^2
Galactans	11.5 ± 1.6[b,c]	-2.58 ± 0.35[d]	0.9628
Arabinans	12.0 ± 1.5[c]	-3.41 ± 0.33[c]	0.9692
Glucans	10.5 ± 1.4[b,c]	-4.66 ± 0.31[a]	0.9658
Protein fraction	8.5 ± 0.6[b]	-1.96 ± 0.13[d]	0.9912
Amino acids	6.1 ± 0.4[a]	-4.14 ± 0.09[b]	0.9906

Different letters in each column indicate that there are statistically significant differences among the slopes at the 90 % of higher confidence level and among the intercepts at 95 % confidence level.

For the experiment carried out in the biggest reactor, other organic acids were also quantified such as succinic, lactic and levulinic acids. In this work, products from retroaldol condensation of C6 sugars such as glycoaldehyde or glyeraldehyde were not detected in the subW extracts.

Among the different polysaccharides determined in the raw material, uronic acids present a great attractive due to its potential as platform chemicals. Galacturonic acid was the most abundant uronic acid determined in the subW extracts with small amounts of glucuronic acid. The final extraction yield obtained from the sum of the individual uronic acids content in all the subW extracts collected along the extraction time has been represented in **Figure 2.6**, expressed as mg/g_{DMR} and percentage yield. The uronic acids yield increased with decreasing residence time due to an enhancement of external mass transfer limitation, as previously explained, but also to a reduction in the degradation of the already solubilized uronic acids due to shorter residence times inside the reactor at high temperatures. As reported in the literature, some characteristic products of uronic acids thermal degradation are 2-furancarboxylic and 5-formyl-2-furancarboxylic acids but these compounds were not measured in this work (Li et al., 2007). In **Figure 2.6**, it can be also observed that by decreasing residence time, galacturonic acid is mainly released as monomer.

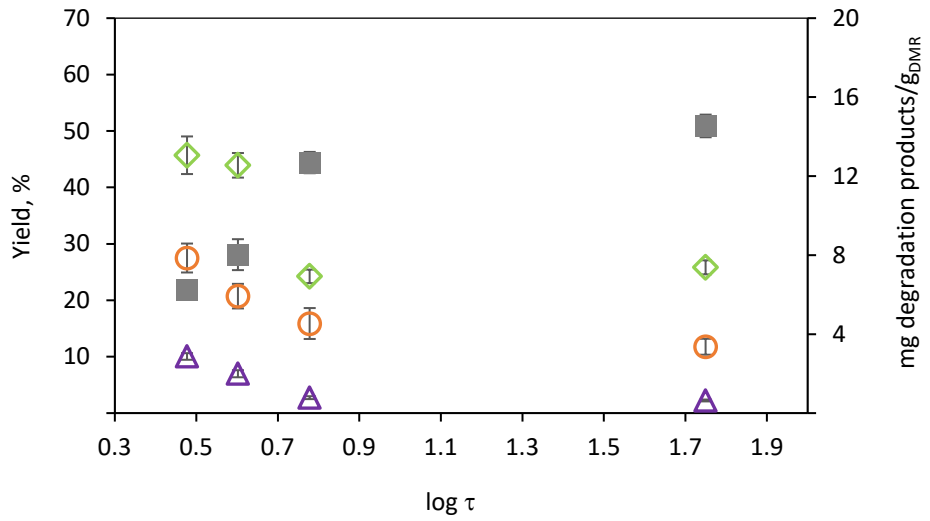

Figure 2.5. Final extraction/hydrolysis yield for the different polysaccharides oligomers as a function of the residence time in the different reactor configurations: glucans (△), arabinans (○), galactans (◇). Final yield of sugars degradation products (■). T = 185 °C.

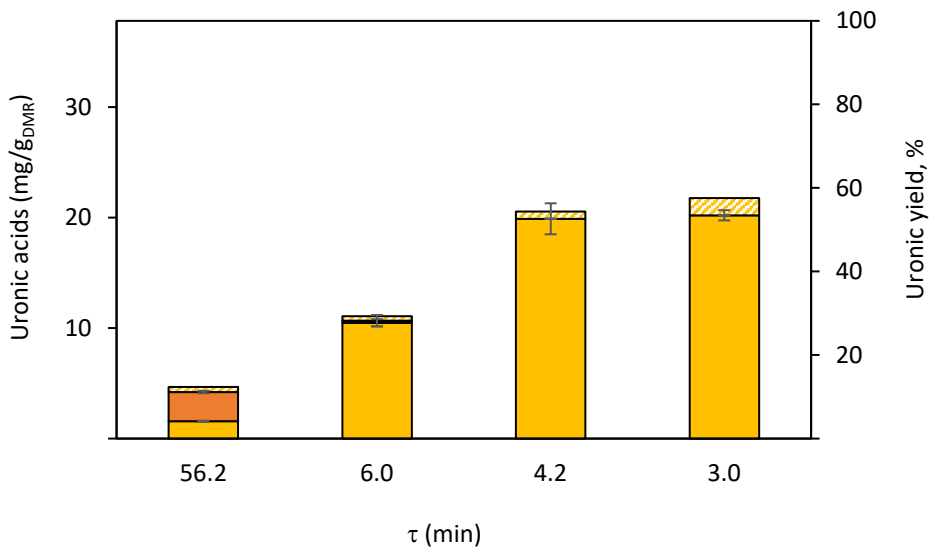

Figure 2.6. Uronic acid yield as a function of the residence time in the different reactor configurations: galacturonic acid as monomer (■) and oligomer (■); glucuronic acid as monomer (▨). T = 185 °C.

3.4 Protein fraction

The solubilisation of the protein fraction of the MR is presented in **Figure 2.7a**. The solubilized protein fraction in the subW extracts was evaluated from the nitrogen content in the extracts, obtained from TOC analyzer measurements by applying the same N conversion factor as for the raw material. The N conversion factor of the macroalgae residue was evaluated from the amino acid profile listed in **Table 2.S-2** and previously evaluated as 4.9 (Trigueros et al., 2021). The low value of the N conversion factor, compared to the commonly used value of 6.25, is due to the presence of non-protein nitrogen compounds such as pigments and inorganic nitrogen (nitrite, nitrate and ammonia) that led to lower NF for algae species (Lourenço et al., 2004). Lourenco et al. (Lourenço et al., 2002) determined an average value of 4.6 ± 0.5 for nine red algae species, with an overall average NF of 4.9 ± 0.6 for different macroalgae species including red, brown and green.

By working at the lowest residence time essayed in this work, 3 min, nearly 100 % of the protein content was recovered in the subW extracts. A comparison of **Figures 2.3** and **2.7** showed higher hydrolysis yields of the protein fraction than of the carbohydrate fraction for all the experiments carried out. This could be attributed to the fact that proteins were not bonded as strongly as the carbohydrate fraction to the algae structure and they were more easily extracted (Pronyk et al., 2011).

A small fraction of the protein content was hydrolysed as free amino acids in the subW extracts (see **Figure 2.7b**). The free amino acids yield was evaluated as the ratio of the sum of all the individual amino acids determined by gas chromatography in the collected subW extracts and the sum of individual amino acids determined in the raw material. The highest free amino acid yield, around 8 %, was obtained for the experiments carried out in the smallest reactor and the lowest residence time. As an example, for the experiment carried out at 3 min of residence time, the accumulative yield of the individual free amino acids has been plotted in **Figure 2.8**. Some of the amino acids were not detected in the subW extracts although they were present in the raw material (**Table 2.S-2**), specifically threonine, methionine, glutamic acid, tryptophan and lysine. The absence of tryptophan and methionine could be attributed to its low content in the macroalgae residue (see **Table 2.S-2**). On the other hand, polar amino acids side groups have been reported to present a high

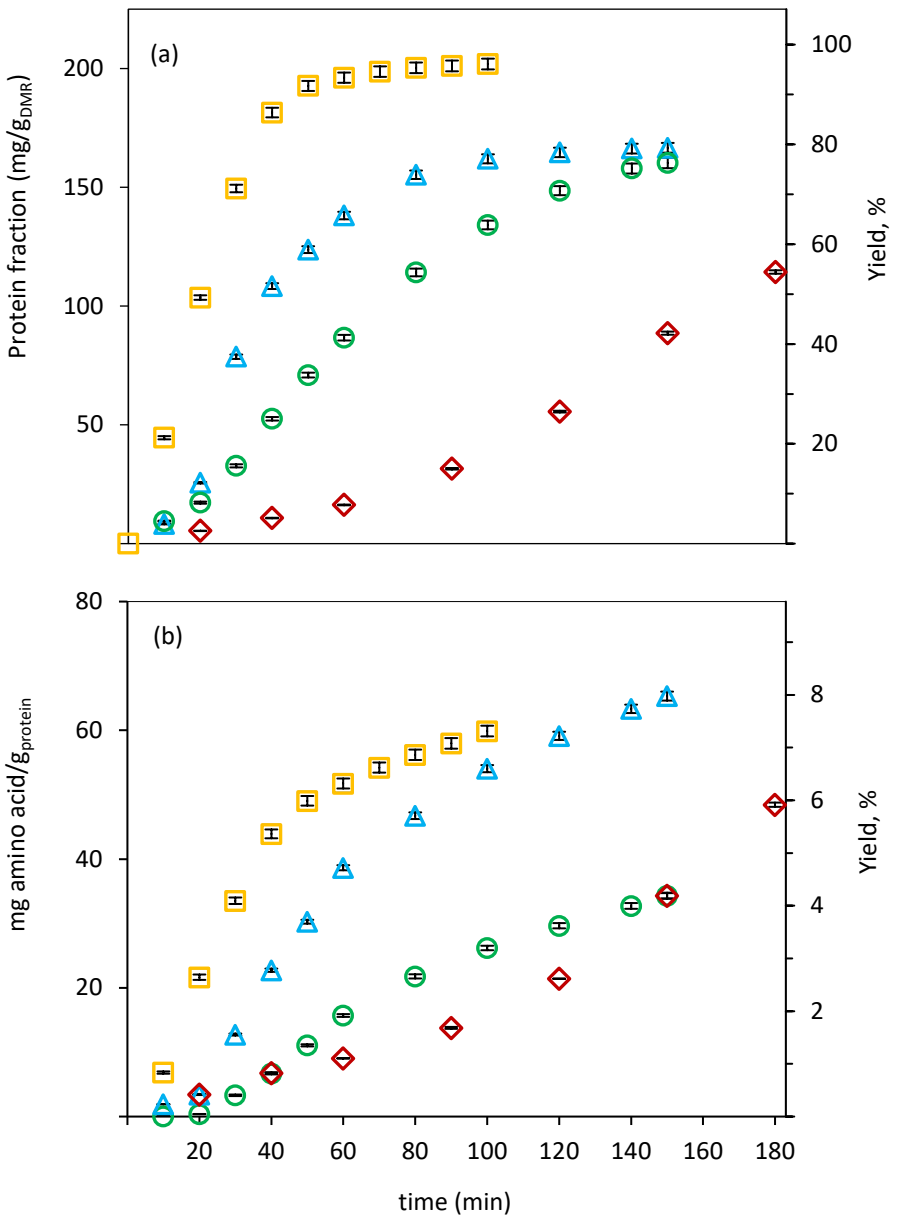

Figure 2.7. Extraction/hydrolysis yield by subW treatment of **(a)** the protein fraction **(b)** free amino acids ($V_{reactor}$ = 27 cm^3 and different residence time 3 min (□), 4.2 min (△), 6 min (○); $V_{reactor}$ = 127 cm^3, 56.2 min of residence time (◇). T = 185 °C.

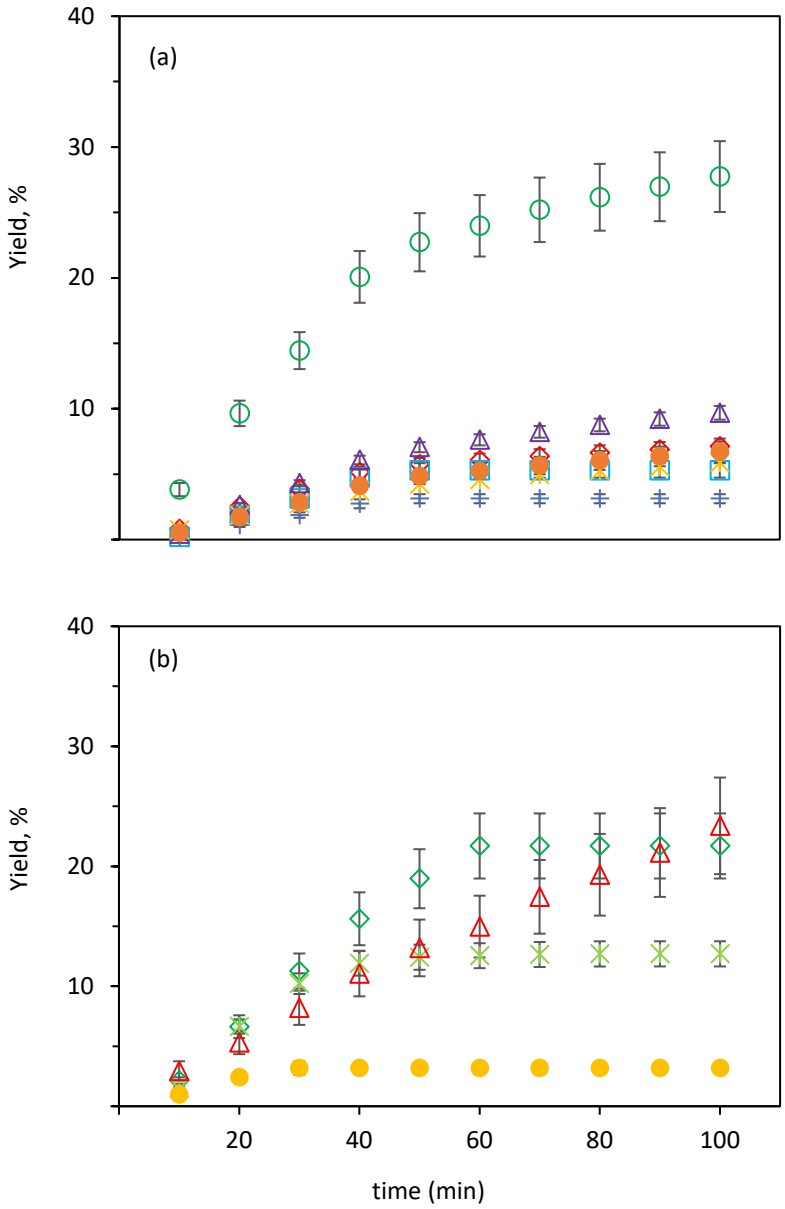

Figure 2.8. Accumulative formation of individual amino acids for a residence time of 3 min and T = 185 °C. Non-polar amino acids **(a)** (◇ alanine, ○ glycine, □ valine, △ leucine, + isoleucine, ✳ proline, ● phenylalanine). **(b)** Polar amino acids (◇ histidine, △ tyrosine, ✳ aspartic acid, ● serine).

tendency to undergo Maillard reactions with carbonyl groups or reducing carbohydrates generated during subW treatment (Lamp et al., 2020). This could justify the low or null yield obtained for threonine, lysine, glutamic and serine. The highest free amino acid yield was obtained for the non-polar amino acid glycine, which is the smallest amino acid. High molecular weight amino acids are more susceptible to degradation not only to ammonia, organic acids and amines but also to other amino acids of lower molecular weight, which could compensate the degradation of these amino acids (Esteban et al., 2010). Similar results were obtained in a previous work where the temperature effect on free amino acid profile and yield was studied in the subW extracts (Trigueros et al., 2021).

Figure 2.9 shows the relationship between the hydrolysis degree and the total yield extraction of free amino acids obtained as the sum of the individual amino acids determined by GC in the subW extracts in relation to the total in raw material. A good correlation has been stablished between both variables. Person's correlation coefficient between the hydrolysis degree and the total extraction yield of free amino acids indicated a statistically non-zero correlations at the 95.0 % confidence level and positive and strong correlation between both parameters (n = 41, R^2 = 0.958).

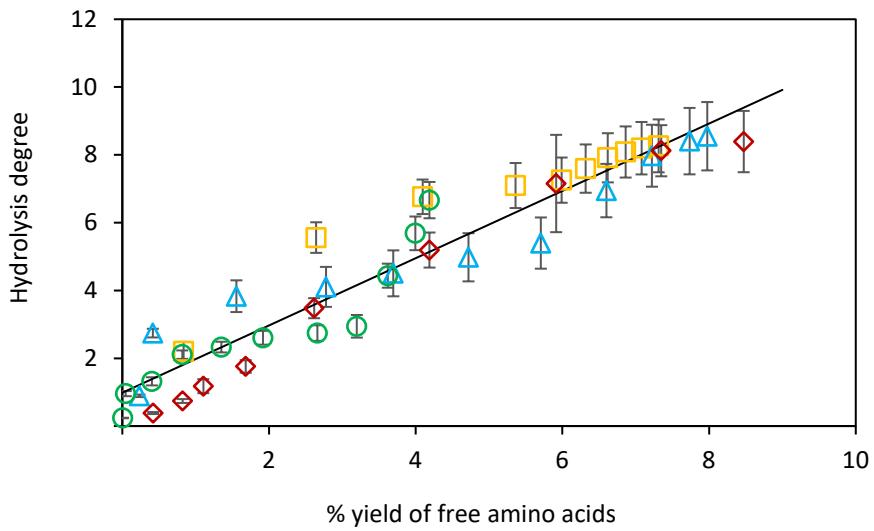

Figure 2.9. Hydrolysis degree as a function of yield percentage of free amino acids as determined by GC (DH = 0.9925 (free amino acids) + 0.984 R^2 = 0.9175). ($V_{reactor}$ = 27 cm^3 and different residence time 3 min (□), 4.2 min (△), 6 min (○); $V_{reactor}$ = 127 cm^3, 56.2 min of residence time (◇). T = 185 °C.

The effect of flow rate on the protein fraction hydrolysis, as small peptides or free amino acids, was similar to the one described for the polysaccharide fraction. The initial extraction/hydrolysis rate increased with flowrate (decreasing residence time), which proved that external mass transfer limitations could play an important role, since higher flow rates would help to enhance diffusion of hydrolysed peptides and amino acids from the biomass surface to the water bulk, similar to the theory proposed by Liu & Wyman (Liu & Wyman, 2003) for hemicellulose dissolution from corn stover in subcritical water. On the other hand, lower residence times would lead to a decrease of the degradation of peptides and amino acids obtaining higher hydrolysis yields. The initial extraction/hydrolysis rate of peptides and free amino acids at the different residence times essayed in this work has been evaluated through the initial slope of the accumulated curves expressed as percentage yield. As for carbohydrates, an Arrhenius type relationship was established between the initial rate and the residence time according to **Equation 2.6** (see **Figure 2.4b**). Parameters of the linear model have been listed in **Table 2.1**. The values of the intercept indicated higher yields for protein fraction solubilisation than for free amino acid release. Statistical analyses of the slopes and intercepts for carbohydrates, protein and free amino acid solubilisation showed that there were not statistically significant differences among the slopes at the 90 % of higher confidence level for carbohydrates and proteins, except for proteins and arabinans, but there were statistically significant differences with the free amino acid initial release. The lowest value of the slope for free amino acid release indicates a lower dependence on increasing flow rate due to higher diffusion coefficients in water for small molecules. Longsworth (Longsworth, 1953) carried out diffusion measurements of amino acids, peptides and sugars in aqueous solutions, at 25 °C, finding that an increase in molar volume led to lower diffusion coefficients. They concluded that higher values of diffusion coefficients can be expected in subW due to lower density and viscosity of water at these conditions, but the order in which components would diffuse would not probably change. These authors also found a progressively diminishing reduction of the diffusion coefficient with molar volume; that is, the difference in the diffusion coefficient was greater for the monomer and dimer than for the dimer and trimer. This could explain the similar effect found for carbohydrates (released as oligomers) and peptides when increasing flow rate, while the release of free amino acids (lower slope value of the Arrhenius relationship) was less affected by increasing flow rate, due to higher diffusivity coefficients.

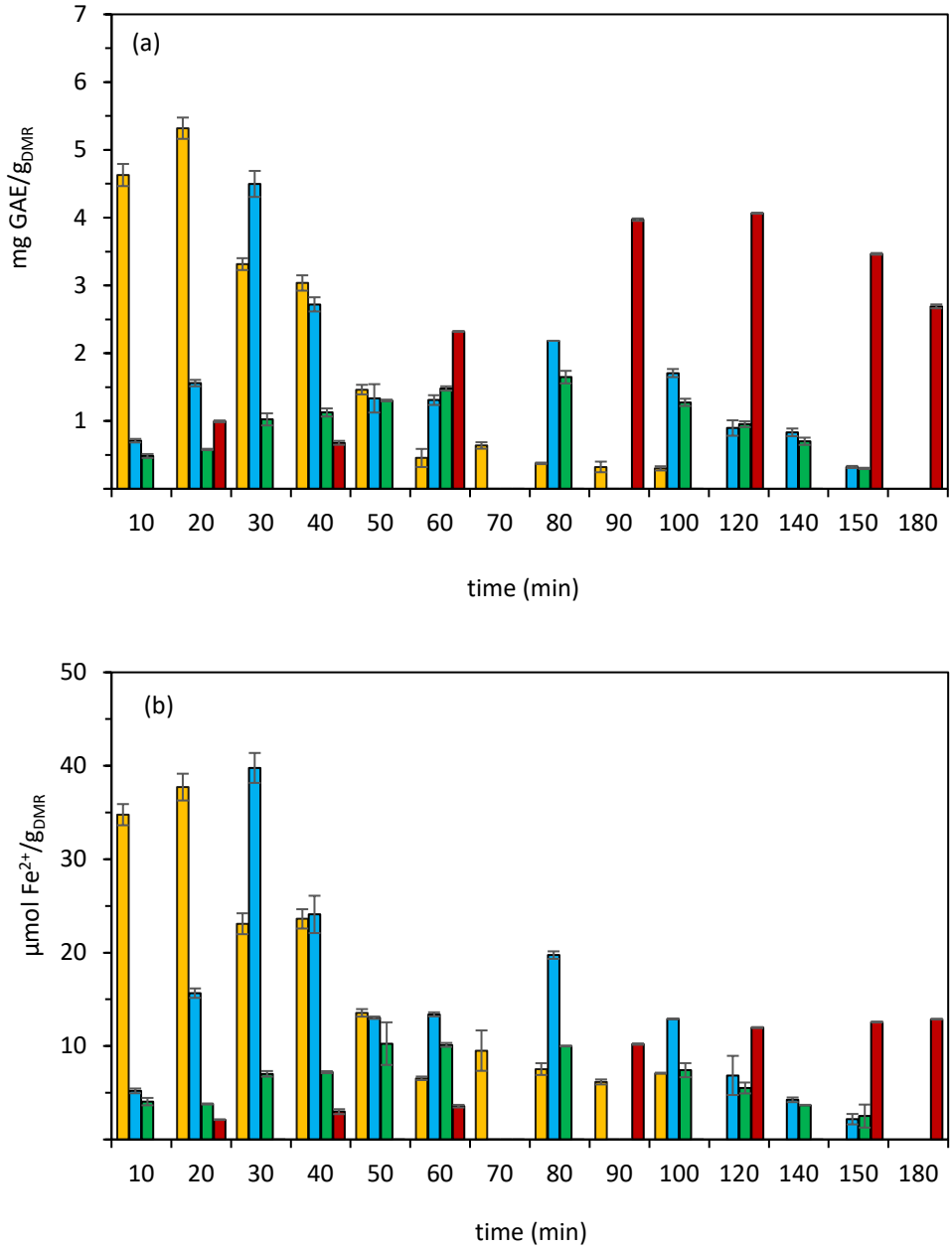

Figure 2.10. **(a)** TPC and **(b)** reducing power of subW extracts collected along the extraction time ($V_{reactor}$ = 27 cm^3 and different residence time 3 min (■), 4.2 min (■), 6 min (■); $V_{reactor}$ = 127 cm^3, 56.2 min of residence time (■). T = 185 °C.

3.5 Total phenolic content and antioxidant activity of SWE extracts

The elution profiles of TPC in the different experiments and the corresponding reducing power, determined according to the FRAP assay, have been plotted in **Figure 2.10**. The maximum TPC release and reducing capacity reached higher levels and appeared sooner by increasing flow rate (decreasing residence time). The analysis of the Pearson product moment correlation indicated a statistically significant non-zero correlation at the 95.0 % confidence level and strong and positive correlation between reducing capacity and TPC (n = 41; R^2 = 0.8137). High TPC final accumulative yield was reached in all the experiments, around 19.9 ± 0.3 mg GAE/g_{DMR}. However, it must be highlighted that, products from browning reactions such as protein-carbohydrate conjugates, melanoidins, and heterocyclic compounds may interfere in the TPC determination by the Folin-Ciocalteu assay and may also contribute to the antioxidant capacity of the collected extracts, as it has been suggested in different publications (Alonso-Riaño et al., 2021; Plaza & Turner, 2015; Trigueros et al., 2021; Wang et al., 2011).

3.6 Total organic carbon in subcritical water extracts and hydrolysis yield

The analysis of TOC in the subW extracts showed faster release of the organic carbon fraction by increasing flow rate as well as higher yields (see **Figure 2.11**). TOC would include solubilized polysaccharides and proteins, as well as their degradation products. Long residence times could have led to degradation of the solubilized products that could also release CO_2 or other gas products, as has been reported in other literature works (Kang & Chun, 2004; Sereewatthanawut et al., 2008). However, gas products were not determined in this work.

The final hydrolysis yield was evaluated according to **Equation 2.2** and showed that the residence time did not have any significant effect on the final hydrolysis yield with values of 63, 61, 59 and 60 % for residence times of 3, 4.2, 6 and 56 min respectively. Similar results were obtained by other authors in the study of hydrothermal treatment of triticale straw,

where flow rate had little effect on dissolved mass (Pronyk et al., 2011). On the contrary, other authors observed that by working at higher flow rates, the reactor loading could become more compact, hindering the mass transfer kinetics (Pinto et al., 2017). Previous work on the same raw material showed an increase on the hydrolysis yield with operating temperature in the range from 129 to 200 °C and a residence time of 56.2 min (Trigueros et al., 2021).

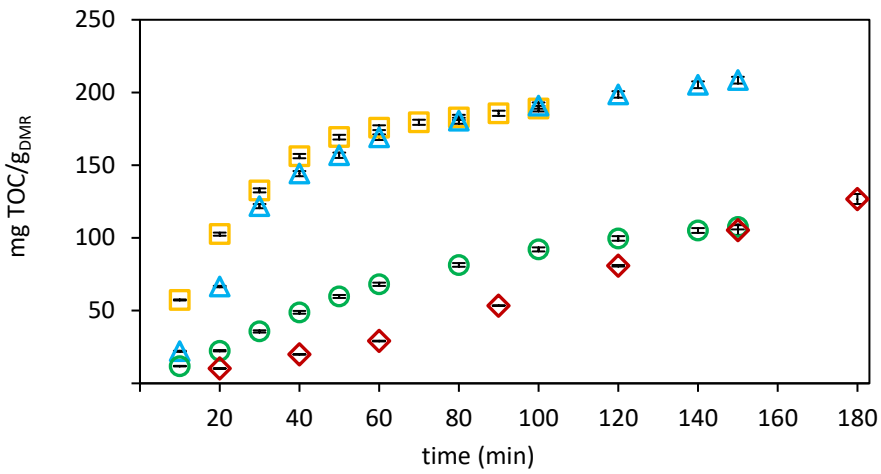

Figure 2.11. Accumulative total organic carbon in the subW extracts ($V_{reactor}$ = 27 cm^3 and different residence time 3 min (□), 4.2 min (△), 6 min (○); $V_{reactor}$ = 127 cm^3, 56.2 min of residence time (◇). T = 185 °C.

Conclusions

The technology of subcritical water allowed hydrolysis of the solid residue generated after agar extraction from red algae. A bypass section before subcritical reactor allowed reaching the operating temperature avoiding the exposure of the sample to high temperatures during the heating procedure. By working at low residence times, higher flow rates, led to higher hydrolysis rates due to enhancing diffusion of hydrolysed biocompounds from biomass surface into the bulk solution. Small release of molecules, such as amino acids, showed a less dependence on increasing flow rate due to higher diffusion coefficients. It was shown no dependence on final hydrolysis yield with residence time.

Supplementary data

Table 2.S-1. Chemical composition of macroalgae residue, MR, expressed as % ± SD in a dry basis.

Compound	*G. sesquipedale*	Macroalgae residue
Extractives	30 ± 2	11.5 ± 0.9
Carbohydrates	38 ± 1	42 ± 2
Glucans	10.7 ± 0.3	23.4 ± 0.9
Galactans	21.3 ± 0.5	10.9 ± 0.5
Arabinans	1.4 ± 0.1	2.9 ± 0.2
Uronic acids	4.3 ± 0.1	3.8 ± 0.1
Lignin	11.3 ± 1	12 ± 1
Soluble	9.5 ± 0.1	8.7 ± 0.1
Insoluble	0.3 ± 0.1	3 ± 1
Proteins*	14.9 ± 0.3	21 ± 1
Lipids	0.7 ± 0.2	0.87 ± 0.09
Ashes	14.9 ± 0.3	22 ± 2

*Proteins include the protein content in the extractive fraction (2.6 %). NF = 4.9 (see **Table 2.S-2** of the manuscript for amino acid profile)

Table 2.S-2. Amino acid profile of macroalgae residue, MR. (*EAA* = essential amino acids, *TAA* = total amino acids).

Amino acid	MR, mg/g_{prot}
Alanine	94 ± 8
Glycine	41 ± 4
Valine	67 ± 7
Leucine	78 ± 8
Isoleucine	45 ± 5
Threonine	36 ± 2
Serine	39 ± 6
Proline	73± 4
Asparragine	97 ± 8
Methionine	8 ± 1
Glutamine	79 ± 5
Phenyalanine	51 ± 6
Lysine	12.0 ± 0.8
Histidine	3.4 ± 0.2
Tyrosine	7.3 ± 0.9
Tryptophan	0.60 ± 0.02
EAA	76 ± 5
TAA	172 ± 9

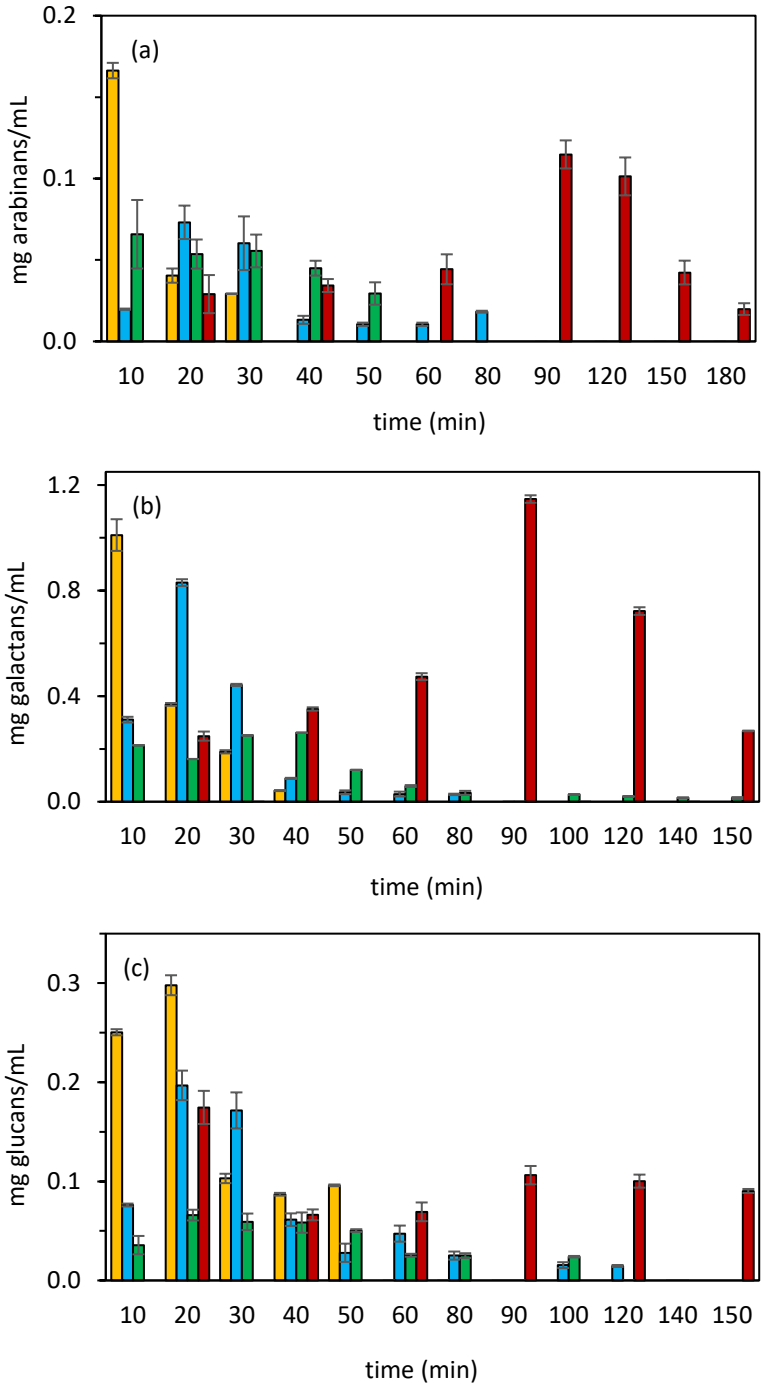

Figure 2.S-1. Elution profile **(a)** arabinans **(b)** galactans **(c)** glucans. ($V_{reactor}$ = 27 cm^3 and different residence time 3 min (■), 4.2 min (■), 6 min (■); $V_{reactor}$ = 127 cm^3, 56.2 min of residence time (■).

References

Adler-Nissen, J., Eriksen, S., & Olsen, H. S. (1983). Improvement of the functionality of vegetable proteins by controlled enzymatic hydrolysis. *Qualitas Plantarum Plant Foods for Human Nutrition*, 32(3–4), 411–423.

Alonso-Riaño, P., Sanz, M. T., Benito-Román, O., Beltrán, S., & Trigueros, E. (2021). Subcritical water as hydrolytic medium to recover and fractionate the protein fraction and phenolic compounds from craft brewer's spent grain. *Food Chemistry*, 351, 129264.

Álvarez-Viñas, M., Flórez-Fernández, N., Torres, M. D., & Domínguez, H. (2019). Successful approaches for a red seaweed biorefinery. *Marine Drugs*, 17(11).

Araki. (1956). Structure of the Agarose Constituent of Agar-agar. *Bulletin of the Chemical Society of Japan*, 29(4), 543.

Benzie, I.F.F., & Strain, J.J. (1996). The Ferric Reducing Ability of Plasma (FRAP) as a Measure of "Antioxidant Power": The FRAP Assay. *Analytical Biochemistry*, 239(1), 70–76.

Brand, S., Hardi, F., Kim, J., & Suh, D.J. (2014). Effect of heating rate on biomass liquefaction: Differences between subcritical water and supercritical ethanol. *Energy*, 68, 420–427.

Ciko, A. M., Jokić, S., Šubarić, D., & Jerković, I. (2018). Overview on the application of modern methods for the extraction of bioactive compounds from marine macroalgae. *Marine Drugs*, 16(10).

Cui, M., Wu, J., Wang, S., Shu, H., Zhang, M., Liu, K., & Liu, K. (2019). Characterization and anti-inflammatory effects of sulfated polysaccharide from the red seaweed *Gelidium pacificum* Okamura. *International Journal of Biological Macromolecules*, 129, 377–385.

Duckworth, M., & Yaphe, W. (1971). The Structure of Agar. *Carbohydrate Research*, 16, 189–197.

Esteban, M.B., García, A.J., Ramos, P., & Márquez, M.C. (2010). Sub-critical water hydrolysis of hog hair for amino acid production. *Bioresource Technology*, 101(7), 2472–2476.

Filisetti-Cozzi, T.M.C.C., & Carpita, N.C. (1991). Measurement of uronic acids without interference from neutral sugars. *Analytical Biochemistry*, 197(1), 157–162.

Friedman, M. (2004). Applications of the Ninhydrin Reaction for Analysis of Amino Acids, Peptides, and Proteins to Agricultural and Biomedical Sciences. *Journal of Agricultural and Food Chemistry*, 52(3), 385–406.

Gallina, G., Cabeza, Á., Grénman, H., Biasi, P., García-Serna, J., & Salmi, T. (2018). Hemicellulose extraction by hot pressurized water pretreatment at 160 °C for 10 different woods: Yield and molecular weight. *Journal of Supercritical Fluids*, 133, 716–725.

Jang, J. S., Cho, Y. K., Jeong, G. T., & Kim, S. K. (2012). Optimization of saccharification and ethanol production by simultaneous saccharification and fermentation (SSF) from seaweed, Saccharina japonica. *Bioprocess and Biosystems Engineering*, 35(1–2), 11–18.

Kang, K. Y., & Chun, B. S. (2004). Behaviour of amino acid production from hydrothermal treatment of fish-derived wastes. *Korean Journal of Chemical Engineering*, 21(6), 1147–1152.

Kumar, S., Gupta, R., Lee, Y. Y., & Gupta, R. B. (2010). Cellulose pretreatment in subcritical water: Effect of temperature on molecular structure and enzymatic reactivity. *Bioresource Technology*, 101(4), 1337–1347.

Lamp, A., Kaltschmitt, M., & Lüdtke, O. (2020). Protein recovery from bioethanol stillage by liquid hot water treatment. *Journal of Supercritical Fluids*, 155.

Li, J., Kisara, K., Danielsson, S., Lindström, M. E., & Gellerstedt, G. (2007). An improved methodology for the quantification of uronic acid units in xylans and other polysaccharides. *Carbohydrate Research*, 342(11), 1442–1449.

Liu, C., & Wyman, C.E. (2003). The effect of flow rate of compressed hot water on xylan, lignin, and total mass removal from corn stover. *Industrial and Engineering Chemistry Research*, 42(21), 5409–5416.

Longsworth, L.G. (1953). Diffusion Measurements, at 25°, of Aqueous Solutions of Amino Acids, Peptides and Sugars. *Journal of the American Chemical Society*, 75(22), 5705–5709.

Lourenço, S.O., Barbarino, E., De-Paula, J.C., Pereira, L.O.D.S., & Lanfer Marquez, U.M. (2002). Amino acid composition, protein content and calculation of nitrogen-to-protein conversion factors for 19 tropical seaweeds. *Phycological Research*, 50(3), 233–241.

Lourenço, S.O., Barbarino, E., Lavín, P.L., Lanfer Marquez, U.M., & Aidar, E. (2004). Distribution of intracellular nitrogen in marine microalgae: Calculation of new nitrogen-to-protein conversion factors. *European Journal of Phycology*, 39(1), 17–32.

Manns, D., Deutschle, A., Saake, B., & Meyer, A. S. (2013). Methodology for quantitative determination of the carbohydrate composition of brown seaweeds (Laminariaceae). *RSC Advances*, 4, 25736–25746.

Mohamad, R., Aki, T., Nakashimada, Y., Okamura, Y., Tajima, T., & Matsumura, Y. (2017). Decomposition kinetics of uronic acids obtained from kelp under hydrothermal condition. *Journal of the Energy Institute*, 90(2), 185–190.

Pińkowska, H., Krzywonos, M., Wolak, P., & Złocińska, A. (2019). Production of uronic acids by hydrothermolysis of pectin as a model substance for plant biomass waste. *Green Processing and Synthesis*, 8(1), 683–690.

Pinto, A.R.R., Antas, F., Santos, R.C.D., Bowra, S., Simões, P., Barreiros, S., & Paiva, A. (2017). Effect of reactor configuration on the subcritical water hydrolysis of recycled paper mill sludge. *Journal of Analytical and Applied Pyrolysis*, 127, 68–74.

Plaza, M., & Turner, C. (2015). Pressurized hot water extraction of bioactives. *Trends in Analytical Chemistry*, 71, 39–54.

Pronyk, C., Mazza, G., & Tamaki, Y. (2011). Production of carbohydrates, lignins, and minor components from triticale straw by hydrothermal treatment. *Journal of Agricultural and Food Chemistry*, 59(8), 3788–3796.

Sánchez-Bastardo, N., Romero, A., & Alonso, E. (2017). Extraction of arabinoxylans from wheat bran using hydrothermal processes assisted by heterogeneous catalysts. *Carbohydrate Polymers*, 160, 143–152.

Sasaki, M., Fang, Z., Fukushima, Y., Adschiri, T., & Arai, K. (2000). Dissolution and hydrolysis of cellulose in subcritical and supercritical water. *Industrial and Engineering Chemistry Research*, 39(8), 2883–2890.

Sereewatthanawut, I., Prapintip, S., Watchiraruji, K., Goto, M., Sasaki, M., & Shotipruk, A. (2008). Extraction of protein and amino acids from deoiled rice bran by subcritical water hydrolysis. *Bioresource Technology*, 99(3), 555–561.

Sinağ, A., Kruse, A., & Rathert, J. (2004). Influence of the Heating Rate and the Type of Catalyst on the Formation of Key Intermediates and on the Generation of Gases during Hydropyrolysis of Glucose in Supercritical Water in a Batch Reactor. *Industrial and Engineering Chemistry Research*, 43(2), 502–508.

Singleton, V. L., Orthofer, R., & Lamuela-Raventós, R. M. (1999). Analysis of Total Phenols and Other Oxidation Substrates and Antioxidants by Means of Folin-Ciocalteu Reagent. *Methods in Enzymology*, 299, 152–178.

Sluiter, J. B., Ruiz, R. O., Scarlata, C. J., Sluiter, A. D., & Templeton, D. W. (2010). Compositional analysis of lignocellulosic feedstocks. 1. Review and description of methods. *Journal of Agricultural and Food Chemistry*, 58(16), 9043–9053.

Thiruvenkadam, S., Izhar, S., Yoshida, H., Danquah, M. K., & Harun, R. (2015). Process application of Subcritical Water Extraction (SWE) for algal bio-products and biofuels production. *Applied Energy*, 154, 815–828.

Trigueros, E., Sanz, M. T., Alonso-Riaño, P., Beltrán, S., Ramos, C., & Melgosa, R. (2021). Recovery of the protein fraction with high antioxidant activity from red seaweed industrial solid residue after agar extraction by subcritical water treatment. *Journal of Applied Phycology*.

Wang, R., Neoh, T. L., Kobayashi, T., & Adachi, S. (2011). Antioxidative capacity of the degradation products of glucuronic and galacturonic acid from subcritical water treatment. *Chemical Engineering and Technology*, 34(9), 1514–1520.

Zhang, J., Wen, C., Zhang, H., Duan, Y., & Ma, H. (2020). Recent advances in the extraction of bioactive compounds with subcritical water: A review. *Trends in Food Science and Technology*, 95, 183–195.

CHAPTER 3

Subcritical water extraction scale-up from laboratory to pilot system for red algae residue after agar extraction valorization

Based on the article:

Trigueros E., Sanz M.T., Beltrán S., Alonso-Riaño P., Ramos C.

"Subcritical water extraction scale-up from laboratory to pilot system for red algae residue after agar extraction valorization".

(Submitted to Journal of Industrial and Engineering Chemistry)

Capítulo 3

Escalado del sistema de extracción con agua subcrítica desde el modelo de laboratorio hasta planta piloto para la valorización del residuo de alga roja tras la extracción del agar

Resumen

Se ha investigado la viabilidad de la extracción con agua subcrítica a escala industrial mediante la ampliación del sistema desde escala de laboratorio hasta planta piloto en la valorización del residuo de alga roja. Se extrajo galactosa, principalmente como oligómero, con rendimientos de 71.4 % (36 minutos) en planta piloto y 74.5 % (45 minutos) en laboratorio. En la fracción de glucanos se obtuvieron rendimientos más bajos (9.5 %) en ambos sistemas y más del 6 % se obtuvo durante los primeros minutos. Tras 20 minutos de extracción, los compuestos de degradación aumentaron, especialmente en escala de laboratorio, probablemente debido a la dificultad para mantener la temperatura en el reactor en planta piloto. Las curvas de extracción para la fracción proteica fueron similares, con rendimientos próximos al 40 %, mientras que el contenido de aminoácidos libres fue superior en escala de laboratorio. El rendimiento más alto se observó para los aminoácidos más pequeños (glicina, alanina y ácido aspártico), mientras que el contenido en aminoácidos polares como ácido glutámico y lisina se redujo. No se detectó lisina en escala piloto. En relación a los compuestos polifenólicos totales (TPC), se observó un aumento de TPC a escala de laboratorio al aumentar el tiempo de extracción, mientras que en planta piloto se alcanzó una fase estacionaria a los 36 minutos. La intensidad de color de los extractos aumentó progresivamente a escala de laboratorio. Se estableció una relación entre TPC, aminoácidos libres e intensidad de color, atribuyéndolo al desarrollo de reacciones de Maillard durante el proceso de extracción con agua subcrítica.

Palabras clave: planta piloto, escala de laboratorio, extracción con agua subcrítica, biorrefinería, residuo macroalga, valorización.

Abstract

The feasibility of industrial-scale subcritical water system through scaling-up from lab to pilot system has been investigated on the red alga solid residue valorization. Galactose was mainly recovered as oligomer fraction with maximum yields of 71.4 (36 minutes) and 74.5 % (45 minutes) for pilot and lab-scale, respectively. Lower yields were determined for glucans, with maximum yields of 9.5 % for both systems, in which more than 6 % was extracted in the first minutes. After 20 minutes of extraction, degraded compounds content increased, especially in laboratory-scale system, probably due to the difficulty to maintain temperature in pilot-scale reactor. Similar extraction curves and yields were determined for protein fraction with final extraction yields close to 40 %, while free amino acids content was higher in laboratory scale. The greatest extraction yield was accounted for the smallest amino acids, such as glycine, alanine and aspartic acid, whereas polar amino acids such as glutamic acid and lysine were reduced, although lysine was not detected in pilot system. Differences in total polyphenolic compounds (TPC) extraction were observed for both systems. Increasing TPC content with time was determined for lab-scale system, while in pilot system a plateau phase was observed after 36 minutes of extraction. Colour intensity progressively increased with time in lab-scale subcritical water extracts. Hence, a relation between TPC, free amino acids and colour was attributed to Maillard reactions occurrence during subcritical water extraction.

Keywords: pilot scale, lab-scale, subcritical water extraction, biorefinery, macroalgae residue, valorization.

1. Introduction

Gelidium sesquipedale solid residue after industrial agar extraction contains high amounts of proteins with all essential amino acids and carbohydrates such as glucans, galactans or arabinans (Trigueros et al., 2021a). Therefore, although it is generally discarded, its reincorporation in the industry as a value-added product is possible within a biorefinery concept.

The term "biorefinery" refers to the production of high-value compounds from biomass, through the integration of green technologies in an economically efficient and environmentally friendly way (Chisti, 2007). Within a biorefinery concept, different technologies are able to transform the starting biomass into its basic constituents, known as “building blocks”, which can be turned into value-added compounds (Cherubini, 2010).

Traditional methods used for bioactive compounds extraction from different raw materials present numerous drawbacks, namely, time-consuming, costly to dispose of used products and harmful to environment and human health (Camel, 2001).

Among green technologies, subcritical water extraction stands out as a great alternative to traditional extraction processes. SWE consists of using hot pressurized water above its boiling point, 100 °C, and below its critical point, 374 °C, which causes many of the properties of water to change, such as density or dielectric constant (Herrero et al., 2006; Zakaria & Mustapa Kamal, 2016). Water dielectric constant, which is related to its polarity, decreases with increasing temperature. The value drops from 80 at room temperature to 40, similar to organic solvents, at 200 °C. As a result, through the dielectric constant modulation with temperature, SWE is able to selectively extract polar or non-polar compounds (Park et al., 2019; Plaza et al., 2010).

SWE systems can be divided into continuous and discontinuous mode. In continuous mode, fresh solvent and sample pass continuously through the reactor, while in discontinuous mode, sample and solvent stay in the reactor for the total treatment time. Parameters to be controlled are temperature and time and, additionally, flow rate solvent in continuous

mode (Ko et al., 2020; Plaza & Turner, 2015). Moreover, a semicontinuous system is possible as a combination of the other modes (Morales-Muñoz et al., 2002). Recently, the results obtained after SWE from *G. sesquipedale* algae residue in semi-continuous mode have been published (Trigueros et al., 2021a). A protein extraction yield of nearly 70 % was reached at 185 °C and 2 mL/min of flow rate.

In order to ensure the viability of industrial-scale SWE for algae residue after agar extraction valorization, a pilot-scale process must be studied (Kwon & Chung, 2015). Generally, the design of the industrial SWE equipment is preceded by the study of laboratory- and pilot-scale systems. However, in many cases, the pilot-scale study stage is eliminated and goes directly from the laboratory to the industrial scale. Hence, the scaling-up process would be much more efficient by incorporating the pilot-scale study to obtain quality data and determination of scale-up factor (Pronyk & Mazza, 2009).

Therefore, the main goal of this research was to prove the feasibility of industrial-scale subcritical water system through scaling-up from lab to pilot system. Accordingly, the purposes of this work were: (1) to study the subcritical water ability for bioactive compounds recovery from alga residue in a discontinuous mode and (2) to compare lab- and pilot-scale subcritical water performance.

2. Material and methods

2.1. Raw material

The raw material used in this work is the industrial solid residue obtained from *Gelidium sesquipedale* after industrial agar extraction and it was provided by Hispanagar (Burgos, Castilla y León, Spain) (https://www.hispanagar.com/es). This residue was oven-dried at 45 °C for 24 hours, with a resulting 5 ± 2 % of humidity. Dried macroalga residue (DMR) was milled by using a Retsch mill and sieving by using a stainless-steel mesh sieve (Cisa Sieving Technologies) to obtain a material feed size lower than 1 mm. Particle size distribution is shown in **Figure 3.1**. As it can be observed, a majority fraction (74.6 %) lower than 0.5 mm

was obtained, while just 2.3 % was higher than 1 mm. DMR fraction below 500 µm particle size ($DMR_{<500}$) was used for subcritical water treatment due to the requirements of the recirculation pump on subcritical water pilot plant. Raw material characterization was carried out according to the NREL protocols (https://www.nrel.gov/bioenergy/biomass-compositional-analysis.html).

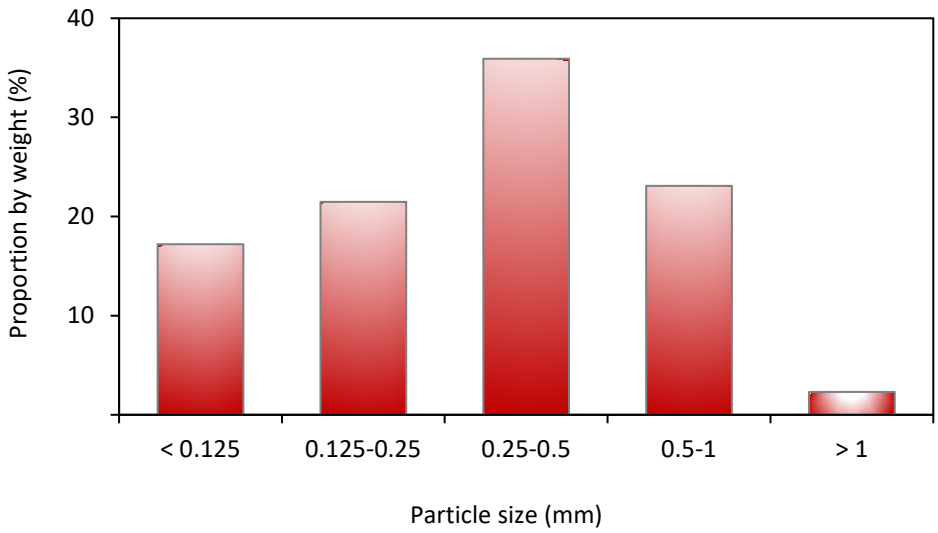

Figure 3.1. Proportion by weight of particle size from dried macroalga residue (DMR).

2.2. Subcritical water equipment

2.2.1. Laboratory-scale SWE

Laboratory-scale subcritical water treatment in a discontinuous mode was performed by using a stainless-steel extractor of 500 mL volume. The heating system consisted of a ceramic heating jacket (230 V, 4000 W, ø95 cm, 160 mm height) covering the reactor, which let the system to reach the working temperature (**Figure 3.2**). A Pt100 sensor connected to a PID system and placed inside the reactor allowed to control and register the temperature during the extraction.

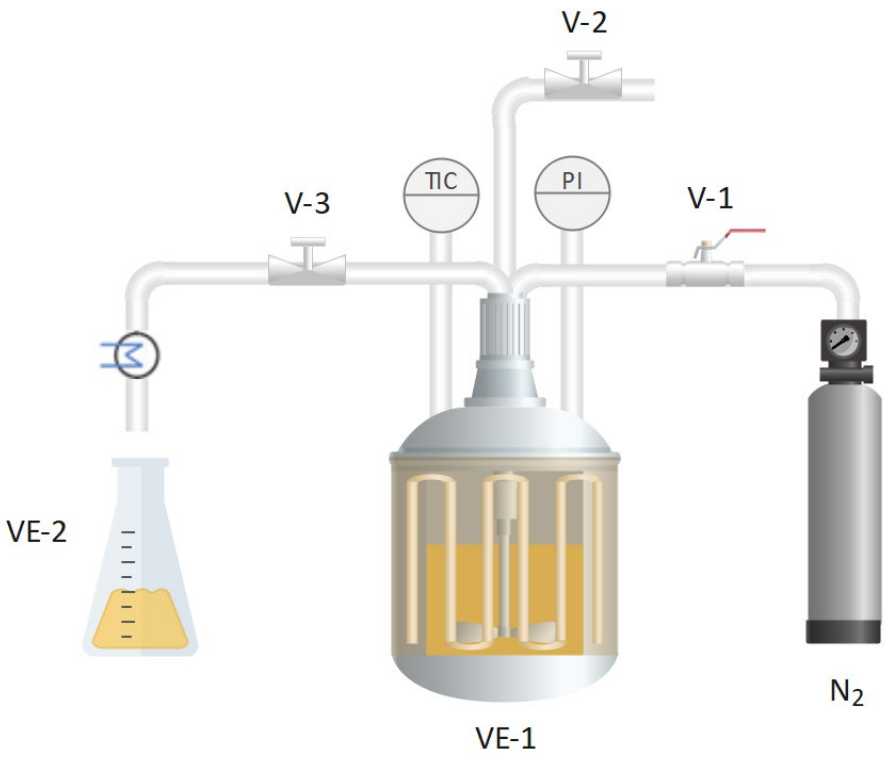

Figure 3.2. Diagram of the laboratory-scale subcritical water equipment. VE-1: extractor; VE-2: sample collector; V-1: pressurization valve; V-2: pressure relief valve; V-3: needle valve.

In a typical run, 17.5 g of $DMR_{<500}$ were charged into the reactor together with 350 mL of deionized water (1:20 sample:solvent (w/v)). The mixture was heated up to the desired temperature at a certain heating rate and pressure was fixed to 50 bar by using nitrogen gas to prevent sample oxidation. Homogenization of the mixture was achieved by mechanical stirring. Extraction/hydrolysis kinetics were followed by withdrawing sample through a sampling pipe submersed in the mixture and provided with a metallic filter to avoid the clogging of the pipe. Laboratory-scale SWE was carried out at 175 °C for a total treatment time of 130 minutes.

2.2.2. Pilot-scale SWE

Subcritical water experiments at pilot-scale level were carried out at Hiperbaric's facilities (Burgos, Spain) by using a discontinuous system.

The main structural elements of the prototype were a reactor of 25 L capacity, a steam boiler as the heating system, a pump to recirculate and homogenize the biomass inside the reactor, a heat exchanger to avoid cooling during the recirculation process and a solid/liquid separation system (**Figure 3.3**). The maximum specifications were 185 °C and 20 bar. Operation and control of the process was performed by self-built Hiperbaric software.

In a typical run, water was initially pre-heated up to 80 °C in the steam boiler and circulated through the heat exchanger. This way, all the system was initially pre-heated at 80 °C. After this pre-heating period, the system was completely drained and the biomass was charged into the reactor. Then, the reactor was filled with the pressurized water at the working temperature, achieved by the steam boiler system. The system was pressurized by using nitrogen gas. Recirculation pump was turned on to enhance external mass transfer in the extraction/hydrolysis process. The pump was able to handle up to a biomass concentration of 40 wt % with a maximum particle size of 0.5 mm, which determined the particle size of the biomass to be used. The heat exchanger placed in the recirculation pipe allowed contact with the steam boiler outlet pipe avoiding the cooling in the recirculation process. A sampling system at the bottom of the reactor allowed sample withdrawal to follow the extraction/hydrolysis kinetics. After extraction was finished, a filtration tank allowed phases separation to obtain a liquid hydrolysate and the solid residue.

Experiments were carried out at 5 % biomass loading, 175 °C and a working pressure of 20 bar.

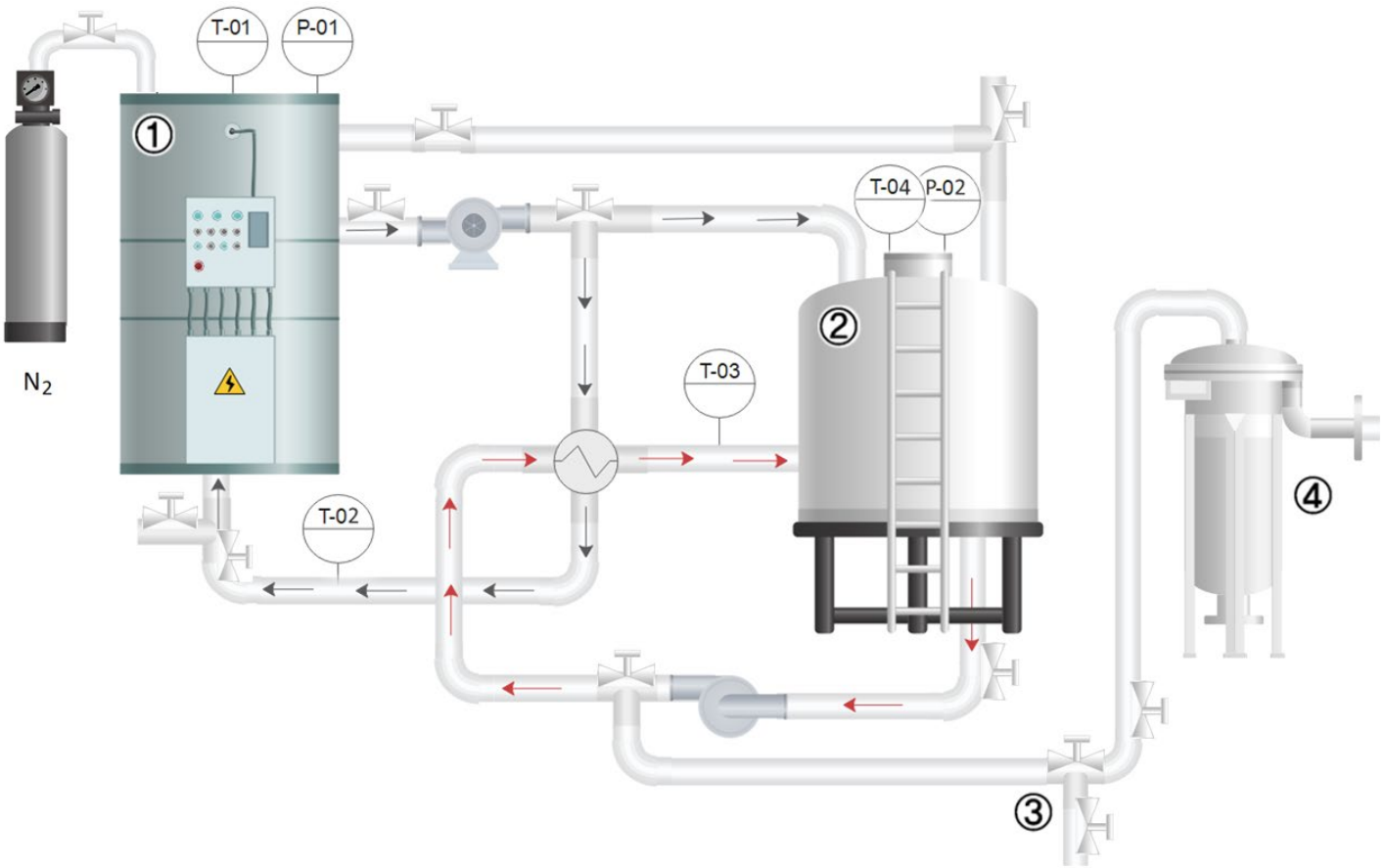

Figure 3.3. Diagram of the pilot-scale subcritical water plant designed and built in Hiperbaric (https://www.hiperbaric.com/es/). 1: steam boiler preheater and water tank; 2: 25 L extractor; 3: liquid sample collector; 4: filtration tank.

2.3. Analytical methods

2.3.1. Sugars and derived compounds

Sugars and derived compounds were measured by HPLC equipped with a Biorad Aminex-HPC-87 H column, a variable wavelength detector (VWD) and a refractive index detector (RID) as described in Trigueros et al. (Trigueros et al., 2021b).

Monomeric sugars and degradation compounds were directly measured in liquid extracts, while oligomeric sugars fraction needed a first acid hydrolysis step in order to release the monomeric sugars for quantification. Monomeric and total sugar yield was estimated according to (Sánchez-Bastardo et al., 2017):

$$Monomer\ yield\ (\%) = \frac{(Monomeric\ Sugar)_{hydrolysate}}{Sugar_{rawmaterial}} \cdot 100 \quad [\mathbf{3.1}]$$

$$Total\ yield\ (\%) = \frac{(Monomeric\ and\ Oligomeric\ Sugar)_{hydrolysate}}{Sugar_{rawmaterial}} \cdot 100 \quad [\mathbf{3.2}]$$

Oligomer yield was calculated by difference between total and monomer yield.

2.3.2. Protein and free amino acids

Total protein content was determined from the nitrogen content by applying a nitrogen factor of 4.9 estimated from the amino acid profile of the raw material (Trigueros et al., 2021a). The nitrogen content was measured by using a TOC/TN analyzer (Shimadzu TOC-V CSN analyzer) using KNO_3 as standard.

Free amino acids were determined by using the EZ:faast Phenomenex procedure as described in Trigueros et al. (Trigueros et al., 2021a). It consists of a first solid extraction, followed by a derivatization step and a final liquid/liquid extraction. Finally, derivatized samples were analyzed by gas chromatography (Hewlett-Packard, 6890 series) with a coupled FID detector.

2.3.3. Total organic carbon

Total carbon and inorganic carbon were measured with a TOC Analyzer Shimadzu by using $C_6H_{14}(COOK)(COOH)$, $NaHCO_3$ and Na_2CO_3 as standards. Total organic carbon (TOC) was calculated by subtracting the inorganic carbon from total carbon content.

2.3.4. Total polyphenol content

Total polyphenol content (TPC) was determined by Folin-Ciocalteu reagent according to Singleton (Singleton et al., 1999) and expressed as mg of gallic acid equivalent (GAE) per gram of $DMR_{<500}$.

2.3.5 Elemental composition

Elemental composition (C, H, N, S) of raw material and solid residue after SW treatment was determined by an organic elemental micro-analyzer equipment (Thermo Scientific Model Flash 2000). Ash content was determined by placing around 0.5 grams of sample in a muffle furnace at 575 ± 25 °C for 24 ± 6 h until constant weight. Oxygen content was determined by difference. The high heating value (HHV) of the raw material and the solid after subW treatment was evaluated by the following equation (Friedl et al., 2005):

$$HHV\ (kJ/kg) = 3.55C^2 - 232C - 2230H + 51.2C \cdot H + 131N + 20600 \qquad [\mathbf{3.3}]$$

2.4. Statistical analysis

All determinations were taken at least in duplicate and expressed as mean ± standard deviation. The Fisher's least significant differences (LSD) method at p value ≤ 0.05 was applied to confirm significant differences. Analyses were carried out by Centurion Statgraphics software.

3. Results and discussion

3.1 Raw material characterization

Composition of DMR and $DMR_{<500}$ is shown in **Table 3.1**. DMR grinding and sieving resulted in a reduction of extractives and insoluble lignin content in $DMR_{<500}$. After grinding and sieving, insoluble lignin accounted only for 0.6 ± 0.2 %, while this content was 3 ± 1 in the DMR, concluding that the insoluble lignin remained mainly in the particle size fractions higher than 0.5 mm, which was around 25 % of the initial weight of the raw material. In this sense, grinding and sieving favoured the sample conditioning before SWE. Moreover, a slight reduction in carbohydrates and protein content in grounded DMR in comparison with DMR was observed, but still high content of carbohydrates (33.2 %) and proteins (17.6 %) was found in $DMR_{<500}$. Particle size distribution of ground DMR is presented in **Figure 3.1**.

Table 3.1. Chemical composition of dried macroalga residue (DMR) and dried macroalga residue < 500 µm ($DMR_{<500}$) fraction.

Compound	DMR	$DMR_{<500}$
Extractives	**11.5 ± 0.9**	**9.6 ± 0.9**
Carbohydrates	**37 ± 2**	**33.2 ± 2.1**
Glucans	23.4 ± 0.9	21.4 ± 1.2
Galactans	10.9 ± 0.5	10.3 ± 1.7
Arabinans	2.9 ± 0.2	1.51 ± 0.11
Lignin	**12 ± 1**	**7.6 ± 0.9**
Soluble	8.7 ± 0.1	7.0 ± 0.9
Insoluble	3 ± 1	0.6 ± 0.2
Proteins*	**21 ± 1**	**17.6 ± 0.5**
Lipids	**0.87 ± 0.09**	**2.3 ± 0.5**
Ashes	**22 ± 2**	**24.9 ± 1**

*Proteins include the protein content in the extractive fraction (1.9 ± 0.1 %).
NF = 4.9

3.2 Heating rate

Temperature profiles along SWE for both lab- and pilot-scale systems are plotted in **Figure 3.4**. On pilot-scale, system was preheated at 80 °C, so 3 and 12 minutes were enough to reach 160 and 170 °C, respectively. At lab-scale system, where water was initially at room temperature, it took 15 and 19 minutes, respectively, to reach such temperatures. In both systems, two different heating rates can be observed. Faster initial rates, of 75.5 °C/min and 11.7 °C/min for pilot plant and laboratory scale, respectively, and slower heating rates of 0.93 °C/min and 2.6 °C/min for pilot and laboratory scale, respectively, were determined. It can be observed that temperature was less stable in pilot plant system since the temperature tended to decrease with reaction time, proving that the heating jacket system allowed a better control of the temperature of the system that determines the efficiency of the process. On pilot-scale system, the temperature dropped throughout the treatment time to 163 °C at the end of the extraction, while at lab-scale system, temperature ranged between 174 and 180 °C all along the experiment, highlighting the importance of recording the temperature in order to explain the conversion reactions that take place inside the reactor during SWE.

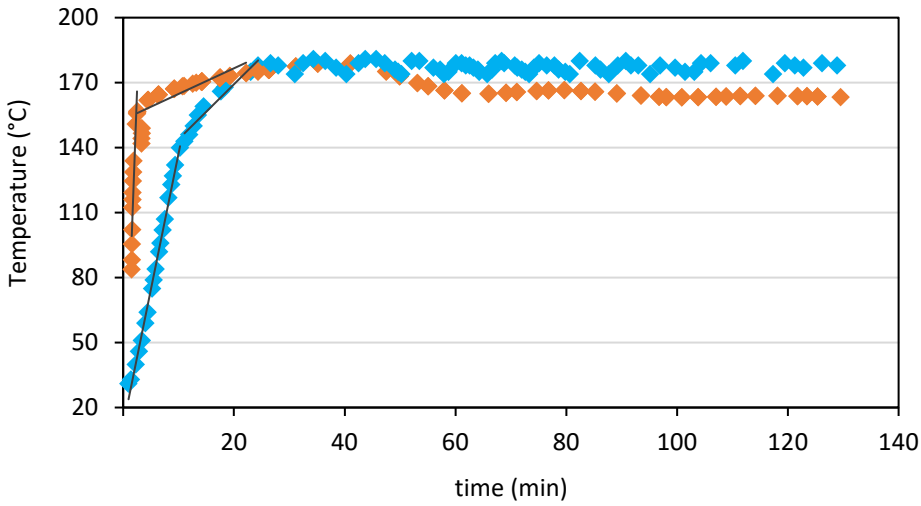

Figure 3.4. Extraction temperature profiles along treatment time at lab-scale (◆) and pilot-scale SWE system (◆) at 175 °C working temperature.

3.3 Polysaccharide fraction extraction/hydrolysis

Figure 3.5 shows the galactose extraction yield along extraction time for both laboratory- and pilot-scale systems. Galactose was released to the extraction medium mainly as oligomer. Small differences were observed in the extraction kinetics between both configurations. A faster galactans extraction was observed for pilot-scale in comparison with lab system, 60.7 and 47.3 %, respectively, in the first ten minutes of treatment. However, maximum oligomer yield was similar for both pilot- and lab-scale systems, 71.4 % (36 minutes) and 74.5 % (45 minutes), respectively. For longer extraction times, galactose degradation rate was higher than its formation rate by hydrolysis.

The extraction yield as monomer fraction was very low in both designs. As a consequence of a faster oligomer extraction at pilot-system, monomers appeared earlier. Nevertheless, at the end of the treatment, monomer yield was slightly higher on the lab-scale system due to a higher galactose oligomer content in subcritical water extracts. These results are consequence of the water ability under subcritical conditions to hydrolyze solubilized galactans into galactose monomers (Yedro et al., 2015).

Much lower hydrolysis yields were obtained for glucans (**Figure 3.6**). A similar trend was observed for laboratory and pilot scale systems with a maximum yield of 9.5 and 9.6 %, respectively, as glucans, because no glucose monomers were detected in the subcritical water extracts. Moreover, final equilibrium extraction yield was achieved after 20 minutes of extraction time. No glucans degradation was observed at longer times since glucose monomer was probably not formed. According to literature, Mohan et al. (Mohan et al., 2015) proved that high temperatures are needed in order to hydrolyze cellulose fraction. Below 250 °C, cellulose does not hydrolyze but dissolves, being able to produce high degree polymerization molecules.

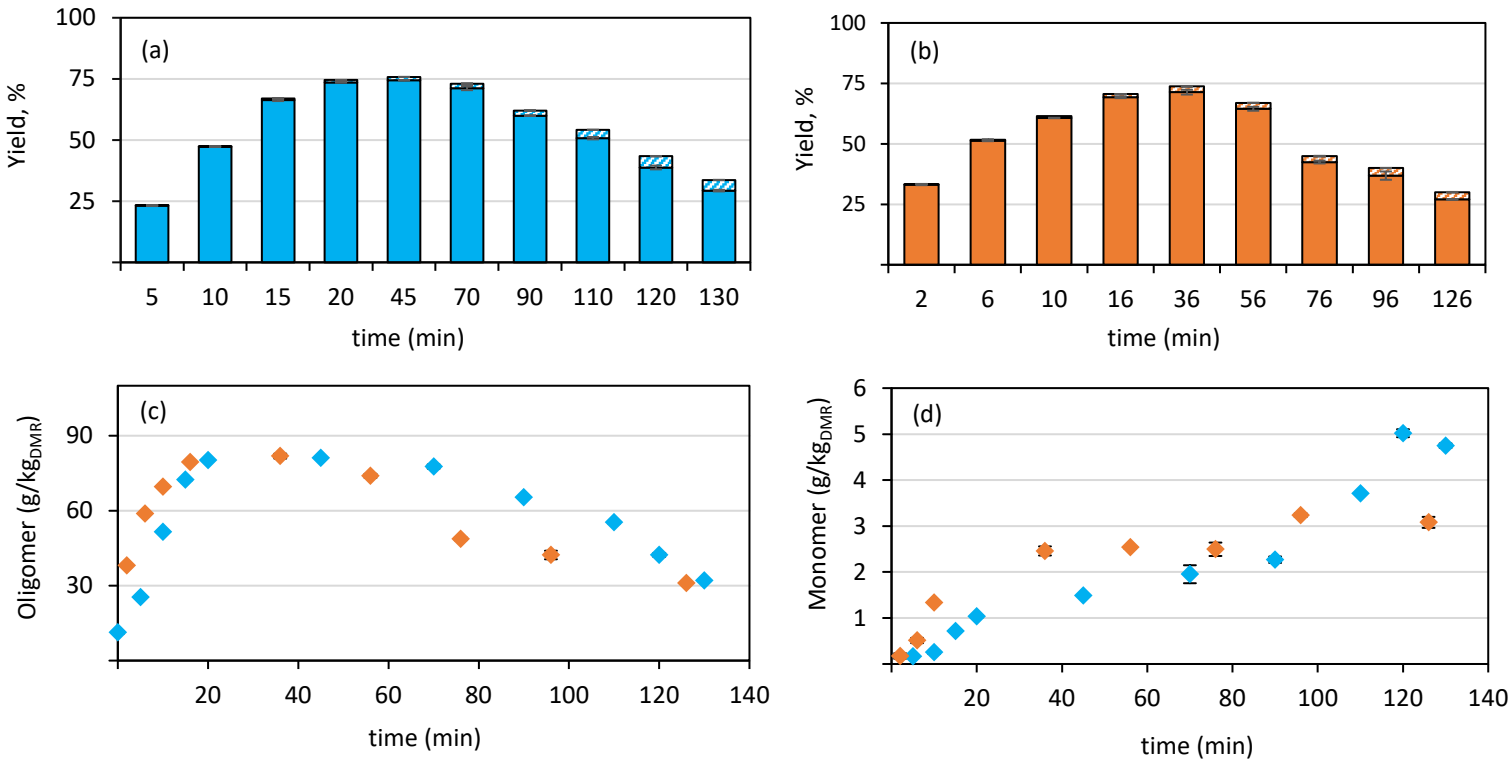

Figure 3.5. Galactose yield along SWE from DMR$_{<500}$ at **(a)** lab-scale and **(b)** pilot-scale as oligomers (■, ■) and monomers (▨, ▨) and galactose fraction content as **(c)** oligomer and **(d)** monomer at lab-scale (◆) and pilot-scale (◆) systems, at 175 °C working temperature.

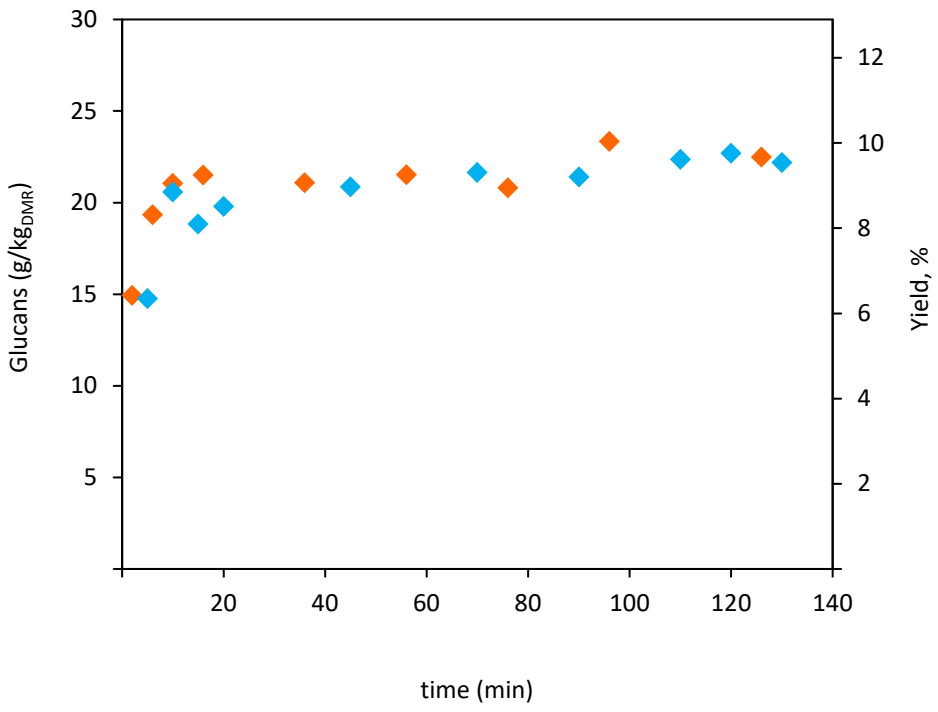

Figure 3.6. Glucose yield and content collected as oligomer fraction in subcritical water extracts at the different time intervals from DMR$_{<500}$ at lab-scale (◆) and pilot-scale (◆) at 175 °C working temperature.

In **Figure 3.7**, the production of sugar-degradation and sugar-dehydration compounds is shown. Acetic acid was the degradation product that was formed preferentially, while sugar dehydration products content such as furfural and 5-hydroxymethylfurfural (HMF) was very low.

A notable increase in degradation products formation, especially at the pilot-scale system, was observed after 30-40 minutes of extraction, agreeing with the maximum in the extraction yield for galactans.

As mentioned before, temperatures above 250 °C are needed to hydrolyze cellulose (Mohan et al., 2015). However, although in this study temperatures below 200 °C were studied, cellulose could be dissolved, resulting in high degree polymerization molecules release to the extraction medium.

For formic acid, big differences were found between the two different systems. While at lab-scale the maximum formic acid concentration was 0.3 g/L, on pilot-system was close to 1.0 g/L. This could be explained because higher content of solubilized oligosaccharides was found at the beginning of the extraction on pilot-system, which may have suffered from degradation reactions and turning into organic acids and other compounds promoted by subcritical water (Cabeza et al., 2016). The same trend was observed for HMF formation at the beginning of the SW treatment. However, at longer extraction times (> 110 minutes), a great increase in the HMF formation at laboratory SW extracts was observed, probably due to a greater monomeric galactose yield at the end of the subcritical water extraction. Furfural content in subcritical water extracts was very similar in both systems and lower than HMF due to low pentoses content in the raw material. Similar results were found by Jeong et al. (Jeong et al., 2012) from *G. amansis* acid hydrolysis. They observed an increase in the formic acid and HMF production at the same time that the amount of glucose in the raw material decreased.

Yoo et al. (Yoo et al., 2020) evaluated the scaling up from laboratory to pilot subcritical water system for β-glucan hydrolysis. They found a greater extraction yield at laboratory system (6.98 %) than in pilot-scale (3.01 %) at 201 °C for ten minutes. However, in this work similar maximum sugars yields were achieved for both systems.

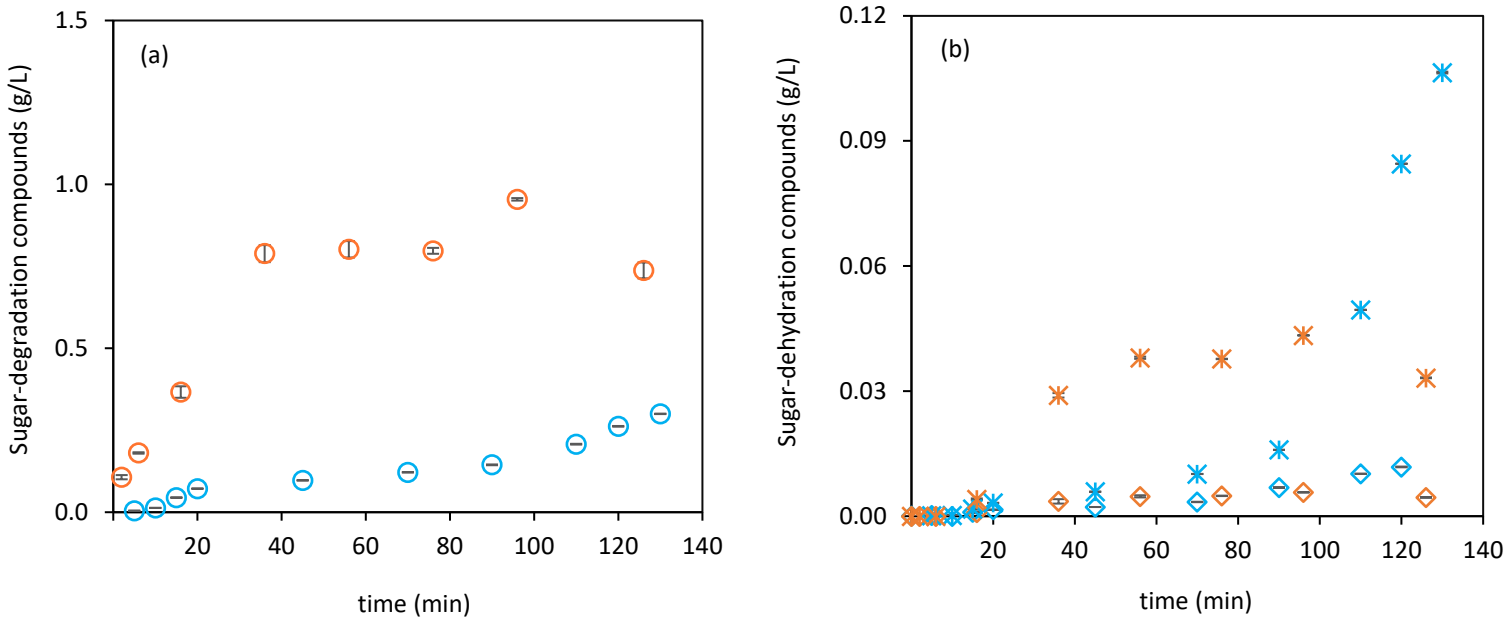

Figure 3.7. **(a)** Sugar-degradation and **(b)** sugar-dehydration compounds (furfural (◇) and 5-hydroxymethylfurfural (∗)) content in subcritical water extracts at the different time intervals from $DMR_{<500}$ at lab-scale (blue) and pilot-scale (orange) at 175 °C working temperature (expressed as g/L subcritical water extract ± standard deviation).

3.4 Protein fraction extraction/hydrolysis

Protein extraction is shown in **Figure 3.8a.** Similar extraction curves were obtained with both systems, although a slightly faster initial extraction/hydrolysis was described for pilot design. This could be related to the faster heating rate due to the preheating of the system. Final protein extraction/hydrolysis yield was 36.8 and 37.5 % for pilot and lab-scale, respectively, showing the good scaling-up process of subcritical water extraction on a larger scale.

The yields obtained in the discontinuous process were lower than in the semicontinuous process (see **Chapter 2**). In a semicontinuous process, fresh water is continuously supplied to the raw material increasing the driving force of the process resulting in higher hydrolysis. A comparison could be established not only in terms of hydrolysis yield, but also amount of biocompounds per liter of water. On the semicontinuous system, maximum yield around 95 % was reached after 70 minutes of extraction, but a very diluted extract was obtained since 560 mL of water were used. However, to achieve the same yield as on discontinuous system, a final water volume of 160 mL was used, less than half volume used at discontinuous system.

Regarding the free amino acids content, a higher formation rate and yield was observed at lab-scale along all the subcritical water treatment (**Figure 3.8b**), with values of 14.2 and 17.8 mg free amino acids/$g_{protein}$ at pilot plant and lab-scale systems, respectively. The lower yields at pilot plant scale could be due to the difficulty to maintain the working temperature during the process on pilot system (see **Figure 3.4**), as higher temperature results in higher protein extraction and hydrolysis, following by the amino acids release, as long as the degradation temperature is not reached (Trigueros et al., 2021a).

Figure 3.9 shows the release curves for individual amino acids by SWE at lab and pilot-scale systems grouped into non-polar and polar amino acids. In both systems, the greatest release for non-polar amino acids was obtained for the smallest amino acids, with 9.6 and 4.7 % for glycine and 2.6 and 1.4 % for alanine at lab and pilot system, respectively. The concentration of the non-polar amino acids continuously increased with increasing extraction time. On the

opposite, concentration of some polar amino acids such as glutamic acid and lysine were reduced as the hydrolysis process progressed, although lysine was not detected in subcritical water extracts from the pilot system. However, aspartic acid was one the most produced amino acids, with 6.1 and 6.4 % release at lab and pilot scale, respectively. Rogalinski et al. (Rogalinski et al., 2005) reported high stability of alanine and glycine at subcritical water conditions, whereas lysine and other polar amino acids usually participate into Maillard reactions with reducing sugars under subcritical conditions (Plaza et al., 2010). Similar results were found in a previous work by using a semicontinuous subcritical water lab-system, where the selectivity towards non-polar amino acids increased by increasing time and temperature (Trigueros et al., 2021a).

Table 3.2 lists the amino acids yields expressed as mg of free amino acids per gram of protein and mg of free amino acids per mg of amino acid in the raw material. In general, low free amino acids yields were obtained. Compared to semicontinuous system, it can be seen that glycine was the most yielded amino acid for both semicontinuous and discontinuous lab-scale systems, but yield at semicontinuous accounted for almost three times the value of discontinuous system. Only serine yield was a little bit higher on discontinuous lab-scale system than at semicontinuous SWE. In general, lower yields were obtained on discontinuous system in comparison with semicontinuous, suggesting a small rate of the protein fraction hydrolysis to free amino acids, mainly on pilot-scale system due to the worse temperature control along the treatment time.

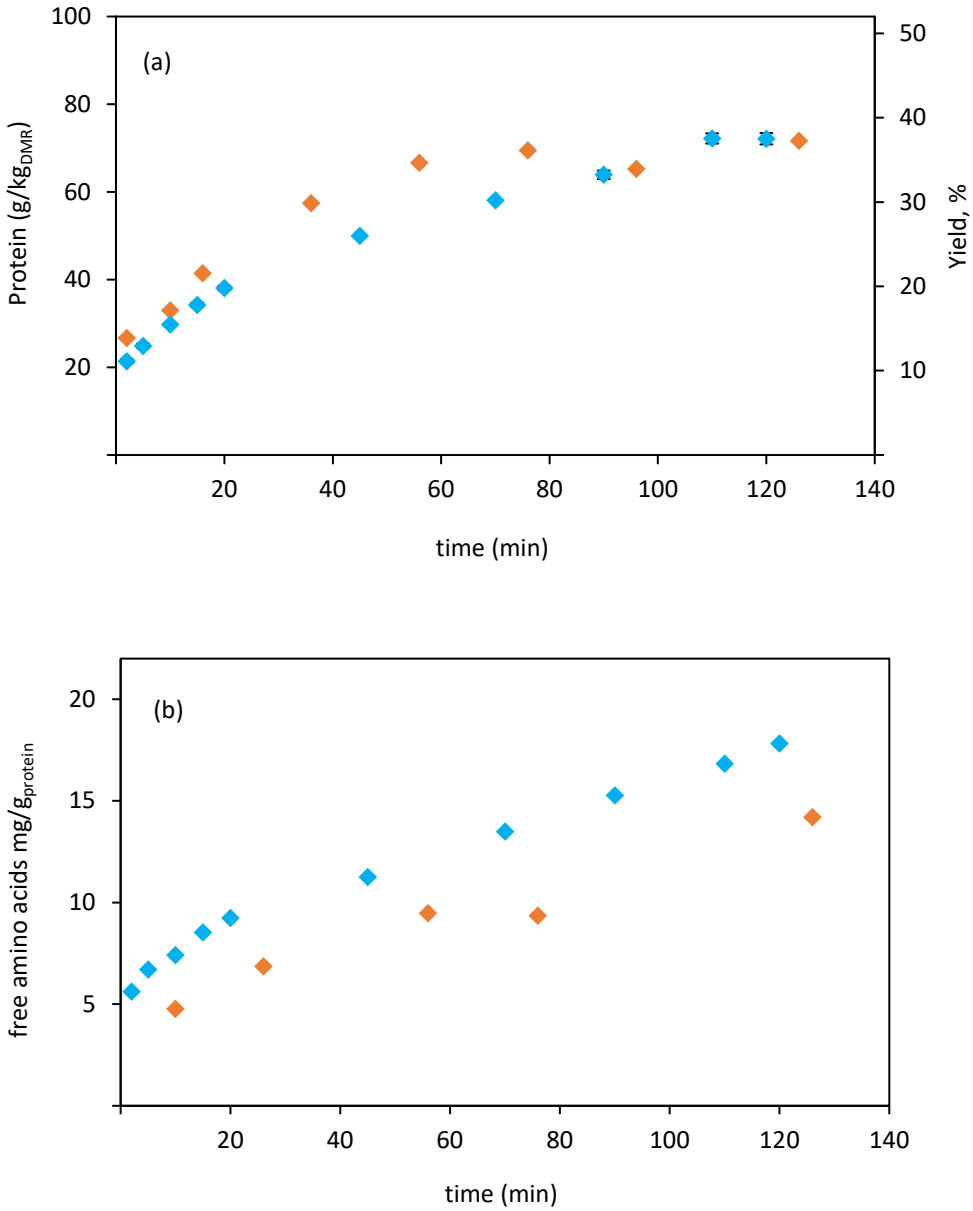

Figure 3.8. **(a)** Protein yield and content and **(b)** free amino acids per protein gram in subcritical water extracts collected at the different time intervals from DMR$_{<500}$ at lab-scale (◆) and pilot-scale (◆) at 175 °C working temperature.

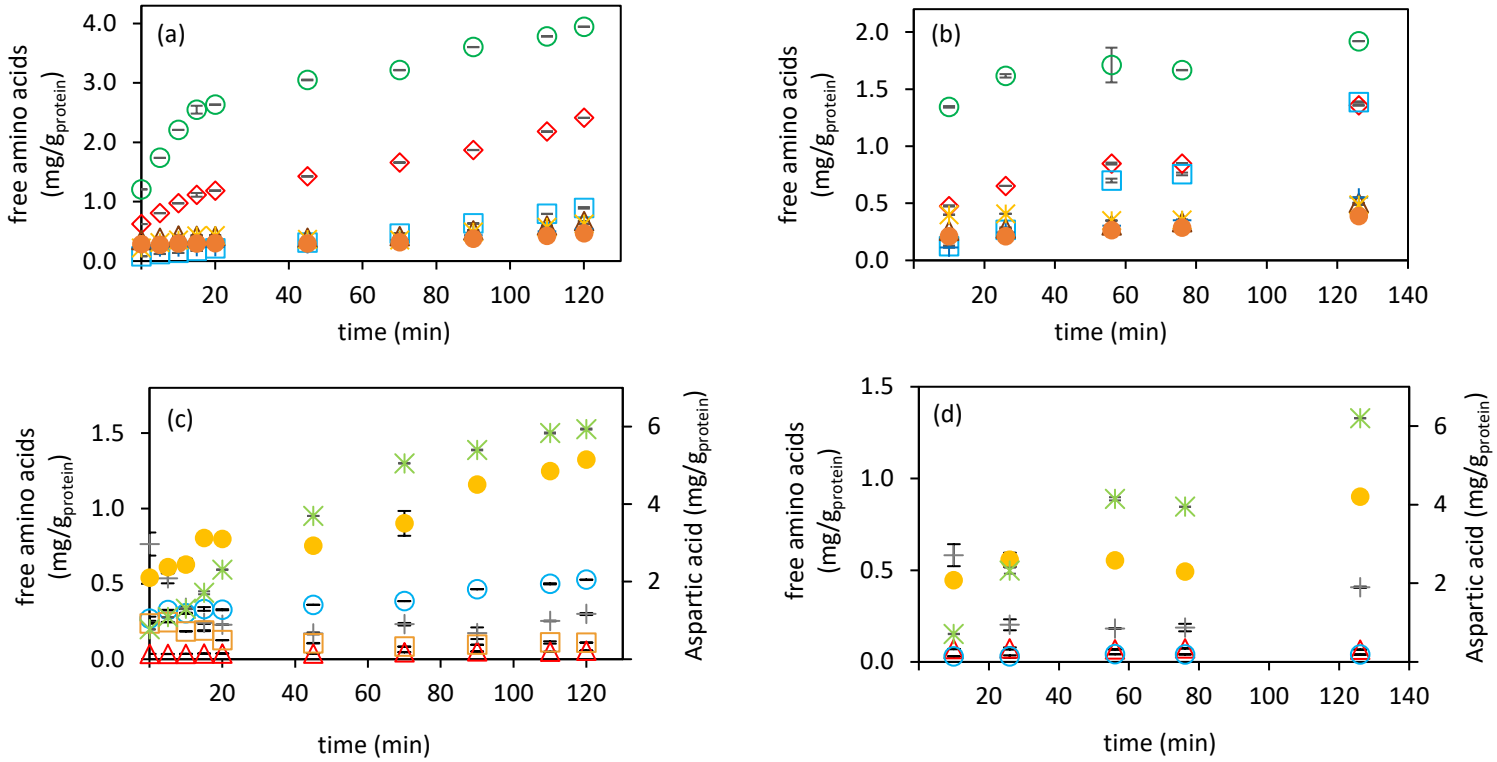

Figure 3.9. Accumulative formation of individual amino acids. Non-polar amino acids at **(a)** lab-scale and at **(b)** pilot-scale (◇ alanine, ○ glycine, □ valine, △ leucine, + isoleucine, ✳ proline, ● phenylalanine). Polar amino acids at **(c)** lab-scale and at **(d)** pilot-scale (principal axes: ○ threonine, □ lysine, △ tyrosine, + glutamic acid, ● serine; secondary axes: ✳ aspartic acid). (experimental data include standard deviations, *n* = 3 technical replicates).

Table 3.2. Individual amino acids yield after SWE at lab-scale and pilot-scale and amino acid profile in macroalgae residue, MR. (*n* = 3 technical replicates).

	Macroalgae residue	Lab-Scale SWE		Pilot-Scale SWE	
	mg/g_{DMR}	$mg/g_{protein}$	Yield (%)	$mg/g_{protein}$	Yield (%)
Alanine	19.8 ± 0.7	2.4 ± 0.01	2.6 ± 0.2	1.4 ± 0.1	1.4 ± 0.1
Glycine	8.6 ± 0.5	3.9 ± 0.01	9.6 ± 0.9	1.9 ± 0.1	4.7 ± 0.2
Valine	14.0 ± 0.9	0.90 ± 0.01	1.3 ± 0.2	1.4 ± 0.1	2.1 ± 0.1
Leucine	16.3 ± 0.8	0.67 ± 0.01	0.86 ± 0.09	0.50 ± 0.01	0.65 ± 0.05
Isoleucine	9.4 ± 0.7	0.54 ± 0.01	1.2 ± 0.1	0.55 ± 0.01	1.2 ± 0.1
Proline	15.4 ± 0.1	0.62 ± 0.01	0.85 ± 0.05	0.49 ± 0.01	0.66 ± 0.05
Phenylalanine	10.6 ± 0.8	0.47 ± 0.01	0.93 ± 0.12	0.39 ± 0.01	0.77 ± 0.05
Threonine	7.5 ± 0.1	0.53 ± 0.01	1.5 ± 0.1	0.04 ± 0.01	0.11 ± 0.02
Lysine	12.0 ± 0.8	0.11 ± 0.01	0.19 ± 0.04	---	---
Histidine	3.4 ± 0.2	---	---	---	---
Tyrosine	7.3 ± 0.9	0.06 ± 0.01	0.17 ± 0.03	0.07 ± 0.01	0.19 ± 0.01
Glutamic acid	16.6 ± 0.2	0.30 ± 0.01	0.38 ± 0.05	0.41 ± 0.01	0.52 ± 0.05
Aspartic acid	20.4 ± 0.8	5.9 ± 0.01	6.1 ± 0.5	6.2 ± 0.1	6.4 ± 0.6
Methionine	1.7 ± 0.2	---	---	---	---
Serine	8.0 ± 0.9	1.3 ± 0.01	3.5 ± 0.6	0.90 ± 0.03	2.4 ± 0.1
Tryptophan	0.60 ± 0.02	---	---	---	---
Essential amino acids	76 ± 5	3.2 ± 0.01	0.90 ± 0.10	2.9 ± 0.1	0.80 ± 0.26
Total amino acids	172 ± 9	17.8 ± 0.02	2.3 ± 0.1	14.2 ± 0.1	1.8 ± 1.3

3.5 Total polyphenol content extracted in SW extracts

Total polyphenol content (TPC) was determined along treatment and it is shown in **Figure 3.10**. At lab-scale a maximum TPC of 17.9 g/kg$_{DMR}$ was achieved while this value decreased down to 9.0 g/kg$_{DMR}$ at pilot plant scale. The lower value reached at pilot plant scale could be attributed to the decrease in operating temperature (see **Figure 3.4**) down to values of 163 °C, 12 °C lower than the values maintained at lab scale by using the heating jacket. It is well documented that Maillard and caramelization reactions can be produced under intense heating conditions in subcritical water extraction between reducing sugars and free amino acids such as lysine and arginine. The higher temperature after 40-60 minutes of extraction at lab scale could induce to Maillard and caramelization reactions, whose products are well known to interfere in the TPC analysis by Folin-Ciocalteu assay (Plaza et al., 2010).

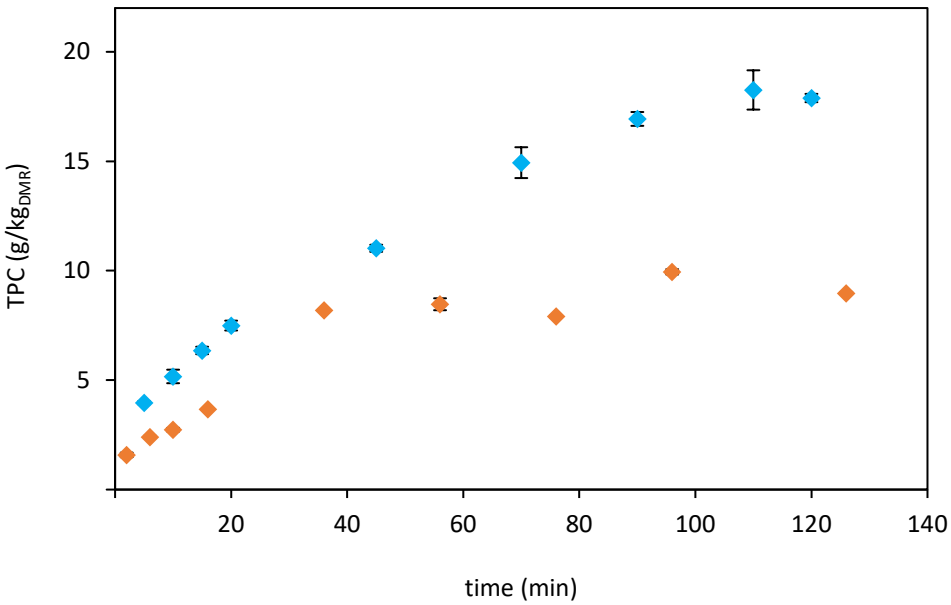

Figure 3.10. TPC content in subcritical water extracts collected at the different time intervals from DMR$_{<500}$ at lab-scale (◆) and pilot-scale (◆) at 175 °C working temperature.

Figure 3.9c showed a continuous decrease in lysine content from 0.27 to 0.11 mg/$g_{protein}$, more than 50 % after 100 minutes of treatment.

Brown colour development is an easy indicator of Maillard reactions occurrence being brown colour intensity proportional to the extent of these reactions (Morales & Jiménez-Pérez, 2001). In **Figure 3.11** is observed how colour intensity in lab-scale SW extracts progressively increased with treatment time towards dark brown colours, proving the occurrence of Maillard reactions. Hence, in this study, the treatment time at which the maximum brown colour development was reached agreed with the maximum of HMF formation and lysine disappearance, which suggests the advancement in the development of the Maillard reaction with extraction time.

He et al. (He et al., 2012) evaluated the TPC formation under subcritical conditions. They found that the increase in time and temperature from 80 to 220 °C resulted in increasing TPC extraction and brown colour intensity, agreeing with high concentrations of 5-HMF in the extracts, owing to the fact that 5-HMF is an important intermediate component produced in Maillard reactions.

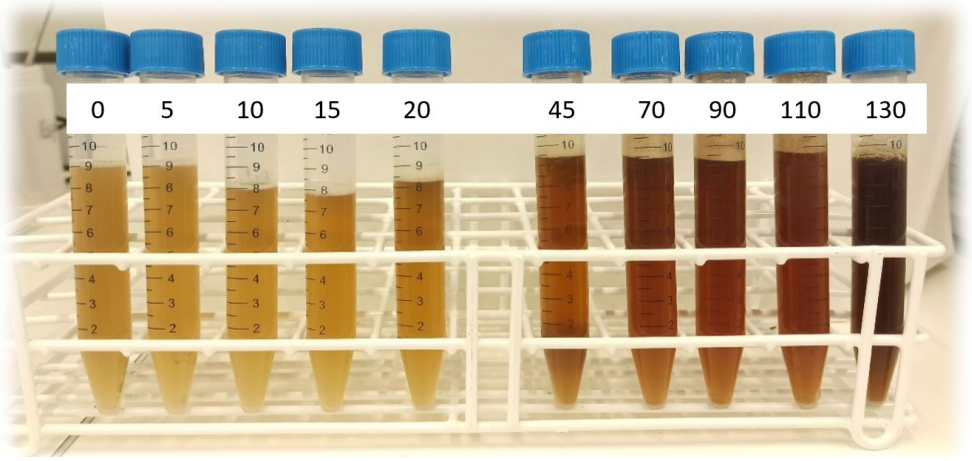

Figure 3.11. Liquid extracts collected at the different time intervals from $DMR_{<500}$ after subcritical water treatment at lab-scale for colour observation. (Numbers above the tubes indicate the minute of treatment at which they were collected).

3.6 Total organic carbon and solid residue

Total organic carbon followed the same trend than TPC (**Figure 3.12**). The longer the extraction time, the more TOC in subcritical water extracts at lab-scale. However, at pilot scale system, due to temperature decrease, a plateau was reached after 36 minutes of treatment.

The solid residues after SWE were analyzed to determine their element composition and listed in **Table 3.3**. This table also lists the elemental composition of the raw material. Sulphur content decreased for both SWE systems as a consequence of the partial extraction of the residual agar present in the alga residue at high temperatures. On lab-scale residue, the reduction hydrogen content was clearly observed as a result of the greater extraction of biocompounds in the liquid extracts during SWE. Consequently, lower H:C molar ratio was obtained. However, for pilot system, a great change was not appreciated due to the lower extraction in comparison with lab system and a higher proportion was obtained due to the decrease in sulphur content.

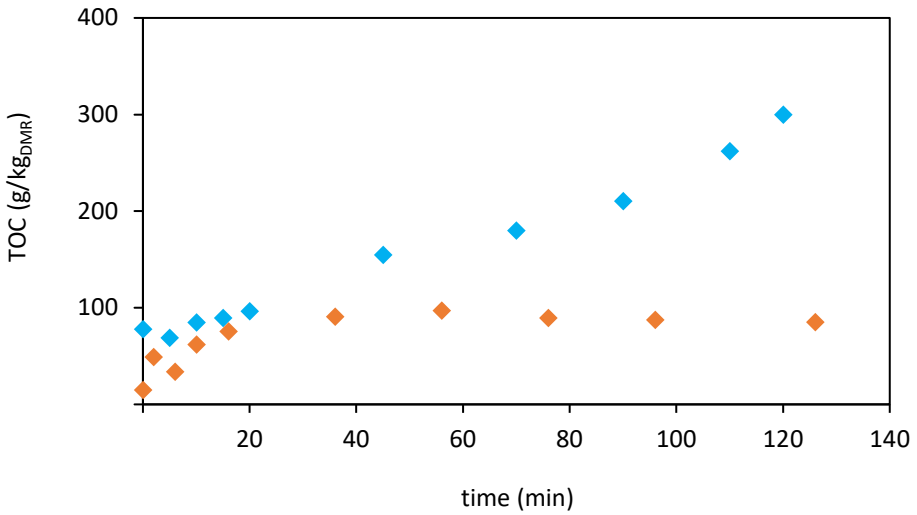

Figure 3.12. TOC content in subcritical water extracts collected at the different time intervals from DMR$_{<500}$ at lab-scale (◆) and pilot-scale (◆) at 175 °C working temperature.

Table 3.3. Elemental analysis, ash content and estimated higher heating value (HHV) of dried macroalga residue (DMR), DMR < 500 µm size fraction ($DMR_{<500}$) and solid residues after SWE on lab-scale and pilot-scale. (Oxygen content was estimated by difference)

Sample	C (%)	N (%)	H (%)	S (%)	O (%)	ashes (%)	H:C	O:C	N:C	HHV (kJ/kg)
DMR	36 ± 1^{a}	4.2 ± 0.4^{b}	5.9 ± 0.2^{b}	0.21 ± 0.05^{ab}	32.3 ± 0.3^{c}	21.8 ± 1.1^{b}	2.0 ± 0.1^{c}	0.68 ± 0.03^{a}	0.11 ± 0.01^{a}	$14{,}987 \pm 466^{a}$
$DMR_{<500}$	38 ± 1^{ab}	3.6 ± 0.1^{ab}	5.6 ± 0.2^{b}	0.70 ± 0.05^{c}	27.2 ± 1.4^{b}	24.9 ± 1.0^{c}	1.8 ± 0.2^{bc}	0.54 ± 0.09^{a}	0.08 ± 0.02^{a}	$15{,}789 \pm 250^{b}$
Residue Lab-Scale	36 ± 1^{a}	3.5 ± 0.1^{a}	4.6 ± 0.2^{a}	0.09 ± 0.08^{a}	23.1 ± 1.4^{a}	32.9 ± 0.7^{d}	1.5 ± 0.1^{a}	0.5 ± 0.1^{a}	0.08 ± 0.02^{a}	$15{,}476 \pm 318^{ab}$
Residue Pilot-Scale	40.7 ± 0.2^{b}	4.2 ± 0.1^{b}	5.80 ± 0.03^{b}	0.22 ± 0.01^{b}	30.4 ± 0.2^{bc}	18.7 ± 0.1^{a}	1.7 ± 0.1^{ab}	0.56 ± 0.01^{a}	0.09 ± 0.01^{a}	$16{,}877 \pm 38^{c}$

Values with different letters in each column are significantly different when applying the Fisher's least significant differences (LSD) method at p value ≤ 0.05 (*C* carbon; *H* Hydrogen; *N* Nitrogen; *S* Sulfur; *O* Oxygen) expressed as % (w/w) ± standard deviation (n = 3 technical replicates)

Conclusions

Subcritical water extraction has been proven to be an efficient technology for bioactive compounds recovery such as carbohydrates, protein and amino acids from algae residue. Scaling up from laboratory to pilot subcritical water system resulted in good and reproducible results with 75.9 and 73.8 % extraction yield for galactans, 9.5 and 9.6 % for glucans and 37.5 and 36.8 % for protein at lab and pilot-scale systems, respectively. Therefore, feasibility of industrial-scale subcritical water system through scaling-up from lab to pilot system has been showed. However, future research about an adequate heating system that allows maintaining the temperature throughout the extraction process in SWE at industrial plant is needed.

References

Cabeza, A., Piqueras, C. M., Sobrón, F., & García-serna, J. (2016). Modeling of biomass fractionation in a lab-scale biorefinery: Solubilization of hemicellulose and cellulose from holm oak wood using subcritical water. *Bioresource Technology*, 200, 90–102.

Camel, V. (2001). Recent extraction techniques for solid matrices - Supercritical fluid extraction, pressurized fluid extraction and microwave-assisted extraction: Their potential and pitfalls. *Analyst*, 126, 1182–1193.

Cherubini, F. (2010). The biorefinery concept: Using biomass instead of oil for producing energy and chemicals. *Energy Conversion and Management*, 51, 1412–1421.

Chisti, Y. (2007). Biodiesel from microalgae. *Biotechnology Advances*, 25, 294–306.

Friedl, A., Padouvas, E., Rotter, H., & Varmuza, K. (2005). Prediction of heating values of biomass fuel from elemental composition. *Analytica Chimica Acta*, 544, 191–198.

He, L., Zhang, X., Xu, H., Xu, C., Yuan, F., Knez, Ž., Novak, Z., & Gao, Y. (2012). Subcritical water extraction of phenolic compounds from pomegranate (*Punica granatum* L.) seed residues and investigation into their antioxidant activities with HPLC-ABTS assay. *Food and Bioproducts Processing*, 90, 215–223.

Herrero, M., Cifuentes, A., & Iban, E. (2006). Sub- and supercritical fluid extraction of functional ingredients from different natural sources: Plants, food-by-products, algae and microalgae A review. *Food Chemistry*, 98, 136–148.

Jeong, T. S., Kim, Y. S., & Oh, K. K. (2012). A kinetic assessment of glucose production from pretreated *Gelidium amansii* by dilute acid hydrolysis. *Renewable Energy*, 42, 207–211.

Ko, M. J., Kwon, M. R., & Chung, M. S. (2020). Pilot-scale subcritical-water extraction of nodakenin and decursin from Angelica gigas Nakai. *Food Science and Biotechnology*, 29(5), 631–639.

Kwon, H. L., & Chung, M. S. (2015). Pilot-scale subcritical solvent extraction of curcuminoids from *Curcuma long* L. *Food Chemistry*, 185, 58–64.

Mohan, M., Timung, R., Deshavath, N.N., Banerjee, T., Goud, V.V., & Dasu, V.V. (2015). Optimization and hydrolysis of cellulose under subcritical water treatment for the production of total reducing sugars. *RSC Advances*, 5, 103265–103275.

Morales, F. J., & Jiménez-Pérez, S. (2001). Free radical scavenging capacity of Maillard reaction products as related to colour and fluorescence. *Food Chemistry*, 72, 119–125.

Morales-Muñoz, S., Luque-García, J.L., & Luque de Castro, M.D. (2002). Pressurized Hot Water Extraction with On-Line Fluorescence Monitoring: a Comparison of the Static, Dynamic, and Static-Dynamic Modes for the Removal of Polycyclic Aromatic Hydrocarbons from Environmental Solid Samples. *Analytical Chemistry*, 74, 4213–4219.

Park, J. S., Jeong, Y. R., & Chun, B. S. (2019). Physiological activities and bioactive compound from laver (*Pyropia yezoensis*) hydrolysates by using subcritical water hydrolysis. *The Journal of Supercritical Fluids*, 148, 130–136.

Plaza, M., Amigo-Benavent, M., del Castillo, M.D., Ibáñez, E., & Herrero, M. (2010). Neoformation of antioxidants in glycation model systems treated under subcritical water extraction conditions. *Food Research International*, 43, 1123–1129.

Plaza, M., & Turner, C. (2015). Pressurized hot water extraction of bioactives. *Trends in Analytical Chemistr*y, 71, 39–54.

Pronyk, C., & Mazza, G. (2009). Design and scale-up of pressurized fluid extractors for food and bioproducts. *Journal of Food Engineering*, 95, 215–226.

Rogalinski, T., Herrmann, S., & Brunner, G. (2005). Production of amino acids from bovine serum albumin by continuous sub-critical water hydrolysis. *Journal of Supercritical Fluids*, 36, 49–58.

Sánchez-Bastardo, N., Romero, A., & Alonso, E. (2017). Extraction of arabinoxylans from wheat bran using hydrothermal processes assisted by heterogeneous catalysts. *Carbohydrate Polymers*, 160, 143–152.

Singleton, V.L., Orthofer, R., & Lamuela-Raventós, R.M. (1999). Analysis of total phenols and other oxidation substrates and antioxidants by means of Folin-Ciocalteu reagent. *Methods in Enzymology*, 25, 281–286.

Trigueros, E., Sanz, M.T., Alonso-Riaño, P., Beltrán, S., Ramos, C., & Melgosa, R. (2021a). Recovery of the protein fraction with high antioxidant activity from red seaweed industrial solid residue after agar extraction by subcritical water treatment. *Journal of Applied Phycology*.

Trigueros, E., Sanz, M.T., Filipigh, A., Beltrán, S., & Riaño, P. (2021b). Enzymatic hydrolysis of the industrial solid residue of red seaweed after agar extraction: extracts characterization and modelling. *Food and Bioproducts Processing*, 126, 356–366.

Yedro, F.M., García-Serna, J., Cantero, D.A., Sobrón, F., & Cocero, M. J. (2015). Hydrothermal fractionation of grape seeds in subcritical water to produce oil extract, sugars and lignin. *Catalysis Today*, 257, 160–168.

Yoo, H.U., Ko, M.J., & Chung, M.S. (2020). Hydrolysis of beta-glucan in oat flour during subcritical-water extraction. *Food Chemistry*, 308.

Zakaria, S.M., & Mustapa Kamal, S.M. (2016). Subcritical Water Extraction of Bioactive Compounds from Plants and Algae: Applications in Pharmaceutical and Food Ingredients. *Food Engineering Reviews*, 8, 23–34.

CHAPTER 4

Enzymatic hydrolysis of the industrial solid residue of red seaweed after agar extraction: Extracts characterization and modelling

Based on the article:

Trigueros E., Sanz M.T., Filipigh A., Beltrán S., Riaño P. (2021). "Enzymatic hydrolysis of the industrial solid residue of red seaweed after agar extraction: Extracts characterization and modelling".

Food and Bioproducts Processing, 126, 356-366

DOI: https://doi.org/10.1016/j.fbp.2021.01.014

Capítulo 4

Hidrólisis enzimática del residuo sólido industrial de alga roja tras la extracción del agar: caracterización de los extractos y modelado

Resumen

Se ha evaluado la eficiencia de la hidrólisis enzimática para la liberación de diferentes biocompuestos como compuestos fenólicos totales (TPC), azúcares y proteínas del residuo sólido industrial de *G. sesquipedale* tras la extracción del agar. Se ha demostrado que la celulasa (0,25 - 8 %, p/p, enzima:residuo sólido, pH = 5) es una enzima eficaz para degradar la pared celular de las algas, lo que favorece la liberación de TPC unidos a la misma, con valores de hasta 7,5 mg de equivalentes de ácido gálico/g de residuo seco de macroalga. Los carbohidratos se liberaron al medio de reacción en forma de monómeros y oligómeros (glucosa, galactosa y arabinosa), con rendimientos superiores al aumentar la concentración de celulasa. Las combinaciones enzimáticas con otras enzimas hidrolíticas, como la xilanasa y la proteasa, no aportaron ninguna mejora en los rendimientos de TPC y azúcares. La proteína también se liberó al medio enzimático con rendimientos de extracción de alrededor del 30 %. El uso de proteasa en condiciones básicas condujo a un aumento en la liberación de la fracción proteica y del contenido de aminoácidos libres con una proporción hidrofóbica superior a la de la materia prima. Las cinéticas de TPC e hidrólisis de proteínas se han ajustado a los modelos power law y Weibull, siendo el modelo Weibull el que mejor se ajusta.

Palabras clave: enzimas hidrolíticas, modelos cinéticos, residuo industrial macroalga, TPC, carbohidratos, proteínas

Abstract

The efficiency of enzymatic hydrolysis for the release of different biocompounds such as total phenolic compounds (TPC), sugars and proteins from the industrial solid residue of *G. sesquipedale* after agar extraction has been evaluated. Cellulase (0.25-8 %, w/w, enzyme: solid residue, pH = 5) has been proved to be an efficient enzyme to degrade the algae cell wall improving the release of the bound TPC with values up to 7.5 mg gallic acid equivalent/g dry macroalgae residue. Monomer and oligomer carbohydrates were released to the reaction medium, namely glucose, galactose and arabinose with higher yields by increasing cellulase concentration. Enzyme combinations with other hydrolytic enzymes, such as xylanase and protease, did not bring any improvement of the TPC and sugar yields. Protein was also released to the enzymatic medium with protein extraction yields around 30 %. The use of protease under basic conditions led to an increase in the release of the protein fraction and of the free amino acids content with a hydrophobic ratio higher than in the raw material. The kinetics of TPC and protein hydrolysis have been fitted to the power law and the Weibull models yielding the Weibull model the best fitting quality.

Keywords: hydrolytic enzymes, kinetic models, macroalgae industrial residue, TPC, carbohydrates, proteins.

1. Introduction

Gelidium sesquipedale is a red alga that is widely used for agar production. The industrial process of agar extraction generates a solid residue that accounts for 15-40 % of the initial dry biomass (Álvarez-Viñas et al., 2019). This solid residue can be used for fodder and fertilizer although most of it is disposed of (Ferrera-Lorenzo, Fuente, Suárez-Ruiz, & Ruiz, 2014). However, it presents a valuable chemical composition with high protein content with all the essential amino acids, carbohydrates and with low insoluble lignin content (Trigueros et al., 2021). To incorporate commercially exploited macroalgae into a biorefinery context, valorization of this solid residue must be considered to reach the concept of zero residues.

Due to the complex chemical structure of macroalgae, it allows to produce different high added values compounds (Ruiz et al., 2015). The most essential step to break the cell wall of the algae to release biomolecules is the pretreatment technique. The pretreatment techniques available for the macroalgae can be classified into four main categories: physical, physicochemical, chemical and biological ones (Shobana et al., 2017).

One of the most attractive technologies for pretreatment of the biomass are those based on hydrothermal processes using different heating sources such as subcritical water (subW) and steam explosion. These techniques can be considered as green and clean technologies since they are based on the use of water as extracting/hydrolytic agent. In steam explosion, the biomass is subjected to high pressure saturated steam (0.69-4.83 MPa) at a temperature of 160-260 °C and then the pressure is suddenly reduced to let the water escape in an explosive way that causes explosion of the biomass (Baruah et al., 2018). SubW uses water as solvent at temperature above its boiling point, 100 °C, and below its critical point 374 °C and pressure high enough to keep water at its liquid state. At these conditions water provides an effective medium for acid- and base-catalyzed reactions. Therefore, an important advantage of these techniques is that the use of catalyst or chemicals is avoided to get biomass hydrolysis.

Recently, subW treatment was applied to the solid residue generated after agar extraction from *G. sesquipedale* (Trigueros et al., 2021). By using a semicontinuous fix-bed reactor configuration, nearly 70 % of the protein content was recovered with nearly 100 mg of free amino acids/$g_{protein}$. SubW treatment also allowed the release of total phenolic compounds to the medium presenting a high antioxidant capacity.

On the other hand, the use of enzyme assisted extraction (EAE) is a promising technology that presents a great potential to improve the extraction efficiency of bioactive components (Sabeena et al., 2020). EAE offers several advantages over conventional extraction methods such as high yield and specificity, being an environmental friendly technology (Wijesinghe & Jeon, 2012). However, the cost of the enzyme is one of the technical limitations for processing large volumes of raw material (Puri et al., 2012). The use of hydrolytic enzymes helps to degrade the cell wall structure thereby enhancing the release of bioactive compounds since some of these compounds are either dispersed in the cell cytoplasm or retained in the cell wall by hydrogen or hydrophobic bonding (Fleurence et al., 1995). Furthermore, antioxidant properties of the hydrolysates are enhanced due to the breakdown of high molecular weight polysaccharides and proteins (T. Wang et al., 2010). In the literature, some studies can be found regarding the use of EAE to increase the extraction of bioactive compounds from different brown, red and green algae (Sabeena et al., 2020) (Hardouin et al., 2014) (T. Wang et al., 2010) (Vásquez et al., 2019). However, only a few studies deal with the use of EAE from the residue generated after phycocoloids extraction from macroalgae. Shukla and Jumar (Shukla et al., 2016) treated the leftover pulp after agar extraction of *Gracilaria Verrucosa* by enzyme hydrolysis to obtain reducing sugars that were later used as fermentation broth to produce ethanol by using *S. cerevisiae*.

The aim of this work was to study the potential of EAE, as an alternative to hydrothermal processes, to improve the release of biocompounds from the industrial solid residue remaining after agar extraction from *G. sesquipedale* by using cellulase, protease and xylanase as hydrolytic enzymes. The main goal of this article was to provide a detailed characterization of the enzymatic extracts, showing the ability of the hydrolytic enzymes to release different biocompounds into the extraction medium. Extraction kinetics and yield of TPC and proteins were determined. The knowledge of the extraction curves is important to determine the time needed to obtain a certain extraction yield and analyze the

characteristics of enzymatic extraction. The presence of other biocompounds in the final extract was also determined, such as the presence of free amino acids and carbohydrates, namely, glucose, galactose and arabinose. To our knowledge, the enzymatic extraction from the solid residue after agar extraction had not been previously reported in literature and results would help to valorize this industrial solid waste.

2. Materials and methods

2.1. Raw material

The raw material used in this work has been provided by Hispanagar (Burgos, Castilla y León, Spain) (https://www.hispanagar.com/es) and it consisted of the solid residue from *G. sesquipedale* after agar extraction. This raw material was oven dried at 45 °C for 24 hours to preserve it and retard microbial growth during storage. This solid residue was called "macroalgae residue", MR. Final moisture content of this by-product was determined gravimetrically by weighing it before and after drying in an oven at 105 °C until constant weight resulting to be 5 ± 2 %. Sample moisture was used to express results per gram of dried MR (DMR).

Biomass characterization was performed according to the NREL protocols (Sluiter et al., 2010). Carbohydrates were quantified by high-performance liquid chromatography (HPLC) with a Bio-Rad Aminex-HPX-87 H column, a variable wavelength detector (VWD) and a refractive index detector (RID) using a mobile phase constituted by 0.005 M sulphuric acid. The column detector was maintained at 40 °C. Uronic acids were determined after acid hydrolysis according to the method of Filisetti-Cozzi (Filisetti-Cozzi & Carpita, 1991).

Protein content in the MR was obtained by the total nitrogen content as measured by the elemental analysis (Thermo Scientific Model Flash 2000) by using the nitrogen factor (NF). The NF was determined according to the amino acid profile of the MR determined after acid and basis hydrolysis. After hydrolysis, the amino acid profile was determined by using the EZ:faast Phenomenex procedure (Trigueros et al., 2021).

2.2. Hydrolytic enzymes

Cellulase, 1,4-(1,3:1,4)-β-D-Glucan 4-glucanohydrolase, EC 3.2.1.4, from *Aspergillus niger* was provided by Sigma-Aldrich. Xylanase, a mixture of xylanase endo-1,4β (EC 3.2.1.8) and xylanase endo-1,3β (EC 3.2.1.32) from *Trichoderma Longibrachiatum* and a protease, proteinase EC 3.2.1.6, from *Bacillus subtilis* were supplied by Biocon.

2.3. Enzymatic hydrolysis

7.5 g of the MR were introduced into a 500 mL jacketed reactor provided with magnetic agitation together with 150 mL of the reaction medium. pH was adjusted by adding HCl or NaOH. Enzyme treatment was carried out at constant temperature of 50 °C. When the temperature was reached, the enzyme was added to the mixture and hydrolysis was carried out for more than 24 h. Samples were withdrawn at regular time intervals to plot the corresponding extraction curves. To stop the hydrolytic reaction, the enzyme was inactivated by heating the withdrawn samples at 100 °C for 5 min and immediately were cooled in ice and kept in the refrigerator until analysis. Samples were centrifuged (Thermo Scientific Sorvall ST16) and filtered through a Whatman n° 542 filter before analysis.

The cellulase concentration, expressed as enzyme:DMR ratio (w/w), was varied in the mass percent range from 0.25 % to 8 %. A control sample at the same extraction temperature but with no enzyme added to the extraction medium was also carried out. Other hydrolytic enzymes such as xylanase and protease were also tested separately and the effect of their association with cellulase was also determined.

2.4. Characterization of the enzymatic liquid extracts

2.4.1. Extraction yield

1.5 mL of the final enzymatic extract was filtered through a 0.22 µm filter and dried at 105 °C to remove the solvent until constant weight. Extraction yield was calculated as the ratio

between the residual weight of the dry extract obtained after removing the solvent by evaporation, by considering the initial volume of the solvent, and the weight of the DMR charged into the enzymatic reactor.

2.4.2. Determination of total phenolic compounds

TPC were evaluated according to the method of Folin Ciocalteu (Singleton et al., 1999). A calibration curve was prepared with standard solutions of gallic acid by following the same colorimetric method and results were expressed as TPC extraction yield, defined as mg of gallic acid equivalent (GAE) per gram of DMR.

2.4.3. Determination of carbohydrates and derived compounds

Identification and quantification of carbohydrates were performed by HPLC as described in **section 2.1**. Monosaccharides and derived products were directly analyzed in the liquid enzymatic hydrolysates previously filtered through 0.22 µm pore size (Scharlab syringe filter). Total sugars were determined after hydrolysis of the sample according to the Laboratory Analytical Procedure (LAP) (Sluiter et al., 2010) to hydrolyze the oligomer sugars. Sugar yield was calculated as monomer yield and oligomer yield (Sánchez-Bastardo et al., 2017):

$$Monomer\ yield\ (\%) = \frac{MS_{enzymatichydrolysate}}{Sugar_{rawmaterial}} \cdot 100 \quad \textbf{[4.1]}$$

$$Total\ yield\ (\%) = \frac{(MS\ and\ OS)_{enzymatichydrolysate}}{Sugar_{rawmaterial}} \cdot 100 \quad \textbf{[4.2]}$$

where *MS* and *OS* are the content of monomeric and oligomeric sugars in the enzymatic hydrolysates.

2.4.4. Protein determination

Total protein content in the enzymatic extracts was determined by using the kit DC (Bio-Rad Laboratories, Hércules-CA, USA) based on the Lowry protocol (Lowry et al., 1951). This assay was chosen since, according to the literature, the Lowry method is recommended to measure protein content in seaweeds and allows a better quantification compared to other methods (Barbarino & Lourenço, 2005). A calibration curve was done by using bovine serum albumin as standard. The protein extraction yield was calculated as:

$$Protein\ yield\ (\%) = \frac{protein_{enzymatichydrolysate}}{protein_{rawmaterial}} \cdot 100 \qquad [4.3]$$

2.4.5 Free amino acids and hydrolysis degree

Free amino acids in the enzymatic extracts were determined by using the EZ:faast Phenomenex kit (see **section 2.1**). The percentage of hydrolysed peptide bonds, the hydrolysis degree (DH), was evaluated by the ninhydrin reaction method according to the Sigma Aldrich protocol. 2 mL of sample were gently mixed with 1 mL of ninhydrin reagent solution and placed into a boiling water bath for 10 min. After that, samples were cooled and 5 mL of 95 % ethanol were added. Absorbance was measured at 570 nm. A calibration curve was obtained by using different standards of a leucine solution that was daily prepared (Friedman, 2004). The DH was evaluated as (Adler-Nissen et al., 1983):

$$DH = h/h_{tot} \cdot 100\ (\%) \qquad [4.4]$$

where *h* is the number of equivalent peptide bonds hydrolysed, expressed as meq/g protein and h_{tot} is the total amount of milimols of individual amino acids per gram in the unhydrolysed protein that can be evaluated from the amino acid profile.

2.5. Modelling of the extraction curves

Modelling of the extraction curves is a useful tool to optimize the extraction process reducing the cost of the process. The use of empirical models helps to simplify the study of

complex systems such as the extraction of biocompounds from plant materials (González-Centeno et al., 2015). In this work, two empirical models that have been previously proposed to model the extraction and recovery of compounds from different types of solid matrix were used to fit the experimental data obtained from the extraction and try to elucidate the extraction mechanism: the power law and the Weibull models (Patricia Alonso-Riaño et al., 2020) (Kitanović et al., 2008). The power law model can be described by the following equation:

$$Extraction\ yield, mg_{biocompound}/g_{DMR} = Bt^n \quad \textbf{[4.5]}$$

where *t* is the extraction time (s), *B* is a constant incorporating the characteristics of the particle-active substance system and *n* is the diffusional exponent.

The Weibull's model was expressed as:

$$Extraction\ yield,\ mg_{biocompound}/g_{DMR} = A\left(1 - exp(-kt^m)\right) \quad \textbf{[4.6]}$$

where *t* is the extraction time (s), *A*, *k* and *m* are the kinetic parameters.

A deep analysis of the kinetic parameters for both models would help to determine the dependence on operating conditions leading to a better design, simulation, optimization and control of further industrial processes (González-Centeno et al., 2015).

To estimate the kinetic parameters, non-linear regression was performed by using the Marquardt algorithm (Statgraphics X64). Experimental results were then compared with those of the model prediction through the values of the Root Mean Square Deviation (RMSD) between experimental and calculated extraction yields:

$$RMSD = \sqrt{\frac{\sum_{i=1}^{n}\left(Yield_{exp} - Yield_{calc}\right)^2}{n}} \cdot 100 \quad \textbf{[4.7]}$$

where *n* is the number of experimental data points in each kinetic curve.

2.6. Statistical analysis

Statistical analyses were conducted using the software Statgraphics X64. The results were presented as a mean ± standard deviation of at least three replicates. To confirm significant differences, the Fisher's least significant differences method at p-value ≤ 0.05 was applied.

3. Results and discussion

3.1. Macroalgae solid residue characterization

Table 4.1 presents the chemical characterization of *G. sesquipedale* solid residue after agar extraction (Trigueros et al., 2021). Chemical composition would depend on the industrial extraction process as well as other intrinsic factors such as origin and season of the collected macroalgae due to different stages of macroalgae development. Polysaccharides accounted for a mass percent of 41 ± 2 % in a dry basis. This fraction consisted mainly of glucans (23.4 ± 0.9 %) and galactans (11.9 ± 0.5 %) with small amounts of arabinans, 2.9 ± 0.2 % and 3.8 ± 0.1 % of uronic acids. The higher content of glucans compared to galactans is due to the efficient reduction of the galactans content during the agar industrial extraction process. Similar results were reported in the literature by Kim et al. (2015) for *Gelidium amansii* after autoclaving treatment of the macroalgae. These authors determined that the main sugars were galactose and glucose, 30.3 ± 0.6 and 21.6 ± 0.4 (mass percent % in a dry basis) in the raw *Gelidium amansii*; however, after autoclaving, due to efficient reduction of the galactan content, the relative content of glucose increased and galactose decreased. After 40 min of autoclaving, these authors determined 13.5 ± 0.3 and 39.6 ± 1.2 (mass percent % in a dry basis) for galactose and glucose, respectively. Lipid content was low, less than 1 %. The lipid content agreed with the range reported in the literature between 0.3 and 3.6 g/100 g dry seaweed for different red, brown and green algae (Rodrigues et al., 2015). Extractives represented 11.5 ± 0.9 %, proteins 21 ± 1 % and ashes 22 ± 2 % of DMR composition. The relative high protein content of the solid residue after agar extraction agreed with the fact that red algae have the highest protein content among the three types

of macroalgae (Postma et al., 2018) with all essential amino acids, being worth its valorization. Insoluble lignin accounted for 3 ± 1 %, as corresponds to third generation biomass.

Table 4.1. Chemical composition of macroalgae residue, MR, expressed as mass percent % ± SD in a dry basis.

Compound	Composition, %
Extractives	**11.5 ± 0.9**
Polysaccharides	**41.0 ± 2.0**
Glucans	23.4 ± 0.9
Galactans	10.9 ± 0.5
Arabinans	2.9 ± 0.2
Uronic acids	3.8 ± 0.1
Lignin	**11.7 ± 1.1**
Soluble	8.7 ± 0.1
Insoluble	3.0 ± 1.0
Proteins*	**21 ± 1**
Lipids	**0.87 ± 0.09**
Ashes	**22 ± 2**

*Proteins include the protein content in the extractive fraction (2.6 %).
NF = 4.9 (see **Table 4.6** for amino acid profile)

3.2. TPC release by cellulase hydrolysis

Figure 4.1 shows the time course of TPC release at different cellulase loading from 0.25 to 8 % (mass percent %, enzyme:MR ratio) at pH = 5. This pH was initially selected since it has been reported in literature as the optimum pH for cellulase activity (Shukla et al., 2016). By increasing the enzyme loading, the initial TPC release rate and the final extraction yield increased. A high cellulase loading led to a more effective cell wall degradation and consequently an improved release of the bound phenolic compounds. Hydrolytic extraction curves indicated that more than 70 % of final TPC release took place in the first 3 h (10800

s) of enzymatic treatment, but up to 24 h of treatment were needed to reach the final extraction equilibrium. Vásques et al. (Vásquez et al., 2019) also reported long hydrolysis time due to the complexity of the algae matrix, between 12 h and 18 h for red and brown algae, respectively. **Figure 4.1** also shows the TPC release when using water as solvent at its natural pH. The low values of TPC extraction yield indicated that the non-enzymatic TPC release is much lower in the experimental conditions evaluated due to the presence of phenolic compounds bound to the cell wall that limits its extraction efficiency (Sabeena et al., 2020).

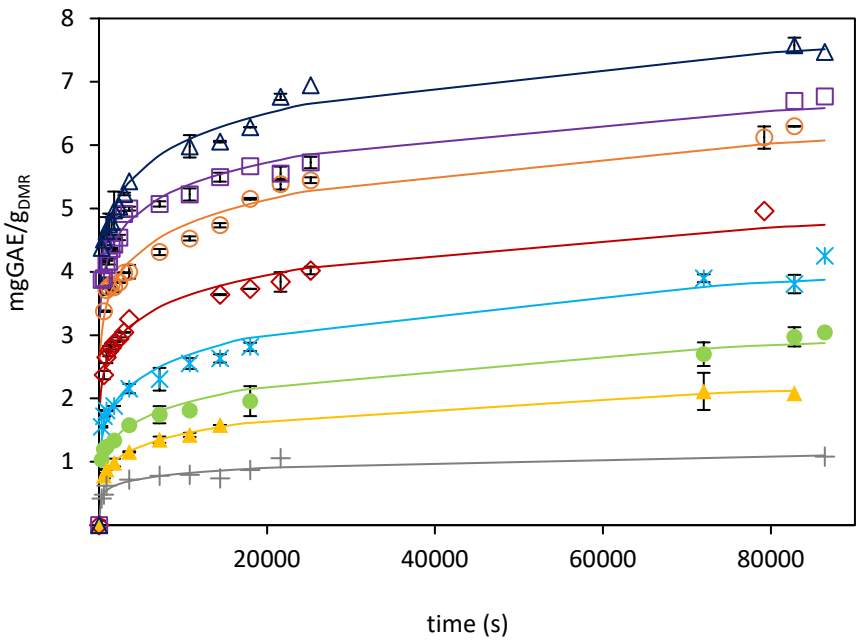

Figure 4.1. TPC extraction kinetics at 50 °C and pH = 5 at different cellulase loadings (▲ 0.25 %, ● 0.5 %, ✳ 1%, ◇ 2%, ○ 4%, □ 6%, △ 8%) and by using water as solvent at its natural pH, (+). The continuous lines represent the Weibull model (**Table 4.3**).

To evaluate the effect of the pH of the hydrolysis medium, enzymatic hydrolysis was carried out at 6 % cellulase loading in water as reaction medium at its natural pH. Results are presented in **Figure 4.2**, where it can be observed that half TPC extraction yield was reached than at pH of 5. Gligor et al. (Gligor et al., 2019) described that an acid pH influences the catalytic activity by modifying the protein configuration and binding capacity to the

substrates, concluding that enzymes usually require acidic pH values. The hydrolytic effect of an acid extraction medium was evaluated by performing the kinetics at pH of 5 in the absence of enzyme (see also **Figure 4.2**). Similar results were obtained as when using 6 % of cellulase in water. This can be due to the fact that an acidic extraction led to hydrogen bonds destabilization resulting in increased cellular wall plasticity (Gligor et al., 2019).

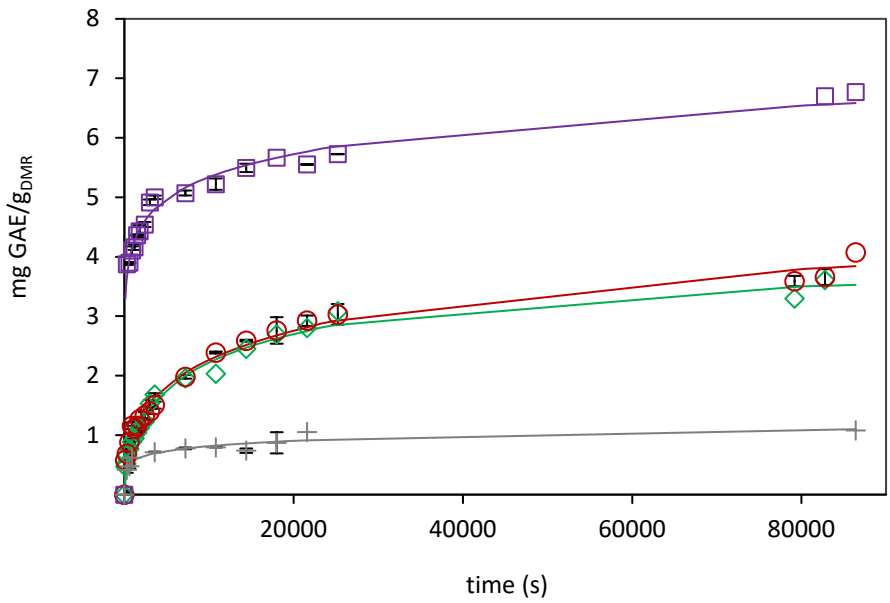

Figure 4.2. TPC extraction kinetics at 50 °C (□ 6% cellulase pH = 5; ◇ 6 % cellulase in water, ○ no cellulase pH = 5, + water as solvent). The continuous lines represent the Weibull model (**Table 4.3**).

The maximum TPC obtained in this work, as determined by the Folin Ciocalteu method, was lower than the values obtained by subW treatment of this solid residue. In previous work, by applying subW (Trigueros et al., 2021), 26 mg GAE/g_{DMR} were obtained in a semicontinuous fix-bed reactor at 200 °C and residence time of 18.7 min. However, at this temperature, Maillard reactions products between sugars and amino acids would interfere in the analysis, that could provide higher TPC values.

The total yield of enzymatic extracts after 24 h ranged from 11.2 ± 0.9 % to 73 ± 2 % at 0.25 and 8 % (w/w) cellulase loading respectively (see **Table 4.2**). These extraction yields were

higher than the value obtained when using water as extraction solvent at its natural pH, 6.1 ± 0.3 %. Similar to TPC release, by increasing enzyme loading, higher total extraction yields were obtained due to the breakdown of the cell wall of the algae and the release of the compounds into the extraction medium (Sabeena et al., 2020). Other extraction yields reported in the literature for enzymatic extracts ranged from 36.0 to 95.1 % for different brown seaweeds by using commercial enzymes (Sabeena et al., 2020).

Table 4.2. Total extraction yield obtained at different cellulase loadings at pH = 5 and for the extraction controls (water, 6% cellulase in water and no enzyme added to medium at pH = 5).

Extraction medium	Extraction yield, %
Water (control)	6.1 ± 0.3[a]
0.25 % cellulase	11.2 ± 0.9[b]
0.5 % cellulase	15.5 ± 0.8[c]
1 % cellulase	22.5 ± 0.7[d]
2 % cellulase	39.5 ± 0.9[e]
4 % cellulase	47.0 ± 1.0[f]
6 % cellulase	60.0 ± 1.0[g]
8 % cellulase	73.0 ± 2.0[h]
6 % cellulase in water (control)	18.0 ± 1.0[c]
No enzyme, pH = 5 (control)	18.0 ± 2.0[c]

Values with different letters are significantly different when applying the Fisher's least significant differences (LSD) method at p-value ≤ 0.05

3.3. Enzymatic hydrolysis by other hydrolytic enzymes and their combination with cellulase

To ensure a complete cell wall breakage, the association of cellulase with other hydrolytic enzymes, such as xylanase and protease, was studied. First, the hydrolytic effect of xylanase and protease, by acting alone, was studied by performing the enzymatic treatment for an enzyme loading of 6 % mass percent and pH = 5 (**Figure 4.3**). It can be observed that cellulase

was the most effective enzyme on weakening the cell wall structure favouring faster TPC release. This result agrees with the recent literature that describes cellulases as enzymes

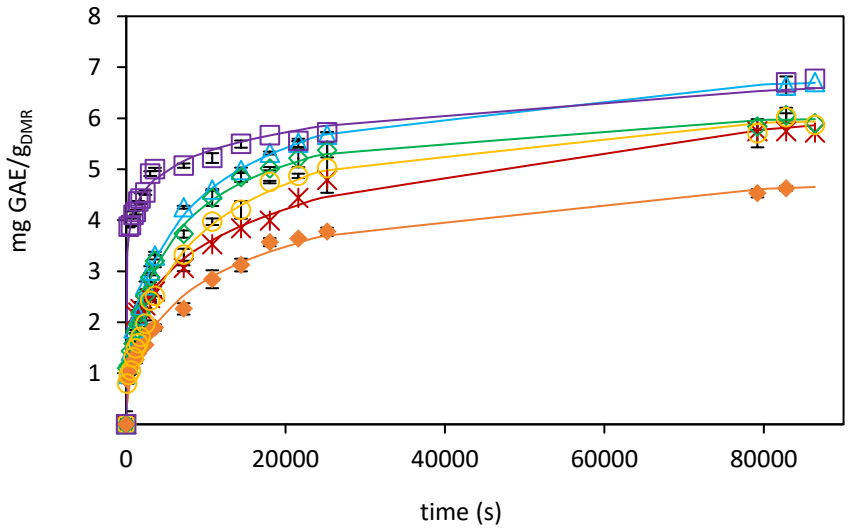

Figure 4.3. TPC extraction kinetics at 50 °C and pH = 5: □ 6% cellulase, △ 6% protease, ✳ 6% xylanase, ◇ 3 % cellulase + 3 % protease, ◆ 3 % cellulase + 3 % xylanase, ○ 2 % cellulase + 2 % protease + 2 % xylanase. The continuous lines represent the Weibull model (**Table 4.3**).

with a high hydrolytic capacity as well as a vast substrate specificity (Gligor et al., 2019). Among the three enzymes, xylanase led to the lowest TPC yield probably due to the structure of the cell wall of the MR since no xylanes were determined in the chemical composition. For the protease, slower extraction kinetics but similar final extraction yield was reached as for cellulase, probably due to the breakdown of the complexes formed between some phenolic compounds and proteins similar to phlorotannins naturally found in brown algae (Sánchez-Camargo et al., 2016). To further analyze the good results obtained by protease, the effect of pH on the protease activity was evaluated in the pH range from 5 to 8, since some proteases can exhibit high activity at high pH value (Faulds et al., 2008). The results are presented in **Figure 4.4** where it can be observed that the hydrolytic activity of the protease used in this work increased as the pH of the reaction medium increased.

TPC extraction curve was also determined for different enzyme combinations: two binary enzyme combinations: 3% cellulase + 3% protease and 3% cellulase + 3% xylanase and a ternary combination 2% cellulase + 2% protease + 2% xylanase (**Figure 4.3**). None of the combinations led to better results than for cellulase. The lowest yield was obtained for the combination of xylanase and cellulase. In this regard, different results have been found in literature regarding the effect of enzyme combinations. Rakariyatahm (Rakariyatham et al., 2019) found that the TPC extraction yield from Longan (*Dimocarpus longan*) peel by combining cellulase, α-amylase, protease and β-glucosidase significantly increased the extraction yield. Hosni et al. (Hosni et al., 2013) reported opposite results for the extraction of essential oils from two different species, *Thymus capitatus* and *Rosmarinus officinalis* leaves. A combination of cellulase and hemicellulase led to a better extraction yield for *T. capitatus* while for *R. officinalis,* lower extraction yield was obtained than for the enzyme acting alone. Boulila et al. (Boulila et al., 2015) recovered bioactive compounds from bay leaves (*Laurus nobilis L.*) by enzymatic treatment with cellulase, hemicellulase, xylanase and the ternary mixture. These authors found that, when enzymes were combined, the extraction yield was reduced suggesting a competitive adsorption to the cell wall polysaccharides that led to steric hindrance to bind the enzymes to the substrate decreasing the breakdown of the cell wall components.

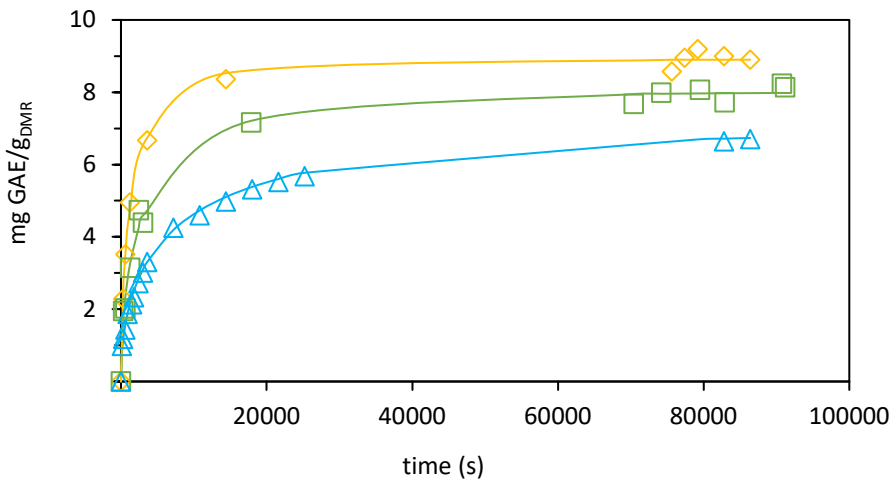

Figure 4.4. TPC extraction kinetics at 50 °C by using 6 % protease at different pH values (△ pH = 5, □ pH = 6, ◇ pH = 8). The continuous lines represent the Weibull model (**Table 4.3**).

3.4. Kinetic models

TPC extraction curves were fitted to the power law and the Weibull models and the corresponding parameters of the models have been listed in **Table 4.3**. According to the low values of the RMSD, both models fitted the extraction kinetics quite well, ranging from 0.032 to 0.650 and from 0.025 to 0.240 for the power law and the Weibull models, respectively.

For the power law model, the diffusional exponent, n, was lower than the unity, as reported for other plant materials (Kitanović et al., 2008). An observation of parameters listed in **Table 4.3** indicates that the type of enzyme and its concentration had a great effect on initial rate and final extraction yield. By observing the parameters reported in **Table 4.3**, for the experiments carried out by using cellulase as biocatalyst, the parameters of the power law model were correlated with the cellulase concentration, in the range from 0.25 to 8 % (mass percent) of catalyst loading:

$$B = 0.255\ [\text{Cellulase}] + 0.281\ (R^2 = 0.945) \quad [\mathbf{4.8}]$$

$$n = -0.029\ \ln [\text{Cellulase}] + 0.169\ (R^2 = 0.892) \quad [\mathbf{4.9}]$$

In the same way, for protease, a correlation was stablished between the pH of the medium in the range from 5 to 8:

$$B = 0.369\ [\text{pH}] - 1.460\ (R^2 = 0.997) \quad [\mathbf{4.10}]$$

$$n = -0.2135\ \ln [\text{pH}] + 0.600\ (R^2 = 0.960) \quad [\mathbf{4.11}]$$

Regarding the Weibull model, the trend observed for the k constant is justified by considering that this parameter is related with the extraction rate. The A constant increased as the final extraction yield also increased since it represents the maximum extraction yield at infinite time. The shape parameter, m, indicated the shape of the extraction curves. In this work, values of $m < 1$ indicates upward concavity. For the experiments carried out with cellulase, different relationships have been also found for the parameters and the cellulase concentration, in the range from 0.25 to 8 % mass percent of cellulase loading:

$A = 2.772 \ln [Cellulase] + 8.524$ ($R^2 = 0.9622$) [**4.12**]

$k = 0.016 [Cellulase] + 0.0416$ ($R^2 = 0.9007$) [**4.13**]

$m = -0.0365 \ln [Cellulase] + 0.2070$ ($R^2 = 0.9531$) [**4.14**]

Regarding the effect of pH for protease, a relationship between the Weibull parameters and the pH of the medium was also determined, in the pH range from 5 to 8:

$A = 3.968 \ln [pH] + 0.719$ ($R^2 = 0.973$) [**4.15**]

$k = 0.001\ pH + 0.004$ ($R^2 = 1.000$) [**4.16**]

$m = 0.1453 \ln [pH] + 0.286$ ($R^2 = 0.914$) [**4.17**]

The Weibull model has been represented in **Figures 4.1-4.4**, where it can be observed the good fitting to the experimental data. This model presented slightly lower RMSD values than the power law model; furthermore, we consider the power law model less realistic since does not approach to a limit with time.

3.5. Sugar release

Cellulase has been found an efficient enzyme to release TPC bound to the cell wall algae due to its hydrolytic action on cell wall increasing its permeability. The disruption of cell wall algae would led to the release of the polysaccharide fraction present in the MR into the extraction medium. Therefore, monomers and oligomers of glucose, galactose and arabinose were determined. The results of the different sugars released from the carbohydrate fraction of the MR after 24 h of enzymatic treatment are presented in **Figures 4.5 (a-c)**. The results have been presented as sugar yields for monomers and oligomers. By increasing the cellulase concentration, the sugar release for glucose, galactose and arabinose also increased. The lowest yield was obtained when using water as solvent with no enzyme added to the medium since no hydrolytic effect took place. At 6% cellulase in water at its natural pH, lower sugars yields were obtained than when pH was adjusted to 5.

Table 4.3. Kinetic parameters for the power law and the Weibull models for TPC enzyme assisted extraction.

Enzyme concentration	Power law			Weibull			
	B	n	RMSD	A	k	m	RMSD
0.25 % C	0.232	0.169	0.032	3.717	0.045	0.259	0.025
0.5 % C	0.312	0.196	0.098	7.949	0.035	0.225	0.110
1 % C	0.470	0.187	0.156	8.580	0.047	0.224	0.181
2 % C	1.023	0.136	0.103	10.188	0.093	0.168	0.114
4 % C	1.355	0.137	0.175	12.325	0.113	0.157	0.171
6 % C	2.054	0.103	0.122	13.062	0.153	0.134	0.133
8 % C	2.075	0.115	0.168	14.579	0.148	0.140	0.153
No enzyme, water*	0.196	0.154	0.067	1.802	0.088	0.208	0.068
No enzyme, pH= 5	0.162	0.281	0.159	5.055	0.014	0.407	0.111
6 % C in water*	0.145	0.287	0.196	3.860	0.010	0.488	0.114
6 % X	0.351	0.249	0.039	10.009	0.022	0.326	0.141
6 % P	0.364	0.264	0.40	6.996	0.009	0.512	0.097
3% C+ 3% P	0.383	0.249	0.455	6.092	0.008	0.551	0.153
3% C+ 3 % X	0.189	0.287	0.233	5.129	0.008	0.505	0.195
2% C+ 2% X+2% P	0.215	0.301	0.428	6.141	0.005	0.582	0.139
6 % P (pH = 6)	0.787	0.206	0.562	8.007	0.0097	0.5584	0.240
6 % P (pH = 8)	1.482	0.161	0.650	8.901	0.012	0.583	0.192

Unless specified experiments were carried out at pH = 5. C: cellulase, X: xylanase, P: protease
(*): natural water pH

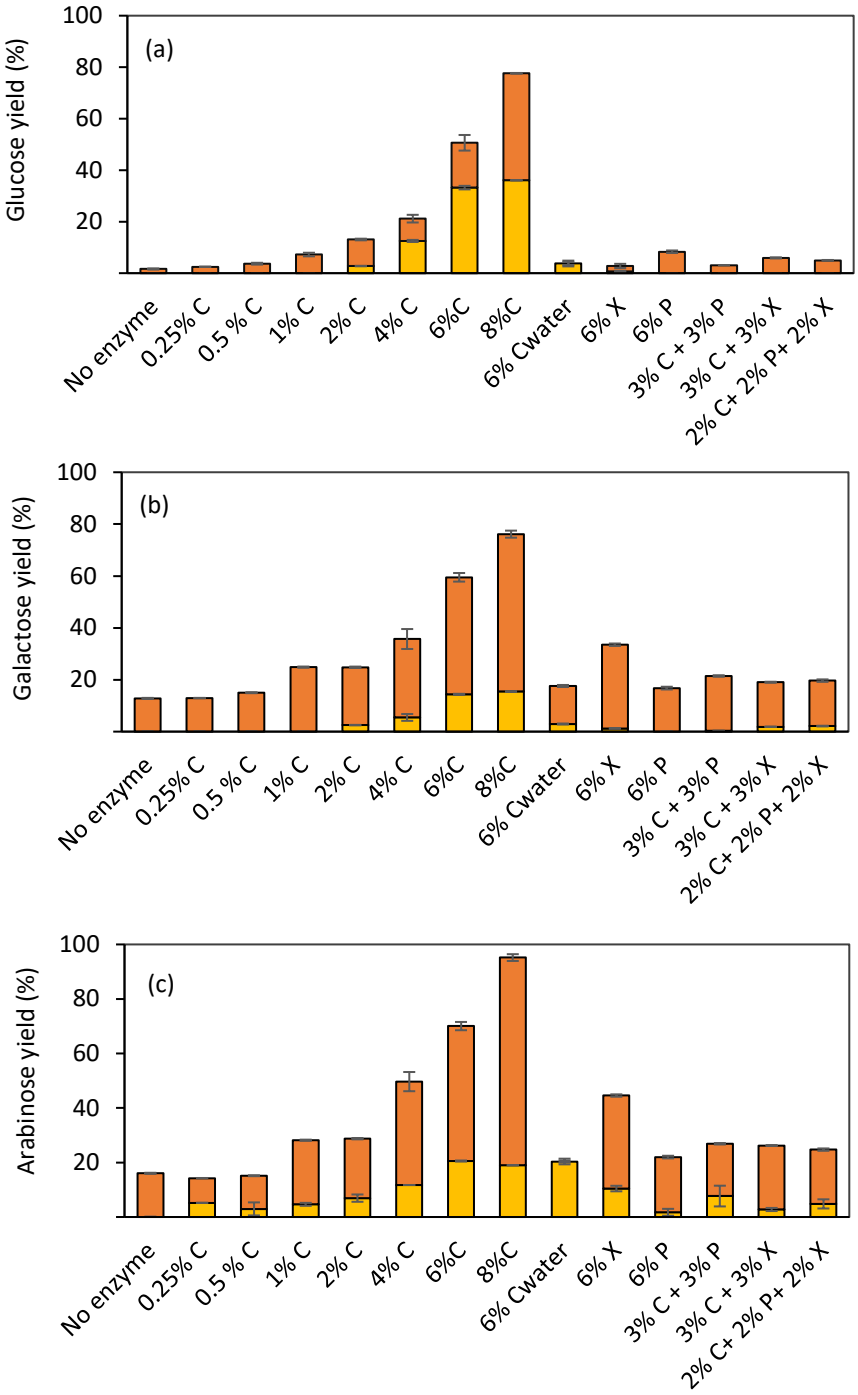

Figure 4.5. Sugars enzymatic yield at 50 °C after 24 h. **(a)** Glucose yield **(b)** Galactose yield, **(c)** Arabinose yield (■ monomer, ■ oligomer) by using different hydrolytic enzymes.

These results followed the same trend as the TPC release and the total extraction yield. The efficient breakdown of the cell walls of the algae by increasing the cellulase concentration led to a higher polysaccharide fraction in the enzymatic extracts.

In case of the glucose, about half of the sugar was released into the extraction medium as monomeric glucose, while the rest was solubilized as oligomers. Regarding galactose and arabinose, less than 20 % of their content in the substrate was released as monomers and the rest as oligomers. In any case, the presence of monomers and oligomers support that these type of enzymes attack randomly the internal sites of the amorphous region of the polysaccharide chain producing small oligosaccharides of different length, as it has been described in literature (Nadar et al., 2018). The higher percentage of glucose as monomer compared to the other sugars, indicated that the cellulase used in this work was more selective towards small chains of glucans to produce glucose as monomer compared to the other oligomer fractions of galactans and arabinans.

In **Figures 4.5a-c**, the results obtained for the other hydrolytic enzymes, protease and xylanase, and their combinations with cellulase have been also presented. At the same enzyme concentration, 6 % (w/w), the best results, in terms of sugar release, were obtained for cellulase. This can be related to the raw material composition being glucans the main component and cellulase would act preferentially over this fraction helping the release of the other polysaccharide components.

For all the enzymes or their combinations, the highest sugar yields were achieved by arabinose followed by galactose and glucose. For instance, at the highest cellulase dose essayed in this work, 8%, the sugar yields were 95 % for arabinose, 76 % for galactose and 77 % for glucose. The lower yields obtained for both hexoses (galactose and glucose) compared to arabinose could be due to monomeric sugar degradation to other compounds via enzymatic conversion of hexoses (see **Figure 4.6**). When using the cellulase, the major sugar degradation compound was lactic acid that accounted up to 100 mg/g_{DMR}. Lactic acid bears a hydroxyl group and an acid function, being able to undergo numerous chemical conversions to useful products. Succinic, acetic and formic acids were also determined as well as small amount of ethanol. Acetic acid was one the major compounds formed when using the other enzymes or their combinations with cellulase, proving that the presence of

other enzymes exert a competitive effect on the enzymatic transformation routes. Degradation products due to dehydration reaction of hexoses such as furfural and 5-hydroxymethylfurfural (HMF) and other degradation products as pyruvaldehyde were not found in the enzymatic extracts. These products have been reported as degradation products from the polysaccharide fraction of biomass by hydrothermal process (Brunner, 2009).

It must be also highlighted that production of organic acids from sugars would decrease the pH of the medium. As a result, the reaction rate would decrease and even deactivation of the enzyme would be accelerated (Wasewar et al., 2003). Furthermore, in literature, it has been described that enzymatic reaction suffer not only substrate inhibition but also competitive inhibition by lactic acid (Wasewar et al., 2003).

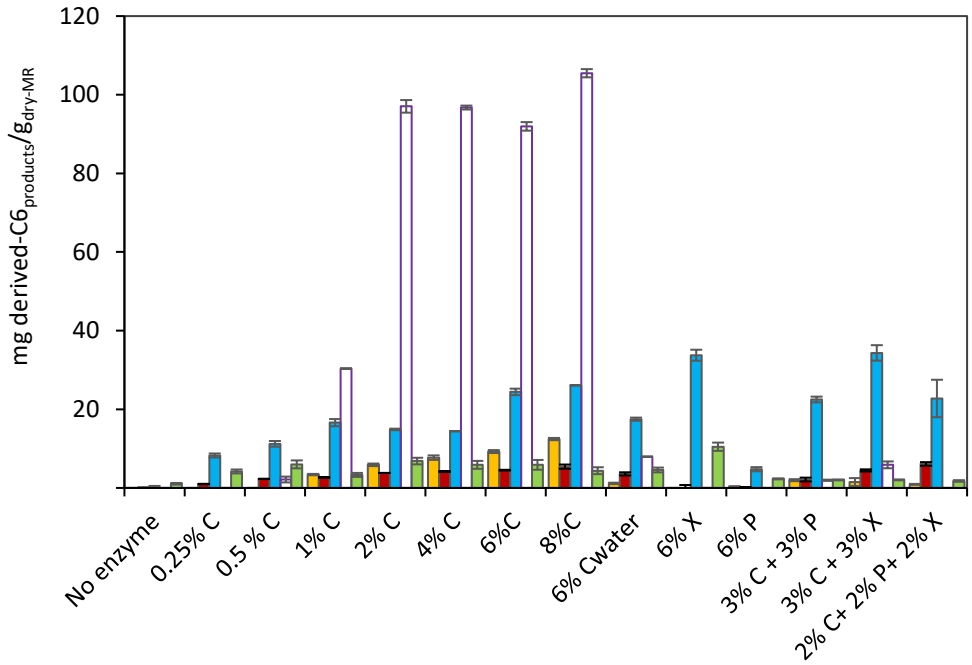

Figure 4.6. Concentration in the enzymatic extracts of sugars degradation products ■ succinic acid ■ formic acid ■ acetic acid, □ lactic acid, ■ ethanol.

3.6. Protein fraction release

Table 4.4 lists the total protein content released in the extraction medium, expressed as mg protein/g_{DMR} and as extraction yield (**Equation 4.3**) for the different enzymes and their combinations. By increasing the cellulase dose, the protein extraction yield also increased; although at concentration higher than 4 % (w/w) no significative differences were observed. This result agrees with literature, that also reported good results by using nonspecific carbohydrases for protein extraction from seaweeds (Vásquez et al., 2019).

Table 4.4. Specific protein yield, mg protein/g_{DMR} and protein extraction yield for the different enzymes and their combinations at pH = 5.

Enzyme	mg protein/g_{DMR}	Extraction yield, %
0.25 % C	21.5 ± 0.1^{a}	10.2 ± 0.1^{a}
0.5 % C	21.8 ± 0.4^{a}	10.4 ± 0.2^{a}
1 % C	24.3 ± 0.1^{b}	11.6 ± 0.1^{b}
2 % C	53.6 ± 0.4^{e}	25.5 ± 0.2^{e}
4 % C	62.0 ± 2.0^{g}	29.3 ± 0.9^{g}
6 % C	62.0 ± 1.0^{g,}	29.5 ± 0.6^{g}
8 % C	63.0 ± 1.0^{g,h}	29.9 ± 0.4^{g,h}
6 % X	50.9 ± 0.5^{d}	24.2 ± 0.3^{d}
6 % P	59.5 ± 0.6^{f}	28.3 ± 0.3^{f}
3 C + 3 % P	64.2 ± 0.5^{h}	30.6 ± 0.2^{h}
3 % C + 3 % X	46.0 ± 1.0^{c}	21.8 ± 0.5^{c}
2 % C + 2 % P + 2 % X	59.2 ± 0.4^{f}	28.2 ± 0.2^{f}

C: cellulase, X: xylanase, P: protease
Values with different letters in each column are significantly different when applying the Fisher's least significant differences (LSD) method at p-value ≤ 0.05

The highest protein extraction yield was determined for the binary enzyme mixture with cellulase and protease. In any case, the slightly higher content of protein determined in the medium in the presence of cellulase compared to protease, at the same enzyme

concentration, 6 %, could be due to the interference of the non-protein compounds released into the medium that also absorb at the same wavelength in the spectrophotometric method such as phenolic compounds and sugars. These compounds were produced in a bigger extent due to the action of the cellulase (see **Figure 4.1** and **4.5**), and it would result in an overestimation of the protein content in the extract (Olivares-molina & Fernández, 2016).

Vásquez et al. (Vásquez et al., 2019) reported a protein extraction yield of 36.1 % for the red algae *Chondracanthus chamisso*i after 12 h of enzymatic treatment with cellulase and a ratio of 1:10 enzyme:seaweed. These authors reported that, according to literature, conventional methods for protein extraction from seaweed, such as chemical or physical extraction , show protein extraction yields between 24 and 59 % for different seaweeds (Bleakley & Hayes, 2017). In this work, by using enzymes, protein extraction yields of the same order were obtained compared to conventional methods but using milder conditions. It must be highlighted that the protein recovery yield achieved by subW treatment of this solid residue was nearly 70 % in a semicontinuous fix-bed reactor configuration at 200 °C and 18.7 min of residence time. At these conditions, the ionic product of water increases that induced lower pH values that favour biomass hydrolysis (Trigueros et al., 2021).

The effect of pH on protein release by the protease has been studied by performing kinetics at different pH values, 5, 6 and 8 (**Figure 4.7**). It can be observed that the protein release was faster with higher yields under basic conditions. At pH = 8, nearly 80 mg protein/g_{DMR} was obtained, which represented a 38 % of protein extraction yield. Protein extraction kinetics at the different pH values were also fitted to the Weibull and the power law models (**Table 4.5**). For protein release, the Weibull model yielded much lower RMSD than the power law model, thus, it has been chosen for being represented in **Figure 4.7**. Regarding the Weibull model, an increase in the pH led to higher values of the A parameter, according to the highest extraction yield.

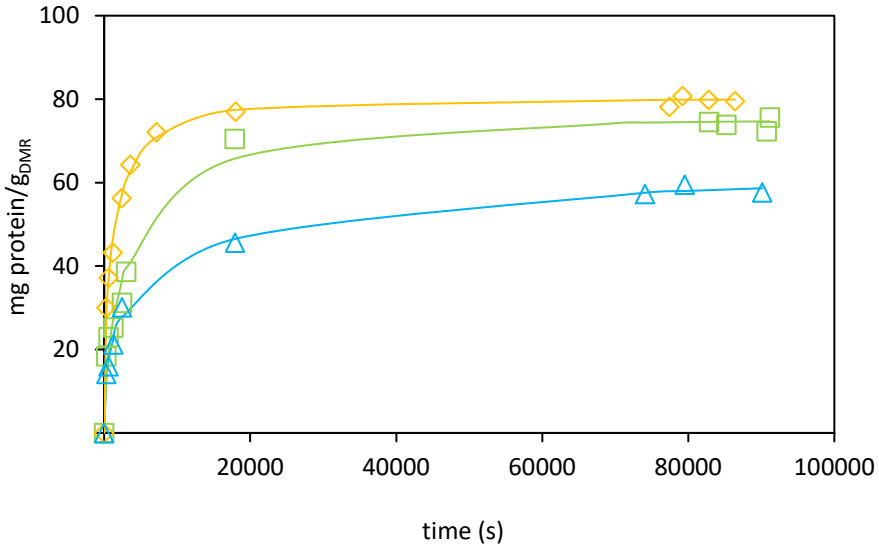

Figure 4.7. Protein extraction kinetics at 50 °C by using 6 % protease at different pH values (△ 5, □ 6, ◇ 8). The continuous lines represent the Weibull model (**Table 4.5**).

Table 4.5. Kinetic parameters for the power law and the Weibull models for protein release by using 6 % protease at different pH values.

	Power law			Weibull			
	B	n	RMSD	A	k	n	RMSD
pH = 5	3.90	0.240	2.7	63.3	0.0220	0.418	1.3
pH = 6	5.89	0.214	8.7	75.04	0.0075	0.575	3.2
pH = 8	18.44	0.111	14.8	79.92	0.0238	0.509	1.5

The individual free amino acid profile in the enzymatic extracts after 24 h at the different pH values has been listed in **Table 4.6**. The hydrolysis yield for each individual amino acid has been evaluated taking into account the amino acid profile in the MR (see also **Table 4.6**). Regarding the amino acid profile of the MR, the major amino acid was aspartic acid, 97 ± 8 mg/g$_{prot\text{-}DMR}$, followed by alanine and glutamic acid. Glutamic and aspartic acids were found to be the main amino acids for many algae, including red algae (Lourenço et al., 2002). The amount of amino acids released increased with the pH of the medium, with the highest

Table 4.6. Amino acid profile of macroalgae residue, MR, and of the protease enzymatic extracts, expressed as mg/$g_{protein\text{-}MR}$. Extraction yield percentage (yield, %) of individual amino acid. Hydrolysis degree (DH) and hydrophobic molar selectivity (HPB/TAA).

	MR	pH = 5		pH = 6		pH = 8	
	mg/$g_{prot\text{-}DMR}$	mg/$g_{prot\text{-}DMR}$	Yield, %	mg/$g_{prot\text{-}DMR}$	Yield, %	mg/$g_{prot\text{-}DMR}$	Yield, %
Ala	94 ± 8	8.4 ± 0.1	9.0 ± 0.9	11.0 ± 0.5	12.0 ± 2.0	11.7 ± 0.3	12.0 ± 1.0
Gly	41 ± 4	2.0 ± 0.1	4.8 ± 0.8	3.1 ± 0.3	8.0 ± 1.0	3.2 ± 0.1	8.0 ± 1.0
Val	67 ± 7	7.6 ± 0.3	11.0 ± 2.0	13.0 ± 1.0	19.0 ± 4.0	13.7 ± 0.2	20.0 ± 3.0
Leu	78 ± 8	11.6 ± 0.5	15.0 ± 2.0	15.0 ± 2.0	19.0 ± 4.0	15.6± 0.2	20.0 ± 2.0
Ile	45 ± 5	6.0 ± 1.0	14.0 ± 5.0	10.1 ± 0.3	23.0 ± 3.0	10.7 ± 0.1	24.0 ± 3.0
Thr	36 ± 2	1.8 ± 0.1	5.1 ± 0.4	3.5 ± 0.3	10.0 ± 1.0	3.2 ± 0.2	9.0 ± 1.0
Ser	39 ± 6	--	--	--	--	--	--
Pro	73 ± 4	1.6 ± 0.3	2.3 ± 0.6	3.5 ± 0.1	4.8 ± 0.4	4.8 ± 0.2	7.0 ± 0.6
Asp	97 ± 8	--	--	--	--	--	--
Met	8 ± 1	0.8 ± 0.1	10.0 ± 3.0	1.5 ± 0.1	19.0 ± 4.0	1.4 ± 0.1	18.0 ± 4.0
Glu	79 ± 5	2.9 ± 0.5	3.6 ± 0.9	8.0 ± 2.0	11.0 ± 3.0	9 ± 2	11.0 ± 3.0
Phe	51 ± 6	7.3 ± 0.3	14.0 ± 2.0	9.2 ± 0.8	18.0 ± 4.0	9.8 ± 0.1	19.0 ± 2.0
Lys	57 ± 7	1.5 ± 0.1	2.7 ± 0.4	1.63 ± 0.04	2.9 ± 0.4	1.9 ± 0.3	3.0 ± 0.9
His	16 ± 2	0.50 ± 0.02	3.0 ± 0.4	0.9± 0.2	6.0 ± 2.0	1.1 ± 0.3	7.0 ± 2.0
Tyr	35 ± 6	4.4 ± 0.7	13.0 ± 4.0	5.4 ± 0.5	16.0 ± 4.0	6.0 ± 0.3	17.0 ± 4.0
Trp	3.0 ± 0.2	1.1 ± 0.2	36.0 ± 9.0	1.2 ± 0.1	41.0 ± 7.0	1.3 ± 0.1	42.0 ± 6.0
EAA	361 ± 39	39 ± 3	11 ± 2	56 ± 5	15 ± 3	59 ± 2	16 ± 2
Total	819 ± 80	58 ± 5	7 ± 1	87 ± 8	11 ± 2	93 ± 4	11 ± 2
HPB/TAA	0.4 ± 0.1	0.64 ± 0.01		0.62 ± 0.01		0.62 ± 0.01	
DH		4.2 ± 0.8[a]		7.70 ± 0.05[b]		9.3 ± 0.8[b]	

Values with different letters are significantly different when applying the Fisher's least significant differences (LSD) method at p-value ≤ 0.05

content at pH = 8, 93 ± 4 mg aa/$g_{protein}$. The total hydrolysis yields were 7 ± 1, 11 ± 2 and 11 ± 2 (%), at pH values of 5, 6 and 8, respectively. This result agrees with the hydrolysis degree (**Equation 4.4**, h_{tot} = 7.24) that also increased by increasing pH of the medium, although no significant differences were observed at pH values of 6 and 8 (**Table 4.6**). The highest content of individual amino acids in the enzymatic hydrolysates corresponds to leucine, valine, alanine, isoleucine and phenylalanine. According to the literature, hydrophobic amino acids includes phenylalanine, leucine, isoleucine, tyrosine, tryptophan, valine, methionine, and proline (Widyarani et al., 2016). Therefore, high selectivity towards hydrophobic amino acids has been obtained by using this protease. Hydrophobic selectivity has been evaluated as the amount of free hydrophobic amino acids relative to the total liberated free amino acids on molar base (**Table 4.6**). It can be observed that the hydrophobic ratio increased in the hydrolysates compared to the MR, reaching values around 0.62-0.64. According to the amino acid profile in the enzymatic hydrolysates, in general, higher yields were obtained for hydrophobic amino acids (see **Figure 4.8**). The highest yield corresponds to tryptophan, due to its small content in the raw material, although concentration in the enzymatic hydrolysates was only 1.3 ± 0.1 mg/$g_{protein}$ (at pH = 8). It can be highlighted that the production of mixtures rich in hydrophobic amino acids is an interesting process based on their potential application in food and feed.

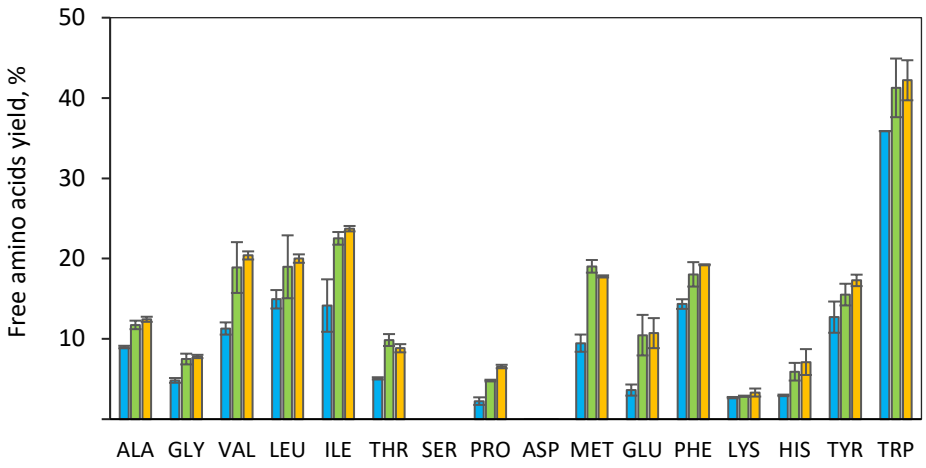

Figure 4.8. Free amino acid yield in the protease enzymatic extracts at different pH values after 24 h (pH = 5 ■; pH = 6 ■; pH = 8 ■).

Conclusions

To incorporate macroalgae into the biorefinery concept, valorization of industrial wastes generated during industrial processing should be considered. It has been shown that EAE provides a mild and efficient technology to valorize the industrial solid waste residue after agar extraction from *G sesquipedale*. The use of hydrolytic enzymes allowed the release into the reaction medium of phenolic compounds bound to the cell wall of the macroalgae, as well as the release of the polysaccharide fraction as monomers and oligomers and the hydrolysis of the protein fraction with a higher content of hydrophobic amino acids compared to the raw material. Cellulase has been found to provide the highest hydrolytic capacity to break down the cell wall algae. It was not observed a competitive adsorption effect to the cell wall polysaccharides by increasing the amount of cellulase in the medium, but the optimum enzyme dose must also take into account economic factors as the enzyme cost. Further works should be performed to determine the extraction curves of the polysaccharide fraction and sugar degradation products.

References

Adler-Nissen, J., Eriksen, S., & Olsen, H.S. (1983). Improvement of the functionality of vegetable proteins by controlled enzymatic hydrolysis. *Qualitas Plantarum Plant Foods for Human Nutrition*, 32, 411–423.

Alonso-Riaño, Patricia, Sanz Diez, M.T., Blanco, B., Beltrán, S., Trigueros, E., & Benito-Román, O. (2020). Water Ultrasound-Assisted Extraction of Polyphenol Compounds from Brewer's Spent Grain: Kinetic Study, Extract Characterization, and Concentration. *Antioxidants*, 9, 265.

Álvarez-Viñas, M., Flórez-Fernández, N., Torres, M.D., & Domínguez, H. (2019). Successful approaches for a red seaweed biorefinery. *Marine Drugs*, 17, 1-18.

Barbarino, E., & Lourenço, S. O. (2005). An evaluation of methods for extraction and quantification of protein from marine macro- and microalgae. *Journal of Applied Phycology*, 17(5), 447–460.

Baruah, J., Nath, B.K., Sharma, R., Kumar, S., Deka, R.C., Baruah, D.C., & Kalita, E. (2018). Recent trends in the pretreatment of lignocellulosic biomass for value-added products. *Frontiers in Energy Research*, 6, 1–19.

Bleakley, S., & Hayes, M. (2017). Algal Proteins: Extraction, Application, and Challenges Concerning Production. *Foods*, 6(5), 33.

Boulila, A., Hassen, I., Haouari, L., Mejri, F., Amor, I. Ben, Casabianca, H., & Hosni, K. (2015). Enzyme-assisted extraction of bioactive compounds from bay leaves (*Laurus nobilis* L.). *Industrial Crops and Products*, 74, 485–493.

Brunner, G. (2009). Near critical and supercritical water. Part I. Hydrolytic and hydrothermal processes. *Journal of Supercritical Fluids*, 47(3), 373–381.

Faulds, C.B., Robertson, J.A., & Waldron, K.W. (2008). Effect of pH on the solubilization of Brewers' spent grain by microbial carbohydrases and proteases. *Journal of Agricultural and Food Chemistry*, 56(16), 7038–7043.

Ferrera-Lorenzo, N., Fuente, E., Suárez-Ruiz, I., & Ruiz, B. (2014). KOH activated carbon from conventional and microwave heating system of a macroalgae waste from the Agar-Agar industry. *Fuel Processing Technology*, 121, 25–31.

Filisetti-Cozzi, T.M.C.C., & Carpita, N.C. (1991). Measurement of uronic acids without interference from neutral sugars. *Analytical Biochemistry*, 197(1), 157–162.

Fleurence, J., Massiani, L., Guyader, O., & Mabeau, S. (1995). Use of enzymatic cell wall degradation for improvement of protein extraction from *Chondrus crispus*, *Gracilaria verrucosa* and *Palmaria palmata*. *Journal of Applied Phycology*, 7(4), 393–397.

Friedman, M. (2004). Applications of the Ninhydrin Reaction for Analysis of Amino Acids, Peptides, and Proteins to Agricultural and Biomedical Sciences. *Journal of Agricultural and Food Chemistry*, 52(3), 385–406.

Gligor, O., Mocan, A., Moldovan, C., Locatelli, M., Crișan, G., & Ferreira, I.C.F.R. (2019). Enzyme-assisted extractions of polyphenols – A comprehensive review. *Trends in Food Science and Technology*, 88, 302–315.

González-Centeno, M.R., Comas-Serra, F., Femenia, A., Rosselló, C., & Simal, S. (2015). Effect of power ultrasound application on aqueous extraction of phenolic compounds and antioxidant capacity from grape pomace (*Vitis vinifera* L.): Experimental kinetics and modeling. *Ultrasonics Sonochemistry*, 22, 506–514.

Hardouin, K., Burlot, A.S., Umami, A., Tanniou, A., Stiger-Pouvreau, V., Widowati, I., Bedoux, G., & Bourgougnon, N. (2014). Biochemical and antiviral activities of enzymatic hydrolysates from different invasive French seaweeds. *Journal of Applied Phycology*, 26(2), 1029–1042.

Hosni, K., Hassen, I., Chaâbane, H., Jemli, M., Dallali, S., Sebei, H., & Casabianca, H. (2013). Enzyme-assisted extraction of essential oils from thyme (*Thymus capitatus* L.) and rosemary (*Rosmarinus officinalis* L.): Impact on yield, chemical composition and antimicrobial activity. *Industrial Crops and Products*, 47, 291–299.

Kim, H.M., Wi, S.G., Jung, S., Song, Y., & Bae, H. J. (2015). Efficient approach for bioethanol production from red seaweed Gelidium amansii. *Bioresource Technology*, 175, 128–134.

Kitanović, S., Milenović, D., & Veljković, V.B. (2008). Empirical kinetic models for the resinoid extraction from aerial parts of St. John's wort (*Hypericum perforatum* L.). *Biochemical Engineering Journal*, 41(1), 1–11.

Lourenço, S.O., Barbarino, E., De-Paula, J.C., Pereira, L.O.D.S., & Lanfer Marquez, U.M. (2002). Amino acid composition, protein content and calculation of nitrogen-to-protein conversion factors for 19 tropical seaweeds. *Phycological Research*, 50(3), 233–241.

Lowry, O.H., Rosebrough, N.J., Farr, A.L., & Randall, R.J. (1951). Protein measurement with the folin reagent. *Journal of Biological Chemistry*, 193, 265–275.

Nadar, S.S., Rao, P., & Rathod, V.K. (2018). Enzyme assisted extraction of biomolecules as an approach to novel extraction technology: A review. *Food Research International*, 108,309–330.

Olivares-molina, A., & Fernández, K. (2016). Comparison of different extraction techniques for obtaining extracts from brown seaweeds and their potential effects as angiotensin I-converting enzyme (ACE) inhibitors. *Journal of Applied Phycology*, 28, 1295–1302.

Postma, P.R., Cerezo-Chinarro, O., Akkerman, R.J., Olivieri, G., Wijffels, R.H., Brandenburg, W. A., & Eppink, M. H. M. (2018). Biorefinery of the macroalgae Ulva lactuca: extraction of proteins and carbohydrates by mild disintegration. *Journal of Applied Phycology*, 30(2), 1281–1293.

Puri, M., Sharma, D., & Barrow, C. J. (2012). Enzyme-assisted extraction of bioactives from plants. *Trends in Biotechnology*, 30(1), 37–44.

Rakariyatham, K., Liu, X., Liu, Z., Wu, S., Shahidi, F., Zhou, D., & Zhu, B. (2019). Improvement of Phenolic Contents and Antioxidant Activities of Longan (Dimocarpus longan) Peel Extracts by Enzymatic Treatment. *Waste and Biomass Valorization*, 11, 3987-4002.

Rodrigues, D., Freitas, A.C., Pereira, L., Rocha-Santos, T.A.P., Vasconcelos, M.W., Roriz, M., Rodríguez-Alcalá, L.M., Gomes, A.M.P., & Duarte, A.C. (2015). Chemical composition of red, brown and green macroalgae from Buarcos bay in Central West Coast of Portugal. *Food Chemistry*, 183, 197–207.

Ruiz, H.A., Rodríguez-Jasso, R.M., Aguedo, M., & Kádár, Z. (2015). Hydrothermal Pretreatments of Macroalgal Biomass for Biorefineries (Springer). In Algal Biorefineries: Volume 2: *Products and Refinery Design*, pp. 467–491.

Sabeena, S. F., Alagarsamy, S., Sattari, Z., Al-Haddad, S., Fakhraldeen, S., Al-Ghunaim, A., & Al-Yamani, F. (2020). Enzyme-assisted extraction of bioactive compounds from brown seaweeds and characterization. *Journal of Applied Phycology*, 32(1), 615–629.

Sánchez-Bastardo, N., Romero, A., & Alonso, E. (2017). Extraction of arabinoxylans from wheat bran using hydrothermal processes assisted by heterogeneous catalysts. *Carbohydrate Polymers*, 160, 143–152.

Sánchez-Camargo, A.D.P., Montero, L., Stiger-Pouvreau, V., Tanniou, A., Cifuentes, A., Herrero, M., & Ibáñez, E. (2016). Considerations on the use of enzyme-assisted extraction in combination with pressurized liquids to recover bioactive compounds from algae. *Food Chemistry*, 192, 67–74.

Shobana, S., Kumar, G., Bakonyi, P., Saratale, G. D., Al-Muhtaseb, A. H., Nemestóthy, N., Bélafi-Bakó, K., Xia, A., & Chang, J. S. (2017). A review on the biomass pretreatment and inhibitor removal methods as key-steps towards efficient macroalgae-based biohydrogen production. *Bioresource Technology*, 244, 1341–1348.

Shukla, R., Kumar, M., Chakraborty, S., Gupta, R., Kumar, S., Sahoo, D., & Kuhad, R.C. (2016). Process development for the production of bioethanol from waste algal biomass of Gracilaria verrucosa. *Bioresource Technology*, 220, 584–589.

Singleton, V. L., Orthofer, R., & Lamuela-Raventós, R.M. (1999). Analysis of Total Phenols and Other Oxidation Substrates and Antioxidants by Means of Folin-Ciocalteu Reagent. *Methods in Enzymology*, 299, 152–178.

Sluiter, J.B., Ruiz, R.O., Scarlata, C.J., Sluiter, A.D., & Templeton, D.W. (2010). Compositional analysis of lignocellulosic feedstocks. 1. Review and description of methods. *Journal of Agricultural and Food Chemistry*, 58, 9043–9053.

Trigueros, E., Sanz, M.T., Alonso-Riaño, P., Beltrán, S., Ramos, C., & Melgosa, R. (2021). Recovery of the protein fraction with high antioxidant activity from red seaweed industrial solid residue after agar extraction by subcritical water treatment. *Journal of Applied Phycology*.

Vásquez, V., Martínez, R., & Bernal, C. (2019). Enzyme-assisted extraction of proteins from the seaweeds Macrocystis pyrifera and Chondracanthus chamissoi: characterization of the extracts and their bioactive potential. *Journal of Applied Phycology*, 31(3), 1999–2010.

Wang, T., Jónsdóttir, R., Kristinsson, H.G., Hreggvidsson, G.O., Jónsson, J.Ó., Thorkelsson, G., & Ólafsdóttir, G. (2010). Enzyme-enhanced extraction of antioxidant ingredients from red algae Palmaria palmata. *LWT - Food Science and Technology*, 43(9), 1387–1393.

Wasewar, K.L., Pangarkar, V.G., Heesink, A.B.M., & Versteeg, G.F. (2003). Intensification of enzymatic conversion of glucose to lactic acid by reactive extraction. *Chemical Engineering Science*, 58, 3385–3393.

Widyarani, Sari, Y.W., Ratnaningsih, E., Sanders, J.P.M., & Bruins, M.E. (2016). Production of hydrophobic amino acids from biobased resources: wheat gluten and rubber seed proteins. *Applied Microbiology and Biotechnology*, 100, 7909–7920.

Wijesinghe, W.A.J.P., & Jeon, Y.J. (2012). Enzyme-assistant extraction (EAE) of bioactive components: A useful approach for recovery of industrially important metabolites from seaweeds: A review. *Fitoterapia*, 83, 6–12.

CHAPTER 5

Fractionation of bioactive compounds from a red alga subcritical water extract by ultrafiltration

Based on the article:

Trigueros E., et al. "Fractionation of bioactive compounds from a red alga subcritical water extract by ultrafiltration".

(Will be submitted to Separation and Purification Technology)

Capítulo 5

Fraccionamiento de compuestos bioactivos mediante ultrafiltración a partir del extracto de alga roja en agua subcrítica

Resumen

Se ha estudiado la viabilidad de un proceso de ultrafiltración (UF) cross-flow en contínuo, con membranas tubulares inorgánicas de TiO_2, para tratar los extractos obtenidos a partir del residuo del alga *Gelidium sesquipedale* mediante tratamiento con agua subcrítica. En un estudio preliminar se usaron membranas multicanal con un corte de peso molecular (MWCO) de 5 a 100 kDa. El mayor MWCO fue suficiente para eliminar el color y la materia coloidal presente en los extractos, conservando una alta capacidad antioxidante (76.7 %). El nitrógeno total (TN) fue uno de los componentes con menor retención en todos los experimentos. La retención de aminoácidos libres no superó el 1 % en ningún caso. Los carbohidratos mostraron el mayor coeficiente de retención (55.4 %), siendo principalmente glucanos, seguido de galactanos. Se obtuvo un menor flujo de permeado con las membranas de menor MWCO debido al aumento en la resistencia total de la membrana, de entre 4 y 5 veces su valor en comparación con la membrana de mayor MWCO, como consecuencia de un mayor ensuciamiento. Se consiguió una mejora en el proceso de UF en términos de un menor ensuciamiento al aumentar la temperatura, así como un proceso más rápido al aumentar el flujo de la alimentación sin alterar la retención. Se estudió un proceso de UF secuencial usando membranas de 100, 5 y 1 kDa. Tras pasar el permeado de la membrana de 100 kDa por la de 5, se obtuvo una suma de retenidos con un 56 % de carbohidratos, mientras que el 81.4 % del TN quedó en los permeados. Al pasar el permeado de la membrana de 5 kDa por la de 1, se retuvo el 83.4 % de los carbohidratos, mientras que el 65.7 % del TN quedó en el permeado.

Palabras clave: ultrafiltración, membranas cerámicas, tecnología de separación, biorrefinería, fraccionamiento de azúcares y proteínas, macroalga.

Abstract

The feasibility of continuous cross-flow ultrafiltration (UF) with TiO_2 tubular inorganic membranes, for the treatment of extracts from *Gelidium sesquipedale* residues obtained by means subcritical water was studied. Multichannel membranes with a molecular weight cut-off (MWCO) from 5 to 100 kDa for a preliminary study were used. Membrane with the highest MWCO was enough for colloidal matter and colour removal, but preserving high antioxidant capacity (76.7 %). Total nitrogen (TN) was one of the lowest rejected compounds for all the performed experiments. Free amino acids rejection did not exceed 1 % in any case. Carbohydrates showed the highest retention coefficient (55.4 %), glucans mostly, followed by galactans. Lower permeate flux was determined for the lowest MWCO membranes because of the increase in total resistance, by almost 4-5 times its value in comparison with the highest MWCO membrane, as a result of a greater fouling. An improvement in ultrafiltration process was observed by increasing temperature, in terms of membrane fouling reduction, and faster ultrafiltration process was developed by increasing feed flow rate without perturbing retention. A sequential ultrafiltration was evaluated by using 100, 5 and 1 kDa membranes. By passing the 100 kDa permeate fraction through the 5 kDa membrane, the sum of all the retained fractions contained 56 % of total carbohydrates, while permeate fractions accounted for 81.4 % total nitrogen. By other side, by passing permeate from 5 kDa to 1 kDa membrane, a sum of retentates with 83.4 % of total carbohydrates and permeates with 65.7 % of total nitrogen were collected.

Keywords: ultrafiltration, ceramic membranes, separation technology, biorefinery, sugars and proteins fractionation, macroalga.

1. Introduction

Red marine seaweeds are frequently exploited for their high content of phycocolloids, such as agar and carrageenans, based on a complex mixture of polysaccharides. Agar is a hydrocolloid widely used in different areas such as microbiology, pharmacy, food or cosmetics (Murano, 1995), which forms a thermoreversible gel when it is dissolved in hot water and cooled (Guerrero et al., 2014).

Gelidium sesquipedale is the major seaweed resource in the Spanish agar industry since it provides the best raw material to obtain the highest quality agar (Carmona et al., 1998; Fernández, 1991; Mouradi-givernaud et al., 1999; Torres et al., 1991). Industrial agar extraction process involves the generation of a solid waste that is usually discarded, despite containing a significant content of valuable compounds (Trigueros et al., 2021).

One profitable way of taking the most benefit from this residue is by turning it into a valuable bio-compounds source. For this purpose, subcritical water extraction (SWE) has shown a great capacity to extract bioactive compounds from different natural sources (Gallina et al., 2016; Herrero et al., 2006; Wataniyakul et al., 2012) and vegetal residues (Alonso-Riaño et al., 2021; He et al., 2012; Munir et al., 2018). The use of SWE to valorize *G. sesquipedale* solid waste was reported in a previous work (see **Chapter 3**). High recovery of the polysaccharide fraction, proteins and free amino acids was achieved by using a discontinuous reactor. However, the extracts were dilute complex mixtures, which means that a suitable separation technique is required to recover, to isolate and concentrate valuable compounds.

In this sense, separation pressure-driven membrane processes have been proven to be an environmentally friendly and cost-effective alternative for the recovery of different valuable compounds from by-products (Saidi et al., 2014; Yu et al., 2016). Ultrafiltration (UF) is widely used for the separation of different molecules in solution based on their size. Common compounds retained by UF membranes include colloidal particles, polymers, polyphenols, colour substances and some sugars (Balakrishnan et al., 2000; Hinková et al., 2000;

Sarmento et al., 2008; Xie et al., 2014). Easy automation and scale up, low energy costs, mild operation conditions, free of toxic solvents and low waste generation are recognised as the main advantages of UF-based processes (Cissé et al., 2011).

Nevertheless, membrane fouling is still a problem in UF technology (Ambrosi et al., 2014; Audinos & Branger, 1992; Takaç et al., 2000). In numerous cases, the permeate flux obtained is still too low to encourage any industrial application. Proteins and carbohydrates in subcritical water extracts from *G. sesquipedal*e may play an important role in fouling, even when using crossflow UF. This dissolved matter, with high gelling properties, can cause severe fouling by accumulating in the pores and spreading across the membrane surface, which could lead to continuous changes in permeate flux and membrane permeability throughout the extract treatment (Marshall et al., 1993; Susanto et al., 2008, 2009).

UF inorganic membranes, especially ceramics, are emerging as an alternative to conventional organic membranes due to their potential advantages, such as high chemical stability in a wide pH and temperature range, high wear resistance, long lifetime, and resistance to harsh chemical cleaning (Fard et al., 2018; Lin, 2019). Hence, all of these outstanding properties make inorganic membranes good candidates to be used for the treatment of subcritical water red algae extracts, especially when a membrane system coupled to a reactor is desired.

The aim of this study is to analyse the feasibility of continuous cross-flow ultrafiltration with TiO_2 tubular inorganic membranes for the treatment of extracts from *Gelidium sesquipedale* residues obtained by means of subcritical water treatment and to optimize the operating process parameters to achieve the maximum separation yield of the subcritical water hydrolysate. Finally, a fractionation process to separate carbohydrates and proteins is proposed.

2. Materials and methods

2.1. Raw material

Gelidium sesquipedale residue after industrial agar extraction was milled and the particle size fraction lower than 0.5 mm was used to perform subcritical water extraction. A subcritical water hydrolysate was obtained at pilot plant scale at Hiperbaric's facilites at 175 °C and 5 % of biomass loading. Hydrolysate composition consisted of 1.05 g/L glucans, 1.73 g/L galactans, 0.42 g/L total polyphenols content (TPC) and 0.7 g/L total nitrogen (TN) (4.0 g/L TOC). Before ultrafiltration experiments, the aqueous extract hydrolysate was diluted with a dilution factor of 4.

2.2. Membranes

Multichannel Filtanium ceramic membranes (Tami Industries) with an active layer of TiO_2 supported on titania with a molecular weight cut-off (MWCO) from 1 to 100 kDa were used (**Figure 5.1**). These membranes consist of a single tubular module (254 mm length and 6 and 10 mm inside and outside diameter, respectively) with seven inner channels and an effective membrane area, as stated by the manufacturer, of 132 cm^2. Further specifications of the membranes are shown in **Table 5.1**.

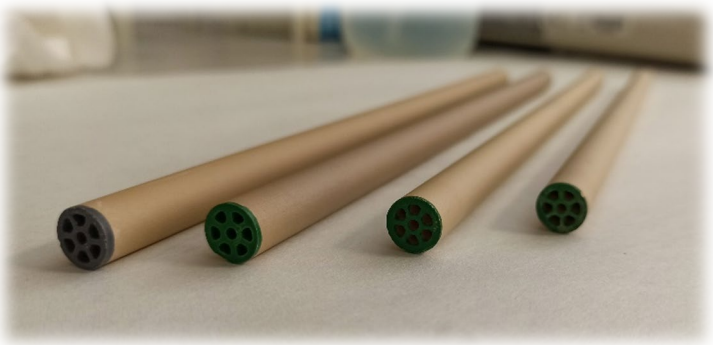

Figure 5.1. Membranes used for the MWCO study. From left to right: 100, 50, 10 and 5 kDa membranes.

Table 5.1. Water permeability (Lp) and membrane hydraulic resistance to water permeation (Rm) experimentally determined at 20 °C.

Membrane	Lp ($L/m^2h \cdot bar$)	Rm (m^{-1}) · 10^{12}
Filtanium™ 100 (MWCO 100 kDa)	212	1.70
Filtanium™ 50 (MWCO 50 kDa)	170	2.11
Filtanium™ 10 (MWCO 10 kDa)	59	6.07
Filtanium™ 5 (MWCO 5 kDa)	47	7.38
Filtanium™ 1 (MWCO 1 kDa)	44	8.23

Maximum transmembrane pressure (TMP) and temperature provided by the manufacturer were 10 bar and 95 °C, respectively, for all 7-channel membranes.

2.3. Equipment and ultrafiltration procedure

The experimental setup shown in **Figure 5.2** was used in all cross-flow ultrafiltration experiments. The feed solution was pumped from a batch stirred glass tank (Pobel) at 20 ± 2 °C to the membrane module by using a Masterflex peristaltic pump (HV-7520-57, with a Masterflex L/S Easy-Load II Head HV-77201-62). A silicone tubing (Materflex L/S 15, 25 ft.) was used. Before starting the UF process, the feed solution was allowed to recirculate through the system without pressure for 10 minutes to homogenize the pipes and, immediately, a feed sample was collected to analyze. Then, the feed flowrate and transmembrane pressure were adjusted to the desired values by using a variable speed drive for the pump and a valve placed after the membrane module. The pressures at the inlet and outlet of the membrane module were measured by using two pressure gauges. Different samples of permeate were collected along time in order to analyze the compounds rejection depending on permeate volume.

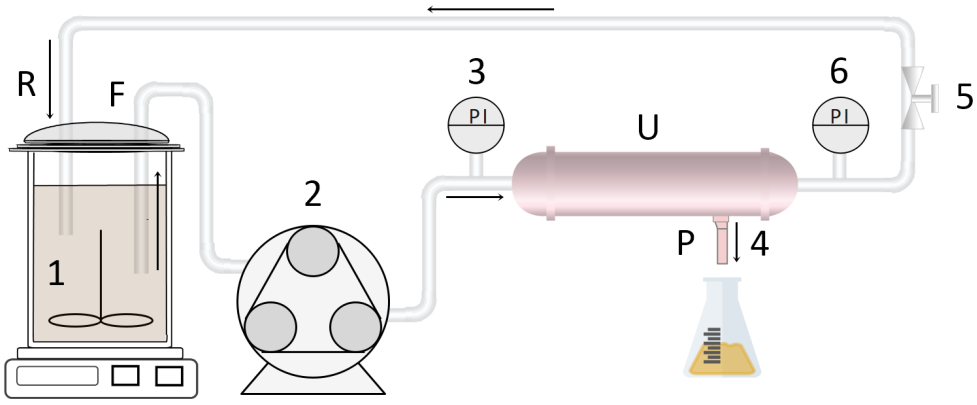

Figure 5.2. Experimental setup for cross-flow ultrafiltration experiments with tubular ceramic membranes. (1) feed tank; (2) peristaltic pump; (3,6) pressure gauge; (U) ultrafiltration module; (4) permeate outlet; (5) regulating valve. F, P and R refer to the feed, permeate and retentate streams.

The experiments were carried out by continuously withdrawing the permeate. The retentate was recycled back to the feed tank and the permeate was collected in the permeate tank. Permeate fluxes (J_p) were determined volumetrically and gravimetrically under different operating conditions: MWCO, temperature (T) and feed flowrate (Q_F). J_P values during ultrafiltration were determined by using the following equation:

$$J_p = \frac{V_p}{A_m \times t} \quad [5.1]$$

where V_p is the volume of permeate collected at time t and A_m is the membrane effective area of each 7-channel tubular membranes.

The permeates collected throughout UF, final retentate, final permeate and feed solution were analyzed in triplicate in all experiments. The initial conditions for ultrafiltration experiments are summarized in **Table 5.2**.

Table 5.2. Ultrafiltration conditions for the experiments performed according to the parameters studied.

Parameter studied	MWCO (kDa)	temperature (°C)	Flow rate (L/h)
Membranes molecular weight cut-off (MWCO)	100	20	11.2
	50	20	11.2
	10	20	11.2
	5	20	11.2
Feed temperature (T)	5	20	11.2
	5	50	11.2
Feed flow rate (Q_F)	5	20	11.2
	5	20	6.6

Membrane fouling was also evaluated for the experiments of **Table 5.2**. Considering a resistance-in-series model, the total resistance of the membrane can be written as (Leberknight et al., 2011):

$$R_t = \frac{TMP}{\mu_p \times J_p} = Rm + Rs \qquad [5.2]$$

where μ_p is the experimental viscosity of the permeate by using hydrolysate extract as feed solution, *Rm* is the membrane hydraulic resistance expressed in m^{-1} and *Rs* is the resistance to filtration due to concentration polarisation and membrane fouling, expressed in m^{-1}. As Rt = Rm in systems with water, Rm was measured experimentally for ultrafiltration of water under different TMP at 20 °C and Rm values are listed in **Table 5.1** for all the membranes.

Once the optimal parameters were established, two independent cycles of sequential UF stages were carried out (**Figure 5.3**). The subcritical water extract was ultrafiltered through a 100 kDa membrane, obtaining a first permeate and retentate. This first permeate from the 100 kDa membrane was then ultrafiltered through a 5 kDa membrane. Subsequently, the resulting permeate stream from 5 kDa membrane was subjected to lyophilization to obtain the concentrated dry extract (Cycle A), while in a third stage (Cycle B), this permeate from 5 kDa membrane was again ultrafiltered through a 1 kDa membrane. The resulting permeate from the 1 kDa membrane was also lyophilized to obtain the concentrated dry extract for cycle B. Samples of each permeate and the retentate fraction were taken and stored at - 18 °C for further analysis.

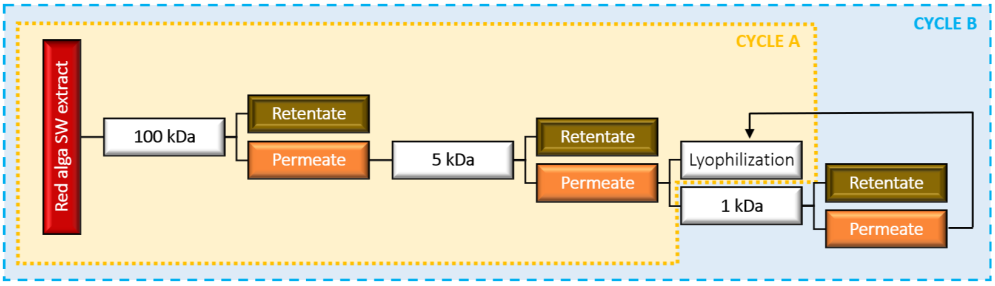

Figure 5.3. Diagram of sequential ultrafiltration carried out by two independent cycles (yellow CYCLE A; blue = CYCLE B)

The ceramic membranes were cleaned at 50 °C after each ultrafiltration run following a procedure that involved rinsing with soapy water and deionized water in order to remove the retentate, cleaning with a 0.17 vol. % aqueous H_3PO_4 solution at 0.25 bar of TMP for 60 minutes, rinsing again with deionized water and finally cleaning with a 0.20 g/L of NaOH solution in deionized water for 60 minutes at 0.25 bar of TMP. The membranes were then rinsed with freshly deionized water and the permeate flux was measured at 20 °C to check flux recovery.

2.4. Lyophilization procedure

The final permeate fractions collected from Cycle A and Cycle B sequential ultrafiltration were submitted to freeze drying. First, samples were frozen at -80 °C for 24 h and then submitted to freeze-drying in a Labconco Freeze Dry System (Labconco Corporation, U.S.A.) at $1.5 \cdot 10^{-4}$ mbar during 48 h. The moisture content of the freeze-dried particles was determined gravimetrically by weighing small amounts of dried particles (around 0.5 g) before and after drying in an oven at 105 °C until constant weight.

2.5. Analytical methods

Particle size distribution (PSD) was evaluated by laser diffraction method by using a Malvern Matersizer 2000 particle size analyzer to determine particle size ranged from 0.02 to 2000 µm.

Total organic carbon (TOC) was determined with a TOC/TN analyzer (Shimadzu TOC-V CSN analyzer) by difference of estimated total and inorganic carbon, using C_6H_{14}(COOK)(COOH), $NaHCO_3$ and Na_2CO_3 as standards.

Total nitrogen (TN) was measured using KNO_3 as standard with the TOC/TN analyzer.

Free amino acids were determined by using EZ:faast Phenomenex procedure and derivatized samples were analyzed by gas chromatography (Hewlett-Packard, 6890 series) as described in (Trigueros et al., 2021).

Carbohydrates determination. Monomeric sugars were directly analyzed by HPLC, while polysaccharides required a previous acid hydrolysis according to NREL protocols. A Biorad Aminex-HPX-87 H column was used, attached to a variable wavelength detector (VWD) and refractive index detector (RID). Polymeric sugars were estimated by using an anhydro correction of 0.9 for C-6 sugars.

Total polyphenolic compounds (TPC) were determined according to Folin-Ciocalteu procedure (Singleton et al., 1999), using gallic acid (GA) as standard.

The reducing capacity was determined by the Ferric Reducing Ability of Plasma (FRAP) method according to Benzie and Strain (Benzie & Strain, 1996).

Total solids were measured by drying the extracts at 105 °C to remove water until constant weight. Total solids were estimated as the ratio between the residual weight of the dry extract after removing water by evaporation and the initial volume of wet extract.

Total solids and FRAP variation of the different fractions analyzed respect to the feed were estimated according to the following equation:

$$Total\ solids\ (TS)\ or\ FRAP\ variation = \frac{TS\ or\ FRAP_{(P,R)}}{TS\ or\ FRAP_{(F)}} \quad [5.3]$$

where *TS or FRAP*$_{(P,R)}$ and *TS or FRAP*$_{(F)}$ are total solids and FRAP of permeate or retentate fractions and feed fraction, respectively.

Colour was measured by a spectrophotometric method by means of absorbance determination at 420 ± 0.4 nm, which allows to calculate the variation respect to the feed by using **equation 5.4** and finally express the loss or gain of colour in permeate and retentate samples.

$$Colour\ variation\ (\%) = \frac{Abs_{(P,R)}}{Abs_{(F)}} \times 100 \quad [5.4]$$

where $Abs_{(P,R)}$ is the absorbance of permeate or retentate and $Abs_{(F)}$ is the feed absorbance.

Compounds observed retention. To measure membrane selectivity for target compounds, the observed retention for each specific compound (R_i) was calculated as:

$$\%\ R_i = 100 \times \left(1 - \frac{C_{ip}}{C_{if}}\right) \quad [5.5]$$

where C_{ip} and C_{if} are compounds concentrations in permeate and feed, respectively.

2.6. Statistical analysis

All determinations were taken at least in triplicate and expressed as mean ± standard deviation. The Fisher's least significant differences (LSD) method at *p* value ≤ 0.05 was applied to confirm significant differences. Analyses were carried out by Centurion Statgraphics software.

3. Results and discussion

3.1. Feed extract

Feed extract used for the ultrafiltration study is an aqueous mixture of organic compounds. Among them, carbohydrates, with a concentration of 2.78 g/L, are mainly constituted by glucans (37.8 %) and galactans (62.2 %). Another major compound is the protein fraction with 3.4 g/L (4.9 nitrogen factor). Free amino acids, present in a relation of 14.7 mg/$g_{protein}$, are composed by 24 % of essential amino acids. Therefore, this aqueous extract, diluted 1:4 for the ultrafiltration study, is a source of valuable bioactive compounds, which make it an excellent substrate for fractionation and concentration by means of membrane technology separation.

3.2. Effect of the molecular weight cut-off on the separation

3.2.1. Permeate and retentate fraction characteristics

Effect of molecular weight cut-off of the membranes on particle size distribution and solid content of the different fractions after ultrafiltration process is shown in **Figure 5.4**. A MWCO of 100 kDa was enough to retain all the colloidal matter from the raw material with a particle size above 0.2 µm, which was also retained with lower MWCO. A similar permeate particle-size profile, with sizes from 0.020 to 0.195 µm was observed for all the membranes.

However, although the permeate fractions showed similar particle-size profiles for all the membranes, total solid determination proved that there was a significant difference between the permeate obtained with the 100 kDa membrane and the rest of the tested membranes (**Figure 5.4b**). The permeate collected after using 100 kDa membrane retained 10 % of total solids from feed, while with lower MWCO membranes a higher retention close to 40 % of total solids was observed.

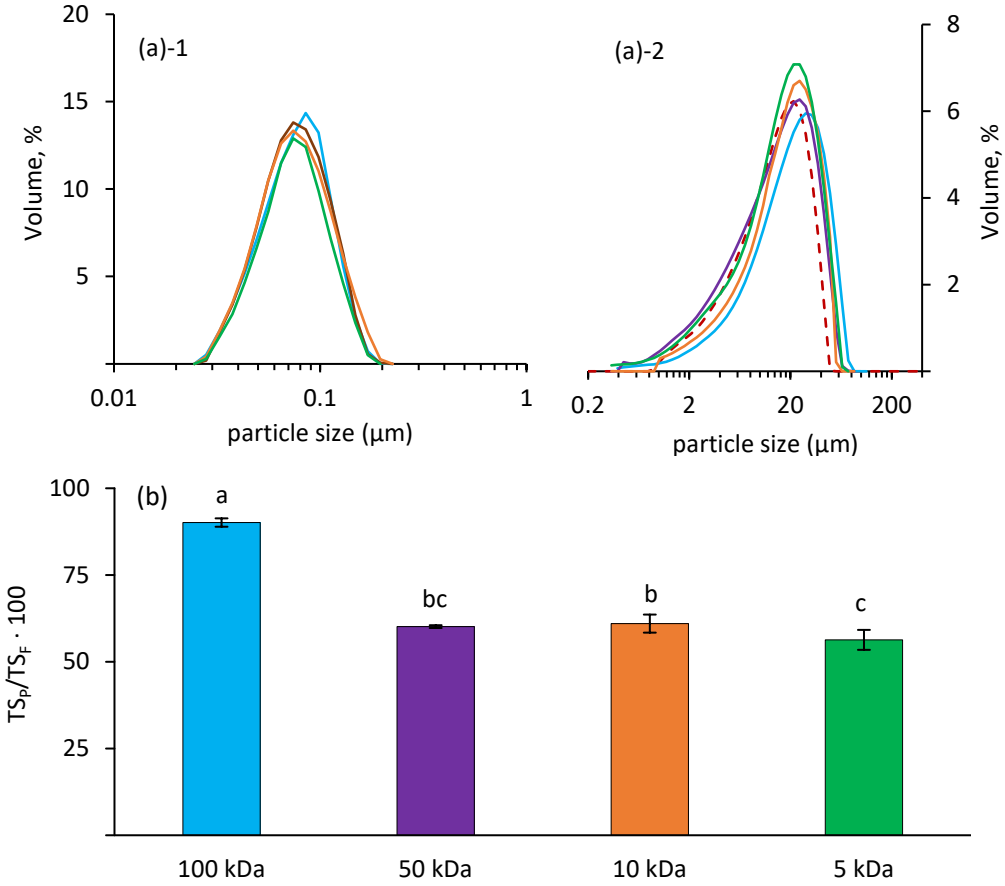

Figure 5.4. (a)-1 Permeate and **(a)-2** retentate particle size distribution after UF at 20 °C and 11.2 L/h (- - - Feed; — 100 kDa; — 50 kDa; — 10 kDa; — 5 kDa). **(b)** Percentage of solids variation in the permeate fraction with respect to feed estimated according to **Equation 5.3**. Values with different letters are significantly different when applying the Fisher's least significant differences (LSD) method at p-value ≤ 0.05. (Experimental data include standard deviations, *n* = 3 technical replicates).

Regarding the colour of the different fractions collected after UF process, a clear colour intensification was observed in the retentate fraction for all the membranes. The lower the molecular weight cut-off of the membrane, the higher the increase in the retentate fraction, although there was no significant difference between 10 and 5 kDa. The opposite effect was observed in permeate fractions. The lower the MWCO, the lower the coloration of the permeate extracts, as it is clearly observed in the attached photographs (**Figure 5.5a**).

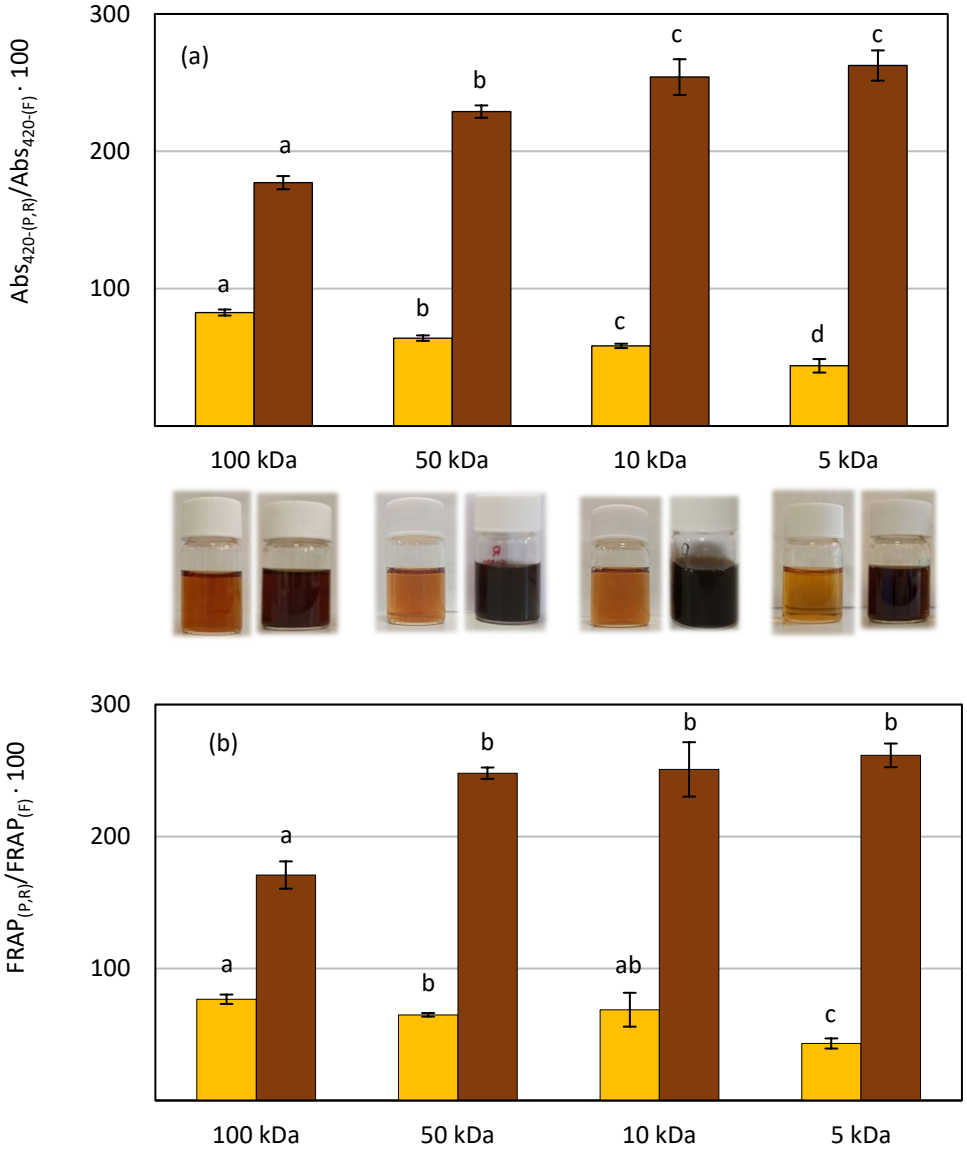

Figure 5.5. (a) Colour and **(b)** FRAP variation of permeate (■) and retentate (■) fraction in relation to feed after UF at 20 °C and 11.2 L/h, estimated according to **Equations 5.4** and **5.3**, respectively. (Photographs of permeate (left) and retentate (right) fractions are shown below each molecular weight cut-off). Values with different letters are significantly different when applying the Fisher's least significant differences (LSD) method at p-value ≤ 0.05. (Experimental data include standard deviations, *n* = 3 technical replicates).

FRAP variation of permeate and retentate fractions respect to initial feed follows the same trend as colour. A progressive increase in the retentate reducing capacity was observed for 100 or lower molecular weight cut-off, but a significant difference was just observed between 100 and 50 kDa (**Figure 5.5b**).

In view of these results, a relation between reducing capacity and colour could be established. Melanoidins are compounds formed as a consequence of Maillard and caramelization reactions at high temperatures between carbonyl and amine groups from reducing sugars and amino acids, respectively (Gu et al., 2009). Maillard reaction products (MRPs) were the main responsible for colour and antioxidant activity on the subcritical water extracts (Trigueros et al., 2021) and these compounds, which absorb mainly at the measured wavelength (420 nm), are generally high molecular weight components (Plaza et al., 2010). According to previous studies, low values of luminosity and yellowness and high values of redness colour parameters corresponded with the highest reducing power, with a strong correlation with the reducing power (at the 95 % confidence level). For this reason, by using high MWCO membranes, it was possible to reach high rejection of MRPs, removing unwanted coloration and preserving between 76.7 and 64.9 % of the starting reducing capacity, with 100 and 50 kDa membranes, respectively. By using the lowest MWCO membrane (5 kDa), just 43.3 % of reducing capacity remained in the permeate fraction.

3.2.2. Bio-compounds rejection

With respect to the rejection of the biocompounds determined in the red alga subcritical water extract, total polyphenols showed the same trend as colour and reducing capacity. Rejection of 21.7 % of TPC was reached with 100 kDa membrane and, although an increase was observed with lower MWCO, there was no significant difference among MWCO lower than 50 kDa (**Figure 5.6**). Hence, 100 and 50 kDa membrane were cut-offs small enough for colloidal material and colour removal, respectively, because of MRPs retention.

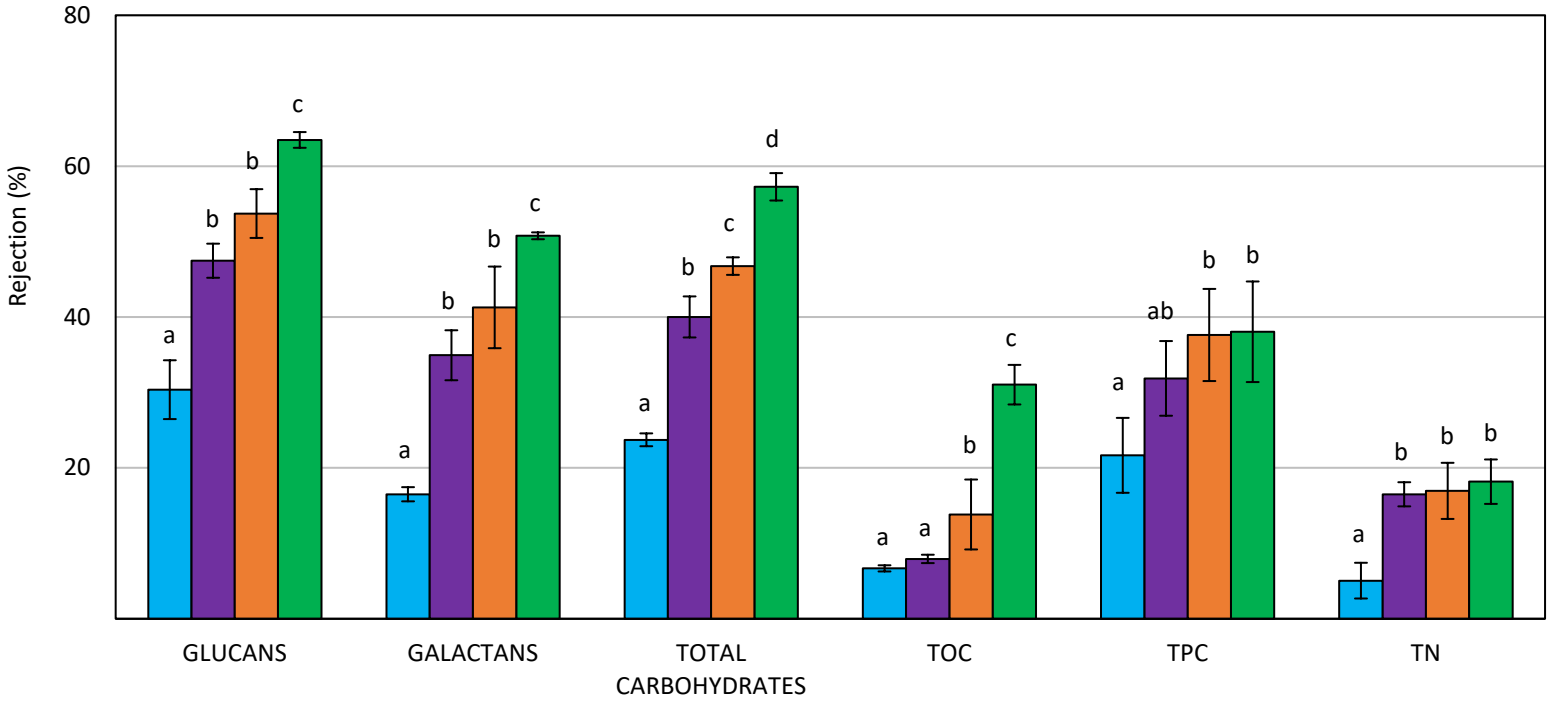

Figure 5.6. Retention percentages estimated by **equation 5.5** of different bioactive compounds by using membranes with different molecular weight cut-off after UF at 20 °C and 11.2 L/h (■ 100 kDa; ■ 50 kDa; ■ 10 kDa; ■ 5 kDa). Values with different letters for each component are significantly different when applying the Fisher's least significant differences (LSD) method at p-value ≤ 0.05. (Experimental data include standard deviations, *n* = 3 technical replicates)

Similar results were found by Tsibranska et al. (Tsibranska et al., 2011) during propolis nanofiltration. By using membranes between 300 and 900 Da, they found that by decreasing the molecular weight cut-off of the membranes, the antioxidant capacity of the retentate increased, at the same time that a decrease was observed in permeate. Also, these results were accompanied by an increase in the retention of total polyphenols and flavonoids.

Additionally, Díaz-Reinoso et al. (Díaz-Reinoso et al., 2009) evaluated the fractionation capacity of different polymeric and ceramic membranes from distilled white grape pomace, first pressed (1.4 MPa, 5 minutes) and washed with water at 60 °C for 1 hour. They determined the greater retention for total solids, polyphenols and antioxidant activity with the ceramic membrane, even at low levels of TMP, which evidenced the great effectiveness of ceramic membranes against organic ones.

Total nitrogen was one of the lowest rejected compounds for all the experiments performed. A significant difference in retention coefficient was just observed between 100 (5.1 %) and 50 kDa (16.5 %) membranes. Moreover, the amino acids retention did not exceed 1 % in any case, due to its low molecular weight making them to permeate.

Yu et al. (Yu et al., 2016) investigated the proteins and polyphenols separation with polymeric (PES) membranes from fresh rapeseed extracts obtained by grinding and mixing the fresh rapeseed stems with water, with a solid to liquid ratio of 1:8. They reached a high protein rejection (64 %) with a 50 kDa membrane, while about the total protein content was rejected with the 10 kDa membrane. On the opposite, just 3 % of retention was achieved for polyphenols with 50 kDa, and no great improvement was observed with lower molecular cut-off. These high levels of protein retention were due to the composition of the raw material, mainly constituted of high molecular weight globulins and albumin proteins, of 300 and from 12 to 14 kDa, respectively. Leberknight et al. (Leberknight et al., 2011) evaluated the protein recovery from corn kernel extract with regenerated cellulose and PES membranes with MWCO of 5 and 100 kDa. The corn kernel extract was obtained by grinding and mixing 40 g of kernel yellow corn in 100 mL of water and adjusting pH at 8.5 by using sodium hydroxide. They found a protein yield in the retentate fraction of 80 %, approximately, for all the tested membranes. However, these results were unexpected because the protein composition in the raw material mainly consisted of 80 and 20 % of

proteins greater than 5 and 100 kDa, respectively. Finally, they concluded that the high retention observed for all the experiments could be explained by the narrowing and/or protein aggregation during filtration by using organic membranes, in relation to the chemicals that constitute them.

The lower retention index obtained for total nitrogen in this work (assuming that most of the nitrogen comes from the protein fraction), was due to the extraction/hydrolysis of the protein fraction in the subcritical water extracts. Water under subcritical conditions presents unique properties as solvent such as lower dielectric constant, which lead to a higher organic compounds solubility in water when temperature increases (Cocero et al., 2018).

Total organic carbon retention increased slightly as the molecular cut-off of the membrane decreased from 100 to 5 kDa, resulting in retention of 31 %.

Carbohydrates showed the highest rejection. Glucans were the most retained components followed by galactans. The lowest rejection values were determined for 100 kDa membrane, with 30.4 and 16.5 for glucans and galactans, respectively. The highest rejection was reached with the lowest MWCO membrane (5 kDa), 63.5 and 50.8 %, respectively. Hence, once again, the relation between MWCO and rejection coefficient was observed, although no significant differences were found between 50 and 10 kDa for glucans and galactans. As a result, a retention above 55 % of total carbohydrates was determined for the lowest MWCO membrane. From these results it can be concluded that in the subcritical water hydrolysates, the carbohydrate fraction present higher molecular size distribution that the peptides obtained in the hydrolysis process under subcritical conditions.

Similarly, high rejection coefficients (> 90 %) of polysaccharides from winery effluents were observed by using PES polymeric membranes (7600 Da) and non-influence of pressure on their retention was observed (Giacobbo et al., 2013).

Polisetti & Ray (Polisetti & Ray, 2020) evaluated the differences between organic and inorganic membranes by using polymeric membranes enriched with inorganic nanoparticles. They found that the addition of increasing concentrations of SiO_2 and TiO_2 promoted a notable improvement in the polyethylene glycol (35 kDa) and polyethylene

oxide (100-600 kDa) rejection coefficients, especially for the membranes with lower molecular weight cut-off. Hence, the trend between the decreasing MWCO and the increase in retention was clearly observed.

3.2.3. Membrane fouling

In spite of the fact that ceramic membranes are potentially more advantageous than organic, the loss of permeate flux due to irreversible fouling because of organic matter is a common challenge, since it could alter the ultrafiltration process and decrease the membrane lifetime (Alresheedi & Basu, 2019).

Dependence of permeate flux and total resistance of the tested membranes with Volume Reduction Factor (VRF) along UF process is shown in **Figure 5.7**. VRF was estimated according to the following equation:

$$VRF = \frac{V_F}{V_R} \qquad [5.6]$$

where V_F and V_R are feed and retentate volume, respectively.

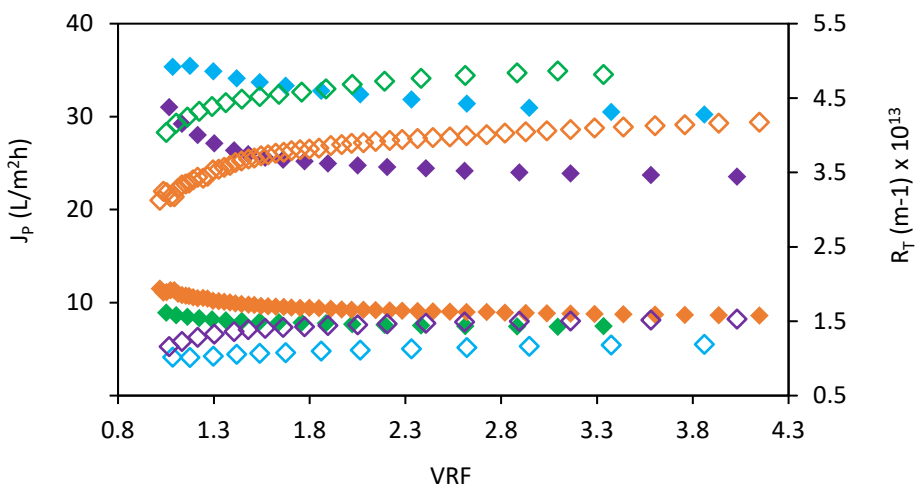

Figure 5.7. Permeate flux (J_P) (principal axis, filled symbols) and total membrane resistance (R_T) (secondary axis, non-filled symbols) estimated by **equation 5.1** and **5.2**, respectively, depending of VRF along UF process at 20 °C and 11.2 L/h.
(◆◇ 100 kDa; ◆◇ 50 kDa; ◆◇ 10 kDa; ◆◇ 5 kDa)

A slight decrease in permeate flux of 14.5, 24.2, 25.1 and 16.2 % for 100, 50, 10 and 5 kDa membranes, respectively, was observed along the ultrafiltration process. With 10 and 5 kDa membranes, obtained permeate flux was very low in comparison with the highest MWCO tested membrane (100 kDa), specifically, 71.1 and 75.7 % lower, respectively. This was related to the big increase in membrane fouling, as shown by the total resistance values, which increase by almost 4 and 5 times its value for 10 and 5 kDa, respectively, in comparison with 100 kDa membrane resistance.

The decrease in permeate flux, accompanied by the increase in total membrane resistance from 1.02-1.19 m^{-1} for 100 kDa to 4.04-4.82 m^{-1} for 5 kDa membrane, could be explained owing to the polarization layer formation over the surface of the membrane with high molecular compounds such as agar, protein or polysaccharides leftover from the initial aqueous extract (Gekas et al., 1993; Marshall et al., 1993). Jarusutthirak et al. (Jarusutthirak et al., 2002) indicate that polysaccharide colloids are responsible for most fouling in UF membranes. However, the growth of this bio-gel layer is limited by the external turbulence caused by the tangential velocity during ultrafiltration in cross-flow operational mode, resulting in lower flux declining and a final steady-state flux value (Rai et al., 2006).

Therefore, in view of these results, despite having found great retention capacity with the lowest MWCO membranes, a great reduction in permeate flux was determined due to a greater fouling rate, which makes the process performance more difficult.

3.3. Temperature and feed flux effects on the membrane fouling

Feed temperature is an important operating parameter in UF, since density and viscosity of the aqueous extract are directly influenced by temperature, which influences the whole ultrafiltration process (Alresheedi & Basu, 2019).

Effect of temperature and feed flow rate on the permeate flux and secondary resistance of the membranes is shown in **Figure 5.8a** (total resistance is the same). As it can be observed, by decreasing feed flow rate from 11.2 to 6.6 L/h no variation was observed in the permeate flux and secondary resistance of the membrane; however, by increasing the feed temperature from 20 to 50 °C, an increase in the permeate flux was achieved at the same

time that secondary resistance of the membrane was reduced. Moreover, it was also observed that this effect was more intense at the beginning of the ultrafiltration process, since similar values of secondary resistance and permeate flux were found at the end of the filtration between different operational conditions.

Similar results were found by Cromey et al. (Cromey et al., 2015) when evaluating the effect of temperature on colloidal suspensions ultrafiltration by using ceramic membranes. They found a great increase in permeate flux, as it was also observed in this work, by increasing feed temperature from 25 to 90 °C.

However, although a decrease in resistance of the membrane at 50 °C was observed in our study, significant differences in rejection coefficients for the components analyzed were not determined by increasing temperature from 20 to 50 °C. Moreover, the UF process remained fairly stable throughout the entire process for all the performed experiments, with practically constant permeate fluxes after the first reduction. This fact can be also observed in **Figure 5.8b** in which TOC and TN concentration of permeate fraction remained constant until the end of the ultrafiltration stage. These results suggest that, once the concentration polarization layer was formed over the membrane, the fouling rate did not increase appreciably for all the experiments, proving again the feasibility of selected ceramic membranes for selected subcritical water extract ultrafiltration. Nevertheless, as mentioned before, an improvement in UF process was observed by increasing temperature, which also could improve the cleaning process of the membrane after UF, as well as its preservation. Moreover, ultrafiltration at higher temperatures could be an option to work with more concentrated extracts with higher fouling rates. By increasing feed flow rate from 6.6 to 11.2 L/h, the ultrafiltration process was accelerated without worsening UF.

Hence, although at industrial scale the increase in temperature would not economically compensate because of the higher energy costs, it could be an interesting operational parameter to take into account for an industrial-scale reactor, in which high temperatures are usually reached. In this sense, a subcritical water reactor coupled to the ultrafiltration system could be an economical and useful alternative, resulting in the improvement of the process by using ceramic membranes, capable of resisting high operational temperatures.

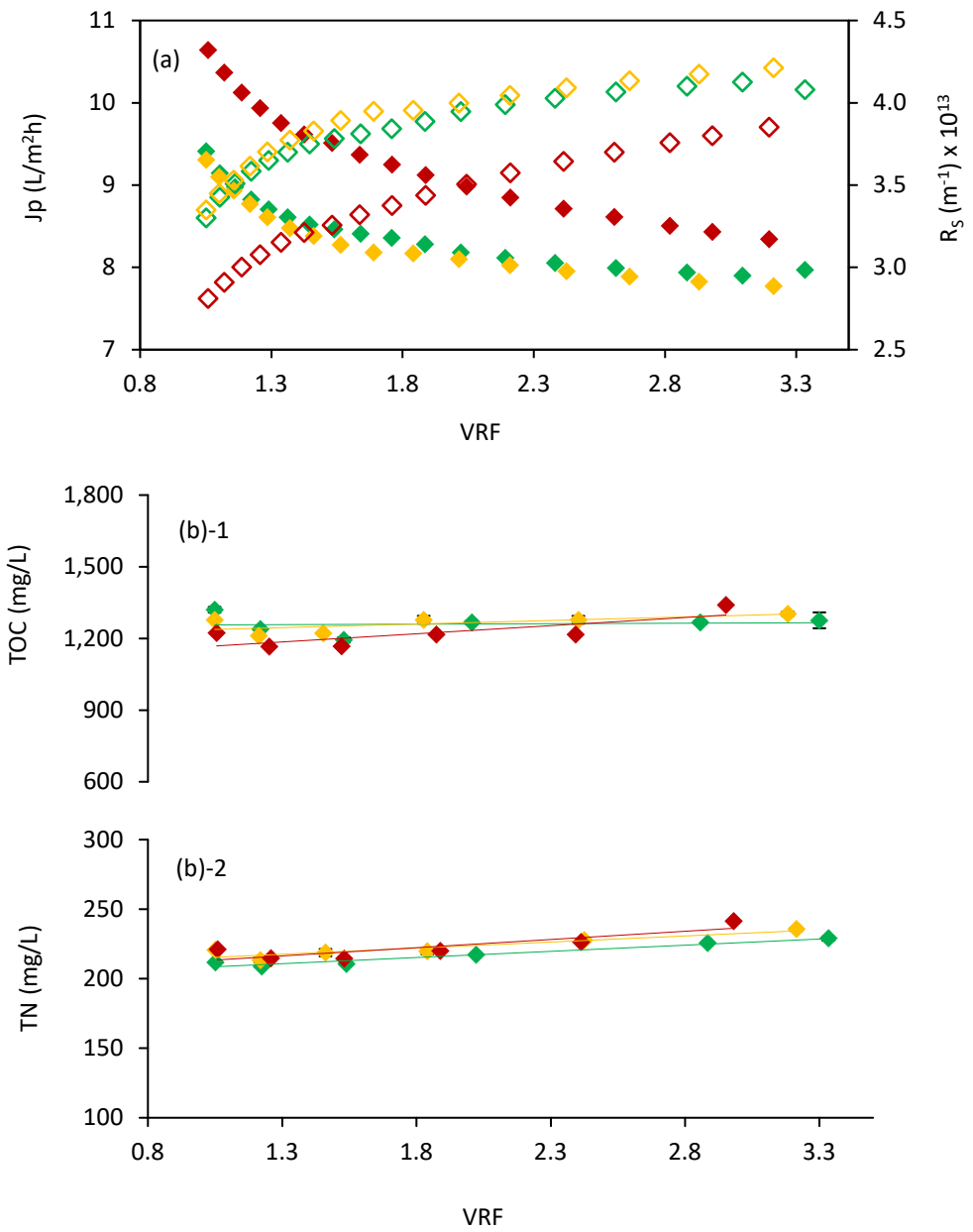

Figure 5.8. (a) Permeate flux (J_P) (principal axis, filled symbols) and secondary resistance (R_S) (secondary axis, non-filled symbols) of the membranes along UF process. **(b)-1** Total Organic Carbon and **(b)-2** Total Nitrogen concentration in permeate fraction along UF for 5 kDa MWCO membrane at different temperatures and feed flow rates.
(◆◇ T = 20 °C, Q_F = 11.2 L/h; ◆◇ T = 20 °C, Q_F = 6.6 L/h; ◆◇ T = 50 °C, Q_F = 11.2 L/h).
(Regression lines are indicated for each experiment).

3.4. Fractionation of bioactive compounds by sequential UF

3.4.1. Permeate and retentate fraction characteristics

In order to fractionate and concentrate carbohydrates and protein fraction, a sequential ultrafiltration was carried out. **Figure 5.9a** shows the reduction in solid content regarding the initial subcritical water hydrolysate. By a sequential ultrafiltration process, most of solid content was removed, remaining 57.7 and 33 % of total solids in permeate fraction after ultrafiltration through the 5 and 1 kDa membrane, respectively. Moreover, the good reproducibility of the ultrafiltration process can be observed, due to no significant differences were observed between replicated stages in Cycle A and Cycle B.

Colour and FRAP followed the same trend (**Figure 5.9b-c**). After the different stages of ultrafiltration, a reduction of colour on the permeate fractions was achieved respect to the original feed. A decrease of 50.8 % in colour intensity was reached with 5 kDa membrane, while a reduction of 70.8 % was observed with 1 kDa membrane. This colour reduction can be also visually observed in the permeate photographs attached.

Regarding the reducing capacity, ultrafiltration of 100 kDa permeate through 5 kDa membrane resulted in a great FRAP decrease of the concentrate. Then, ultrafiltration of 5kDa permeate through 1 kDa membrane promoted a lighter but significant reduction, preserving a reducing capacity of 15 % respect to the initial subcritical water extract.

3.4.2. Bio-compounds rejection

Resulting rejected coefficient after sequential ultrafiltration are shown in **Figure 5.10**. The good reproducibility of the results obtained in both independent ultrafiltration cycles was also observed.

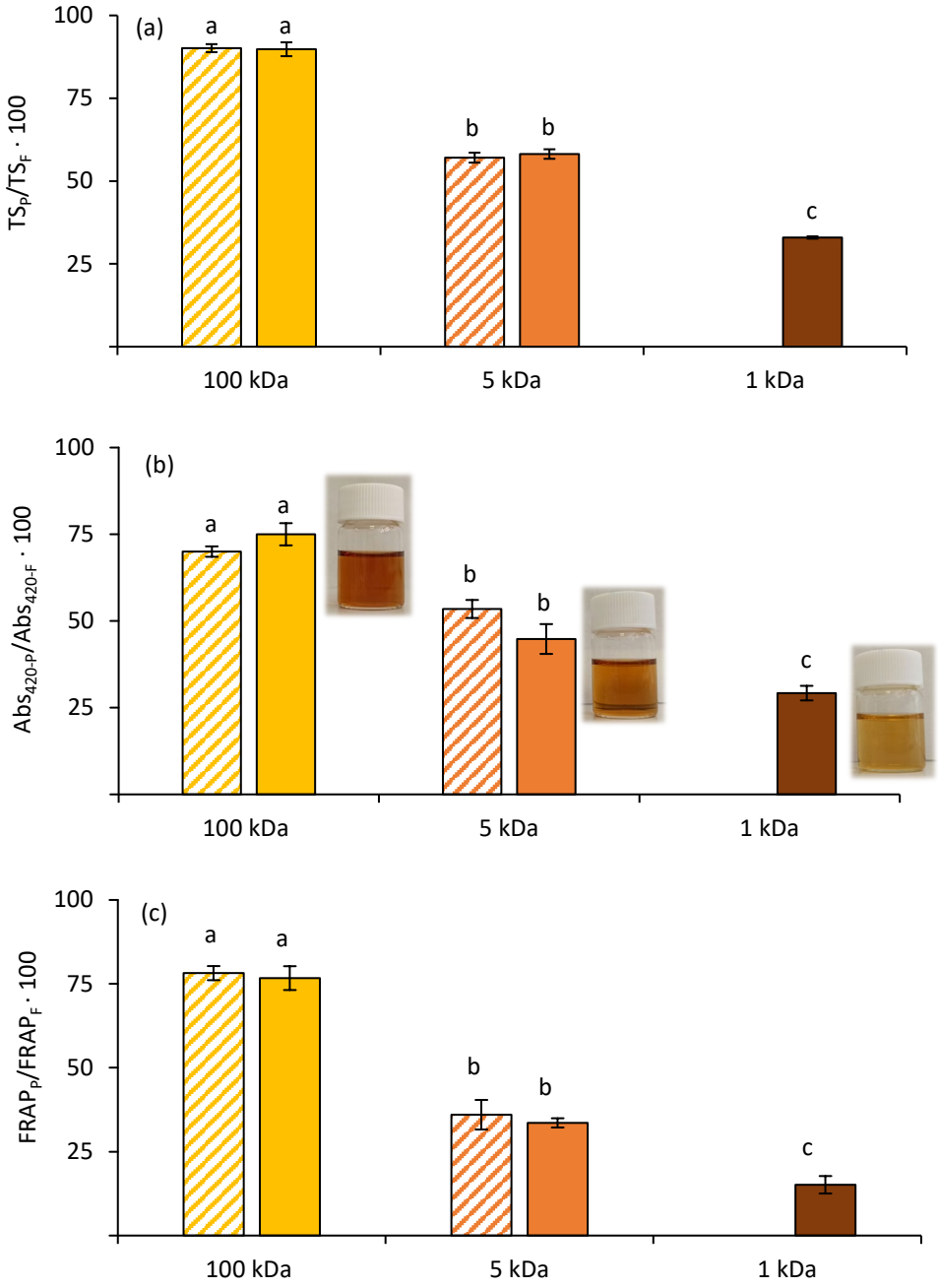

Figure 5.9. Percentage of variation of **(a)** Total Solids **(b)** Colour and **(c)** FRAP of permeate respect to the original feed after sequential UF estimated according to **Equations 5.3** and **5.4**. (Cycle A: ▨ 100 kDa; ▨ 5 kDa; Cycle B: ■ 100 kDa; ■ 5 kDa; ■ 1 kDa). Values with different letters are significantly different when applying the Fisher's least significant differences (LSD) method at p-value ≤ 0.05. (Experimental data include standard deviations, *n* = 3 technical replicates).

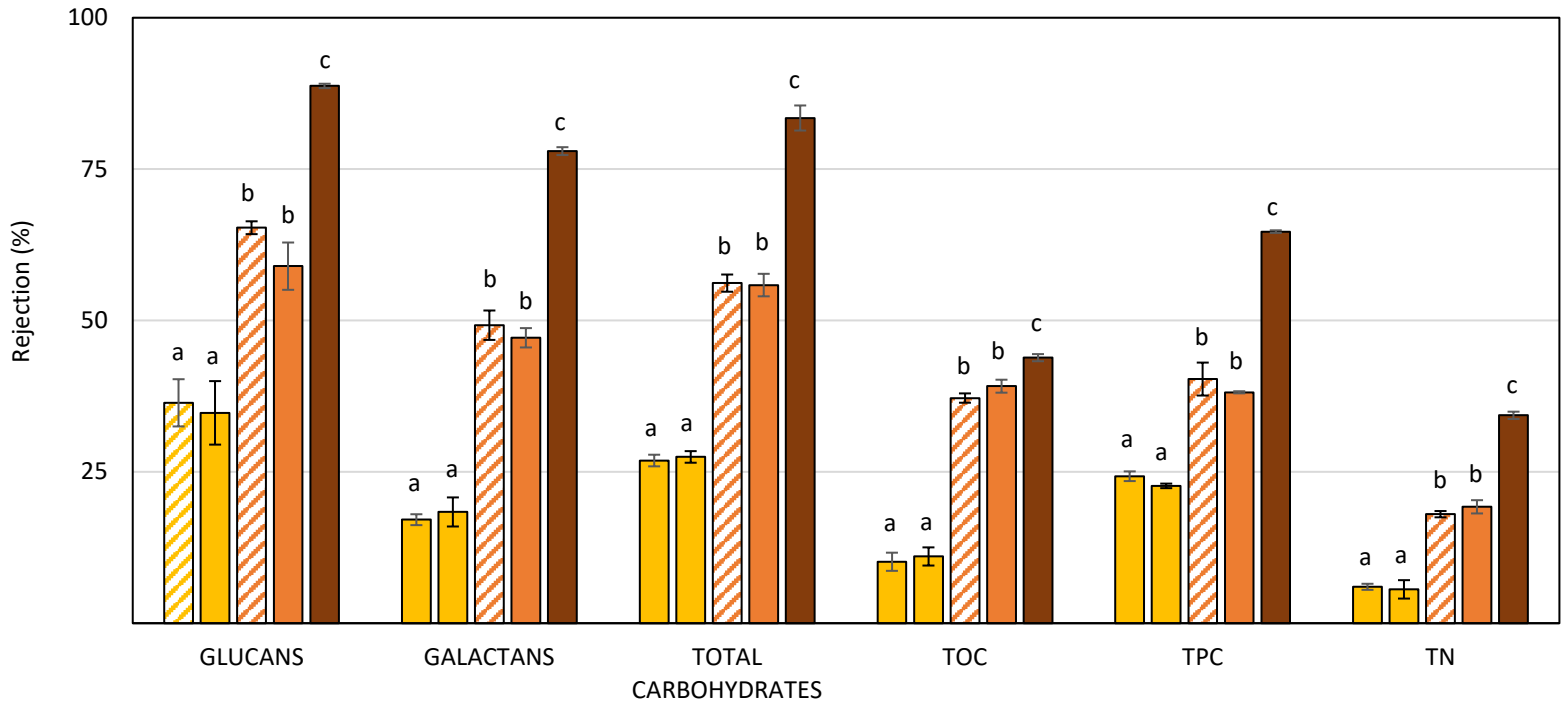

Figure 5.10. Retention coefficients estimated by **Equation 5.5** of different bioactive compounds respect to the original feed after sequential UF (Cycle A: ▨ 100 kDa; ▨ 5 kDa; Cycle B: ■ 100 kDa; ■ 5 kDa; ■ 1 kDa). Values with different letters for each component are significantly different when applying the Fisher's least significant differences (LSD) method at p-value ≤ 0.05. (Experimental data include standard deviations, *n* = 3 technical replicates).

By passing 100 kDa permeate fraction through the 5 kDa membrane (Cycle A), a significant increase in rejection coefficients for all the compounds analyzed was observed, but it was more intense for total carbohydrates. However, total nitrogen retention was not greatly affected by this ultrafiltration step, since just 18.6 % of retention was observed after ultrafiltration through 5 kDa membrane.

By passing permeate fraction from 5 kDa membrane through the 1 kDa membrane (Cycle B), carbohydrates retention still continued to increase significantly, obtaining a total final rejection of 83.4 %. Nevertheless, total nitrogen rejection values stayed small, lower than 35 % respect to the initial feed content.

According to these results, after the first two sequential ultrafiltration stages (Cycle A), the sum of all the retained fractions contained 56 % of total carbohydrates, while permeate fractions accounted for 81.4 % total nitrogen. On the other hand, at the end of the complete three-stages sequential UF (Cycle B), a sum of retentates with 83.4 % of total carbohydrates and permeates with 65.7 % of total nitrogen were collected.

Moreover, more than 60 % of total polyphenol content as determined by the Folin-Ciocalteu assay remained in the retentate fraction after complete sequential UF. In previous work, stronger correlations were determined for TPC and reducing capacity than for other components determined in the hydrolysates as peptides and free amino acids (Trigueros et al., 2021), as it can be also seen in this work.

Tsibranska et al. (Tsibranska et al., 2011) reached rejection coefficients for total polyphenols and flavonoids from 30 % to 94 % by a sequential nanofiltration. As feed concentration in sequential filtration was lower than in direct filtration, they observed an improvement in filtration performance because of greater permeate flux.

Therefore, the sequential ultrafiltration process showed the ability to fractionate and concentrate the carbohydrate and protein content in retentate and permeate fractions, respectively, from the red alga subcritical water extract studied in this work. Lyophilization by freeze-drying showed a high recovery yield of 98.7 and 98.9 % for two-stages (Cycle A) and three-stages (Cycle B) sequential ultrafiltration, respectively.

Conclusions

Cross-flow ultrafiltration with TiO_2 tubular inorganic membranes has proven to be a suitable separation technology to fractionate subcritical water extracts from macroalgae residue. By decreasing molecular weight cut-off of the membranes, higher retention coefficients were determined for carbohydrates and TPC. TN rejection coefficient below 20 % was found for all the membranes. Although increasing feed temperature resulted in lower secondary resistance of the membrane and higher permeate flux, rejection coefficients were not significant different. Feed flow rate had not influence on the ultrafiltration process. By a sequential ultrafiltration was possible to fractionate and concentrate the carbohydrate and protein fractions from the subcritical water extract. A sum of retentates with 83.4 % of total carbohydrates and permeates with 65.7 % of total nitrogen were collected after sequential ultrafiltration by using 100, 5 and 1 kDa membranes.

References

Alonso-Riaño, P., Sanz, M.T., Benito-Román, O., Beltrán, S., & Trigueros, E. (2021). Subcritical water as hydrolytic medium to recover and fractionate the protein fraction and phenolic compounds from craft brewer's spent grain. *Food Chemistry* (Vol. 351).

Alresheedi, M. T., & Basu, O. D. (2019). Effects of feed water temperature on irreversible fouling of ceramic ultrafiltration membranes. *Journal of Water Process Engineering*, 31.

Ambrosi, A., Cardozo, N.S.M., & Tessaro, I.C. (2014). Membrane Separation Processes for the Beer Industry: A Review and State of the Art. *Food and Bioprocess Technology*, 7(4), 921–936.

Audinos, R., & Branger, J.L. (1992). Ultrafiltration concentration of enzyme hydrolysates. *Journal of Membrane Science*, 68, 195–204.

Balakrishnan, M., Dua, M., & Bhagat, J.J. (2000). Effect of operating parameters on sugarcane juice ultrafiltration: Results of a field experience. *Separation and Purification Technology*, 19, 209–220.

Benzie, I.F.F., & Strain, J.J. (1996). The Ferric Reducing Ability of Plasma (FRAP) as a Measure of "Antioxidant Power": The FRAP Assay. *Analytical Biochemistry*, 239, 70–76.

Carmona, R., Vergara, J.J., Lahaye, M., & Niell, F.X. (1998). Light quality affects morphology and polysaccharide yield and composition of *Gelidium sesquipedale* (Rhodophyceae). *Journal of Applied Phycology*, 10, 323–331.

Cissé, M., Vaillant, F., Bouquet, S., Pallet, D., Lutin, F., Reynes, M., & Dornier, M. (2011). Athermal concentration by osmotic evaporation of roselle extract, apple and grape juices and impact on quality. *Innovative Food Science and Emerging Technologies*, 12, 352–360.

Cocero, M.J., Cabeza, Á., Abad, N., Adamovic, T., Vaquerizo, L., Martínez, C.M., & Pazo-cepeda, M.V. (2018). The Journal of Supercritical Fluids Understanding biomass fractionation in subcritical & supercritical water. *The Journal of Supercritical Fluids*, *133*, 550–565.

Cromey, T., Lee, S.J., & Kim, J.H. (2015). Effect of Elevated Temperature on Ceramic Ultrafiltration of Colloidal Suspensions. *Journal of Environmental Engineering*, 141(6), 04014096.

Díaz-Reinoso, B., Moure, A., Domínguez, H., & Parajó, J.C. (2009). Ultra- and nanofiltration of aqueous extracts from distilled fermented grape pomace. *Journal of Food Engineering*, 91, 587–593.

Fard, A.K., McKay, G., Buekenhoudt, A., Al Sulaiti, H., Motmans, F., Khraisheh, M., & Atieh, M. (2018). Inorganic membranes: Preparation and application for water treatment and desalination. *Materials*, 11.

Fernández, C. (1991). Biological and economic importance of the genus Gelidium in Spain. *Informes Técnicos de Scientia Marina*, 163, 1–20.

Gallina, G., Cabeza, Á., Biasi, P., & García-Serna, J. (2016). Optimal conditions for hemicelluloses extraction from Eucalyptus globulus wood: Hydrothermal treatment in a semi-continuous reactor. *Fuel Processing Technology*, 148, 350–360.

Gekas, V., Aimar, P., Lafaille, J. P., & Sanchez, V. (1993). A simulation study of the adsorption-concentration polarisation interplay in protein ultrafiltration. *Chemical Engineering Science*, 48(15), 2753–2765.

Giacobbo, A., Oliveira, M., Duarte, E.C.N.F., Mira, H.M.C., Bernardes, A. M., & de Pinho, M.N. (2013). Ultrafiltration Based Process for the Recovery of Polysaccharides and Polyphenols from Winery Effluents. *Separation Science and Technology*, 48, 438–444.

Gu, F., Kim, J.M., Hayat, K., Xia, S., Feng, B., & Zhang, X. (2009). Characteristics and antioxidant activity of ultrafiltrated Maillard reaction products from a casein-glucose model system. *Food Chemistry*, 117, 48–54.

Guerrero, P., Etxabide, A., Leceta, I., Peñalba, M., & de la Caba, K. (2014). Extraction of agar from *Gelidium sesquipedale* (Rodhopyta) and surface characterization of agar based films. *Carbohydrate Polymers*, 99, 491–498.

He, L., Zhang, X., Xu, H., Xu, C., Yuan, F., Knez, Ž., Novak, Z., & Gao, Y. (2012). Subcritical water extraction of phenolic compounds from pomegranate (*Punica granatum* L.) seed residues and investigation into their antioxidant activities with HPLC-ABTS assay. *Food and Bioproducts Processing*, 90, 215–223.

Herrero, M., Cifuentes, A., & Iban, E. (2006). Sub- and supercritical fluid extraction of functional ingredients from different natural sources: Plants, food-by-products, algae and microalgae A review. *Food Chemistry*, 98, 136–148.

Hinková, A., Bubník, Z., Kadlec, P., Pour, V., & Štarhová, H. (2000). Membrane filtration in the sugar industry. *Chemical Papers*, 54(6), 375–382.

Jarusutthirak, C., Amy, G., & Croué, J. P. (2002). Fouling characteristics of wastewater effluent organic matter (EfOM) isolates on NF and UF membranes. *Desalination*, 145, 247–255.

Leberknight, J., Wielenga, B., Lee-Jewett, A., & Menkhaus, T.J. (2011). Recovery of high value protein from a corn ethanol process by ultrafiltration and an exploration of the associated membrane fouling. *Journal of Membrane Science*, 366, 405–412.

Lin, Y.S. (2019). Inorganic Membranes for Process Intensification: Challenges and Perspective. *Industrial and Engineering Chemistry Research*, 58, 5787–5796.

Marshall, A.D., Munro, P.A., & Trägårdh, G. (1993). The effect of protein fouling in microfiltration and ultrafiltration on permeate flux, protein retention and selectivity: A literature review. *Desalination*, 91, 65–108.

Mouradi-givernaud, A., Hassani, L.A., Givernaud, T., & Lemoine, Y. (1999). Biology and agar composition of Gelidium sesquipedale harvested along the Atlantic coast of Morocco. *Hydrobiologia*, 398/399, 391–395.

Munir, M.T., Kheirkhah, H., Baroutian, S., Quek, S.Y., & Young, B.R. (2018). Subcritical water extraction of bioactive compounds from waste onion skin. *Journal of Cleaner Production*, 183, 487–494.

Murano, E. (1995). Chemical structure and quality of agars from *Gracilaria*. *Journal of Applied Phycology*, 7, 245–254.

Plaza, M., Amigo-Benavent, M., del Castillo, M.D., Ibáñez, E., & Herrero, M. (2010). Neoformation of antioxidants in glycation model systems treated under subcritical water extraction conditions. *Food Research International*, 43, 1123–1129.

Polisetti, V., & Ray, P. (2020). Nano SiO2 and TiO2 embedded polyacrylonitrile/polyvinylidene fluoride ultrafiltration membranes: Improvement in flux and antifouling properties. *Journal of Applied Polymer Science*, 138(1).

Rai, P., Majumdar, G.C., Jayanti, V.K., Dasgupta, S., & De, S. (2006). Alternative pretreatment methods to enzymatic treatment for clarification of mosambi juice using ultrafiltration. *Journal of Food Process Engineering*, 29, 202–218.

Saidi, S., Deratani, A., Belleville, M.P., & Amar, R. Ben. (2014). Production and fractionation of tuna by-product protein hydrolysate by ultrafiltration and nanofiltration: Impact on interesting peptides fractions and nutritional properties. *Food Research International*, 65, 453–461.

Sarmento, L.A.V., Machado, R.A.F., Petrus, J.C.C., Tamanini, T.R., & Bolzan, A. (2008). Extraction of polyphenols from cocoa seeds and concentration through polymeric membranes. *Journal of Supercritical Fluids*, 45, 64–69.

Singleton, V.L., Orthofer, R., & Lamuela-Raventós, R.M. (1999). Analysis of total phenols and other oxidation substrates and antioxidants by means of Folin-Ciocalteu reagent. *Polyphenols and Flavonoids*, 25, 281–286.

Susanto, H., Arafat, H., Janssen, E.M.L., & Ulbricht, M. (2008). Ultrafiltration of polysaccharide-protein mixtures: Elucidation of fouling mechanisms and fouling control by membrane surface modification. *Separation and Purification Technology*, 63, 558–565.

Susanto, H., Feng, Y., & Ulbricht, M. (2009). Fouling behaviour of aqueous solutions of polyphenolic compounds during ultrafiltration. *Journal of Food Engineering*, 91(2), 333–340.

Takaç, S., Elmas, S., Çalik, P., Özdamar, T.H. (2000). Separation of the protease enzymes of Bacillus licheniformis from the fermentation medium by crossflow ultrafiltration. *Journal of Chemical Technology and Biotechnology*, 75(6), 491–499.

Torres, M., Niell, F. X., & Algarra, P. (1991). Photosynthesis of *Gelidium sesquipedale*: effects of temperature and light on pigment concentration, C/N ratio and cell-wall polysaccharides. *Hydrobiologia*, 221, 77–82.

Trigueros, E., Sanz, M.T., Alonso-Riaño, P., Beltrán, S., Ramos, C., & Melgosa, R. (2021). Recovery of the protein fraction with high antioxidant activity from red seaweed industrial solid residue after agar extraction by subcritical water treatment. *Journal of Applied Phycology.*

Tsibranska, H., Peev, G.A., & Tylkowski, B. (2011). Fractionation of Biologically Active Compounds Extracted from Propolis by Nanofiltration. *Journal of Membrane Science & Technology*, 1(4), 1–5.

Wataniyakul, P., Pavasant, P., Goto, M., & Shotipruk, A. (2012). Microwave pretreatment of defatted rice bran for enhanced recovery of total phenolic compounds extracted by subcritical water. *Bioresource Technology*, 124, 18–22.

Xie, J.H., Shen, M. Y., Nie, S. P., Zhao, Q., Li, C., & Xie, M.Y. (2014). Separation of water-soluble polysaccharides from Cyclocarya paliurus by ultrafiltration process. *Carbohydrate Polymers*, 101, 479–483.

Yu, X., Bogaert, L., Hu, R., Bals, O., Grimi, N., & Vorobiev, E. (2016). A combined coagulation–ultrafiltration method for enhanced separation of proteins and polyphenols. *Separation Science and Technology*, 51(6), 1030–1041.

CONCLUSIONS

CONCLUSIONS

Although each chapter contains its own conclusions from the different experimental studies carried out in this PhD Thesis, the following general conclusions can be established:

- Macroalgae residue from *Gelidium sesquipedale* after industrial agar extraction constitute a source of valuable bioactive compounds such as carbohydrates, proteins with all essential amino acids and high antioxidant activity.

- Subcritical water extraction (SWE) has proven to be a green technology capable of recovering bioactive compounds with high yields from macroalgae residue through a complete by-product valorization.

- Extraction/hydrolysis during subcritical water extraction showed to be highly influenced by the temperature, the heating rate and the residence time.

- Enzymatic assisted extraction (EAE) has also proven to be an efficient technology to valorize the industrial alga solid waste after agar extraction.

- Longer times were needed for EAE and lower yields of biocompounds extraction/hydrolysis were observed in comparison with SWE.

- Ultrafiltration with tubular inorganic membranes has proven to be a suitable separation technology to fractionate subcritical water extracts from macroalgae residue. The most influential parameter in separation process was the MWCO of the membrane. By increasing the temperature an improvement in the process was achieved by reducing the fouling of the membrane.

- Further research about functional properties of concentrated and isolated biocompounds is needed in order to study their possible applications to be reincorporated into industrial processes.

CURRICULUM VITAE

Ester Trigueros Andrés

Born in March 24th, 1993 in Palencia (Spain)

Contact

e-mail: esther.t.a@hotmail.com
Scopus author ID: 57203857162
ORCID: https://orcid.org/0000-0003-1701-0523
ResearcherID: AAF-9791-2021

Education

2016-present	Bachelor's Degree in Chemistry University of National Distance Education, Spain
2018-2021	PhD student in Advances in Food Science and Biotechnology University of Burgos, Spain
2015-2016	Master's Degree in Food Safety and Biotechnology University of Burgos, Spain
2011-2015	Bachelor's Degree in Human Nutrition and Dietetics University of Valladolid, Spain

Employment

2018-2021	PhD scholarship in the Department of Biotechnology and Food Science, University of Burgos, Spain (Ref.: BOCYL-D-07062018-6)
2016-2018	Dietitian in C.S. Hermanas Hospitalarias, Palencia, Spain
2015-2016	Research technician scholarship in the Department of Biotechnology and Food Science, University of Burgos, Spain
2014 (3 months)	Scholarship for academic internship in C.H. Benito Menni, Valladolid, Spain

Short research visit

2021 (3 months) *(Virtual)*	Marine and Environmental Sciences Centre (MARE), Polytechnic of Leiria, Peniche, Portugal

Publications compiled in the PhD Thesis

1. Trigueros E., et al. Fractionation of bioactive compounds from a red alga subcritical water extract by ultrafiltration. *Separation and Purification Technology* (will be summited).
2. Trigueros E., Sanz M.T., Beltrán S., Alonso-Riaño P., Ramos C. Subcritical water extraction scale-up from laboratory to pilot system for red algae residue after agar extraction valorization. *Journal of Industrial and Engineering Chemistry*. (submitted).
3. Trigueros E., Sanz M.T., Beltrán S., Alonso-Riaño P., Ramos C. Effect of heating rate and residence time on subcritical water macroalgae residue hydrolysis. *Journal of Cleaner Production* (submitted).
4. Trigueros E., Sanz M.T., Filipigh A., Beltrán S., Riaño P. (2021). Enzymatic hydrolysis of the industrial solid residue of red seaweed after agar extraction: extracts characterization and modelling. *Food and Bioproducts Processing,* 126, pp. 356-366.
5. Trigueros E., Sanz M.T., Alonso-Riaño P., Beltrán S., Ramos C., Melgosa R. (2021). Recovery of the protein fraction with high antioxidant activity from red seaweed industrial solid residue after agar extraction by subcritical water treatment. *Journal of Applied Phycology.*

Co-authored publications

6. Alonso-Riaño P., Sanz M.T., Benito-Román O., Beltrán S., Trigueros E. (2021). Subcritical water as hydrolytic medium to recover and fractionate the protein fraction and phenolic compounds from craft brewer's spent grain. *Food Chemistry*, 351.
7. Melgosa R., Trigueros E., Sanz M.T., Cardeira M., Rodrigues L., Fernández N., Matias A.A., Bronze M.R., Marques M., Paiva A., Simoes P. (2020). Supercritical CO2 and subcritical water technologies for the production of bioactive extracts from sardine (Sardina pilchardus) waste. *Journal of Supercritical Fluids,* 164.
8. Alonso P, Sanz M.T., Blanco B, Beltrán S, Trigueros E, Benito O. (2020). Water Ultrasound-Assisted Extraction of Polyphenol Compounds from Brewer's Spent Grain: Kinetic Study, Extract Characterization, and Concentration. *Antioxidants,* 9(3), 265.
9. Illera A., Sanz T., Trigueros E., Beltrán S., Melgosa R. (2018). Effect of high pressure carbon dioxide on tomato juice: Inactivation kinetics of pectin methylesterase and polygalacturonase and determination of other quality parameters. *Journal of Food Engineering,* 239, pp. 64-71.

Oral communications

Trigueros E., Alonso-Riaño P., Sanz M.T., Beltrán S., Ramos C., Benito-Román O. "Hydrothermal fractionation of *Gelidium sesquipedale* alga residue by subcritical water extraction" in *18th European Meeting on Supercritical Fluids.* May 2021, Bordeaux (France).

Trigueros E., Riaño P., Sanz M.T., Beltrán, S. "Valorización del residuo del alga roja tras la extracción de agar mediante tratamiento con agua subcrítica y extracción enzimática asistida" in *VII Jornadas de Doctorandos de la Universidad de Burgos*. March 2021, Burgos (Spain).

Trigueros E., Sanz M.T., Alonso-Riaño P., Beltrán S., Ramos C. "Hydrolysis of the protein fraction of the industrial solid residue from red algae after agar extraction" in *First Greenering International Conference*. February 2021, Costa da Caparica (Portugal).

Trigueros E., Alonso-Riaño P., Sanz M.T., Ramos C., Benito-Román O., Beltrán S. "Recovery of proteins and free amino acids from Gelidium sesquipedale alga residue by subcritical water extraction (SWE)" in *First Iberian Meeting on Supercritical Fluids*. February 2020, Santiago de Compostela (Spain).

Poster presentations

Trigueros E., Alonso-Riaño P., Melgosa R., Sanz M.T., Benito-Román O., Beltrán B. "Recovery of bioactive compounds from Gelidium sesquipedale alga by subcritical water extraction (SWE)" in *17th European Meeting on Supercritical Fluids.* April 2019, Ciudad Real (Spain).

Trigueros E., Illera A.E., Sanz M.T., Melgosa R., Solaesa A.G., Beltrán A., "Effect of HPCD Treatment on Enzyme Inactivation and other Properties of Tomate Juice" in *16th European Meeting on Supercritical Fluids*. April 2017, Lisbon (Portugal).